ISAS - INTERNATIONAL SCHOOL FOR ADVANCED STUDIES

The Mass Distribution Function of Groups of Galaxies

Thesis submitted to the
International School for Advanced Studies, Trieste, Italy
– Astrophysics Sector –
in partial fulfilment of the requirements for the degree of

Doctor Philosophiae

Candidate:
Armando Pisani

Supervisor:
Prof. Dennis W. Sciama

Academic Year 1989/90

TRIESTE

SISSA - SCUOLA INTERNAZIONALE SUPERIORE DI STUDI AVANZATI
TRIESTE
Strada Costiera 11

The Mass Distribution Function of Groups of Galaxies

Thesis submitted to the
International School for Advanced Studies, Trieste, Italy
– Astrophysics Sector –
in partial fulfilment of the requirements for the degree of

Doctor Philosophiae

Candidate:
Armando Pisani

Supervisor:
Prof. Dennis W. Sciama

Academic Year 1989/90

to my wife Antonella

Contents

List of Tables iv

List of Figures vii

Acknowledgements x

Abstract xi

Introduction 1

1 From observations to an estimate of physical parameters 4
- 1.1 Introduction . . . 4
- 1.2 Samples of galaxies . . . 4
- 1.3 Catalogues of groups of galaxies . . . 7
  - 1.3.1 The *friends-of-friends* algorithm . . . 8
  - 1.3.2 The Three-dimensional hierarchical clustering membership criterion . . . 11
- 1.4 The estimate of group parameters . . . 16
  - 1.4.1 The distance . . . 16
  - 1.4.2 The luminosity . . . 18
  - 1.4.3 The size of groups . . . 21
  - 1.4.4 The velocity dispersion . . . 23
  - 1.4.5 The time scale . . . 26
  - 1.4.6 The mass . . . 27
  - 1.4.7 The virial estimators . . . 28
  - 1.4.8 The non-virial estimators . . . 39

2 The available catalogues of galaxy groups 43
- 2.1 Introduction . . . 43
- 2.2 The GH83 catalogue . . . 43
- 2.3 The RGH89 catalogue . . . 45
- 2.4 The S89 catalogue . . . 46
- 2.5 The T87 catalogue . . . 47

2.6 The V84 catalogue 49

3 Analysis of the data and discussion of the results 53
3.1 Introduction 53
3.2 Analysis of the GH83 groups 54
3.2.1 Generalities 54
3.2.2 Analysis of the biases 57
3.2.3 Analysis of groups physical parameters 66
3.2.4 A procedure to recover distant faint groups 71
3.2.5 Summary 77
3.3 Analysis of T87 groups 79
3.3.1 Generalities 79
3.3.2 Analysis of groups physical parameters 83
3.3.3 A test of the procedure to recover faint distant groups 88
3.3.4 Summary 94
3.4 Analysis of V84 groups 95
3.4.1 Generalities 95
3.4.2 Analysis of groups physical parameters 98
3.4.3 Summary 101
3.5 Analysis of *RGH*89 groups 104
3.6 Analysis of S89 groups 111
3.7 Comparison among catalogues 122

Summary and Conclusion 131

A Tables of results 134
A.1 The GH83 Groups 135
A.2 The T87 groups 145
A.3 The V84 groups 153
A.4 The RGH89 groups 159
A.5 The S89 groups 162
A.6 Comparison among catalogues 168

Bibliography 170

List of Tables

2.1 Summary of the features of the GH83 catalogue 44
2.2 Summary of the features of the RHG89 catalogue 45
2.3 Summary of the features of the S89 catalogue 46
2.4 Summary of the features of the T87 catalogue 47
2.5 Summary of the features of the V84 catalogue 52
2.6 Summary of the features of all the catalogues 52

A.1 List of GH83 parameters 135
A.2 List of GH83 mass estimators-statistical parameters. 136
A.3 Spearman correlation for $GH83$. 136
A.4 Spearman correlation for $GH83(D \leq 20\ Mpc)$. 137
A.5 Spearman correlation for $GH83(D \leq 30\ Mpc)$. 137
A.6 Spearman correlation for $GH83(D \leq 25\ Mpc)$. 138
A.7 The Kolmogorov-Smirnov test comparison of mass and other main parameter distributions for different fractions of GH83 139
A.8 List of $GH83(D \leq 20\ Mpc)$ parameters. 140
A.9 List of $GH83(D \leq 20\ Mpc)$ mass estimators-statistical parameters. 141
A.10 The Kolmogorov-Smirnov test for different velocity dispersion estimators ($GH83$). 141
A.11 The Kolmogorov-Smirnov test for different mass estimators ($GH83$). 142
A.12 The Kolmogorov-Smirnov test for different virial radius estimators ($GH83$). 142
A.13 List of $GH83$ mass corrected for the evolutionary effect and related parameters. 143
A.14 List of $GH83(D \leq 20\ Mpc)$ mass corrected for the evolutionary effect and related parameters. 143
A.15 Effect of the evolutionary correction on the mass distribution ($GH83$). 144
A.16 Effect of the value of Ω on the evolutionary correction for $GH83$. 144
A.17 List of T87 parameters. 145
A.18 List of T87 mass estimators-statistical parameters. 145

A.19 Spearman correlation for $T87$. 146
A.20 List of $T87(D \leq 20\ Mpc)$ parameters. 147
A.21 List of $T87(D \leq 20\ Mpc)$ mass estimators-statistical parameters. 147
A.22 Spearman correlation for $T87(D \leq 20\ Mpc)$. 148
A.23 The Kolmogorov-Smirnov test of different mass estimators ($T87$). 149
A.24 The Kolmogorov-Smirnov test for mass and other group parameters distributions in different fractions of $T87$. 149
A.25 List of $T87$ mass corrected for the evolutionary effect and related parameters. 150
A.26 List of $T87(D < 20\ Mpc)$ mass corrected for the evolutionary effect and related parameters. 150
A.27 Effect of the evolutionary correction on the mass distribution ($T87$). 151
A.28 Effect of the value of Ω on the evolutionary correction for $T87$.151
A.29 The effect of the magnitude limit m_c on the observed mass distributions for $T87(D \leq 20\ Mpc)$. 151
A.30 Effect of the faint distant groups correction test for $T87$. . . 152
A.31 The efficiency of faint distant groups recovery tested for $T87$. 152
A.32 List of V84 parameters. 153
A.33 List of V84 mass estimators-statistical parameters. 153
A.34 Spearman correlation for $V84$. 154
A.35 Spearman correlation for $V84(D \leq 20\ Mpc)$. 154
A.36 List of $V84(D \leq 20\ Mpc)$ parameters. 155
A.37 List of $V84(D \leq 20\ Mpc)$ mass estimators-statistical parameters. 155
A.38 The Kolmogorov-Smirnov test for different mass estimators in $V84$ and its nearby fraction. 156
A.39 The Kolmogorov-Smirnov test for parameters of groups in different fractions of $V84$. 156
A.40 List of $V84$ mass corrected for the evolutionary effect and related parameters. 157
A.41 List of $V84(D \leq 20\ Mpc)$ mass corrected for the evolutionary effect and related parameters. 157
A.42 Effect of the evolutionary correction on the mass distribution for $V84$. 158
A.43 Effect of the value of Ω on the evolutionary correction for $V84$.158
A.44 List of RGH89 parameters. 159
A.45 List of RGH89 mass estimators-statistical parameters. . . . 159
A.46 Spearman correlation for $RGH89$. 160
A.47 The Kolmogorov-Smirnov test for different mass estimators in $RGH89$. 160

A.48 The Kolmogorov-Smirnov test of different velocity dispersion and virial radius estimator distributions ($RGH89$). 161
A.49 List of $RGH89$ mass corrected for the evolutionary effect and related parameters. 161
A.50 Effect of Ω on the evolutionary correction for $RGH89$. . . . 161
A.51 List of $S89$ parameters. 162
A.52 List of $S89$ mass estimators-statistical parameters. 162
A.53 Spearman correlation for $S89$. 163
A.54 The Kolmogorov-Smirnov test for group parameters distributions in different fractions of $S89$. 163
A.55 List of $S89(D \leq 20\ Mpc)$ parameters. 164
A.56 List of $S89(D \leq 20\ Mpc)$ mass estimators-statistical parameters. 164
A.57 Spearman correlation for $S89(D \leq 20\ Mpc)$. 165
A.58 The Kolmogorov-Smirnov test for mass estimators in $S89$ and the nearby fraction. 165
A.59 List of $S89$ mass corrected for the evolutionary effect and related parameters. 166
A.60 List of $S89(D \leq 20\ Mpc)$ mass corrected for the evolutionary effect and related parameters. 166
A.61 Effect of the evolutionary correction on the mass distribution for $S89$. 167
A.62 Effect of the value of Ω on the evolutionary correction. . . . 167
A.63 Summary of statistical features of the mass distributions of groups in different catalogues. 168
A.64 The Kruskal-Wallis test the set $\mathcal{C}$ of whole catalogues and within 20 Mpc from us. 168
A.65 The Kruskal-Wallis test for the set $\mathcal{C}_{f.o.f.}$ of whole catalogues and of the KS pairwise test for $GH83$ and $S89$ within 20 Mpc from us. 168
A.66 The Kolmogorov-Smirnov test for pairwise comparison between catalogues. 169
A.67 The Kolmogorov-Smirnov test for pairwise comparison between catalogues within 20 Mpc from us. 169

List of Figures

1.1 An example of friends-of-friends isodensity contours 10
1.2 An example of a dendrogram for a hierarchical clustering identification algorithm 12
1.3 Dendrogram using force hierarchy 15
1.4 The radius versus time relation. 34
1.5 The smoothed evolution curve: virial versus dynamical state. 37
1.6 The time evolution curve 38

3.1 The GH83 group coordinate maps (part 1). 55
3.2 The GH83 group coordinate maps (part 2). 56
3.3 The incompleteness function for the GH83 sample. 57
3.4 The lost fraction of luminosity and number as functions of the distance from us. 59
3.5 The estimated total numbers of group members N_g versus distance D_g for $GH83$. 60
3.6 The group luminosity versus distance for $GH83$. 61
3.7 The Kolmogorov-Smirnov test comparing the distribution of $\mathcal{M}_{Vu}$ obtained from the whole $GH83$ and $GH83(D \leq 20\ Mpc)$. 65
3.8 The unweighted virial mass versus the unweighted virial radius for the $GH83$ groups. 67
3.9 The Kolmogorov-Smirnov comparison between the virial and projected mass distributions for the $GH83$ groups. 69
3.10 The unweighted virial mass versus the corrected velocity dispersion ($GH83$). 70
3.11 The distributions of the dynamical state τ and the virial α for the $GH83$ groups. 72
3.12 The curve $\alpha(\tau)$ for the $GH83$ groups. 73
3.13 The Kolmogorov-Smirnov comparison between the observed and evolutionary corrected mass distributions of the GH83 groups. 74
3.14 Effect of the faint distant groups correction on the mass of $GH83$ groups. 78
3.15 The T87 group coordinate maps (part 1). 80
3.16 The T87 group coordinate maps (part 2). 81

3.17 The group luminosity versus distance for the $T87$ groups. . 82
3.18 The Kolmogorov-Smirnov comparison between the virial mass and the projected mass distributions for the $T87$ groups. . . 85
3.19 The Kolmogorov-Smirnov comparison between the observed and evolutionary corrected mass distributions of the $T87$ groups. 86
3.20 The distributions of the dynamical state τ and of the virial α for the $T87$ groups. 87
3.21 The curve $\alpha(\tau)$ for the $T87$ groups. 88
3.22 The B_T^0 magnitude distribution for the $T87$ galaxies. 89
3.23 The Kolmogorov-Smirnov comparison between the observed mass distribution and the distribution obtained excluding faint members of $T87$ groups. 90
3.24 The spatial distribution of the $T87(D \leq 20\ Mpc)$ groups. . 92
3.25 The Kolmogorov-Smirnov comparison between the observed mass distribution and the distribution obtained from the faint distant groups recovery procedure for $T87$. 93
3.26 The V84 group coordinate maps (part 1). 96
3.27 The V84 group coordinate maps (part 2). 97
3.28 The B_T magnitude distribution for the $V84$ galaxies. 98
3.29 The group luminosity versus distance for the $V84$ groups. . 99
3.30 The Kolmogorov-Smirnov comparison between the virial mass and the projected mass distributions of $V84$ groups. 100
3.31 The Kolmogorov-Smirnov comparison between the observed and evolutionary corrected mass distribution of the $V84$ groups. 102
3.32 The distribution of the dynamical state τ and the virial α for the $V84$ groups. 103
3.33 The curve $\alpha(\tau)$ for the $V84$ groups. 104
3.34 The RGH89 group coordinate maps (part 1). 106
3.35 The RGH89 group coordinate maps (part 2). 107
3.36 The group luminosity versus distance for the $RGH89$ catalogue. 108
3.37 The distributions of the dynamical state τ and of the virial α for the $RGH89$ groups. 110
3.38 The curve $\alpha(\tau)$ for the $RGH89$ groups. 111
3.39 The KS comparison between the observed and evolutionary corrected mass distribution of the $RGH89$ groups. 112
3.40 The Kolmogorov-Smirnov comparison between the virial and projected mass estimators for $RGH89$. 113
3.41 The S89 group coordinate maps (part 1). 114
3.42 The S89 group coordinate maps (part 2). 115
3.43 The B_T magnitude distribution of the $S89$ galaxies. 116
3.44 The group luminosity versus distance for the $S89$ catalogue. 117

3.45 The Kolmogorov-Smirnov comparison between the mass distribution of the groups of the whole $S89$ and its nearby fraction. 118
3.46 The Kolmogorov-Smirnov comparison between the distributions of the virial mass and the projected mass for the $S89$ groups. 120
3.47 The distributions of the dynamical state τ and of the virial α for the $S89$ groups. 121
3.48 The curve $\alpha(\tau)$ for the $S89$ groups. 122
3.49 The Kolmogorov-Smirnov comparison between the observed and evolutionary corrected mass distribution of the $S89$ groups. 123
3.50 The mass distribution function of all catalogues. 125
3.51 The mass distribution for groups within 20 Mpc. 127
3.52 The mass distribution for the bias-free subcatalogues. . . . 128
3.53 The velocity dispersion distribution for all catalogues. . . . 130

Acknowledgements

There are many people I have to thank for the help they have continuously given me. First I thank my supervisor Professor D.W. Sciama and Professors Giuliano Giuricin, Fabio Mardirossian and Marino Mezzetti both for their fundamental scientific support to my work and their friendly encouragement. I also thank the S.I.S.S.A. students José Acosta and Mauro Orlandini for their most valuable advice and discussion. For the same reason I thank many other people, but especially Andrea Biviano and Marisa Girardi as well as Manolis Plionis and Riccardo Valdarnini. In particular I thank Phil Cuddeford for his careful and critical reading of the manuscript and my sister Antonella for her patient correction of my English. I thank Daniela Siri for the great help she gave me during the four years I have spent as a S.I.S.S.A. student. Finally a great contribution to this work has come from the support of my wife and our families.

Abstract

Since the appearance of the widely used model proposed by Press and Schechter (1974), much theoretical work was devoted to the study of the mass function of cosmic structures. In fact, the mass function can provide constraints on the cosmological model of the large scale structure of the Universe. Groups of galaxies may represent an example of cosmic structures quite suitable for this analysis. In fact they have been observed by many authors and many catalogues of data are now available. Moreover, the estimation of the mass of each group is not too uncertain since many redshifts of group members are available in new catalogues.

The first estimate of cosmological parameters using groups of galaxies is due to Gott and Turner (1977) who used their group catalogue (Turner and Gott 1976) to estimate the index n of the power spectrum of primordial density fluctuations. Now a much richer and more accurate amount of data is available so that the estimation of the group mass function and the comparison with theoretical models can be performed on more solid observational grounds.

I consider five different group catalogues available in the literature: Geller and Huchra (1983); Tully (1987b); Vennik (1984); Ramella, Geller and Huchra (1989) and Maia, da Costa and Latham (1989). The features of each catalogue are analysed in detail and particular attention is paid to the effect of observational biases. Several mass estimators proposed in the literature are considered and the dependence of the derived mass function on the estimator used is tested. In the literature it is commonly assumed that groups have reached a stationary dynamical equilibrium so that the conditions required by the virial theorem hold. This assumption is tested for the groups of each catalogue using a general method whose main features are described. Finally the set of all five group catalogues is tested in order to determine whether they give homogeneous distributions not only for the mass but also for all the main physical parameters of galaxy groups.

The main results I obtained can be outlined in the following points:

- In each catalogue all mass estimators yield nearly the same mass distribution, so that all considered mass estimators seem to be homogeneous.

- In each catalogue the groups are likely to be in a phase characterized by strong dynamical evolution and only a small fraction of the observed groups ($\sim 10\%$) have reached the virial equilibrium; hence, I have tried to correct the mass of each group in order to account for the non-virialized dynamical state.

- The set of five catalogues analysed is not homogeneous not only with respect to the mass distribution but also with respect to the distributions of all main physical parameters of groups.

- The group catalogue property mainly responsible for the detected inhomogeneity seems to be the group identification algorithm, although other features of catalogues may play a non-negligible role.

- The analysis to groups within 20 Mpc from us is also considered in order to reduce the observational bias that seems to affect all the catalogues; the main results, concerning the inhomogeneity of catalogues, the stability against various mass estimators and the dynamical state of groups, do not change; hence, it seems that the presence of observational bias does not significantly affect the results obtained.

These results suggest the need of a new definition for groups of galaxies and consequently the introduction of a new identification algorithm that could possibly overcome the inhomogeneity shown by present catalogues. A useful tool to test new identification algorithms can be provided by numerical simulations of galaxy clustering.

The mass distribution functions that I have obtained from the various catalogues can be profitably compared with theoretical predictions (e.g. Press and Shechter, 1974) in order to extract valuable constraints on the cosmological models of the formation and development of the large scale structure of the universe.

Introduction

Recently, a great deal of attention has been paid to the mass function of cosmic structures, namely the abundance $f(\mathcal{M})$ of bound objects of cosmological scale with a given mass $\mathcal{M}$ ([1]). Some works about $f(\mathcal{M})$ concern more refined theoretical models to derive the analytical expression of $f(\mathcal{M})$ from general considerations (Lucchin, 1990a, 1990b; Colafrancesco, Lucchin and Matarrese, 1988; Peacock, 1990 and references therein). In other cases, some theoretical assumptions are tested by using numerical simulations (Efstathiou, Frenk and White, 1988; Nolthenius and White, 1987). It is possible to show (Gott and Rees, 1975) that the mass function $f(\mathcal{M})$ is linked to some cosmological parameters of great interest and can give information independent of other fundamental functions like the covariance function $\xi(r)$.

Another topic, strictly related to $f(\mathcal{M})$, is the formation and evolution of systems of galaxies (Limber, 1959; Smith, 1982; Smith, 1984; Giuricin et al. 1984; Saslaw, 1985; Evrard, 1987; Perea et al. 1990) which is of fundamental importance for the dynamical estimate of the mass of galaxy systems.

It is clear that $f(\mathcal{M})$ plays an important role both in cosmological models and astrophysics of galactic systems.

An example of cosmic structures suitable for an observational estimate of the mass distribution is given by groups of galaxies. This kind of structure is quite abundant in the universe and contributes to trace the large

[1] It is possible to define the mass function of a class of objects, by saying that the number fraction of objects with mass $\mathcal{M} \pm d\mathcal{M}$ is: $dn = f(\mathcal{M})d(\mathcal{M}/\mathcal{M}_0)$, where $\mathcal{M}_0$ is a scale factor. The mass distribution function or simply mass distribution $\mathcal{N}(\mathcal{M})$ is defined by the number fraction of objects with mass smaller than $\mathcal{M}$: $\mathcal{N}(\mathcal{M}) = \mathcal{N}_0 \int_0^{\mathcal{M}} f(\mathcal{M})d\mathcal{M}$. The mass distribution is generally normalized: $\mathcal{N}(\mathcal{M}) \in (0,1)$, and $\mathcal{N}_0$ is a normalization factor. For observational reasons it is possible to obtain a statistically reliable estimate of the mass distribution $\mathcal{N}(\mathcal{M})$ rather than of the mass function $f(\mathcal{M})$. Because of this, $\mathcal{N}(\mathcal{M})$ is the main topic of the present work rather than $f(\mathcal{M})$.

scale structure quite reliably (Geller 1988). Groups of galaxies are well observed and the uncertainty on the estimate of their main physical parameters is not too large and can be compensated by a sufficiently large number of observations. The first attempt to estimate the mass distribution of groups of galaxies is due to Gott and Turner (1977, hereafter GT77) and a lot of work on theoretical models for the mass function refers to the results of GT77 as the observational bench-mark even today. The recent accomplishment of galaxy surveys complete in magnitude and red-shift, and giving a considerable amount of information, allows us to obtain new group catalogues using procedures that fully exploit the information now available which was beyond the observational limits of GT77. The new wealth of data allows me to confront the problem of the estimate of the observational mass distribution on a rather solid and wide data base. The present work considers the groups of galaxies of five different catalogues: Geller and Huchra (1983), Vennik (1984), Tully (1987b), Maia, da Costa and Latham (1989), and Ramella, Geller and Huchra (1989). All these catalogues have different basic features and have been obtained using different procedures, assuming different search parameters. In order to evaluate and compare in a suitable way the information contained in these catalogues I considered some basic points: a) the main features of the underlying galaxy sample for each group catalogue, namely the completeness, depth, extension in solid angle, presence of corrections for absorption and/or systemic motions; b) the algorithm adopted to compile the group catalogue and the basic parameters that characterize the resulting list of groups; c) the estimate of basic physical properties of groups, in particular several estimators quoted in the literature are considered for the mass, stressing the hypotheses that support the derivation of the estimators, the effect of incompleteness and observational biases.

The relevance of the group definition and of the consequent identification algorithm was discussed also by Nolthenius and White (1987) on the basis of numerical simulations and comparing the results with the C.f.A. survey groups (Geller and Huchra 1983; Huchra and Geller 1982). Their results are compared with what I obtained in the last chapter of the present work.

The structure of the present thesis follows the points outlined above. The first chapter describes in general and shortly the main features of the galaxy samples, the group catalogues based on those samples and the identification algorithms used to produce them. A large part of the first chapter is dedicated to the description of the estimate of physical parameters of groups on the basis of the available data. In particular the derivation of the mass estimator is discussed and the basic assumptions are stressed. The second chapter lists the detailed features of the group catalogues used in the present work. The third chapter reports the analysis of the data for

each catalogue. The estimate of the mass distribution is then described. Particular attention is paid to the dynamical state of groups and to the importance of the observational bias for the main conclusions. Finally, the mass distributions of different catalogues are compared in order to test the homogeneity of catalogues. The probable future developments of the work are also indicated.

Chapter 1

From observations to an estimate of physical parameters

Abstract

The main features of a catalogue of galaxy groups and of the underlying sample of galaxies are described and analysed. Particular attention is paid to the procedure adopted in order to obtain the group catalogue, and to the estimation of basic physical parameters of groups as well as to the hypotheses underlying their derivation.

1.1 Introduction

In this chapter I describe the information that can be obtained from the groups of galaxies belonging to a catalogue and what are the main features of the catalogue that influence such information. To this aim the main point to be discussed concerns the characteristics (completeness, depth, magnitude system, etc.) of the sample of galaxies, the identification algorithm that produces the group catalogue, the effect of observational biases and the hypotheses underlying the estimation of the physical parameters of groups. In particular I focus on the dynamical state of groups, which is of fundamental relevance for estimating their mass.

1.2 Samples of galaxies

From the point of view of the statistical analysis of group properties there are some characteristics of the sample, which the group catalogue is

derived from, that deserve careful attention. Some of the more important characteristics are described below.

System of magnitudes In order to compute parameters such as the total luminosity for each group, information on the luminosity of each group member is required. To compare parameters which have been obtained from different samples of galaxies, it is necessary to check if the magnitude systems used in both samples are the same. Usually the magnitudes of the galaxies are given in the $B(0)$ system of Zwicky as in Huchra and Geller (1982), Geller and Huchra (1983), Ramella, Huchra and Geller (1989) (hereafter HG82, GH83, RGH89 respectively), but other authors use the total blue magnitude system B_T, (in de Vaucouleurs et al. 1976; Vennik 1984; Tully 1987a). It is possible to assume that $B(0)$ and B_T^0 are related approximately by:

$$B_T \sim B(0) - 0.26 \tag{1.1}$$

(Felten 1985), and therefore the confusion between these two different magnitude systems can introduce systematic errors.

Absorption There is more than one source of absorption and weakening of galactic magnitudes: one is the absorption within the galaxy, indicated by $A_B^{i=0}$ that one would observe if the galaxy were seen face-on ($i = 0$). Generally $A_B^{i=0}$ depends upon the inclination i of the galaxy and for elliptical and $S0$ galaxies it is assumed to be zero. Another source of absorption is due to our Galaxy, A_B^b, mainly based on measurements of galactic HI column densities along the line of sight, which mainly depends on the galactic latitude b. The absorption affects the magnitude in the following way:

$$B_T^{b,i} = B_T - A_B^b - A_B^{i=0} \tag{1.2}$$

(Tully 1987a), so the correction for absorption can introduce systematic differences in the magnitude of galaxies belonging to different samples.

Velocity correction Generally the velocity (in km/s) of each galaxy is corrected for the infall motion towards the centre of the Virgo cluster using the relation:

$$V_{corr.} = V_{in}[\sin(\delta)\sin(\delta_V) + \cos(\delta)\cos(\delta_V)\cos(\alpha - \alpha_V)] \tag{1.3}$$

where α_V and δ_V are the coordinates of the centre of the Virgo cluster ($\alpha_V = 12^h27'.8$ and $\delta_V = 10°33'$) and V_{in} is the infall velocity (assumed to be $V_{in} \sim 300Km/s$) (HG82, GH83, Tully 1987a, RGH89).

Coordinate range A sample of galaxies occupies a limited portion of the whole sky solid angle ($= 4\pi$) and a limited range of red-shifts (V). This fact is due to observational problems. In any case a sample gives an image of a particular region of physical space and in order to compare the behaviour of galaxies in different samples, occupying different regions of space, one should either suppose that the physical conditions in the two regions are the same or restrict the comparison to the region shared by both samples. In other words, if one detects a significantly different behaviour for two samples of galaxies occupying two different regions of the sky, one should not forget the possibility that in different regions of space the evolutionary history of galaxies and structures formed by galaxies might be influenced by different present and initial environmental conditions[1].

Completeness This is a rather important concept. In the literature we can generally find magnitude complete samples of galaxies with a completeness limit of, say, m_c (apparent value). This means that within the coordinate limits of the sample, all the galaxies appearing with a magnitude $m \leq m_c$ are detected and listed in the sample (i.e., none is missing). This "fact" allows for certain considerations such as the application of correction procedures and statistical techniques that would otherwise be meaningless.

Other samples are complete in apparent diameter, containing all the galaxies with a larger size than a fixed limit. Although a significant correlation exists between the absolute luminosity and the absolute diameter of galaxies (Giuricin et al., 1989; Girardi et al., 1990) the completeness in apparent diameter is not easily converted to a magnitude completeness for that sample. This is due to the spread in distance of galaxies.

Further parameters In some cases it is possible to have additional information about those galaxies for which we have particularly detailed observations. One of the most useful parameters we would like to know is the total mass of each galaxy. In the *Nearby Galaxy Catalog* due to Tully (1987a), the total mass of the galaxies is listed when available, and it is estimated, on the basis of the Keplerian formula, from the rotation velocity and the dimensions of the system. In other cases, the mass of neutral hydrogen within the galaxy is given, computed from the HI flux and its distance. The value of each galaxy mass is particularly important for computing an estimate of the total energy of the group.

[1]This is mainly due to the fact that we presently do not know if our samples are fair representations of the large scale universe (Geller 1988).

The linear diameter (in Kpc) may also be listed and may be obtained from the angular diameter of a given isophote, generally at $25 Bmag./arcsec^2$, and the distance of the galaxy. The size of the galaxy is needed if we want to compare it with the size of the whole group in order to obtain an indication of the collision frequency between group members.
In some cases it is possible to have the corrected color indices $(B-V)_0^T$ and $(U-B)_0^T$.

We should bear all these points in mind when we compare results obtained from different samples of galaxies. Now we will see which parameters characterize a catalogue of groups of galaxies.

1.3 Catalogues of groups of galaxies

In order to obtain a catalogue of groups, we must solve two problems. First we need a definition for a group of galaxies and, second, we need an algorithm that identifies all the sets of galaxies satisfying our definition of group and that are present in our sample.

A first definition of a group of galaxies is due to de Vaucouleurs (1975), which is a system of galaxies physically and dynamically associated. A later definition (HG82) calls "group" a collection of galaxies whose number density enhancement exceeds that of the background by a given factor. In this way one can define a whole set of group catalogues, on the basis of the same sample of galaxies, label each catalogue by a critical density contrast, and then study the relation between the group properties and the catalogue parameters.

The group identification algorithm (GIA) is a procedure that decides whether a galaxy is member of a group or not. The correct definition of a GIA is non trivial and the first approach to this problem dates back to de Vaucouleurs (1975), Sandage and Tamman (1975) and Sandage (1975). The first GIA were based on a subjective criterion. The author of the group catalogue compiled the member list on the basis of similarity of redshifts, magnitudes, morphology and positions among the available galaxies he had. Catalogues compiled in this way have been used as a reference for all the later improvements of more automatic and objective algorithms. The subsequent algorithms were in fairly good agreement with the first (more subjective) ones and the improvements mainly concerned a more effective control of the biases due both to the galaxy sample and to the algorithm itself.

A first automatic algorithm called *observer blind* was introduced by Turner and Gott (1976). It worked on a two-dimensional space and identified groups as density enhancements on the surface of the sky, since at that

time no sample of galaxies was complete in red-shift space. The main drawback of this algorithm was its inability to take into account the distance of the galaxies and groups.

The compilation of samples of galaxies with known red-shifts made it possible to introduce algorithms working on a quasi-three-dimensional space. I will illustrate the main features of two different algorithms of this kind. Let us consider first of all which are the properties that a GIA should have in order to produce a catalogue of groups suitable for a statistical analysis:

1. It should depend on a small number of parameters, and the resulting catalogue of groups should not be very sensitive to the exact value of these parameters.

2. It should be objective in the sense that membership criteria based on human judgement should be avoided.

3. It should be suitable to the analysis of selection effects.

4. It should produce a catalogue of groups independent of the order in which it processes galaxies.

5. Finally, it should be easy to apply to a computer code.

We now briefly discuss two different GIAs satisfying the above requirements.

1.3.1 The *friends-of-friends* algorithm

A general method to find isodensity contours for the galaxy distribution (called *friends of friends*) is described and adopted by HG82, GH83, S89 and RGH89. It was run by these authors on magnitude limited samples of galaxies. The procedure is in principle very simple. It is essentially a percolation-type algorithm[2], but instead of having only one three-dimensional linking cutoff, the nature of the quasi-three-dimensional space of the observed galaxies suggested the introduction of two linking cutoffs (D_L and V_L) opportunely scaled with distance.

The algorithm begins with a galaxy not yet assigned to a group and search around it for a companion, in the quasi-three-dimensional space

[2]Suppose you have a three-dimensional distribution of points, the percolation algorithm isolates sets or *clusters* of points whose members have the nearest neighbour closer than a cutoff distance called the *percolation distance*. A good description of percolation theory is due to Stauffer (1985).

(α, δ, V), satisfying the relations:

$$D_{12} = 2 \sin\left(\frac{\theta_{12}}{2}\right) \cdot \frac{V}{H_0} \leq D_L(V_1, V_2, m_1, m_2) \tag{1.4}$$

where

$$V = (V_1 + V_2)/2 \tag{1.5}$$

and

$$V_{12} = \mid V_1 - V_2 \mid \leq V_L(V_1, V_2, m_1, m_2) \tag{1.6}$$

where V_1 and V_2 refer to the red-shifts of the galaxy and its companion, m_1 and m_2 are their apparent magnitudes and θ_{12} is the angular separation between the galaxies. In the case that no companion galaxy is found to satisfy these relations, this is entered in the list of *isolated* galaxies, while all the companions found are considered as members of the group. The process then starts again with another galaxy until no further members are found.

In this way the output of the GIA is obviously dependent on the choice of D_L and V_L. The most naive possibility is to take both these quantities constant. This allows us to take into account the fact that the projected angular separation between galaxies changes with distance, but it ignores all other selection effects. It is easy to understand that at large distances the galaxies are undersampled because of the limit in magnitude: the fainter galaxies are missed. In order to account for this effect, HG82 assumed that the galaxy luminosity function $\phi(L)$[3] is independent of position and distance[4] and that at large distances only the faintest galaxies are missed. In this case they take:

$$D_L = D_0 \cdot \left[\frac{\int_{-\infty}^{M_{12}} \phi(M)dM}{\int_{-\infty}^{M_{lim}} \phi(M)dM}\right]^{-1/3} \tag{1.7}$$

where

$$M_{lim} = m_c - 25 - 5 \log\left(\frac{V_F}{H_0}\right) \tag{1.8}$$

and

$$M_{12} = m_c - 25 - 5 \log\left(\frac{V}{H_0}\right) \tag{1.9}$$

where m_c indicates the completeness limit magnitude of the galaxy sample and D_0 is the projected separation in Mpc chosen at some fiducial red-shift V_F. In this way the volume searched by the algorithm is weighted

[3]The number of galaxies with a luminosity between L and $L + dL$ per unit volume (Mpc^{-3}).

[4]In a recent work Binggeli et al. (1988) show that there are good reasons to believe the opposite.

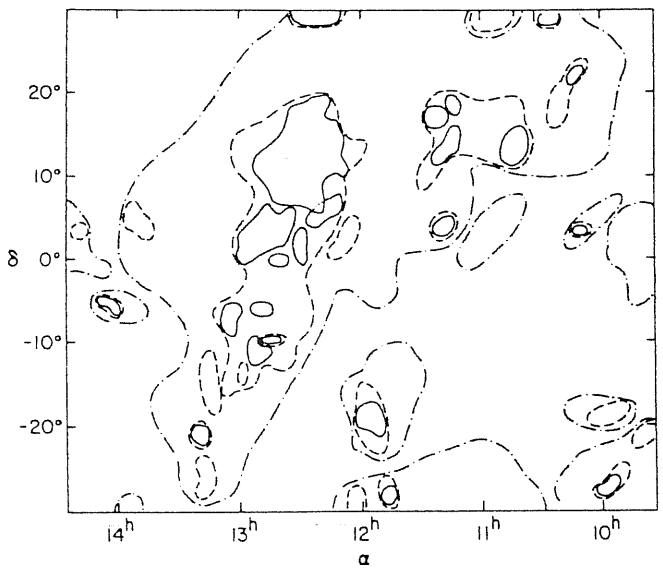

Figure 1.1: An example of friends-of-friends isodensity contours. The dashed-dotted line traces the contour for a density enhancement factor of 2, while the dashed line corresponds to a factor of 20 and the solid line to a factor of 100, (HG82).

by the number density of galaxies that could be observed in a magnitude limited sample taken at the distance V/H_0. Then the isodensity contour (see fig. 1.1) surrounding the group represents a fixed number density excess relative to the mean density of the sample:

$$\frac{\delta\rho_N}{\rho_N} = \frac{3}{4\pi D_0^3}\left[\int_{-\infty}^{M_{lim}} \phi(M)dM\right]^{-1} - 1. \tag{1.10}$$

The limiting velocity is scaled in the same way as D_L:

$$V_L = V_0 \cdot \left[\frac{\int_{-\infty}^{M_{12}} \phi(M)dM}{\int_{-\infty}^{M_{lim}} \phi(M)dM}\right]^{-1/3}. \tag{1.11}$$

Analysing this algorithm, HG82 concluded that it is commutative[5] and produced a unique group catalogue for any choice of selection parameters (D_0 and V_0) and galaxy sample. They then considered a grid of values of selection parameters and chose the value that led to the most stable group catalogue.

In conclusion, we can say that the HG82 algorithm can be characterized by essentially two parameters: $\delta\rho_N/\rho_N$ and V_0. For example, the GH83

[5]If galaxy 1 finds as companion galaxy 2, then galaxy 2 finds galaxy 1.

group catalogue is produced by the *friends of friends* GIA with $\delta\rho_N/\rho_N = 20$ and $V_0 = 600 Km/s$.

Although this kind of GIA satisfies all the requirements listed above, it is still affected by some problems. The contamination by *interlopers*[6] is not completely eliminated. The consequence of this fact is that the estimate of dynamical quantities can be seriously biased towards higher values. Mezzetti et al. (1985) and Giuricin et al. (1986) tried to evaluate the fraction of interlopers in the GH83 group catalogue by assuming that the galaxies were uniformly and non uniformly distributed in the sampled universe. They found that the expected fraction of interlopers is a few per cent on average. A general way to analyse this problem is to use a code of numerical simulation of galaxy clustering and then to construct an artificial group catalogue obtained with the same GIA used in the real data case. So it is possible to study the properties of groups obtained with such a GIA and all the biases relative to the observational procedures. This kind of analysis was performed by Nolthenius and White (1987). They compared the properties of the HG82 and GH83 groups with those of an artificial catalogue obtained by applying the same GIA on an N-body simulation of galaxy clustering in a universe dominated by cold dark matter (Davis et al. 1985). The conclusion they reached suggests (*i*) that the uncertainty in galaxy positions and red-shifts causes a loss of information independent of the GIA, (*ii*) that the group properties can depend very strongly on the selection criterion (GIA), and (*iii*) that the contamination by interlopers may be severe in small groups. A different kind of simulation performed by RGH89 led to the conclusion that $\sim 30\%$ of the groups with less than 5 members were artifacts of the GIA.

Another drawback of this GIA comes from its tendency to be insensitive to extended low-density contrast groups and to the presence of substructures within single groups.

1.3.2 The Three-dimensional hierarchical clustering membership criterion

Materne (1978) proposed a different kind of GIA: a technique called *three-dimensional hierarchical clustering*. The method was introduced mainly to determine the cluster structure of nearby galaxies.

Let us indicate the units of our sample by u_i and a group[7] by $\{u_1, u_2, \cdots, u_n\}$, with a total of m units ($n \leq m$), so that the method develops

[6]Galaxies that are considered as members of a group only because of an accidental projection effect, without being actually bounded to the group.

[7]Materne in his paper used only the term *cluster* meaning a set of merged units, stressing that his method made no difference between clusters and groups. Here I use the term groups, since I am not working with any cluster.

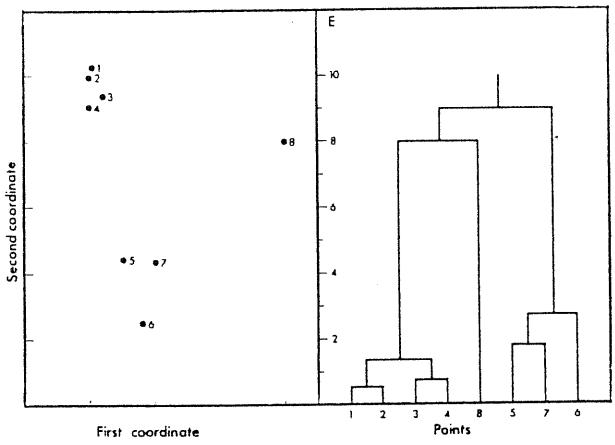

Figure 1.2: An example of a dendrogram for a hierarchical clustering identification algorithm. Left panel: a two dimensional distribution of points. Right panel: how the single units merge to form the hierarchy according to criterion E (Materne 1978).

the hierarchy proceeding through the following points:

1. We start with each separate unit forming a group so that the catalogue G^0 is given by:
$$G^0 = (\{u_1\}, \cdots, \{u_m\}). \tag{1.12}$$

2. At each intermediate step of the process, the couple of units or groups that optimizes a given parameter (for example the mutual distance) is merged and forms a separate group.

3. At the final step (after $n-1$ mergers) we will have all the units merged to only one group, and the catalogue is:
$$G^{n-1} = (\{u_1, u_2, \cdots, u_m\}). \tag{1.13}$$

In order to show how this works, we consider a simple example. Suppose we have a two-dimensional sample of eight units ($m = 8$): $u_1, \cdots, u_8$. Fig. 1.2 shows the map of the units and, on the right side, the process of merging with the resulting hierarchy. This kind of graph is called a *dendrogram*. Suppose also that we have defined a function E of the available coordinates of each pair of units. We call E the *merging criterion* in the sense that the pair having the smallest E is merged to form a single group and a horizontal bar, joining the centres of the two previously separate units in the dendrogram, indicates the value of E at which the merging

occurs. On the ordinate axis is the merging criterion function E. The first units that merge into a group are $\{1\}$ and $\{2\}$, next $\{3\}$ and $\{4\}$, then the two groups just formed $\{1,2\}$ and $\{3,4\}$. Later the units $\{5\}$, $\{7\}$ and $\{6\}$ merge to an independent group. It is possible to notice that in the hierarchy driven by E, the group $\{1,2,3,4\}$ is more *compact* than the group $\{5,7,6\}$, because it is formed at lower values of E. Finally at a high value of E the two groups and the separate unit $\{8\}$ merge. If our units represent galaxies in the sky, we can indicate the unit $\{8\}$ as a *field* galaxy. The limiting value E_0, where the merging process stops and below which one accepts the groups as real, has to be found by an inspection of the whole dendrogram. From fig. 1.2 it is clear that we can choose E_0 quite freely in the range $3.5 < E_0 < 8$. It is also clear that the value of E_0 defines the limits of what one calls a group of galaxies. As an example, we can say that for the catalogue of Turner and Gott (1976) the merging criterion function E is the surface density enhancement and $E_0 = 10^{2/3}$.

It is not difficult to see that the choice of E is not unique. As an example one can think that the units forming a real group are those found at the least distance one from another, hence the merging criterion can be based on the mutual distance between the centroids of the units or groups. But this choice of E implies the possibility that, as a consequence of a merging, the minimum distance E between two groups decreases: it is said that a *reversal* occurs. In this case the hierarchy has no meaningful interpretation. Another choice is based on the idea that the real group members probably share a coherent motion and so the position and velocity dispersions within the groups is less than in the field. In this case E is taken to be the velocity dispersion of all the units and groups in the sample. At each step the pair of units that shows the smallest increase in E is merged. This process is called the *Ward criterion*. Materne (1978) applied this criterion to test his method to a sample of galaxies in the Leo region, obtaining quite good results: he detected five different clusters of galaxies which seemed to be physical objects as a result of four independent tests. Tully (1980) has claimed that the Ward criterion produces groups biased towards small sizes. He considered a sample of 36 galaxies in the region of $NGC1023$ ($l = 144°$, $b = -20°$), then applying the above procedure he compared the hierarchies obtained from two different merging criteria. The first method takes for E the centroid distance, weighting the positions of the units with the luminosity. The resulting hierarchy was dependent on the assumption that the luminosity equals the mass of the units and on the coupling between the projected and line of sight distances. Tully (1980) suggests that the centroid method is quite unphysical. The second method he adopted considered the gravitational force between units as a more physical parameter. In fact the method merges the pairs that

minimize the quantity:

$$\frac{1}{F_{tj}} \propto \frac{r_{tj}^2}{L_{max}} \tag{1.14}$$

where L_{max} is the larger luminosity of L_t and L_j and r_{tj} is the separation between the t^{th} and the j^{th} units or groups. This method is not without its problems. Since at each merging the value of L_{max} increases, the possibility of reversals increases and the *contrast* between the groups and the field reduces because the separations are weighted with very small quantities. Nonetheless the sequence of mergers has a more physical meaning. In order to quantify the physical reality of groups, Tully took the inverse luminosity density l_{tj}:

$$\frac{1}{l_{tj}} = \frac{\frac{4}{3}\pi r_{tj}^3}{L_{max}}. \tag{1.15}$$

If ρ_c is the critical density for closure, then:

$$\rho_c = l\left(\frac{\mathcal{M}}{\mathcal{L}}\right)_c. \tag{1.16}$$

So a group is bound if its $\mathcal{M}/\mathcal{L}$ ratio is larger than the critical value. Fig. 1.3 shows the dendrogram obtained with this method. Now choosing the critical value for $\mathcal{M}/\mathcal{L}$ and cutting the dendrogram horizontally it is possible to see which groups are bound systems and which are not.

The problem of computing the three-dimensional distance between units was discussed by Materne (1978). He concluded that the usual polar coordinate system (α, δ, v) did not work. A correct procedure is to treat the values of α, δ and v as independent numbers. But the values of the redshifts v must be scaled properly in order to be compared. A possibility is to define a new coordinate $x = \chi v$ and retain χ as a free parameter. An estimate of χ may be obtained for well known clusters by comparing the velocity-direction size with the size in the sky that the cluster would have if it had a given velocity (e.g. $1000 Km/s$). However Tully (1980) used a pure Hubble flow model to evaluate the line of sight separations between units. Then, after having performed the clustering method, he analysed the effect of departures from the Hubble flow. The conclusion was that for both hierarchies he obtained that the effect of non-Hubble flows was negligible although in the case of the force hierarchy they were stronger. Materne (1979) proposed a method of assigning a probability density function for group membership by assuming a model for the distribution of the velocities and positions. In this way the problem of the separations is treated in a more general and quantitative way. Unfortunately it is dependent on the assumed model for the positions and velocities of the galaxies.

Summarizing I can say that the advantage of this method is that it offers the opportunity of recognizing the presence of substructures within

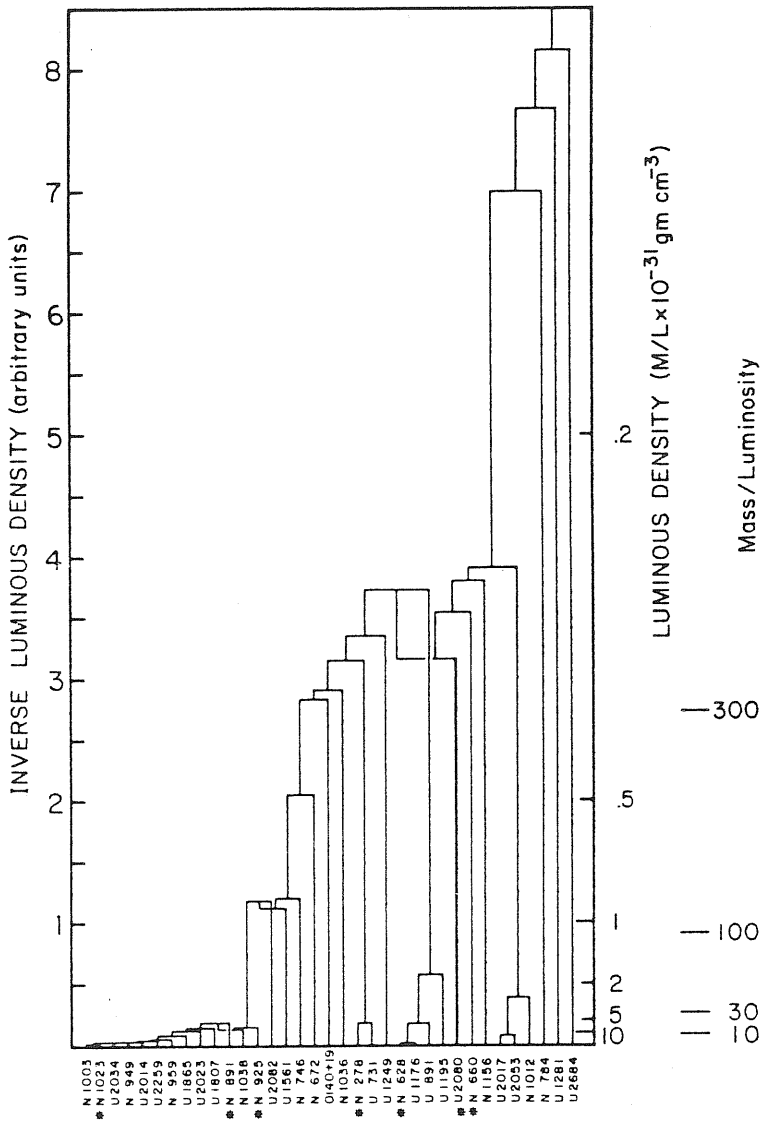

Figure 1.3: Dendrogram using force hierarchy: the sequence of mergers is plotted as a function of the inverse mass (i.e. luminosity) density (Tully 1980).

the identified groups or clusters of galaxies, and of seeing which clusters might form larger structures such as superclusters. Of course it is possible to have many different types of merging criterion function E according to the definition of the galaxy group we consider. The criterion adopted in order to merge galaxies at each step is of fundamental importance and, with a critical value defining the limit at which the merging process stops, it completely characterizes the GIA. Before applying this GIA to a sample of galaxies it is necessary to assume a calibration of the velocities so that two different sorts of coordinates (i.e. position angles and red-shifts) can be combined to give a three-dimensional distance.

I consider later two catalogues of groups obtained adopting this GIA: one is due to Tully (1987b) and the other to Vennik (1984). Both catalogues are based on different galaxy samples and adopted different merging criteria. Tully chose the luminosity density enhancement for E, while Vennik chose the number density enhancement. I will describe both catalogues in the next chapter.

1.4 The estimate of group parameters

We can consider the following quantities for each galaxy in a group catalogue: position angles α_i and δ_i, red-shift $V_i(Km/s)$, apparent magnitude m_i and its morphological type T_i (RC2), where $i = 1, \ldots, n_g$ and n_g is the number of galaxies in the group.

1.4.1 The distance

We define the **distance** of a group by:

$$D_g = \frac{\sum_{i=1}^{n_g} V_{||i}}{n_g H_0} = \frac{< V_{||i} >}{H_0} \tag{1.17}$$

It is assumed that the arithmetical mean of the projected velocities (corrected for Virgo infall) is a good estimator of the distance: the effect of peculiar motions is considered negligible[8]. The uncertainty of this quantity comes from the measurement errors on the red-shifts and H_0[9], but also from the fact that the total number of member of the group N_g is generally

[8]Some authors (see for example Davis and Peebles 1983; Lynden-Bell et al. 1988) claim that the Big Attractor has a non-negligible effect on the velocity field of the local supercluster. Such large scale streaming motions can in principle be taken into account only with models that are presently under debate.

[9]Throughout my work I assume $H_0 = 100\ Km/(s\ Mpc)$. This holds every time the H_0 dependence is not specified.

greater than n_g because the fainter galaxies in a group can be missed if the group is far enough away[10].

For groups of galaxies obtained from a magnitude complete galaxy sample, it is possible to introduce a further distance parameter: the **visibility distance** $D_g^{(v)}$. A group of galaxies contains, by definition, at least three members, otherwise it is called a binary system. Suppose that a group is observed at an average distance D_g and has n_g members each with a luminosity L_i (where $i = 1, \ldots, n_g$), and suppose also that we order the luminosities in such a way that $L_{i+1} \leq L_i$. We can imagine moving the group further and further far away by placing it at increasing values of D (distance from us). In this way the number of observable members reduces every time D reaches a value such that the luminosity corresponding to the completeness-limit magnitude (i.e., m_c) $L_c = L(D, m_c)$ reaches the value of the faintest group member $min\{L_i\}$. This is due to the fact that the number of members observed in a group, called **observed richness**, depends generally on its distance D and on m_c[11]:

$$n_g = \#_\iota[L_\iota \geq L_c(D, m_c)] = \sum_{\iota=1}^{N_g} \theta(L_\iota - L_c(D, m_c)). \tag{1.18}$$

It is then clear why in general groups are incomplete:

$$n_g \leq N_g. \tag{1.19}$$

When D is so large that L_c reaches L_3, then if we move the group to slightly larger D, it disappears from the group catalogue since it becomes a binary system. So we can define the visibility distance of the group as:

$$n_g(D_g^{(v)}) = 3. \tag{1.20}$$

The value of $D_g^{(v)}$ depends on the completeness limit m_c and on L_3.

When the value of the morphological type T is available for each member galaxy, it is possible to define the **relative composition** of the group $C(E, S0, S, IP)$ as the fraction of galaxies with T in the range of spirals

[10]Because of this fact I introduce two different kinds of indices: when summing the observed quantities I use latin indices as i, j, k ranging from 1 to n_g; when I sum in the ideal situation in which all the N_g members of the group are observed, I use greek indices as ι, κ, λ that range from 1 to N_g.

[11]Here $\theta(x)$ is the step function defined by:

$$\theta(x) = \begin{cases} 1 & \text{if } x \geq 0 \\ 0 & \text{if } x < 0 \end{cases}$$

while the function $\#_i[P(i)]$ for $i = 1, \ldots, N$ is defined as the number of times the statement $P(i)$ is true, consequently we have $0 \leq \#_i[P(i)] \leq N$.

S ($1 \leq T \leq 9$), lenticulars $S0$ ($-3 \leq T \leq 0$), ellipticals E ($T \leq -4$) or peculiar and/or irregular $I\&P$ ($T \geq 10$):

$$\mathcal{C}(S, S0, E, IP) = \left(\frac{n_E}{n_g}, \frac{n_{S0}}{n_g}, \frac{n_S}{n_g}, \frac{n_{IP}}{n_g}\right). \tag{1.21}$$

1.4.2 The luminosity

The **seen luminosity** L_{sg} accounts only for the galaxies we can observe from Earth:

$$L_{sg} = \sum_{i=1}^{n_g} L_i, \tag{1.22}$$

where[12]:

$$L_i = L(D_g, m_{B,i}) = 1.556 \cdot 10^{12} \cdot D_g^2 dex(-0.4 m_{B,i}). \tag{1.23}$$

The range spanned by member luminosity is bound by L_{max} and L_{min}:

$$L_{min} = min\{L_i\}, \quad L_{max} = max\{L_i\}. \tag{1.24}$$

It is possible to estimate the mass of each galaxy if we assume a suitable value for $\frac{\mathcal{M}}{\mathcal{L}}$ possibly depending on the morphological type T

$$\mathcal{M}_i = \left(\frac{\mathcal{M}}{\mathcal{L}}\right)_{T_i} \cdot L_i. \tag{1.25}$$

For example we can attribute different amounts of dark matter by using different relative values of $\frac{\mathcal{M}}{\mathcal{L}}(T)$ which depend on the morphological type T of group members in this way :

$$\begin{array}{lll} w = 1 & : & (\mathcal{M}/\mathcal{L})(E : S0 : S) = 1 : 1 : 1 \\ w = 3 & : & (\mathcal{M}/\mathcal{L})(E : S0 : S) = 3 : 3 : 1 \\ w = 5 & : & (\mathcal{M}/\mathcal{L})(E : S0 : S) = 5 : 5 : 1 \\ w = 10 & : & (\mathcal{M}/\mathcal{L})(E : S0 : S) = 10 : 10 : 1 \end{array} \tag{1.26}$$

so that we can state:

$$\mathcal{M}_i(w) = \begin{cases} w \cdot L_i & \text{if } T_i \leq 0 \\ L_i & \text{if } T_i > 0 \end{cases} \tag{1.27}$$

It often happens that the luminosity of the galaxies is unknown and so the same mass is attributed to all the galaxies by assuming:

$$\mathcal{M}_i = 1 \quad \forall i = 1, \ldots, n_g. \tag{1.28}$$

[12]Here $dex(x) \equiv 10^x$.

In the case that we are dealing with a magnitude complete sample of galaxies and m_c is the limiting completeness magnitude of the sample, we can estimate the **total luminosity** L_{Tg} of the group by adopting the expression for the galaxy luminosity (or absolute magnitude M) function, if it exists for the considered sample; here we consider the Schechter (1976) form for the galaxy luminosity function:

$$\phi(l)dl \equiv \phi_\star l^{-\alpha} \exp(-l)dl \tag{1.29}$$

with:

$$l \equiv L/L_\star. \tag{1.30}$$

The parameters $\phi_\star$, α, and $L_\star$ or $M_\star$ depend on the sample of galaxies (Binggeli et al. 1985 and references therein) even though they are often considered as universal. Now introduce the function $f(\alpha; l)$ by:

$$\phi(l)dl \equiv \phi_\star f(\alpha; l)dl. \tag{1.31}$$

It is not possible to allow l to vary from 0 to $+\infty$ and in fact this would cause the estimate of the value of the total number N_T of galaxies present within a given volume $\mathcal{V}$ to diverge:

$$N_T = \mathcal{V} \int_0^{+\infty} \phi(l)dl \rightarrow +\infty. \tag{1.32}$$

If we take a non-zero value for the lower limit for galaxy luminosity within a group, $L_{lim} \simeq 0.0066 \cdot L_\star$[13], then the value of the total luminosity due to galaxies within a group is given by:

$$L_{Tg} = \int_{l_{min}}^{+\infty} l \cdot L_\star \phi(l)dl \tag{1.33}$$

but, in a similar way we can say that the seen fraction L_{sg} of the total luminosity is:

$$L_{sg} = \int_{l_c}^{+\infty} l \cdot L_\star \phi(l)dl \tag{1.34}$$

where the lower integration limit is: $l_c = L_c/L_\star$. Using the definition of $f(\alpha; l)$, we can set:

$$L_{sg} = \phi_\star \cdot L_\star \int_{l_c}^{+\infty} l \cdot f(\alpha; l)dl, \tag{1.35}$$

[13]The exact value assumed for $L_{lim}/L_\star$ is not very relevant for the derived estimates of group properties, in fact the values $L_{lim}/L_\star = 0.176$ and 0.01 are also found in literature, but in a previous work (Mezzetti et al. 1985) we have shown that the estimate of the group parameters is not sensitive to this ratio. The quoted value of 0.0066 corresponds to the minimum observed luminosity in the Geller and Huchra (1983) group.

so that the value of the normalization parameter $\phi_\star$ is:

$$\phi_\star = \frac{L_{sg}}{L_\star \int_{l_{lim}}^{+\infty} l f(\alpha; l) dl}. \tag{1.36}$$

Finally we can express the estimate of the total group luminosity as a function of the observed group luminosity:

$$L_{Tg} = L_{sg} \cdot \frac{\int_{l_{lim}}^{+\infty} l f(\alpha; l) dl}{\int_{l_c}^{+\infty} l f(\alpha; l) dl}. \tag{1.37}$$

Similarly we can evaluate the total number of member galaxies. If the seen members amount to n_g then we can express this value as:

$$n_g = \phi_\star \int_{l_c}^{+\infty} f(\alpha; l) dl, \tag{1.38}$$

so that the total number N_g of members would be:

$$N_g = \phi_\star \int_{l_{lim}}^{+\infty} f(\alpha; l) dl = n_g \cdot \frac{\int_{l_{lim}}^{+\infty} f(\alpha; l) dl}{\int_{l_c}^{+\infty} f(\alpha; l) dl}. \tag{1.39}$$

This point deserves a little care. In fact this sort of correction can introduce some bias in the values of N_g and L_{Tg} since the total quantities depend on distance. In fact we have that $N_g \propto n_g$ and $L_{Tg} \propto L_{sg}$. At large distances the Malmquist bias is likely to play a non negligible role in increasing the average value of n_g and L_{sg}, since only the brightest galaxies are observable. This is clearly what figs. 3.5 and 3.6 show for the GH83 catalogue of groups. Hence this kind of correction is not unbiased when the distance from us is so large that the Malmquist bias is effective. In the case of GH83, this distance is probably of the order of 20 Mpc.

As a first application of the quantities defined here, we can say that the ratios λ_g and ν_g, defined by:

$$\lambda_g \equiv \frac{L_{sg}}{L_{Tg}} \tag{1.40}$$

and by:

$$\nu_g \equiv \frac{n_g}{N_g} \tag{1.41}$$

can tell us the fraction of the whole group membership or total luminosity that we can observe. This gives us an idea of the incompleteness effect in number and luminosity. Once the parameters of the luminosity function are specified, the value of λ_g and ν_g depends on the distance from us D_g as is shown in fig. 3.4. In order to obtain a reliable conclusion about the estimated dynamical parameter, it is useful to drop the groups whose values of λ_g and ν_g are too low, for example $\lambda_g \leq 0.75$ as in Giuricin et al. (1988).

1.4.3 The size of groups

There is more than one size estimator quoted in the literature. Some of these are linked to the dynamical state of the groups, others are geometrical. However some hypotheses are common to all size estimators.

If we suppose that it were possible to observe a group of galaxies from so many directions that we could reconstruct the exact positions $\vec{r}_\iota$ of all the galaxies and their velocities $\vec{v}_\iota$, at some instant, then it would not be difficult to estimate the size of the whole system. Unfortunately the true physical data are degraded by observational effects mainly due to projection, false membership, non-equilibrium and incompleteness. The extent of this loss of information is essentially unknown, but we can have an idea of it by using numerical simulations (Nolthenius and White 1987).

As far as the projection effects are concerned, we can introduce a rough correction only for the averaged values. These corrections are based on the assumption that the distribution of the positions of the member galaxies within a group is spherical, and so the inclination angles ϑ between the three dimensional vectors connecting two galaxies $\vec{r}_{ij}$ and the line of sight are randomly distributed among all the possible values. On the basis of this assumption the observed position vector $\vec{r}_{\perp,i}$ and the three dimensional vector $\vec{r}_i$ satisfy the following relations:

$$<\mid \vec{r}_{\perp i} \mid>=<\mid \vec{r}_i \mid \sin(\vartheta_i) >=< \vec{r}_i > \cdot < \sin(\vartheta_i) >= \frac{2}{\pi} <\mid \vec{r}_i \mid> . \quad (1.42)$$

Unfortunately, groups of galaxies are not very rich systems-the number of their members has a median value of 4 (GH82, Mezzetti et al. 1985), whereas the above relation between the projected and three-dimensional radii holds when the number of objects is large.

One of the first size estimators I consider is the **mean pairwise separation** R_p, defined by[14]:

$$R_p = \frac{4}{\pi} D_g \frac{\sum_{(i,j)} r_{\perp ij}}{\frac{n_g(n_g-1)}{2}} \quad (1.43)$$

with the projected distance[15] between the i^{th} and j^{th} galaxies given, in units of D_g, by

$$r_{\perp ij} = 2\tan(\phi_{ij}). \quad (1.44)$$

[14]Here I introduce a new symbol. If $f(i,j)$ is a symmetric function of two indices $i,j = 1,\ldots,N$, then $\sum_{(i,j)} f(i,j) \equiv \sum_{i=1}^{N-1} \sum_{j=i+1}^{N} f(i,j)$, so the sum symbol with two indices in brackets indicates the sum over all non equal pairs.

[15]In order to avoid unphysical singularities, a minimum value for the separation between pairs of member galaxies is assumed to be 0.05 Mpc. The resulting values of the main parameters of groups do not change significantly if we double this value.

The angle ϕ_{ij} is defined by

$$\cos(\phi_{ij}) = \sin(\delta_i)\sin(\delta_j) + \cos(\delta_i)\cos(\delta_j)\cos(\alpha_i - \alpha_j), \tag{1.45}$$

and the factor $4/\pi$ is due to projection effects in the hypotheses already discussed about the distribution of member positions. The R_p defined above is generally believed to be a good estimator of the group radius. Another estimator, linked to the potential energy of the whole group, is the **virial radius** R_V, defined by setting the potential energy U:

$$U = -G\frac{\mathcal{M}^2}{R_V} = -G\sum_{(\iota,\kappa)}\frac{\mathcal{M}_\iota \mathcal{M}_\kappa}{\mid \vec{r}_{\iota\kappa} \mid} \tag{1.46}$$

and taking projection effects into account trough the factor $\pi/2$:

$$R_V = \frac{\pi}{2} D_g \frac{\left(\sum_{i=1}^{n_g} \mathcal{M}_i\right)^2}{\sum_{(i,j)} \frac{\mathcal{M}_i \mathcal{M}_j}{r_{\perp ij}}}. \tag{1.47}$$

In case the masses are obtained by the luminosity of each galaxy as in eq. 1.25, then we say to have the **luminosity weighted virial radius** $R_V(w)$ in the following way:

$$R_V(w) = \frac{\pi}{2} D_g \frac{\left(\sum_{i=1}^{n_g} \mathcal{M}_i(w)\right)^2}{\sum_{(i,j)} \frac{\mathcal{M}_i(w) \mathcal{M}_j(w)}{r_{\perp ij}}}. \tag{1.48}$$

The values $\mathcal{M}_i(w)$ are defined by eqs. 1.27 and 1.26. In case the luminosities are not available we have:

$$R_{Vu} = \frac{\pi}{2} D_g \frac{n_g^2}{\sum_{(i,j)} \frac{1}{r_{\perp ij}}}. \tag{1.49}$$

We will call this estimator the **unweighted virial radius.** Some authors (Heisler et al. 1985) justify the assumption of eq. 1.28 by the observation that the mass and the luminosity of galaxies are poorly correlated and, performing simulations of groups of galaxies with constant masses, they found no significant difference in the behaviour of groups when they allowed the galaxies to have different masses. I must stress that Heisler et al. (1985) were only interested in the behaviour of the mass estimators for groups of galaxies-nothing was reported about the behaviour of other physical parameters. It would be very important to evaluate the error due to the assumption, in most cases probably not correct, that all the galaxies have the same mass. For example, if we suppose that on average different morphological types of galaxies have different masses, then the presence

of morphological segregation (Mezzetti et al. 1985) would imply a segregation of mass and then a systematic difference in the mass weighted and unweighted virial radius estimators. In some cases an estimate of the mass[16] of the single member galaxies is listed in catalogues (Tully 1987a). In the case that a whole group has all its members with known masses, one could see the effect of different weighting in the virial estimator of radius. Unfortunately this test has a meaning only in the case that the number of suitable groups is large enough.

Another estimator of group size was introduced by Jackson (1975): the **moment-of-inertia radius** R_I[17] defined by:

$$R_I = \left(\frac{3}{2} \frac{\sum_i \mathcal{M}_i r_{\perp i}^2}{\sum_i \mathcal{M}_i} \right)^{1/2} \tag{1.50}$$

where $r_{\perp i}$ indicates the projected distance of the i^{th} galaxy from the centre of the system: $r_{\perp i}^2 = x_i^2 + y_i^2$, and the factor 3/2 is due to the fact that, in the case of a spherically symmetric distribution of positions, $r_{\perp i}^2 = 2/3(r_i^2)$ on average. In this case we have the same weighting problem found for the virial estimator and generally the luminosities are used instead of the masses, with a constant $\mathcal{M}/\mathcal{L}$ ratio and using eq. 1.25. The result is dependent on the position of the centre of the group and if we miss some faint galaxies the computed R_I will be wrong by an unknown amount. Only in the case that we know the masses of all the member galaxies and we take as the origin of the r_i the centre of mass of the group can we guess that the galaxies we miss are so faint that their masses and positions will not too greatly affect the assumed position of the centre of mass.

Finally I want to stress that no size estimator is corrected for the incompleteness effect. Only the observed members are taken into account.

1.4.4 The velocity dispersion

As we have seen, it is possible to define a quantity (the virial radius R_V) which is in some way related to the potential energy of the group. We would like to have another quantity related to the total kinetic energy T of the group. If $\vec{v}_\iota$ is the velocity of the ι^{th} galaxy relative to the rest frame of the group, we can define V^2 by:

$$T = \frac{1}{2}\mathcal{M}V^2 = \frac{1}{2}\sum_{\iota=1}^{N_g} \mathcal{M}_\iota \mid \vec{v}_\iota \mid^2 \tag{1.51}$$

[16]The mass reported by Tully was obtained on the basis of the Keplerian formula when the rotation velocity and dimensions of the galaxy were available.

[17]It is possible to extend the definition of R_I for different values of the weight w as in the case of the virial radius $R_V(w)$, but R_I is not used in this work so I prefer not to increase the number of estimators without a real need of them.

so that:

$$V^2 = \frac{\sum_\iota \mathcal{M}_\iota v_\iota^2}{\sum_\iota \mathcal{M}_\iota} = < v^2 >_{\mathcal{M}} . \tag{1.52}$$

This quantity is the **mass weighted velocity dispersion** of the group, in fact it is the mass-weighted mean square of the velocities of the group galaxies relative to the centre of mass of the group. The main drawback of this quantity is that we cannot directly measure it. In fact we only know the radial components of the velocities $V_{||i}$, while the three-dimensional velocity dispersion V^2 can only be estimated by assuming a model for the velocity distribution of the galaxies. If this distribution is isotropic, then the dispersion of each Cartesian component is the same and equal to $V^2/3$. Generally the masses can be inferred by eq. 1.25. Again assuming eq. 1.28 to hold:

$$V_{obs}^2 = 3\frac{\sum_{i=1}^{n_g}(V_{||i} - V_{||g})^2}{n_g} = 3var(V_{||}) \tag{1.53}$$

which is the estimated three-dimensional number-weighted velocity dispersion, which I will refer to as the **observed velocity dispersion.** In order to be closer to the ideal quantity defined in eq. 1.52 it is worth defining a **luminosity-weighted observed velocity dispersion** as in the case of the virial radius:

$$V_{g,obs}^2(w) = 3\frac{\sum_{i=1}^{n_g} \mathcal{M}_i(w)[V_{||i} - (\sum_i \mathcal{M}_i(w)V_{||i})/(\sum_i \mathcal{M}_i(w))]^2}{\sum_i \mathcal{M}_i(w)}. \tag{1.54}$$

In the case that all the member galaxies have the same mass, the unweighted velocity dispersion $V_{n,obs}^2$ is defined similarly to $V_{g,obs}^2$. Apart from the projection effect, we must correct the velocity dispersion for other biases and effects. In fact, since the velocity dispersion is a quadratic function of the velocities, a bias is introduced by observational errors. If we suppose that the observed velocity V_i, the true velocity W_i and the error ϵ_i are related by:

$$V_i = W_i + \epsilon_i \tag{1.55}$$

and assume that the variable ϵ_i is gaussian, then:

$$E[\epsilon_i] = 0 , \qquad E[\epsilon_i^2] = \Delta_i^2 \tag{1.56}$$

where E[x] is the expectation value function. In the case that the values of ϵ_i and W_i are not correlated (i.e., $E[W_i\epsilon_i] = 0$), we can write:

$$E[V_i^2] = E[W_i^2] + \Delta_i^2 \tag{1.57}$$

so the observed velocity dispersion turns out to be systematically larger than the unbiased estimate (see Giuricin et al. 1982 for a complete discussion). The amount of the correction for observational errors is:

$$\Delta V^2(w) = 3\left[\sum_i \mathcal{M}_i(w)\delta_i^2 - \frac{\sum_i \mathcal{M}_i^2(w)\delta_i^2}{\sum_i \mathcal{M}_i(w)}\right] \tag{1.58}$$

and so the corrected mass-weighted velocity dispersion is:

$$V_g^2(w) = V_{g,obs}^2 - \Delta V^2(w). \tag{1.59}$$

Similarly, for equal mass members, we can obtain:

$$V_n^2 = V_{n,obs}^2 - \Delta V^2. \tag{1.60}$$

In the case that the observational errors are so large that the values of V_n^2 and V_g^2 are negative, the group is rejected. Another point we must consider, although it is relevant only for quite distant ($D_g \geq 30 Mpc$) groups, is the relation linking the velocity v_i of the i^{th} galaxy relative to the rest frame of the group and the velocity V_i of the same galaxy relative to us (Danese et al. 1979):

$$v_i = \frac{V_i - < V >}{1 + \frac{<V>}{c}} \tag{1.61}$$

where c is the speed of light and $< V >= \sum_i V_i / n_g$.

Finally one should not neglect the fact that generally some of the group members are not observed because of their low apparent magnitude, so that the number of observed members is always less than or equal to the true number (eq. 1.19). We have already discussed a possible method to estimate N_g in this way it is possible to introduce a correction to account for the incompleteness of the sampling: $(N_g - 1)n_g/[(n_g - 1)N_g]$ (Kendall and Stewart 1977, vol. 1, p. 319).

The expression of the estimator of the velocity dispersion, corrected for the effects of projection, incompleteness, observational errors and group global motion is:

$$\sigma_v^2 = 3\frac{\sum_{\iota=1}^{N_g} v_\iota^2}{N_g} \approx \frac{N_g - 1}{N_g}\frac{n_g}{n_g - 1}\frac{3}{(1+ < V > /c)^2}\frac{1}{n_g}\left[\sum_{i=1}^{n_g}(V_i - < V >)^2 - V_{sv}^2\right] \tag{1.62}$$

with:

$$V_{sv}^2 = (n_g - 1) < \Delta^2 >= \frac{n_g - 1}{n_g}\sum_{i=1}^{n_g}\Delta_i^2. \tag{1.63}$$

This is the **corrected velocity dispersion** in the case that the mass $\mathcal{M}_j$ and the velocity v_j of the group galaxies are not correlated, so that we can say that the group is in *velocity equipartition.*

Usually, one can justify the assumption of velocity equipartition by claiming that the groups are dynamically young systems in the sense that two-body relaxation has not had time to thermalize the energy spectrum, so that there is not yet a correlation between the velocity and the mass of group members. This problem has also been studied in previous work (Giuricin et al. 1982 and references therein), which has confirmed the reliability of these hypotheses on the basis of the available samples.

It would be simple to solve this problem if we knew the total velocity and the mass of each galaxy within a group. Apart from the unknown amount of peculiar velocity of the whole group discussed in a previous point, the knowledge of member velocity is affected by observational errors and projection effects. As a consequence, we can evaluate the total velocity (tangential + radial) only on the basis of some model of the member velocity distribution within groups. The simplest assumption is to adopt a Gaussian isotropic distribution, but in this case we would admit that the process of violent relaxation (Lynden-Bell 1967) has strongly modified the original phase space distribution leading the system to an equilibrium configuration that can be described by a superposition of many Gaussian distributions. Moreover two-body interactions cause the mass and velocity of members to be (anti-) correlated. This would mean that our estimator of the characteristic velocity within a group is wrong.

We can test our assumptions about the dynamical condition of groups of galaxies only by numerical simulations; an approach surely not without its own problems (Smith, 1977). The best simulation should be able to describe at least the local supercluster evolving from different initial conditions and for different models of the universe ($\Omega = 1, \Omega = 0.1$, cold, hot or warm dark matter) in such a way that a point-like object in the simulation is representative of a galaxy with a given mass. In this way we would be able to study the complete evolutionary history of groups also in relation with their environment. Unfortunately modern techniques are not yet able to reach such a resolution. In fact the numerical simulations now available either represent the evolution of an *isolated* group of galaxies for small length scales or, for large length scales, they simulate the universe on a scale so large that details of galaxy groups are not attainable.

From the observational point of view, we cannot verify the lack of correlation between the galaxy velocity and mass within a group since we do not know the values of masses and total three-dimensional velocities of each group member. Assuming a total velocity on the basis of a model distribution will bring us back to the problem of the dynamical state of groups.

1.4.5 The time scale

The introduction of a time scale for a group of galaxies is required in order to check one of the basic assumptions of the usual analysis of group properties. In fact one has to assume that the group is a bound system of galaxies and, to test this hypothesis, it is possible to compare the time

scale of internal dynamical evolution with the age of the universe[18]. Let me introduce some definitions. As an estimate of group time scale one generally adopts the ratio between the size of the group and a characteristic velocity of the galaxies in the group. This ratio is called crossing time. Remembering eqs. 1.47 and 1.52, we can define the (unweighted) **virial crossing time** $\mathcal{T}_V$ as:

$$\mathcal{T}_V \equiv \left(\frac{3}{5}\right)^{3/2} \frac{R_{Vu}}{\sigma_v} \tag{1.64}$$

where the factor $(3/5)^{3/2}$ is due to the first definition of this quantity (Gott and Turner 1977). Of course the virial crossing time is affected by all the problems discussed for R_V and V.

An alternative to $\mathcal{T}_V$ is given by the **linear crossing time** $\mathcal{T}_L$, defined as the ratio between the mean pairwise separation and the mean pairwise difference of velocities between group galaxies:

$$\mathcal{T}_L \equiv \frac{2}{\pi} \frac{R_p}{\frac{\sum_{(i,j)} |V_{\parallel i} - V_{\parallel j}|}{n_g(n_g-1)/2}}. \tag{1.65}$$

Here it is implicitly assumed that the mean pairwise difference between galaxy velocities is a good estimator of what we call the characteristic velocity of group galaxies. In fact it seems that this estimator of the crossing time is less affected by interlopers than the virial one (Faber and Gallagher 1979, Rood and Dickel 1978). A second advantage of $\mathcal{T}_L$ is due to its geometrical nature[19] in the sense that it is not dependent on the dynamics of the group.

In order to overcome biases connected with the virial estimator, Jackson (1975) introduced the **moment-of-inertia crossing time** $\mathcal{T}_I$:

$$\mathcal{T}_I \equiv \frac{R_I}{V}, \tag{1.66}$$

(see eq. 1.50) which is more suitable for the analysis of groups in relation to the Hubble flow in order to have some indication of whether they are bound or not.

1.4.6 The mass

This is the most important parameter for this work and I analyse it in more details than the other parameters. The principal aim of my discussion is to clarify the relation existing between our estimate of the mass and

[18]It is more correct to use the time elapsed since the formation of the galaxies which now appear within the group instead of the age of the universe.

[19]If we accept the hypothesis of spherical symmetry of groups.

the true physical mass of the group. Two factors play a relevant role in this analysis: the observations of the group members and the simplifying assumptions we have to accept in order to apply the estimators proposed by the theory. From this point of view I think it is convenient to distinguish two main families of mass estimators: the virial estimators[20] based on the application of the virial theorem, and the non-virial family containing every other kind of mass estimator. I discuss the two families separately and then compare them on the basis of the observed data.

1.4.7 The virial estimators

First of all, let me give a short derivation of the (scalar) virial theorem. Suppose we have a system of N particles with masses $\mathcal{M}_\iota$, $\iota = 1, \ldots, N$, positions $\vec{r}_\iota$ and velocities $\vec{v}_\iota$, evolving with a given potential energy U which is a homogeneous function of the coordinates $\vec{r}_\iota = (x_\iota, y_\iota, z_\iota)$ and that the motion is bound in a limited region of space. In this case it exists a very simple relation between the time-averaged values of the kinetic and potential energy of the system. This relation is called the (scalar) virial theorem. Note that kinetic energy T is a quadratic function of the velocities:

$$2T = \sum_\iota \frac{\partial T}{\partial \vec{v}_\iota} \cdot \vec{v}_\iota \tag{1.67}$$

with:

$$\frac{\partial}{\partial \vec{v}} \equiv \nabla_{\vec{v}} = \left(\frac{\partial}{\partial v_x}, \frac{\partial}{\partial v_y}, \frac{\partial}{\partial v_z}\right). \tag{1.68}$$

Introducing the impulses $\vec{p}_\iota = \nabla_{\vec{v}_\iota} T$, we have:

$$2T = \sum_\iota \vec{p}_\iota \cdot \vec{v}_\iota = \frac{d}{dt}\left(\sum_\iota \vec{p}_\iota \cdot \vec{v}_\iota\right) - \sum_\iota \vec{r}_\iota \cdot \dot{\vec{p}}_\iota \tag{1.69}$$

We define the time averaged value of a function $f(t)$ by:

$$< f >_t = \lim_{\tau \to +\infty} \frac{1}{\tau} \int_0^\tau f(t) dt. \tag{1.70}$$

It is easy to see that in the case that the function $f(t)$ has a primitive function $F(t)$ (i.e., $f(t) = \frac{dF(t)}{dt}$) then:

$$< f >_t = \lim_{\tau \to +\infty} \frac{F(\tau) - F(0)}{\tau}, \tag{1.71}$$

[20]The use of the plural is caused by the fact that depending on the weight adopted (i.e., number, luminosity or mass) the mass estimated by the virial theorem may assume different values. So it is better to distinguish the estimators which use different kinds of weights.

and if $F(t)$ is a bounded function then $< f >_t = 0$. The above equation holds in particular if the function $F(t)$ is periodic with period τ, so that $F(\tau) = F(0)$.

Applying these observations to our case, we can say that if our system is bound in a limited region of space, then the function $I \equiv \sum_\iota \vec{p}_\iota \cdot \vec{r}_\iota$ is bounded and we can write:

$$\frac{d}{dt}\left(\sum_\iota \vec{p}_\iota \cdot \vec{r}_\iota\right) = 2T + \sum_\iota \vec{r}_\iota \cdot \dot{\vec{p}}_\iota. \tag{1.72}$$

Taking the time average of both sides:

$$< \frac{d}{dt}\left(\sum_\iota \vec{p}_\iota \cdot \vec{r}_\iota\right) >_t = 2 < T >_t + < \sum_\iota \vec{r}_\iota \cdot \dot{\vec{p}}_\iota >_t \tag{1.73}$$

but, because $I \equiv \sum_i \vec{p}_i \vec{r}_i$ is bounded, we have

$$< \dot{I} >_t = 0. \tag{1.74}$$

Introducing the equations of motion:

$$\dot{\vec{p}}_\iota = -\frac{\partial U}{\partial \vec{r}_\iota}, \tag{1.75}$$

we finally have:

$$2 < T >_t - < \sum_\iota \vec{r}_\iota \cdot \frac{\partial U}{\partial \vec{r}_\iota} >_t = 0. \tag{1.76}$$

This is the most general expression of the virial theorem. Now we introduce the assumption that U is a homogeneous function of the coordinates of degree k, obtaining:

$$2 < T >_t - k < U >_t = 0. \tag{1.77}$$

In the case of gravitational potential energy: $k = -1$, so:

$$2 < T >_t + < U >_t = 0 \tag{1.78}$$

and the total energy E is:

$$E = < T >_t + < U >_t = - < T >_t . \tag{1.79}$$

Equation 1.78 is the expression we will use and is the **virial theorem** for gravitational systems.

Returning to the astrophysical problem, all we have are instantaneous values of the angular positions and radial velocities from us of some of the member galaxies. It is clear that, without any further assumption, the virial theorem is useless. In fact, we cannot compute any time-averaged

quantities appearing in eq. 1.78 since, in order to do that, we should integrate $T(t)$ and $U(t)$ throughout all the past history of the group, which we do not know. We have already discussed how to correct for projection and incompleteness-what we need now is an assumption about the dynamical state of the system. The most straightforward assumption is to take groups as stationary systems, but it is not obvious that even in the stationary regime we can substitute the instantaneous values of, say, T in place of $< T >_t$. It is more correct to proceed as follows. Let us think of the system as a continuous distribution of matter described by a phase-space density $f(\vec{r}, \vec{v}, t)$ generally dependent on time. After a rather violent initial evolution (Lynden-Bell, 1967; Shu, 1978), we can assume that the system reaches, after a sufficiently long time, an equilibrium configuration (Gott and Rees, 1975) in which the phase-space density f_0 is no longer time dependent:

$$f(\vec{r}, \vec{v}, t) \rightsquigarrow f_0(\vec{r}, \vec{v}) \tag{1.80}$$

and in this sense we assume the hypothesis of the steady state of the group. Considering eq. 1.72 and using the fact that U is a homogeneous function of the positions of degree -1, we can write:

$$\frac{d}{dt}\left(\sum_\iota \vec{p}_\iota \cdot \vec{r}_\iota\right) = 2T + U \tag{1.81}$$

which holds at any time t. Now, observing that the moment of inertia $\mathcal{I}$ satisfies the following relation:

$$\frac{d}{dt}\left(\sum_\iota \vec{p}_\iota \cdot \vec{r}_\iota\right) = \frac{1}{2}\frac{d^2}{dt^2}\mathcal{I} \tag{1.82}$$

since

$$\mathcal{I} \equiv \sum_\iota \mathcal{M}_\iota \vec{r}_\iota^{\,2}, \tag{1.83}$$

we can state:

$$\frac{1}{2}\frac{d^2}{dt^2}\mathcal{I} = 2T + U \tag{1.84}$$

at every stage of the dynamical evolution of the system. Assuming a steady state for the group (eq. 1.80) we are allowed to write:

$$\mathcal{I} = const(t) \;\Rightarrow\; 2T + U = 0. \tag{1.85}$$

Finally, inserting the observed values of velocities, masses and positions in the last equation, it is possible to estimate the mass of the system. In other words it is possible to rewrite eq. 1.77 (see eqs. 1.46 and 1.52) as:

$$\sum_\iota \mathcal{M}_\iota v_\iota^2 - G\sum_{(\iota,\kappa)} \frac{\mathcal{M}_\iota \mathcal{M}_\kappa}{r_{\iota\kappa}} = 0 \tag{1.86}$$

hence the virial mass $\mathcal{M}_V$ should satisfy:

$$\mathcal{M}_V V^2 - G\frac{\mathcal{M}_V^2}{R_V} = 0, \tag{1.87}$$

which implies

$$\mathcal{M}_V = \frac{V^2 R_V}{G}, \tag{1.88}$$

or, more explicitly:

$$\mathcal{M}_V = \frac{(\sum_\iota \mathcal{M}_\iota)\sum_\iota \mathcal{M}_\iota v_\iota^2}{G\sum_{(\iota,\kappa)} \frac{\mathcal{M}_\iota \mathcal{M}_\kappa}{r_{\iota\kappa}}}. \tag{1.89}$$

This is the ideal expression of the **virial mass**. We would be able to measure this quantity if we knew, for every member of the group, the value of the mass $\mathcal{M}_\iota$, velocity $\vec{v}_\iota$ and three-dimensional position $\vec{r}_\iota$.

Let me summarize the hypotheses supporting the expression in eq. 1.89 for the virial mass estimator:

1. the system is a bound and isolated collection of point-like masses,

2. the system is in a steady state, in the sense that it is described by an average phase-space density $f_0(\vec{r},\vec{v})$ which is independent of time (eq. 1.80), or, similarly, it is possible to assume that $< X >_t \simeq X_{obs.}$ for every observable quantity X of interest.

I would like to examine these assumptions in detail and the methods that are available to check them. In the first point the term *isolated* means that the system is not affected by other objects. A careful examination of the environmental effect can probably be studied by numerical simulations. Giuricin et al. (1988) proposed a simple criterion to determine if the presence of external forces affects the internal evolution of the system. For each pair of groups they introduced a parameter Γ defined as:

$$\Gamma = \left[\frac{D_{ij}}{R_{p,i} + R_{p,j}}\right]^2 \tag{1.90}$$

where D_{ij} is the distance between the two groups and $R_{p,i}$ and $R_{p,j}$ are the mean pairwise separations of the groups. In the case that both groups have the same mass, Γ indicates the ratio between the internal and external forces, if in the region of space examined only the groups are present. Giuricin et al. (1988) chose to exclude the pairs of groups having $\Gamma \leq 1$.

Let me now turn to discuss the hypothesis that the groups are bound systems. A classical criterion to check this assumption is based on the concept of crossing time $\mathcal{T}$, i.e., the time required for a member galaxy to cross the whole group. If $\mathcal{T}$ is shorter than the Hubble time H_0^{-1}, then the

group must be bound, otherwise it can be that the group is unbound or bound but not yet relaxed.

In principle the most straightforward way of checking this point is to examine the density excess $\delta\rho/\rho$ of the group with respect to the mean density of the Universe. As Gott and Rees (1975) have shown, for a bound spherical system at maximum expansion, we have:

$$\frac{\delta\rho}{\rho} = \frac{\pi^2}{4\Omega(H_0 t_0)^2} - 1 \tag{1.91}$$

where t_0 is the present age of the universe. So for $\Omega = 0.1,\ 0.15,\ 1.0$ we have $\delta\rho/\rho = 30,\ 22,\ 4.6$ respectively. On the other hand, for an unbound system, we have a maximum value of $\delta\rho/\rho$ as:

$$\frac{\delta\rho}{\rho} = \frac{4}{9\Omega(H_0 t_0)^2} - 1. \tag{1.92}$$

Putting $\Omega = 0.02,\ 0.1,\ 0.2$ we obtain $\delta\rho/\rho = 23,\ 4.5,\ 2.1$ respectively. For this criterion to be helpful, it is necessary that the mass is distributed as light, but, since we do not know anything about the distribution of dark matter, our estimate of $\delta\rho/\rho$ can be as much as an order of magnitude higher than the true value. So we can draw no conclusion from this argument.

The simplest alternative to the previous method is to compare the estimate of the crossing time with the Hubble time, and in the case that $\mathcal{T}H_0 < 1$ to deduce that the group is probably bound. It has been shown by Jackson (1975) that the virial crossing time (eq. 1.64) is not a good indicator to test whether a group is bound or expanding following the Hubble flow. He introduced the definition of a new crossing time defined by eq. 1.66. If the group is expanding with the Hubble flow, then:

$$v_{\|i} = H_0 z_i. \tag{1.93}$$

If (x_i, y_i, z_i) is the position of the i^{th} galaxy in the coordinate system at rest with the group and centred at the centroid of the group, and the z axis lies along the line of sight, we have:

$$V^2 = 3\frac{1}{\mathcal{M}} H_0^2 \sum_i \mathcal{M}_i z_i^2 \sim \frac{H_0^2}{\mathcal{M}} \sum_i \mathcal{M}_i (x_i^2 + y_i^2 + z_i^2) \equiv H_0^2 R_I^2, \tag{1.94}$$

where R_I is the moment-of-inertia radius (see eq. 1.50). The approximation used here is valid in the limit of a large number of randomly positioned galaxies, which is unfortunately not the case for groups. However we can claim that $V \sim H_0 R_I$. Finally Jackson proposed comparing the crossing time he defined with the Hubble time, so that bound groups should satisfy the relation:

$$\mathcal{T}_I H_0 < 1. \tag{1.95}$$

Sargent and Turner (1977) proposed another statistical method to check whether a group is expanding or not. Using the positions and red-shifts they introduced a parameter $< \vartheta >$ which is the mean value of the angle between the pair separation vector in the red-shift space and the plane of the sky. They showed that if a system is spherical and follows the unperturbed Hubble flow, then $< \vartheta >= 32.7°$. But if the self-gravity of the system is effective in slowing down the expansion rate (even for unbound systems) then $< \vartheta > < 32.7°$. It is useful to note that during the collapse phase of a bound group $< \vartheta > > 32.7°$. Sargent and Turner (1977) also gave a recipe (equation 4 of their paper) to obtain $< \vartheta >$ from H_p/H_0, where H_p is the group's internal Hubble constant. The observation of a value of $< \vartheta > < 32.7°$ for a group would only mean that the group is not at an advanced state of collapse, but not that it is necessarily unbound.

Giuricin et al. (1988) introduced a generalization of the previous method based on the ratio:

$$F = \frac{H_0 \sigma_d}{\sigma_v} \tag{1.96}$$

where σ_v and σ_d are the standard deviations of the radial velocities $(V/\sqrt{3})$ and of the distance from us. For a spherical density enhancement the Hubble flow is slowed down by a factor $H_p/H_0 = 1/F$. If the system is unbound, then F lies in the range:

$$1 \leq F \leq \frac{3H_0 t_0}{2} \tag{1.97}$$

while for a bound system in expansion:

$$\frac{3H_0 t_0}{2} \leq F \leq +\infty. \tag{1.98}$$

After the maximum expansion, for a homogeneous spherical system,

$$F = H_0 \mathcal{T} = H_0 t_0 / \beta \tag{1.99}$$

(see eq. 1.119 for the definition of β). The problem with this method is given by the fact that to evaluate σ_d it is necessary to have *true* galaxy distances, derived independently from red-shifts. The Tully-Fisher and Faber-Jackson relations may be helpful, but the data in the literature are affected by prohibitively large errors. Alternatively one can assume that the groups are spherical systems and then it is possible to evaluate σ_d directly from the distribution of the member galaxies of each group on the celestial sphere. In this case $\sigma_d \simeq R_I/\sqrt{3}$, and $F \simeq H_0 \mathcal{T}_I$. But for a spherical system $F = H_0 \mathcal{T}_I = H_0 \mathcal{T}$. Thus, in principle, it is possible to check the consistency among F, σ_d, and $< \vartheta >$ (linked to F).

Another quite delicate point concerns the assumption that the groups are made only of galaxies. One may ask how the picture changes if we

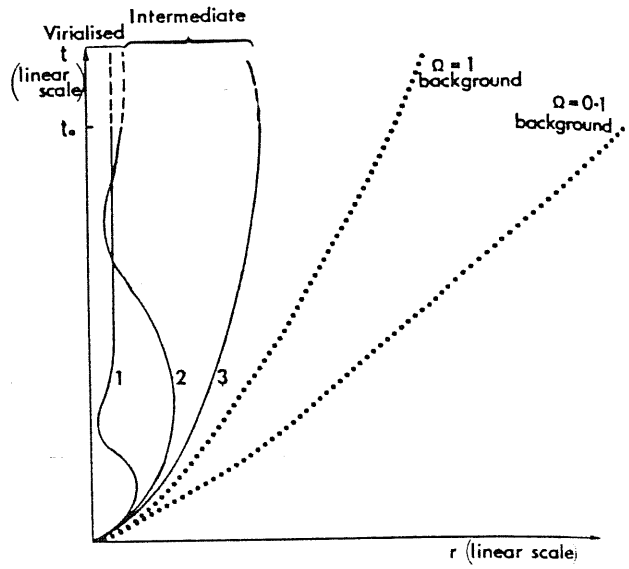

Figure 1.4: The radius versus time relation for spherical inhomogeneities of given mass for different values of the initial density enhancement $\delta\rho/\rho$ (Gott and Rees 1975).

allow a massive and diffuse background to be present within the groups. There are several methods proposed (Saslaw 1985, p. 311 and 374-377) to determine the mass of a system with a diffuse background in addition to point masses. In general all these methods assume a model for the group and by maximum likelihood techniques it is possible to estimate the properties of the group related to the adopted model. Unfortunately this technique is rather model-dependent and works quite well when one knows in advance what one is looking for. In any case this point is very interesting and deserves further attention.

Let me now discuss the assumptions about the dynamical state of groups. In order to be general and to consider the possibility that some groups may still be far away from the equilibrium phase, it is necessary to adopt a model for the formation and evolution of these systems. If we accept the gravitational instability picture described by Gunn and Gott (1972), then the time evolution of the size of the system is shown in fig. 1.4 from Gott and Rees (1975). The early evolution of the physical system was studied extensively by Lynden-Bell (1967), Shu (1978) and Merritt (1983). Giuricin et al. (1988) have recently proposed a simple and general method to correct the usual estimate of the virial mass (eq. 1.89) in order to take into account the actual dynamical state of the group. The method proceeds as follows.

In the evolutionary model of Gunn and Gott (1972), they consider a bound system of galaxies evolving with time t. If the processes relevant in the evolution are non-dissipative and the total energy $\mathcal{E}$ is conserved, then at any time:

$$\mathcal{E} = T + U < 0. \tag{1.100}$$

Since eqs. 1.77 and 1.80 do not hold necessarily, we define a parameter α giving the instantaneous ratio between the kinetic and potential energies in absolute value:

$$\alpha \equiv \frac{T(t)}{\mid U(t) \mid} \tag{1.101}$$

which is in general a function of time. Since

$$\mathcal{E} = T(t) + U(t) = \alpha(t) \mid U(t) \mid + U(t) = \mid U(t) \mid (\alpha(t) - 1) < 0 \tag{1.102}$$

we have

$$\alpha(t) \in (0, 1). \tag{1.103}$$

If we now insert eqs. 1.46 and 1.52 we have:

$$\frac{1}{2}\mathcal{M}_{V,\alpha}V^2(t) = \alpha G\frac{\mathcal{M}^2_{V,\alpha}}{R_V(t)}, \tag{1.104}$$

where the time dependence of the quantities is stressed. The evolutionary-corrected virial mass is given by:

$$\mathcal{M}_{V,\alpha}(t) = \frac{V^2(t)R_V(t)}{2\alpha(t)G}. \tag{1.105}$$

At a sufficiently late epoch t_0 the system reaches virial relaxation and

$$T(t_0)/ \mid U(t_0 \mid = 1/2, \tag{1.106}$$

so that

$$\mathcal{M}_{V,1/2}(t_0) = \mathcal{M}_V, \tag{1.107}$$

the steady state quantity defined in eq. 1.89. The correction factor μ accounting for the possibly non-virialized dynamical state can be defined by:

$$\mu = \frac{\mathcal{M}_{V,\alpha}}{\mathcal{M}_V} = \frac{1}{2\alpha}. \tag{1.108}$$

It is possible to express the time dependence of $V^2(t)$ and of $R_V(t)$ in terms of $\alpha(t)$ by using the conservation of energy. If we suppose to know that, at some instant taken as the beginning of the system's evolution t_m, $\alpha(t_m) = \alpha_m$ and $R_V(t_m) = R_m$, then:

$$T(t_m) + U(t_m) = T(t) + U(t) \tag{1.109}$$

so that

$$(\alpha_m - 1) \mid U(t_m) \mid = (\alpha - 1) \mid U \mid . \tag{1.110}$$

Supposing that the mass M is conserved:

$$(\alpha_m - 1) G \frac{\mathcal{M}^2}{R_m} = \frac{1}{2} \mathcal{M} V^2 - G \frac{\mathcal{M}^2}{R}, \tag{1.111}$$

and therefore:

$$V^2 = \frac{2G\mathcal{M}}{R} \left[1 - (1 - \alpha_m) \frac{R}{R_m} \right]. \tag{1.112}$$

From eq. 1.105 we can write:

$$\alpha = 1 - (1 - \alpha_m) \frac{R}{R_m}, \tag{1.113}$$

or:

$$R(t) = R_m \frac{1 - \alpha(t)}{1 - \alpha_m}. \tag{1.114}$$

At the time when equilibrium is reached:

$$R(t_0) = R_f = \frac{R_m}{2(1 - \alpha_m)}, \tag{1.115}$$

and by using eq. 1.114 it is possible to obtain $V^2(t)$ from eq. 1.112. Similarly it is possible to express the instantaneous value of the virial crossing time (eq. 1.64) as a function of α:

$$\mathcal{T}_{cr} = \mathcal{T}_V \frac{2(1 - \alpha)^{3/2}}{\alpha^{1/2}}, \tag{1.116}$$

where $\mathcal{T}_V$ is the virial crossing time computed in equilibrium conditions. Another convenient time scale was introduced by Cavaliere et al. (1977, 1986): the collapse time defined by:

$$\mathcal{T}_{coll} = 2\pi \left(\frac{3}{10} \right)^{3/2} \frac{G\mathcal{M}^{5/2}}{\mid \mathcal{E} \mid^{3/2}}, \tag{1.117}$$

At virial equilibrium we have: $\mathcal{T}_{coll} = 2\pi\mathcal{T}_V$. Using numerical simulations, Peebles (1970) has shown that a system reaches virialization at a time t_V approximately equal to $(3/2)\mathcal{T}_{coll} = 3\pi\mathcal{T}_V$, hence for a given evolutionary model the dynamical state of the system α is a function of the time Δt elapsed since the beginning of the expansion and $\mathcal{T}_{coll}$ or $\mathcal{T}_V$. Fig. 1.5 shows the smoothed version of the results of numerical simulations of systems composed of 15 point-like masses with a Schechter-type mass function and $\alpha_m = 0$ (Giuricin et al. 1984). The plotted curve is the function $\alpha(\tau)$ where:

$$\tau = \frac{\Delta t}{\mathcal{T}_V} = \frac{t_f - t}{\mathcal{T}_V} \tag{1.118}$$

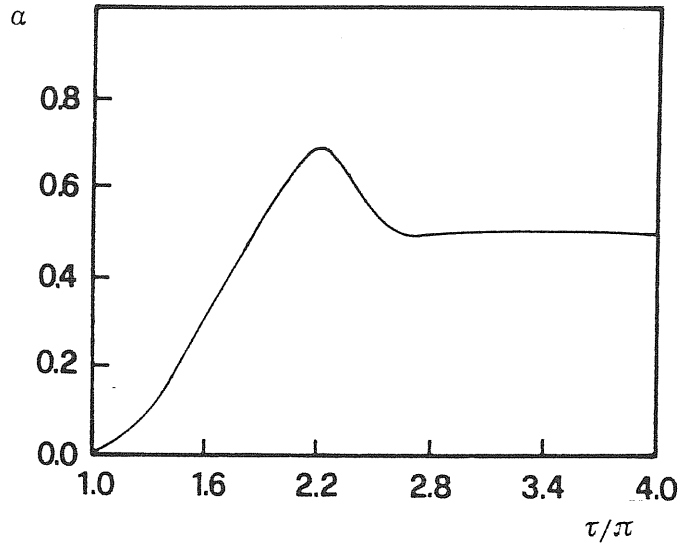

Figure 1.5: The smoothed evolution curve $\alpha(\tau)$ (Giuricin et al. 1984)

is called the *dynamical state* and counts the time from the beginning of the growing fluctuations in units of $\mathcal{T}_V$, and $t = 0$ indicates the present epoch. A bound system, whose size is proportional to $(1 - \alpha)$, typically expands approximately with the Hubble flow for $\tau < \pi$, collapses for $\pi < \tau < 2\pi$, re-expands for $2\pi < \tau < 3\pi$ and eventually reaches the virial equilibrium for $\tau > 3\pi$.

Following this method, the present ($t = 0$) value of τ can be expressed as a function of the observed virial crossing time $\mathcal{T}_V$ by inverting the eq. 1.116. Since in some models it is possible to have singularities due to $\alpha_m = 0$ it is better to use $\beta(\tau)$ defined by:

$$\beta(\tau) = \frac{t_f - t}{\mathcal{T}_{cr}} = \frac{\tau}{2} \frac{\alpha^{1/2}}{(1-\alpha)^{3/2}}. \tag{1.119}$$

Fig. 1.6 shows the curve $\beta(\tau)$ for the adopted evolutionary model. To obtain $\beta(t = 0) = t_f/\mathcal{T}_{cr}$ it is necessary to assume a value for t_f. In the standard Fridman Cosmology the fractional change in t_f is less than 10^{-3} when the corresponding z_f changes from $+\infty$ to ~ 100, hence a large error is not incurred by assuming $t_f \simeq t_0$, the present age of the universe[21]. In the case that a three-fold solution is obtained for τ, each value of τ is weighted by $1/3$ in order to avoid the increase in the observed points due to multiple solutions. Examining figs. 1.5 and 1.6 it is possible to notice that groups with $\beta(t = 0) < 8$ (corresponding to the second local minimum)

[21]In fact for $\Omega = 1$, $H_0 t_f \simeq 2/3$, and for $\Omega = 0.1$, $H_0 t_f \simeq 0.898$.

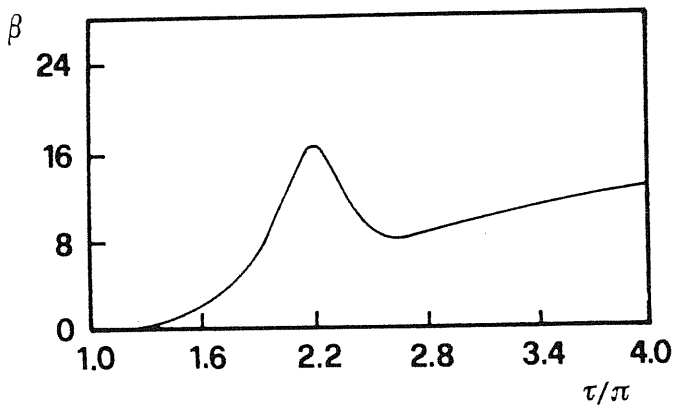

Figure 1.6: The time evolution curve for $\beta(\tau)$ for the model described (Giuricin et al. 1988).

are likely to still be on the collapsing phase, whereas for the groups with $8 \leq \beta(t=0) \leq 17$ there are three possible dynamical phases: the collapse, reexpansion and relaxation phases. Once we have τ, it is easy to compute α and then correct the virial mass. It is worth stressing that the adopted smoothed curve has a wide error band and this kind of correction has only a statistical meaning. More reliable results are subject to the availability of better simulations. In any case Giuricin et al. (1988) applied this method to a subsample of GH groups belonging to the Local Supercluster and found that $\sim 75\%$ of them are likely to be in the collapsing phase, not yet virialized. They have also shown that the median corrected values of the mass and mass to light ratio (for various choices of Ω) were larger by a factor of two than the uncorrected virial estimates. I will show later the results obtained using this method and its effect on the mass distributions of groups.

At the end of this section I will give explicitly the expression for the virial mass estimator used in this work. Whenever possible the largest number of different estimators has been computed in order to test the dependence of the results on the weighting procedures.

Since in no case was complete information available about the masses of each single member galaxy, it was impossible to use the expression for the virial mass closest to the ideal definition given in eq. 1.89. In the case that the values of the luminosities L_i of all the member galaxies were available, the virial mass (in solar units) was estimated by:

$$\mathcal{M}_{vir}(w) = 2.325 \cdot 10^8 \sigma_v^2 R_V(w). \qquad (1.120)$$

This is the **luminosity-weighted virial mass estimator**. Since there is evidence (see chapter 3) that groups are rather unevolved systems, the

equipartition of velocity seems a suitable assumption for the evaluation of the velocity dispersion of these galaxy systems. The factor is due to the units used, σ_v^2 is the corrected velocity dispersion (in Km^2/s^2) defined in eq. 1.62 and $R_V(w)$ is the virial radius (in Mpc) defined in eq. 1.48. In the case that the weight w is not specified, the value $w = 1$ is assumed.

An estimate of the uncertainty due to projection effects, incompleteness and a non-stationary dynamical condition is discussed by Giuricin et al. (1984) as a result of numerical simulations[22]. They claim that the contribution due to observational errors in the red-shifts and magnitudes is negligible with respect to the contribution of ε to the total uncertainty of the mass estimate, hence $\varepsilon(n_g, N_g)$ will be considered a good estimation of the uncertainty of $log(\mathcal{M})$.

Recall that all the quantities I discuss in this work are estimated by assuming $H_0 = 100Km/(sMpc)$. All the masses of the individual galaxies have been estimated by eq. 1.25 always adopting the same value of $\mathcal{M}/\mathcal{L}$.

In the case that the L_i were unknown, the **unweighted virial mass estimator** was used:

$$\mathcal{M}_{Vu} = 2.325 \cdot 10^8 \sigma_v^2 R_{Vu}, \tag{1.121}$$

where $R_{V,u}$ is the unweighted virial radius defined in eq. 1.49 and σ_v^2 is the same as in eq. 1.120.

Heisler, Tremaine and Bahcall (1985, hereafter HTB) introduced a slightly different expression for the virial estimator of group mass. They defined:

$$\mathcal{M}_{VT} = \frac{3\pi n_g}{2G} \frac{\sum_i (V_{\|i} - < V_\| >)^2}{\sum_{(i,j)} 1/r_{\perp,ij}}. \tag{1.122}$$

I call this quantity the **HTB virial mass estimator** to distinguish it from the others. I also considered this expression for the sake of completeness and to compare the results obtained with the previous two expressions.

1.4.8 The non-virial estimators

Following a different argument with respect to the previous section, Bahcall and Tremaine (1981, hereafter BT) and later HTB introduced an alternative mass estimator in order to avoid the drawbacks of the virial one. In fact BT studied the behaviour of the virial estimator for a system of N test (massless) particles orbiting around a central point-like object with a given mass $\mathcal{M}$. They found that for this kind of system, the virial mass estimator[23] was: *i*) biased, in the sense that the average value of $< \mathcal{M}_{VT} >$

[22] It is possible to express the standard deviation of the decimal logarithm of the virial mass estimator $\varepsilon(n_g, N_g)$ as a function of the observed n_g and true N_g values of group members by a relation derived by Giuricin et al. (1984).

[23] The definition of the virial mass used by BT is slightly different from that used by HTB (eq. 1.122).

(virial mass of the central body) was not necessarily equal to the true mass $\mathcal{M}$; *ii*) inefficient, in the sense that the variance of $\mathcal{M}_{VT}$ is large; *iii*) inconsistent, that is: $\mathcal{M}_{VT}$ does not converge to $\mathcal{M}$ in the limit of $N \to +\infty$. HTB examined systems of objects all having the same or comparable mass and found that all the estimators they used performed equally well.

Let us consider a continuous system evolving under the action of gravitational forces and described in the phase-space by the function $f(\vec{r}, \vec{v}, t)$. If the system is collisionless, then the collisionless Boltzmann equation holds:

$$\frac{\partial f}{\partial t} + \vec{v} \cdot \nabla_{\vec{r}} f + \dot{\vec{v}} \cdot \nabla_{\vec{v}} f = 0, \tag{1.123}$$

the volume mass density is:

$$\rho(\vec{r}, t) = \int f(\vec{r}, \vec{v}, t) d\vec{v} \tag{1.124}$$

while the total mass is:

$$\mathcal{M} = \int f(\vec{r}, \vec{v}, t) d\vec{r} d\vec{v}. \tag{1.125}$$

If we take first moments of eq. 1.123 with respect to velocity and consider a stationary system with spherical symmetry, we obtain:

$$\frac{d}{dr}(\rho \sigma_r^2) = -\rho \frac{dU}{dr} - \frac{2\rho}{r^2}(\sigma_r^2 - \sigma_T^2) \tag{1.126}$$

where U is the potential energy, σ_r^2 and σ_T^2 are the radial and tangential one-dimensional velocity dispersions. If the system has only radial orbits:

$$\sigma_T^2 = 0 \tag{1.127}$$

then, multiplying by r^4 and integrating eq. 1.126 over volume we have:

$$2 \int r^3 \rho \sigma_r^2 dr = \int r^4 \rho \frac{dU}{dr} dr \tag{1.128}$$

but, since $\sigma_z^2 = \sigma_r^2 \cos^2(\theta)$ and $r_\perp = r \sin(\theta)$ where θ is the angle between $\vec{v}$ and the line of sight, because of the spherical symmetry we can write:

$$< v_z^2 r_\perp >= \frac{1}{\mathcal{M}} \int \rho \sigma_r^2 r^3 \sin^2(\theta) \cos^2(\theta) d\theta dr = \frac{\pi^2}{4\mathcal{M}} \int \rho \sigma_r^2 r^3 dr. \tag{1.129}$$

Inserting the relations:

$$\frac{dU}{dr} = \frac{G\mathcal{M}(r)}{r^2} \tag{1.130}$$

and

$$\rho = \frac{d\mathcal{M}}{dr} \frac{1}{4\pi r^2} \tag{1.131}$$

we obtain

$$< v_z^2 r_\perp >= \frac{\pi G}{64}\mathcal{M}. \tag{1.132}$$

So the mass of the system satisfies the relation:

$$\mathcal{M} = \frac{64}{\pi G} < v_z^2 r_\perp > \tag{1.133}$$

for radial orbits. Similarly it is possible to show that:

$$\mathcal{M} = \frac{32}{\pi G} < v_z^2 r_\perp > \tag{1.134}$$

for isotropic orbits. In general the quantity $\mathcal{M}_P$ defined by:

$$\mathcal{M}_P = \frac{f_P}{G} < v_z^2 r_\perp > \tag{1.135}$$

is called the **ideal projected mass** and the parameter f_P depends on the distribution of the orbits. In the case of a discrete system $\mathcal{M}_P$ becomes:

$$\mathcal{M}_P = \frac{f_P}{G}\frac{\sum_\iota v_{z,\iota}^2 r_{\perp,\iota}}{N_g} \tag{1.136}$$

on the assumption that there is no correlation between the mass and the luminosity of the galaxies (Yahil 1977; Rubin et al. 1982) so that all the galaxy masses can be taken to be equal to a given value: in this way the average in eq. 1.135 becomes a number average as in eq. 1.136.

HTB tested the projected mass estimator by numerical simulations in order to choose the best value for the orbit parameter f_P. They recommended that, in the case that no information about the orbit distribution is available, the assumption of isotropic orbits $f_P = 32/\pi$ is the best choice. Another important point is the fact that in eq. 1.136 the positions and velocities are referred to the rest frame of the group and the centre of this system is placed at the centre of mass of the group. Unfortunately, since we do not generally observe all the members of the group, our estimation of the position of its centre is not necessarily correct. In fact if we call $\vec{R}_i = (X_i, Y_i, Z_i)$ the observed position vector relative to the geometrical centre of the group defined by $< (X, Y, Z,) >= 0$, and $V_{||,i}$ the line-of-sight component of the velocity from us, we have that $(V_{||,i} - < V_{||} >)^2 R_{\perp,i}$ is generally smaller (HTB) than $v_{||,i}^2 r_{\perp,i}$. HTB account for this effect by rewriting eq. 1.136 as:

$$\mathcal{M}_P = \frac{f_P}{G(n_g - \alpha)}\sum_{i=1}^{n_g}(V_{||,i} - < V_{||} >)^2 R_{\perp,i} \tag{1.137}$$

where $\alpha = 1.5$ as a result of numerical experiments. BT and HTB claim that the projected mass estimator avoids some of the problems of the virial mass estimator in particular it is less sensitive to the interlopers.

By modifying eq. 1.137, HTB introduced two more estimators. They call **median mass estimator** the quantity:

$$\mathcal{M}_{Me} = \frac{f_{Me}}{G} med_{i,j}\{(V_{\|,i} - V_{\|,j})^2 R_{\perp,ij}\}. \tag{1.138}$$

Since the median $med_i\{x\}$ of an ordered vector x_i, $i = 1, \ldots, n$ is relatively insensitive to its extreme values, $\mathcal{M}_{Me}$ should be quite insensitive to the interlopers that are mainly responsible for the high values of $(V_{\|,i} - V_{\|,j})^2 R_{\perp,ij}$. The best estimate of the parameter f_{Me} HTB obtained from their test is $f_{Me} = 6.5$.

HTB also introduced the **average mass estimator** defined by:

$$\mathcal{M}_{Av} = \frac{2 f_{Av}}{G n_g (n_g - 1)} \sum_{(i,j)} (V_{\|,i} - V_{\|,j})^2 R_{\perp,ij} \tag{1.139}$$

in this case $f_{Av} = 2.8$ was the advised value for the orbit parameter. This estimator should share the sensitivity to interlopers that the virial and projected mass estimators have. It was also used by Barnes (1984) and Van Moorsel (1982), and I consider it for the sake of completeness.

It is not hard to recognize that the assumptions supporting the expression for the projected mass estimator (eq. 1.137) are:

1. The system is bound and isolated,
2. it has spherical symmetry,
3. it is in a steady state,
4. it is made of point-like objects all with the same individual mass.

These are the same hypotheses which are needed for the virial family of mass estimators. This is quite an important point since in every group both virial and non-virial estimators are available, but unfortunately this also means that they are not independent and so comparison between them does not tells us much about the real physical mass of the system. It merely informs us about the relative reliabilities of two different procedures which are based on the same basic assumptions.

Chapter 2

The available catalogues of galaxy groups

Abstract

The set of five different catalogues analysed in the present work is described in detail. Particular attention is devoted to the features of the underlying galaxy samples and to the group identification algorithms for each group catalogue.

2.1 Introduction

In this chapter I review the observational data used in my work: namely five distinct group catalogues compiled quite recently and complete in redshift. In the previous chapter I have described all the quantities needed to perform this analysis and their relevance, now for each catalogue I describe the features of the input data since in some cases they are not exactly what is present in the original catalogues. Some of the groups have been excluded from the used catalogues for different reasons that I will explain in each case, for some other catalogues the information about the total blue magnitude was missing and has been taken from other more complete surveys, and so on. In conclusion, because of these changes in the original catalogues, I think it is useful to clarify the exact features of the catalogues effectively used.

2.2 The GH83 catalogue

The integral version of this catalogue, containing 176 groups, was obtained by GH83 from the Centre for Astrophysics Red-Shift Survey containing all the galaxies present in the Zwicky and Nilson (1973) sample. The

Table 2.1: Summary of the features of the GH83 catalogue.

magnitude system	$B(0)$
absorption corr.	no
completeness	$m_{B(0)} \leq 14.5$
velocity corr.	yes
coord. range	$\{b^{II} \geq 40°;\ \delta \geq 0°\} \cup$ $\{b^{II} \leq -30°;\ \delta \geq -2°.5\}$
GIA	friends-of-friends $\delta\rho/\rho = 20;\ V_0 = 600 Km/s$
Luminosity function	Schechter type : $M_\star = -19.4$, $\phi_\star = 0.0143 Mpc^{-3}$, $\alpha = -1.3$
no. of groups	141

coordinate range of the sample is $\{b^{II} \geq 40°;\ \delta \geq 0°\} \cup \{b^{II} \leq -30°;\ \delta \geq -2°.5\}$. The magnitude values are given in the $B(0)$ system of Zwicky (Huchra 1976), and the sample is complete in magnitude up to $m_{B(0)} = 14.5$. Because of the high galactic latitudes covered by the sample, the values of the apparent magnitudes are not corrected for the absorption effect. However this correction is negligible (HG82, GH83). The red-shift of each galaxy is corrected for the infall towards the centre of the Virgo cluster according to eq. 1.3. In order to compile the group catalogue the friends-of-friends GIA has been applied. The set of parameters leading to the most stable and reliable group catalogue was: $V_0 = 600 Km/s$, $\delta\rho/\rho = 20$ or equivalently: $D_0 = 0.52 Mpc$, and $V_F = 1000 km/s$. The expression of the luminosity function used in D_L and V_L was of the Schechter type with the following parameters: $\phi_\star = 0.0143 gal.mag.^{-1} Mpc^{-3}$, $\alpha = -1.30$ and $M_\star = -19.40$. The galaxy sample contained 2390 galaxies: 1451 (= 61%) were assigned to groups, 280 (= 12%) were in binary systems and 659 (= 27%) were members of no system (i.e., isolated). Some of the 176 groups identified by HG were nuclei or fractions of well known large clusters as in the case of group number 106 which is the Virgo cluster. These groups have been omitted. The same has been done with the groups contaminated by interlopers (see GH83). In this way I have tried to reduce the biases due to incompleteness and interlopers. The total number of groups that satisfies these requirements is 141. In the case of this catalogue all the quantities discussed in the previous chapter are calculable, so GH83 is a good source of information. The main features of the $GH83$ group catalogue are listed in Tab. 2.1.

Table 2.2: Summary of the features of the RHG89 catalogue.

magnitude system	$B(0)$
absorption corr.	no
completeness	$m_{B(0)} \leq 15.5$
velocity corr.	no
coord. range	$\{8^h \leq \alpha \leq 17^h$, $26°.5 \leq \delta \leq 38°.5\}$
GIA	friends-of-friends $\delta\rho/\rho = 80$, $V_0 = 350 Km/s$
Luminosity function	Schechter type : $M_\star = -19.15$, $\phi_\star = 0.025 Mpc^{-3}$, $\alpha = -1.2$
no. of groups	49

2.3 The RGH89 catalogue

This catalogue was obtained from an extension of the Centre for Astrophysics survey complete up to $m_{B(0)} = 15.5$ containing 1766 galaxies of the Zwicky and Nilson catalogue within $8^h \leq \alpha \leq 17^h$ and $26°.5 \leq \delta \leq 38°.5$ covering $0.42 sterad.$ of the sky. The catalogue of groups is obtained by applying the friends-of-friends GIA with the following values for the search parameters: $D_0 = 0.27\ Mpc$ (corresponding to $\delta\rho/\rho = 80$), $V_0 = 350 Km/s$ and $V_F = 1000 Km/s$, so that $D_0 = 0.27 Mpc$. The whole catalogue includes 128 groups with a total of 778 members. The luminosity function used to scale D_L and V_L is taken to be of Schechter (1976) form. The parameters $\phi_\star = 0.025 Mpc^{-3}$, $M_\star = -19.15$ and $\alpha = -1.2$ are those determined by the CfA survey (de Lapparent et al. 1989). Finally the galactic magnitudes were not corrected for the absorption effect and no correction was applied to the observed velocities because of the depth of the sample ($cz \leq 1500 Km/s$). I had at my disposal only a fraction of the whole sample of groups made available by M. Ramella. They correspond to the first slice of the whole survey published by Huchra et al. (1988). In order to avoid considering groups that miss galaxies because they are too close to the limits of the slice, I excluded from the catalogue the groups closer than two harmonic radii to the edge of the slice. The data reported in Tab. 2.2 describe the properties of the catalogue I used. As in the previous case, all the discussed parameters were computable for this catalogue.

Table 2.3: Summary of the features of the S89 catalogue.

magnitude system	B_T
absorption corr.	no
completeness	no
velocity corr.	yes
coord. range	$\{b^{II} \leq -30°,\ \delta < -17°.5\}$
GIA	friends-of-friends $\delta\rho/\rho = 20,\ V_0 = 600 Km/s$
Luminosity fn.	-
no. of groups	84

2.4 The S89 catalogue

This catalogue is due to Maia et al. (1989, hereafter S89) and is based on the Southern Sky Red-shift Survey (SSRS, da Costa et al. 1988). This sample counts 2028 galaxies drawn from the ESO/Uppsala Survey of the ESO(B) Sky Atlas (Lauberts 1982) satisfying the conditions: $\log(D(0)) \geq 0.1$ and $b^{II} \leq -30°$, $\delta < -17°.5$. Here $D(0)$ is the face-on diameter and SSRS is a diameter-complete sample. In their analysis Maia et al. (1989) considered all the galaxies having $V < 1200 Km/s$ (1534 galaxies) and corrected the velocity of each one by a dipole virgocentric flow model according to HG. They applied a friends-of-friends GIA slightly modified because of the completeness in diameter of their sample. Moreover, instead of using the Schechter form, they fitted the luminosity function with their data as in da Costa et al. (1988). Their GIA was characterized by: $\delta\rho/\rho = 20$ and $V_0 = 600 Km/s$ with $V_F = 1000 Km/s$. About 35% of the SSRS galaxies were assigned to groups, 14% to binary systems and 51% were isolated. These fractions are quite different from those obtained by GH, probably reflecting the absence of large agglomerates of galaxies such as the Coma and Virgo clusters in the South.

The magnitudes of galaxies were obtained from Lauberts and Valentijn (1989) when available and were given in the B_T system of de Vaucouleurs et al. (1976). The number of groups having all members with known magnitude was 81: only one less than the total number of groups in the catalogue. The main features of the $S89$ group catalogue are listed in Tab. 2.3.

Table 2.4: Summary of the features of the T87 catalogue.

magnitude system	B_T^0
absorption corr.	yes
completeness	no
velocity corr.	yes
coord. range	all unobscured sky
GIA merging crit. reality crit. 3-dim. free param.	3-dim. hierarchical cl. max. $F_{ij} = LR_{ij}^{-2}$ lum. density $\rho = LR_{ij}^{-3}$, $\rho \geq \rho_g = 2.5 \cdot 10^9 L_\odot Mpc^{-3}$ $V_l = 300 Km/s$
no. of groups	157

2.5 The T87 catalogue

Tully (1987b) tried to identify groups of galaxies while taking into account the Large Scale Structure that contains them. He used the *Nearby Galaxies Catalog* (NBG, Tully 1987a) and the *Nearby Galaxies Atlas* (Tully and Fisher 1987) containing information about 2367 galaxies distributed over the whole unobscured sky with $V_0 \leq 3000\ Km/s$. Two major sources contribute to the NBG catalogue. All Shapley-Ames (1932) galaxies satisfying the velocity cutoff (1053 galaxies, Sandage 1978, Sandage and Tamman 1981) are included in $T87$, and this assures completeness across the sky to $B_T^{b,i} \leq 12.0$. The NBG catalogue also includes the results of an all-sky HI survey. Other sources are given by observations made from the northern hemisphere described by Fisher and Tully (1981), while Reif et al. (1982) and Chamaraux et al. (1989) observed from the southern hemisphere. All these sources provide 1515 redshifts to the NBG catalogue. However the group catalogue also contains member galaxies below the completeness limit.

Summarizing it is possible to say that the NBG catalogue covers quite uniformly the entire unobscured sky. The values of the velocities are corrected for a systemic velocity of 300 Km/s towards $l = 90°$, $b = 0°$ (i.e., the centre of the Virgo cluster).

The GIA adopted by Tully (1987a) is the three-dimensional hierarchical clustering method described in §1.3.2 but with slightly different features relative to its previous version (Tully 1980). He solves the problem concerning the three-dimensional separation of the units by considering two different regimes for the difference in radial velocities. In the first case the difference

between the velocities is very large and is assumed to be due to the Hubble flow, so that the line of sight separation is directly obtained. In the case of a very small difference between radial velocities, the separation is taken directly from the positions on the celestial sphere. In all intermediate cases the separation is obtained from an algorithm that allows to pass from one to the other limiting case in a smooth way. This process is regulated by a free parameter: the limiting differential velocity V_l: if the difference of radial velocities is lower than V_l then we are in the low velocity case. Tully (1987a) concluded that the value 300 Km/s for V_l gives the most robust results: a change of ± 100 Km/s does not affect the properties of the resulting groups in the majority of cases. According to the hierarchical nature of the adopted GIA, at each step of the clustering process the units present in the sample are merged to form richer and larger entities. At the first step all the galaxies in the sample are separate units and Tully considered for each pair (i,j), $i,j = 1,\ldots,N = 2367$ the quantity $F_{ij} = L_{max}R_{ij}^{-2}$ where $L_{max} = max\{L_i, L_j\}$ and R_{ij} is the distance between the two galaxies. On the assumption that the luminosity L_i equals the mass $\mathcal{M}_i$ for every galaxy in the sample, this F_{ij} is a measure of the gravitational force between the i^{th} and j^{th} galaxy. The pairs having the largest F_{ij} value are merged to form a new unit t with a total luminosity $L_t = L_i + L_j$ and with a position given by the luminosity weighted average of the i and j member positions. Then at the following steps of the process the sample is formed by different kinds of object: galaxies and new units of previously merged galaxies. The procedure then repeats until all the galaxies are merged to form a single unit containing N members.

While the hierarchy is developed by this parameter, membership is judged on the basis of the luminosity density $\rho = LR_{ij}^{-3}$. In this way, assuming that there is a universal value of the $\mathcal{M}/\mathcal{L}$ ratio, it is possible to specify a critical value ρ_g such that those groups having a higher value of ρ have collapsed by the present epoch, while those groups having a lower value have not yet collapsed. On the basis of empirical considerations, Tully took $\rho_g = 2.5 \cdot 10^9 L_\odot Mpc^{-3}$, uncertain by a factor of two. This value of ρ_g should define groups with crossing times less than the age of the universe, but Tully (1987a) admits that he has not considered the consequences of alternative definitions of ρ on membership. As an example, one could consider what happens if L is replaced with the total luminosity of the two groups instead of that of the brightest component. In order to check the hypothesis that the identified groups were actually bound and collapsed objects, Tully considered three tests. The first is based on the crossing time and he adopted the Jackson definition given in eq. 1.66. The median value of the best data, obtained from the 49 groups having at least five members, is smaller than the Hubble time: $\mathcal{T}_I H_0 \leq 0.3$, hence these groups are probably bound. The second test considered the collapse time t_c defined by Gunn and Gott

(1972). For the same 49 groups of the first test he obtained $t_c H_0 = 0.6$ as the median value and in 98% of these cases $t_c < 2H_0^{-1}$, thus concluding that these groups have already collapsed or are collapsing. In fact, clusters are expected to virialize after about $1.5t_c$ through the violent relaxation process and this condition is indeed satisfied by half of the groups. The third test was devoted to a search for interlopers. It was based on previous studies of group properties (Byrd and Valtonen 1985), showing that fainter prospective group members tend to be redshifted with respect to the group mean. This observation was interpreted as being due to the presence of interlopers, but other more controversial interpretations are possible (Arp 1970; Jaakola 1971; Arp and Sulentic 1985; Mezzetti et al. 1988). The result seemed to indicate the absence of interlopers in these groups. Summarizing the outcome of these tests, Tully (1987a) suggested that most of the groups had probably collapsed, thus satisfying the requirements of the identification process, and that half of them were virialized.

Another result of this identification procedure was the identification of objects that Tully called *associations*: systems of galaxies showing a core-halo structure, probably not bound, and identified by a critical value of ρ which is an order of magnitude lower than that identifying groups.

Finally the outcome of Tully's analysis is a list of 366 systems of two or more members involving 1525 galaxies (i.e., 64% of the 2367 galaxies forming the whole sample), a further 508 (21%) systems lie in associations, 303 systems (13%) lie outside groups and associations but are identified with other structures (clouds), and 31 (1%) systems are not identified with any higher order structure. In my analysis I have retained only 172 groups with a total of 941 member galaxies excluding all the pairs, associations and isolated galaxies. I also excluded groups with negative mean velocity and those groups showing too large an observational error in the member velocities since they would have $\sigma_v^2 < 0$. In fact, considering eq. 1.62, excessive values of the observational errors Δ_i^2 would cause the corrected velocity dispersion σ_v^2 to be negative and hence meaningless. The main features of the $T87$ group catalogue are listed in Tab. 2.4.

2.6 The V84 catalogue

Vennik (1984) applied the three-dimensional hierarchical clustering technique to a sample of galaxies in the northern hemisphere ($\delta \geq -2°30'$). The region surrounding Virgo ($11^h50^m < \alpha < 13^h$, $-2°30' < \delta < 20°$) was excluded because of its strong deviation from the Hubble flow. The galaxy sample contains only objects with known redshifts and with velocities less than $3500 Km/s$ while the mean velocity of the groups found is less than $3200 Km/s$, covering in this way the major part of the Local Superclus-

ter. The redshifts are obtained mainly from Fisher and Tully (1982), and also from Rood (1980), RC2, Huchra et al. (1983) and finally Vennik et al. (1982, 1984). All the heliocentric velocities are corrected for the solar motion around the Virgo cluster. The equatorial coordinates and apparent B_T magnitudes come from the Uppsala General Catalogue (UGC) of Nilson (1973), while the morphological types come from RC2 or UGC. The sample obtained in this way is by no means complete in any sense.

Vennik (1984) adopted the three-dimensional hierarchical clustering technique as GIA. This kind of technique is specified by the merging criterion function and by the coupling between the redshift and line-of-sight separations between galaxies. Vennik assumed, according to Rood and Dickel (1978), that the intrinsic distribution of velocities of galaxy groups is Gaussian with a characteristic dispersion of σ around the centre of mass velocity v_p. He then claimed that the probability of having a galaxy velocity of $v = v_p + \Delta v$ is given by $\exp[-\Delta v^2/2\sigma^2]$. In a similar way the probability of an accidental projection (interloper) of a galaxy with a given Δv on the system is: $1 - \exp[-\Delta v^2/2\sigma^2])$. Assuming that $r_{ij} = \Delta v_{ij}/H_0$ ($\Delta v_{ij} = v_i - v_j$) is the line-of-sight separation for a pure Hubble flow between the j^{th} and the i^{th} galaxy with velocities v_j and v_i respectively, then the line-of-sight separation can be calibrated by:

$$r'_{ij} = r_{ij}\left[1 - \exp\left(\frac{-\Delta v_{ij}^2}{2\sigma^2}\right)\right]. \tag{2.1}$$

In this way the observed line-of-sight separations r_{ij} are weighted by the probability of accidental superposition in a smooth way without a sharp cutoff in Δv. The intrinsic dispersion σ here characterizes the relation between the line-of-sight and the redshift distances. Vennik considers σ as a free parameter which is adjusted in order to obtain the most reliable membership assignment.

The distance between two units (groups or galaxies) in the quasi-three-dimensional space (α, δ, v) is given by:

$$D_{ij}^2 = R_{ij}^2 + (r'_{ij})^2 - 2R_{ij}r'_{ij}\cos(\pi/2 + s_{ij}/2) \tag{2.2}$$

with $v_i < v_j$ and $R_{ij} = 2v_i/H_0 \sin(s_{ij}/2)$ where Vennik assumes $H_0 = 75Km/(sMpc)$ and s_{ij} is defined by:

$$\cos s_{ij} = \cos[\Delta\alpha\cos(\delta_i)]\cos(\Delta\delta) + \sin[\Delta\alpha\cos(\delta_i)]\sin(\Delta\delta)\cos(\psi) \tag{2.3}$$

and

$$\cot\psi = \cos(\pi/e - \delta_i)/\cot(\Delta\alpha/2), \quad \delta_i < \delta_j \tag{2.4}$$

and $\Delta\alpha = \mid \alpha_i - \alpha_j \mid$ and $\Delta\delta = \mid \delta_i - \delta_j \mid$.

The merging criterion function adopted by Vennik is the same as in the case of Tully (1987b) the maximization of the force between two units F_{ij} has more physical sense:

$$F_{ij} = \mathcal{M}_{max} R_{ij}^{-2}, \quad \mathcal{M}_{max} = max\{\mathcal{M}_i, \mathcal{M}_j\}. \tag{2.5}$$

Here the masses are estimated from the luminosities by assuming a standard mass to luminosity ratio:

$$\mathcal{M}_i = \left(\frac{\mathcal{M}}{\mathcal{L}}\right) L_i \tag{2.6}$$

with a dependence on the morphological type defined by:

$$\frac{\mathcal{M}}{\mathcal{L}}(E : S0 : S) = 2 : 2 : 1. \tag{2.7}$$

The merging of the i^{th} and j^{th} unit leads to a new unit with a mass equal to the sum of all members' mass computed according to the previous relation and placed at its centre of mass.

Vennik judged the reality of the obtained systems by using the number density contrast between the system and its environment. At each level of the force hierarchy Vennik computed the number density as:

$$\rho_n = \frac{3n}{4\pi r^3} \tag{2.8}$$

where n is the number of galaxies in a given system and r is an estimate of its radius:

$$r = R_{ij} \frac{max\{\mathcal{M}_i, \mathcal{M}_j\}}{\mathcal{M}_i + \mathcal{M}_j}. \tag{2.9}$$

The reason for to this choice instead of taking the mass density is the fact that Vennik also wanted to consider systems formed by a massive central galaxy surrounded by dwarf satellites. The critical value of ρ_n separating real and non real groups can be considered as the second free parameter of this GIA. Because of the fact that the sample of galaxies was not complete, Vennik could not fix a universal value for the number density enhancement above the mean of the sample. An estimate of this value for the Local Group gives $\log \rho_n = 0.10$ but, if we move this group farther and farther away, the fainter galaxies become invisible and the group size decreases so that the number density is no longer the same but tends to increase. Therefore Vennik considered it more reliable to define a group on the basis of a jump in the hierarchy. In other words, when a really isolated galaxy is merged into a group, the density shows a strong decrease. Then examining the sequence of jumps in the hierarchy, one can have an idea about the isolation of the groups: the higher the jumps, the better the groups are distinguished and form real physical systems. In summary, Vennik's groups

Table 2.5: Summary of the features of the V84 catalogue.

magnitude system	B_T
absorption corr.	no
completeness	no
velocity corr.	yes
coord. range	northern sky
GIA merging crit. reality crit. 3-dim. free param.	3-dim. hierarchical cl. max. $F_{ij} = \mathcal{M}/\mathcal{L}LR_{ij}^{-2}$ num. density $\rho_n = 3n/(4\pi r^3)$, $\sigma = 300Km/s$
no. of groups	109

Table 2.6: Summary of the features of all the catalogues.

	GH83	RGH88	S89	V84	T87
mag.sys.	$B(0)$	$B(0)$	B_T	B_T^0	B_T
abs.	no	no	no	yes	no
comp.	$m_{B(0)} \leq 14.5$	$m_{B(0)} \leq 15.5$	no	no	no
vel. cr.	yes	no	no	yes	no
GIA	f. of f.	f. of f.	f. of f.	h.c.	h.c.

are identified by direct inspection of the hierarchical structure described by a dendrogram, taking into consideration mergers at high density level ($\log \rho_n \geq 0.0$) and limiting the group at a transition to a significantly lower density level. The force-hierarchy depends on the assumed value for σ, and the value giving the most stable group membership and internal dispersion is $300km/s$. Analysing the dendrogram obtained in this way, Vennik obtained 116 groups, 9 of which are divided into two subgroups called A and B, which I have relabelled 0 and 1 for reasons linked to my computer code. Unfortunately not all of these groups were suitable for my analysis and I excluded those having too high an observational error in the redshifts. In this way I used a total of 109 groups. The main features of the $V84$ group catalogues are listed in Tab. 2.5.

Chapter 3

Analysis of the data and discussion of the results

Abstract

To complete the study of group catalogues described in the first chapter, I analyse the properties of the physical parameters of groups in each catalogue by considering the largest number of available estimators. Particular attention is paid to observational bias and an attempt to reduce it is considered. The dynamical state of groups is studied and its consequence on the estimation of group mass is described. All catalogues are compared in order to test the dependence of group properties on the particular catalogue they belong to.

3.1 Introduction

In this chapter I discuss in full detail the results obtained from the analysis of each group catalogue. The peculiarities of each case will be stressed since they are of great help to understand different catalogues, their common features and the main differences among them.

Since the distributions of the relevant parameters are unknown, I preferred to use a non-parametric description of the results obtained and of the comparison among them. This allows me to avoid assumptions about the behaviour of the computed parameters and to follow a general procedure to reach conclusions about the studied groups.

In some cases I refer to subcatalogues formed by groups satisfying a given property. For example $GH83(D \leq 20\ Mpc)$ indicated the set of groups in $GH83$ catalogue and observed within 20 Mpc from us. Another example is $T87(L_{max} > 0, D \leq 20\ Mpc)$ which indicates the set of groups in the $T87$ catalogue, observed within 20 Mpc from us and having at least one member with known luminosity. In fact, in the case that all members

do not have a known magnitude, the luminosity of them all as well as that of the whole group is considered zero. It is also worth pointing out that the units used to express the values of the computed parameters are: solar units for the mass and the luminosities ($\mathcal{M}_\odot$ and $L_\odot$), megaparsecs (Mpc) for the distance from us and the sizes of groups, Hubble time (H_0^{-1}) for the crossing times and kilometers per second (Km/s) for the velocity dispersion and average velocity.

3.2 Analysis of the GH83 groups

3.2.1 Generalities

The groups contained in this catalogue show a wide range of variation for the computed parameters described in the previous chapter. In particular the distance from us ranges from 2 Mpc to 78 Mpc and so the observed 141 groups span quite well the extent of the Local Supercluster.

A first image of the content of GH83 is given by the map of the group positions in the supergalactic coordinate frame (XSL, YSL, ZSL) in fig. 3.1 and 3.2.

Here it is possible to notice regions of the space without objects in them. This is due to the fact that GH83 does not completely cover the whole sky solid angle as it appears clearly in fig. 3.2. The function $\omega_{GH83}(\alpha, \delta)$ defines the catalogue solid angle:

$$\omega_{GH83}(\alpha, \delta) \equiv \begin{cases} 1 & \text{if } (\alpha, \delta) \in \mathcal{A}_{GH83} \\ 0 & \text{otherwise} \end{cases} \tag{3.1}$$

where $\mathcal{A}_{GH83}$ is fixed by the coordinate limits as in Tab. 2.1[1], and amounts to 2.72 *sterad*, corresponding to 22% of the whole sky solid angle ($\mathcal{A}_0 = 4\pi = 12.57$ *sterad*). Remembering that the most distant group of GH83 lies at $D_{max} = 77.7\ Mpc$, the volume[2] spanned by GH83 is:

$$\mathcal{V}_{GH83} = \int_0^{D_{max}} \int_0^{2\pi} \int_{-\pi/2}^{\pi/2} \omega_{GH83}(\alpha, \delta) r^2 \sin(\delta) d\delta d\alpha dr = 4.26 \cdot 10^5\ Mpc^3 \tag{3.2}$$

so that the average number density of observed groups in GH83 is:

$$\bar{\rho}_n^{(obs)}(GH83) = 3.31\ 10^{-4}\ Mpc^{-3}. \tag{3.3}$$

A list of the computed parameters and their statistical characteristics is reported in Tab. A.1.

[1]Due to the large number of tables, I have decided to place all tables in appendix A.

[2]The volume of the catalogues quoted in this chapter have been computed by adopting a Monte Carlo algorithm with a required accuracy of 0.01. The results have been confirmed using different routines.

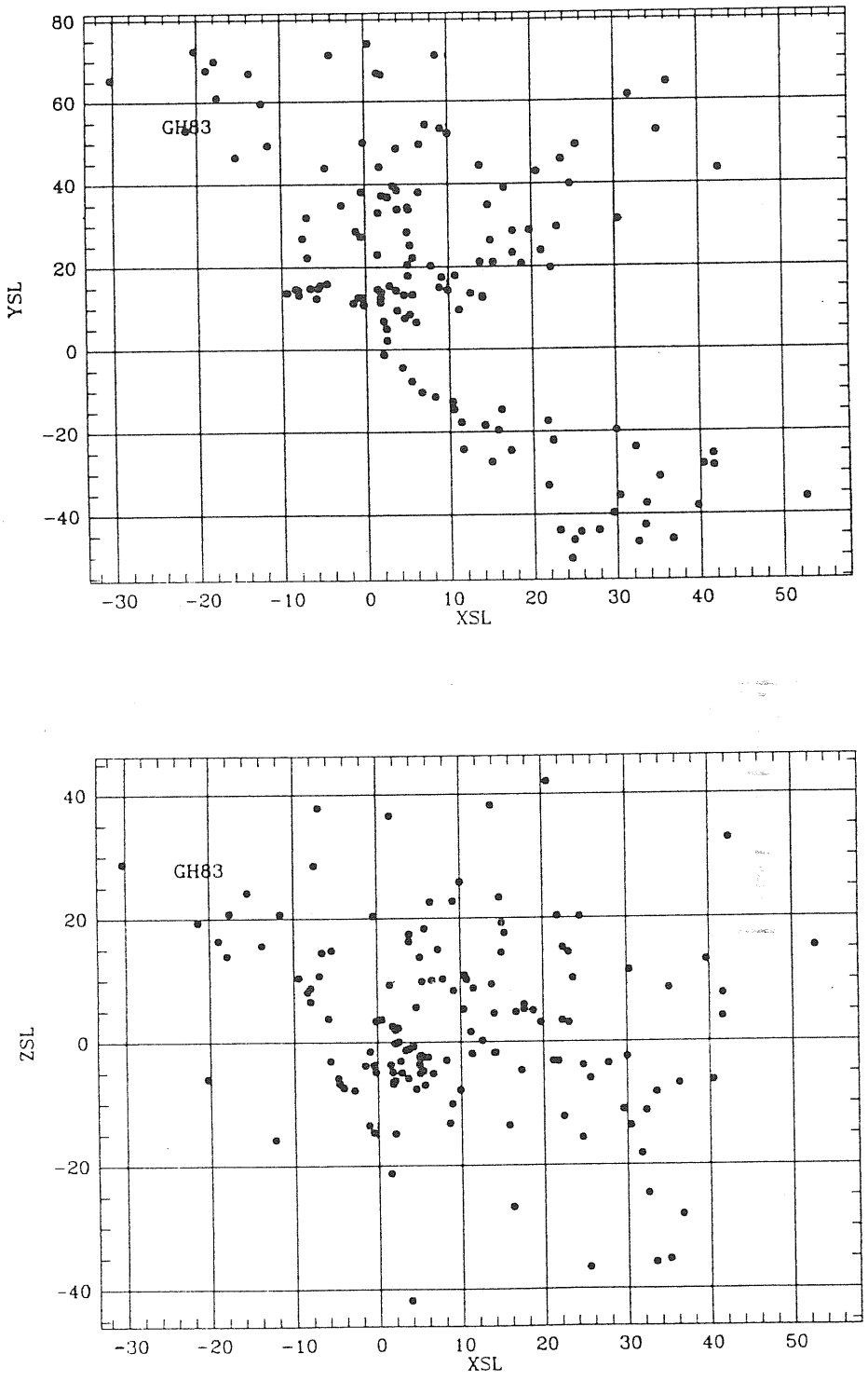

Figure 3.1: The GH83 map in the supergalactic coordinate frame (part 1), the values of the coordinates are given in *Mpc*.

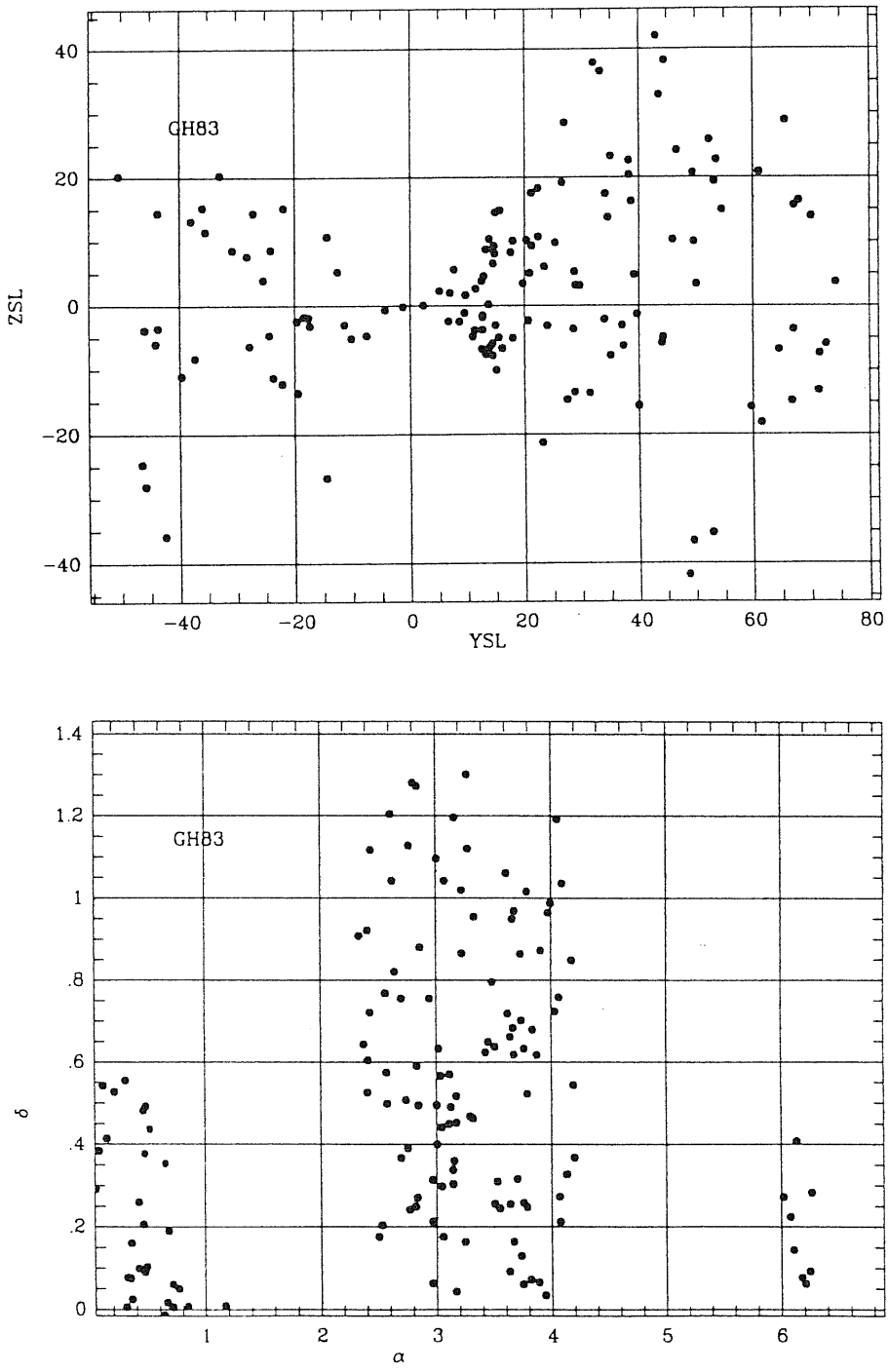

Figure 3.2: The GH83 group coordinate maps (part 2). Upper graph: positions in the supergalactic coordinate frame (in units of *Mpc*. Lower graph: the (α, δ) map in units of *rad*. Recall that these coordinates are defined in the intervals: $\alpha \in (0, 2\pi)$, $\delta \in (-\pi/2, \pi/2)$. The *obscured* regions lacking groups are quite evident.

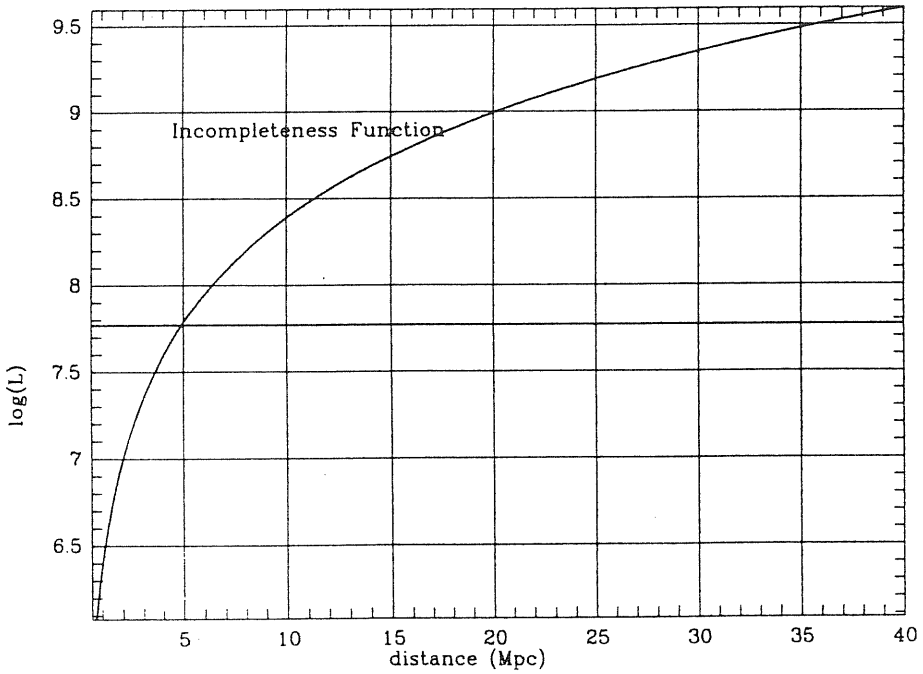

Figure 3.3: The incompleteness function for the GH83 sample, here $m_c = 14.5$. The horizontal straight line indicates the value assumed for the minimum possible value for the luminosity of a galaxy in this sample: $\log(L_{min}/L_\odot) = 7.77$

3.2.2 Analysis of the biases

A very well known problem affecting magnitude-limited samples of galaxies is the Malmquist bias. This is introduced by the fact that the galaxies listed in the sample are those having an apparent magnitude m smaller than a fixed value m_c, the completeness limit. At a distance D from us, the total luminosity L_c corresponding to m_c is given by $L_c = L(D, m_c) \propto D^2$ (see eq. 1.23). In this way as we move far away increasing D, the number of galaxies that we can observe decreases causing us to have a misleading image of the more distant regions of the sampled space. I call here *incompleteness function* the relation between L_c and D. An example of this function for the GH83 catalogue with $m_c = 14.5$ is shown in fig. 3.3.

The main drawback of the undersampling occurring at large distances is that we underestimate the median and average value of, for example, the group luminosity and hence overestimate the mass to luminosity ratio of groups. If we are interested in the general behaviour of groups, we cannot analyse a catalogue affected by this bias since an unknown amount

of information is lost. What we observe is then an unfair representation of the real group distribution.

A typical manifestation of the Malmquist bias is the increasing of the minimum luminosity of group galaxies with distance from us. GH83 is strongly affected by the Malmquist bias, in fact the minimum value of the galaxy luminosity increases monotonically with distance by ~ 2.4 orders of magnitude from the closest to the farthest group. A quantitative description of this trend is given by the Spearman rank correlation coefficient r of the relevant parameters with distance, listed in Tab. A.3. The hypothesis of independence $\mid r \mid = 0$ is tested against real correlation $\mid r \mid > 0$, and the critical region of the test is taken as 0.05 (i.e., if the significance S results smaller than the critical value of 0.05 then the tested hypothesis is rejected, otherwise it is accepted).

Going back to fig. 3.3 it appears that GH83 is free from the Malmquist bias only within 5 Mpc (see also fig. 3.4), a very small value. So a larger and larger fraction of groups that can actually exist in the volume within D_{max} is missed because of the fact that they are at a distance such that L_c is larger than the luminosity of all their members or at least of the third brightest galaxy in the group. If we assume that the distribution of the galaxy luminosity within groups is given by the Schechter (1976) function given by Geller and Huchra (1983) (see eq. 1.29) then it is possible to compute the fraction of the luminosity and number of group galaxies that we lose because of this bias. Recalling the definition of number visibility ν_g (eq. 1.41) and luminosity visibility λ_g (see eq. 1.40), the lost fraction is given by $(1-\lambda_g(D))$ and $(1-\nu_g(D))$ respectively; both these functions are shown in fig. 3.4. It is possible to note the different behaviour of the two curves: the number fraction of the missed galaxies increases more quickly than the luminosity fraction. This means that, for example, at a distance of $30Mpc$ we can observe only the richest groups since nearly 90% of the member galaxies are fainter than $L_c(30Mpc)$, and also means that the observed fraction of galaxies contributes to the total group luminosity by a fraction of nearly 35%([3]). The different behaviour of λ_g and ν_g is due to the different exponent of the linear term in the expression of $\phi(l)$, i.e., the α parameter in $f(\alpha; l)$ differs for λ_g and ν_g in eqs. 1.41 and 1.40.

This point deserves careful attention. In fact, we can statistically recover the total group luminosity L_{Tg} and members N_g by eqs. 1.33 and 1.39, but there are other very important dynamical parameters that cannot be corrected for the missed fraction of members: the radius and the crossing time estimators. It is easy to notice that at a distance of only 10 Mpc we lose nearly one half of the members. This fact has strong

[3]All these statements have only a statistical meaning, of course. It would be wrong to apply them to single groups.

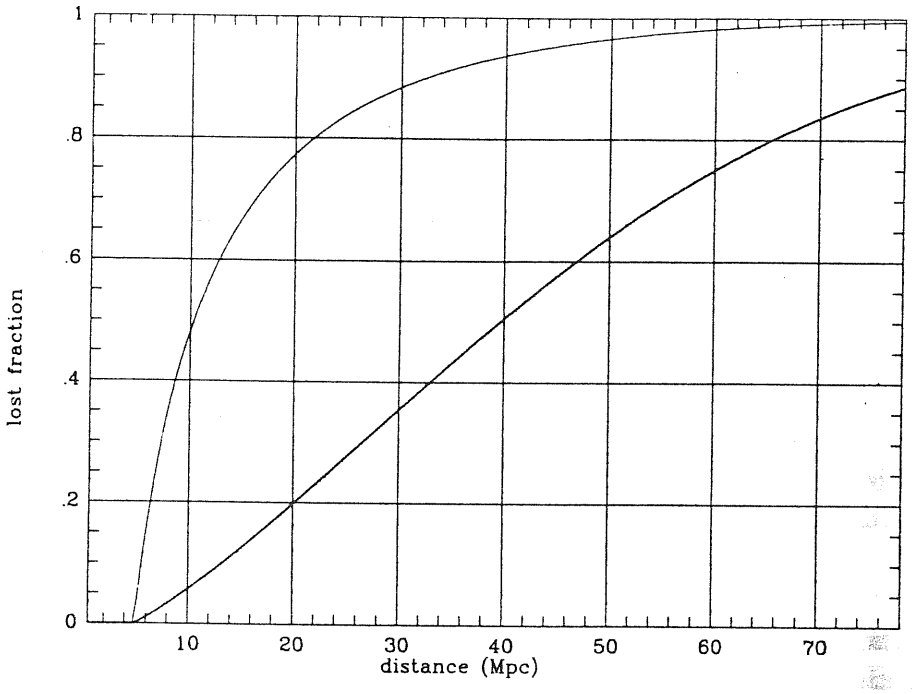

Figure 3.4: The lost fraction of luminosity (heavier line) and number (lighter line) as functions of the distance from us. Both are computed for the Schechter function with the parameters reported in tab. 2.1 and with $\log(L_{min}/L_{\odot}) = 7.77$ and $m_c = 14.5$.

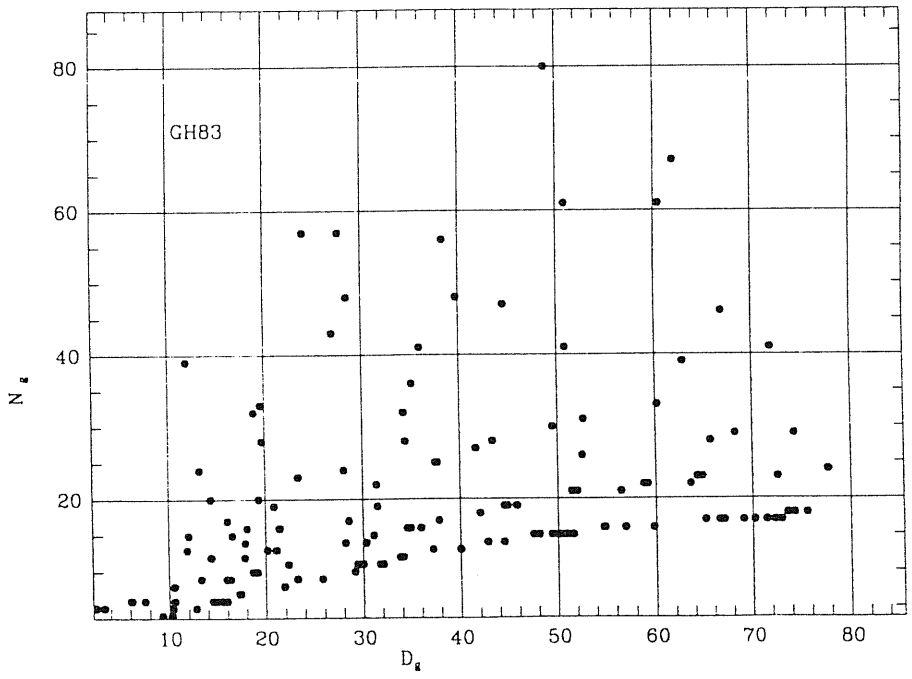

Figure 3.5: The estimated total numbers of group member N_g as a function of the group distance D_g. It appears clearly that the correction is not unbiased at large distances.

consequences for the uncertainty in the estimated mass as was shown by the numerical experiments of Aarseth and Saslaw (1972), by Saslaw (1985, part 3, pp. 303-311) and more recently by Giuricin et al. (1984). A quite rough correction for the unseen members is applied only to the velocity dispersion (eq. 1.62). The dependence of the virial mass on the second power of the velocity dispersion and on the first power of the radius causes the high correlation observed between the virial mass and the velocity dispersion $r[\log(\mathcal{M}_{Vu}), \log(\sigma_v)] = 0.95$ with $S = 2.8 \cdot 10^{-19}$. The much smaller correlation between the same mass and the virial radius $r[\log(\mathcal{M}_{Vu}), \log(R_{Vu})] = 0.16$ with $S = 0.31$, is the reason for the attention paid to the velocity dispersion estimate. It is more important to correct σ_v rather than R_{Vu} for the incompleteness effect in order to refine the estimate of the mass.

On the other hand it is important to consider the fact that the correction technique adopted to estimate L_{Tg} and N_g is not free of bias. This appears clearly in figs. 3.5 and 3.6. Since we can estimate the fraction of number and light we lose, the total correction ΔL (and ΔN) increases both with

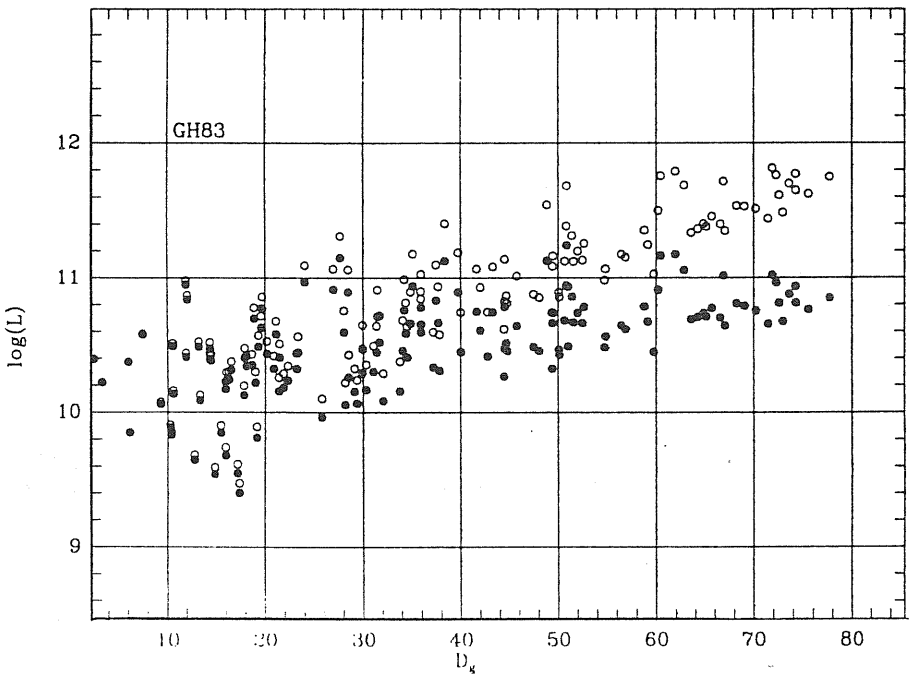

Figure 3.6: The decimal logarithm of group luminosity versus group distance. The black dots indicate the observed luminosity L_{sg}, while the open circles indicate the estimated total luminosity L_{Tg}.

distance and with the observed value:

$$\Delta L = L_{Tg} - L_{sg} = \left(\frac{1}{\lambda_g(D)} - 1\right) L_{sg} \tag{3.4}$$

and

$$\Delta N = N_g - n_g = \left(\frac{1}{\nu_g(D)} - 1\right) n_g. \tag{3.5}$$

These corrections are probably reliable only if their values are not too large, otherwise it is likely that they introduce further errors and undesired trends with distance and observations.

A way to dispose of these problems could be to cut the sample at a distance such that the lost fraction of light and members of groups is sufficiently low. Unfortunately, this remedy turns out to be worse than the Malmquist bias itself. In fact, if we consider only groups within 10 Mpc, our catalogue reduces to six groups, an irrelevant number for a statistical analysis. Let me define $D_{\lambda n}$ (and similarly $D_{\nu n}$) as the distance within which the fraction of the observed luminosity of the group amounts to n %; in symbols:

$$\lambda_g(D_{\lambda n}) = n/100. \tag{3.6}$$

So the Malmquist bias disappears if we cut the sample at $D_{\lambda 100}$, but this value leaves us with an insufficient number of groups. In fact $D_{\lambda 100} = 5\ Mpc$ and $N_{obs}(D_g \leq D_{\lambda 100}) = 2$. This means that only an irrelevant fraction of GH83 is free of this bias.

By inspection of fig. 3.6 it appears that there is an absolute minimum in the curve defined by the lower bound of the $(logL_{sg}, D_g)$ points at $\sim 18 - 20Mpc$. This suggests the possibility of cutting $GH83$ at $20Mpc$. This choice implies:

$$\lambda_g(D = 20Mpc) = 0.80\ ,\ \ \nu_g(D = 20Mpc) = 0.25. \tag{3.7}$$

Although this choice does not seems particular ingenious, it allows us to restrict our attention to a large enough catalogue of groups for our statistical purposes. In fact $N_{obs}(D_g \leq D_\star = 20Mpc) = 38$, which is not too low. In order to check quantitatively the reliability of this choice, it is worth testing the correlations existing between pairs of the computed parameters of groups. The cut at 20 Mpc is accepted as reasonable if the groups of $GH83(D_g \leq 20\ Mpc)$ show no correlation between parameters that should be independent such as the luminosity and distance. It is worth noting that the correlation between the mass $\mathcal{M}_{V_u}$ and the distance is also reduced below the significant value ($S > 0.05$). The same effect is observed for the velocity dispersion and the virial radius. The test of independence between the parameter pairs has been carried out using the Spearman correlation coefficient r and the results are reported in Tab. A.4.

For the sake of completeness other choices of $D_\star$ were considered and some of the resulting correlations are given in Tabs. A.5, and A.6.

This analysis gave comforting results. The comparison among the independence tests performed for different choices of $D_\star$ allows me to conclude that there is no strong dependence on the particular value of the distance cutoff $D_\star$. In fact both the observed (L_{sg}) and the estimated total (L_{Tg}) luminosities are independent of distance D_g as is reasonable for a fair sample. Moreover, the mass estimators share the same independence. This is a rather important fact. A good correlation is found between the luminosity and the richness of groups both in the observed pair (L_{sg}, n_g) and in the estimated total quantity pair (L_{Tg}, N_g). Unfortunately a certain amount of undesired correlation is present between N_g and D_g, which can be understood from the high value of the lost fraction in richness at $20Mpc$: $(1 - \nu(20Mpc)) = 0.75$. It is not advisable to decrease $D_\star$ in order to remove this correlation because of the consequent further decrease of the number of groups present within $D_\star$. These results seem to indicate that the choice of cutting the sample at 20 Mpc is quite reasonable. This is also supported by Tully (1987b) who claims that his sample of galaxies (from which T87 is obtained) is complete up to $m_B \leq 12.0$ within $19 - 20$ Mpc. Moreover, taking $D_\star = 20$ Mpc makes me quite confident that the Local Supercluster is well contained within this distance.

We are now left with a subcatalogue $GH83(D \leq 20Mpc)$ which contains only 38 groups: nearly one third of the whole GH83 content. The main drawback of this reduction is the lower resolution of the statistical test needed to analyse the distribution of group parameters both when comparing the performances of two different estimators of the same physical quantity and when comparing the observed distribution of an estimator with a theoretical prediction. The non-parametrical test suitable for the statistical analysis is the Kolmogorov-Smirnov (KS) test. The error bands, and hence the resolution, of this test is strictly dependent on the amount N of available data and goes as $N^{-1/2}$. Therefore, if N is reduced from 141 to 38, the error band increases by a factor of $(141/38)^{1/2} = 1.93$ and similarly the resolution of the test decreases. This means that a different behaviour of, say, two estimators of the group mass which are really different must show a difference in their observed distributions amounting in $GH83(D \leq D_\star)$ to nearly twice the value it would have if revealed in the whole GH83. In other words an insufficient but real difference in the estimators would not be revealed in the nearby subcatalogue $GH83(D \leq D_\star)$.

A first question we must answer concerns the relation between the general statistical properties of $GH83(D \leq D_\star)$, and also $GH83$ and $GH83(D > D_\star)$. In order to clarify this point, I considered the observed distributions of all the parameters appearing in Tab. A.1 obtained from the whole $GH83$ and from the two subcatalogues. The results of this comparison

gives us an idea of the relevance of the undersampling of the far away regions of the catalogue. The characteristics of the parameters obtained from $GH83(D \leq D_\star)$ are shown in Tab. A.8.

Performing the KS-test between the distribution of the nearby and distant subcatalogues I obtained that every mass estimator shows a strong difference in its distribution obtained from the nearby (i.e., $GH83(D \leq 20Mpc)$) and the distant (i.e., $GH83(D > 20Mpc)$) subcatalogues (see Tab. A.7 column B). An example of this test is shown in fig. 3.7. On the other hand, only $\mathcal{M}_{VT}$, $\mathcal{M}_{Me}$ and $\mathcal{M}_{Av}$ show a non-negligible difference between $GH83$ and $GH83(D \leq 20\ Mpc)$. For the other estimators the significance S is always quite low, although not critically, it is possible to say that the stability is marginal. From the results in column C of Tab. A.7 it seems that the distributions of all the mass estimators in $GH83$ are dominated by the distant fraction of the catalogue, while the results in column B seem to indicate that strong differences ($S < 0.05$) between $GH83(D \leq 20Mpc)$ and $GH83(D > 20Mpc)$ become marginal ($0.10 < S < 0.05$) differences between $GH83(D \leq 20Mpc)$ and GH83. This result might also depend partially on the different number of groups forming the compared catalogues. In any case there is evidence that the mass distribution of $GH83$ is dominated by the contribution of the most strongly biased fraction: $GH83(D > 20\ Mpc)$, no matter what estimator is considered.

The behaviour of the other parameters is quite similar. It is worth noting that the splitting of $GH8$ into two subcatalogues causes strong differences in the distributions of N_g, but not of n_g, consistent with the previous discussion about the Malmquist bias. Other main parameters such as σ_v and $\mathcal{T}_V$ are stable against the splitting of the catalogue, while the size estimators such as R_p and R_{Vu} change quite strongly.

It is likely that when a strong difference detected between a parameter distribution in $GH83(D \leq 20Mpc)$ and $GH83(D > 20Mpc)$ persists, albeit weaker when comparing $GH83(D \leq 20Mpc)$ and $GH83$, then the difference is real and the catalogue size difference does not play the major role in producing the observed results.

In conclusion it is better to perform the analysis only on the nearby subcatalogue if reliable conclusions are to be reached. However the results obtained for the whole catalogue are also reported, for the sake of completeness. In the case that I want to illustrate a result by a graph, and this result holds for both the whole catalogue and its nearby fraction, I prefer to show the graph concerning the whole catalogue because of its better statistical resolution. This convention about graphs applies to all catalogues.

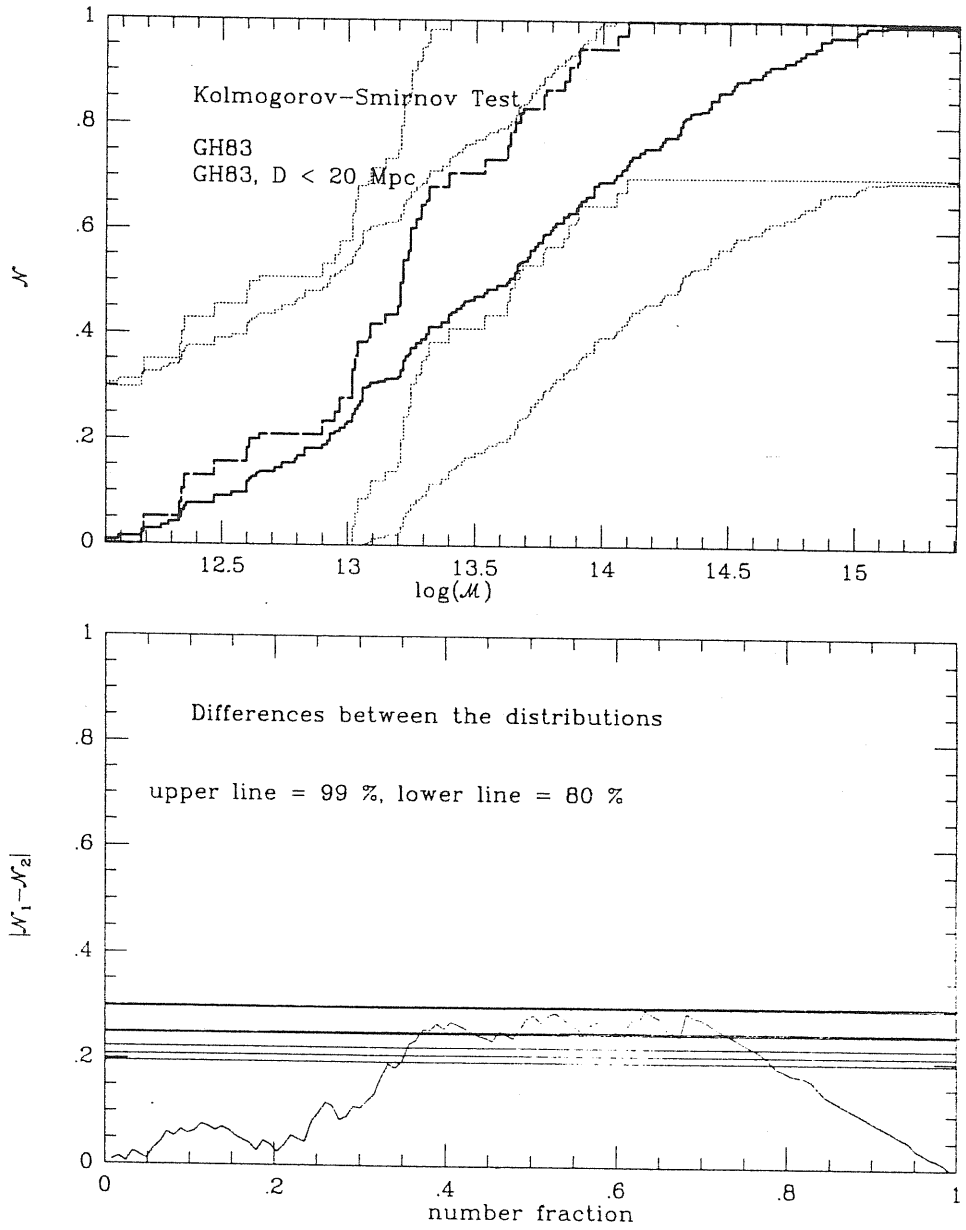

Figure 3.7: The KS test comparing the distribution of $\mathcal{M}_{V_u}$ obtained from the whole $GH83$ (solid) and $GH83(D \leq 20\ Mpc)$ (long-dashed). The dotted step functions indicate the 99% confidence band. In the lower panel the difference between the two distributions is plotted as a function of the steps of the two distributions.

3.2.3 Analysis of groups physical parameters

In the last sections I illustrated the reasons for limiting the study of $GH83$ within $D_\star = 20Mpc$. The *nearby* fraction of GH83 contains, as already shown, 38 groups. The volume covered by $GH83(D \leq D_\star)$ is:

$$\mathcal{V}_{GH83(D \leq D_\star)} = 7.29 \cdot 10^3 Mpc^3 \tag{3.8}$$

and the average observed number density of groups is:

$$\bar{\rho}_n^{(obs)}[GH83(D \leq D_\star)] = 5.2 \cdot 10^{-3} Mpc^{-3}. \tag{3.9}$$

A first point to discuss is the possible dependence of the observed distribution of a given parameter on the estimator used. This obviously concerns those parameters that can be estimated in more than one way: the mass, the radius and the velocity dispersion. The KS pairwise comparison of the various mass estimators used is reported in Tab. A.11. It is clear that all the estimators perform equally well and that there is no dependence on the way we compute the mass of groups: the distribution of this important physical parameter is insensitive to the estimator adopted. This is quite an important result which makes us quite confident that it is possible to refer to the mass of a group without ambiguity.

The same KS pairwise comparison was applied to the virial radius estimators R_{Vu} and $R_V(w)$ for $w = 1$, 3, 5 and 10. The results are listed in Tab. A.12. They seem to indicate the presence of a significant difference between two extreme cases: $R_V(w)$ and R_{Vu} for $w = 5$ and $w = 10$. In all other cases no appreciable difference is found. This fact might mean that a certain amount of morphological segregation is present within groups. This result has been discussed in previous work (Mezzetti et al. 1985, Giuricin et al. 1988) but no attention was paid to the Malmquist bias. Besides, it is generally believed that the mass is a power function of the galaxy luminosity so that a weight that only takes into account the morphological type leads to a poor estimate of the galaxy mass. In Tabs. A.1 and A.8 the median and average values are listed and the difference is clear. The presence of morphological segregation may justify a more careful attention to the luminosity-weighting procedure. On the other hand, the poor correlation between the mass and the virial radius (see fig. 3.8) indicates that the adopted weights are of little consequence on the estimated mass distribution. This is confirmed by direct comparison of weighted and unweighted mass estimators (see Tab. A.11).

The velocity dispersion of groups is estimated by the fully corrected expression of σ_v in velocity equipartition, that is to say without weighting with the luminosity. Another estimator is V_n, not including the incompleteness and global motion corrections. Finally, in the expressions $V_g(w)$ the

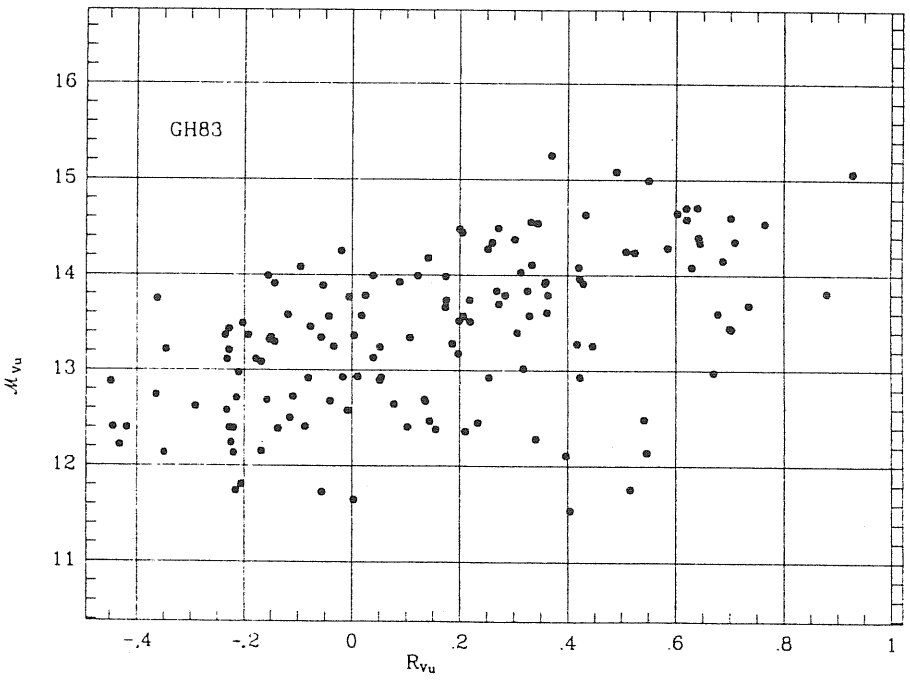

Figure 3.8: The unweighted virial mass $\mathcal{M}_{Vu}$ vs. the unweighted virial radius R_{Vu}.

mass is taken into account although in a quite rough way. A first result is the similarity of the distributions of σ_v and V_n: the corrections applied to the observed velocity dispersion are irrelevant. They do not produce a sensitive effect on the global distribution of the velocity dispersion of $GH83(D \leq D_\star)$ groups (see also Tabs. A.10, A.1 and A.8). On the other hand the comparison of σ_v and $V_g(w = 10)$ ($S = 0.04$) suggests the use of a more appropriate expression for the velocity distribution. Also in this case I think that the composition of groups has a non-negligible effect on the results. On the other hand, the weighting w does not significantly affect the distribution of $V_g(w)$. The significant difference found between σ_v and $V_g(w)$ for $w = 5$ and $w = 10$ is similar to that found in the case of the virial radius. The point here is that the dynamical state of most of the groups supports the assumption of velocity equipartition, rather than energy equipartition and so indicates σ_v as the more suitable estimator for the velocity dispersion. In any case the good stability of the mass distribution for all possible choices of estimator makes the weighting problem not very relevant for mass estimators.

The relevance of the velocity dispersion for estimating the mass of groups is shown in fig. 3.10.

Recent numerical simulations (Perea, del Olmo and Moles 1990) seem to show that when the masses of the single particles forming the group are unknown, the unweighted virial mass estimator is the more reliable. Because of these remarks and the fact that for three out of five group catalogues that I examined the weighted parameters are not available the unweighted virial mass $\mathcal{M}_{Vu}$ is retained as representative of the mass distribution of the groups in various catalogues. In any case the pairwise KS test comparison gives no significant difference between the mass estimator distributions. The comparison between the unweighted virial mass $\mathcal{M}_{Vu}$ and the projected mass $\mathcal{M}_P$ for the whole $GH83$ is shown in fig. 3.9. Moreover the Kruskal-Wallis (Ledermann, 1982, vol. VI; hereafter KW) test applied to all the nine mass estimators available gives a significance $S = 0.88$ for $GH83(D \leq 20\ Mpc)$ and $S = 0.48$ for the whole $GH83$. This means that there is good evidence that all the mass estimators have the same underlying (parent) distribution.

Another point relevant to the discussion is the effect of the correction (see pages 35- 38) to apply to the virial mass of groups accounting for their dynamical state. A large fraction of groups ($\sim 90\%$) is found in the region of $\alpha(\tau)$[4] with $\tau \leq 3 \cdot \pi$, while nearly 80% have $\tau \leq 2 \cdot \pi$. Recall that following the method described by Giuricin et al. (1988), a group expands approximately with the Hubble flow for $\tau < \pi$, it collapses for

[4]Please do not confuse the right ascension α with the virial $\alpha(\tau)$ although they are indicated by the same symbol.

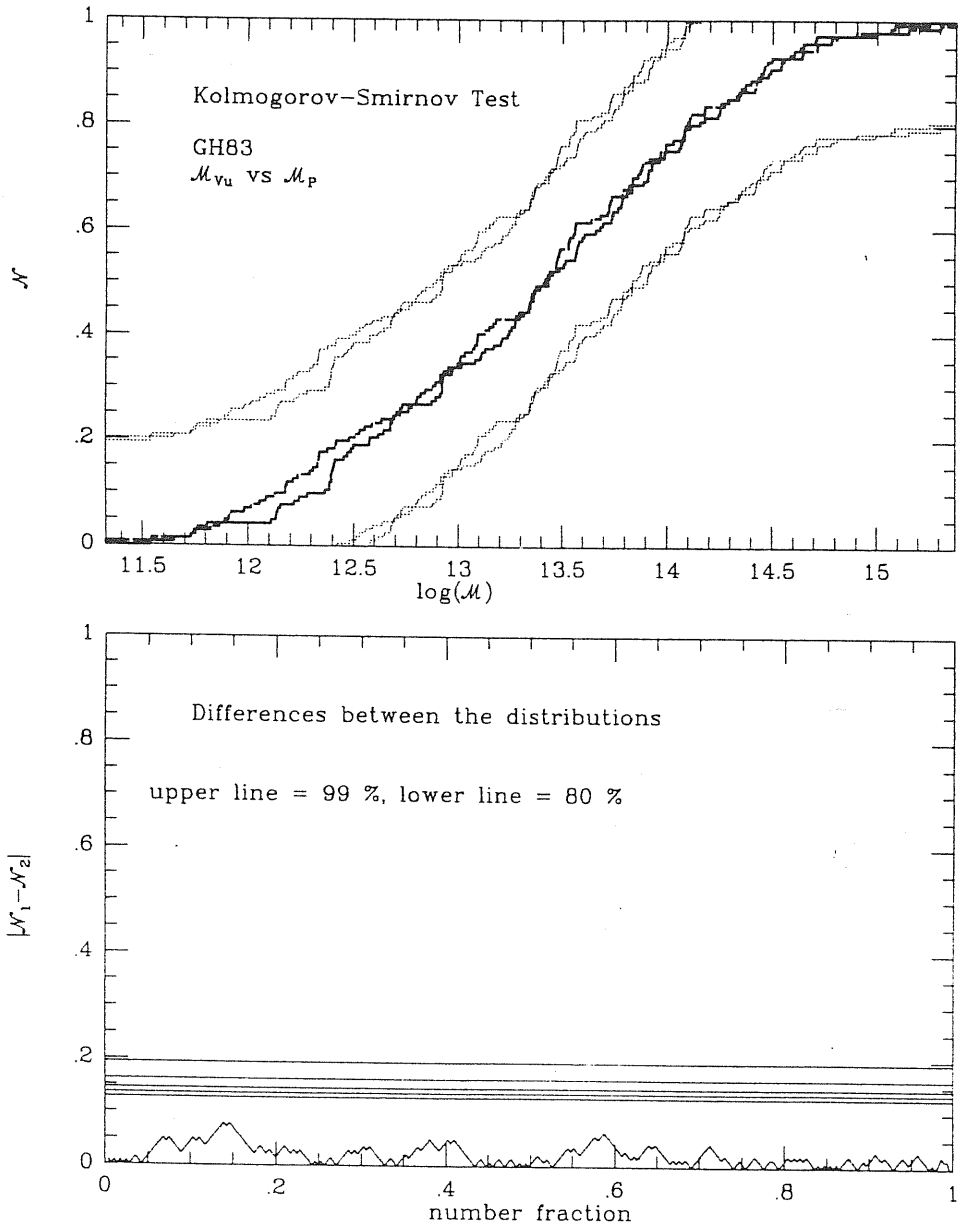

Figure 3.9: The KS comparison between the virial $\mathcal{M}_{Vu}$ (solid line) and projected $\mathcal{M}_P$ (long-dashed line) mass distributions for the $GH83$ groups.

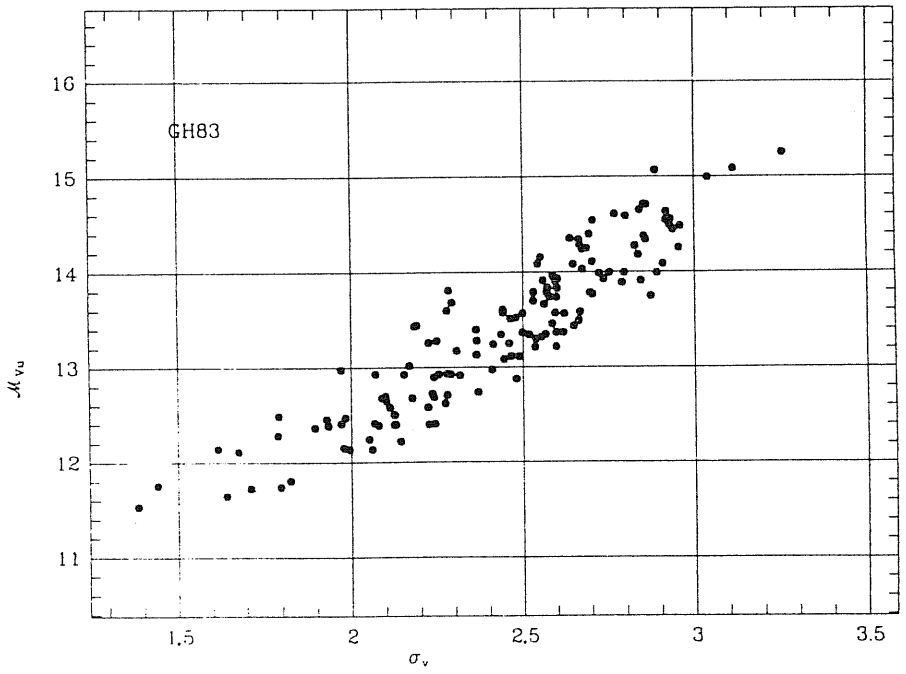

Figure 3.10: The unweighted virial mass $\mathcal{M}_{Vu}$ versus the corrected velocity dispersion σ_v for the whole $GH83$.

$\pi < \tau < 2\pi$, reexpands for $2\pi < \tau < 3\pi$ and eventually becomes relaxed for $\tau > 3\pi$. This means that they are in the phase of contraction after the decoupling from pure Hubble flow. The distributions of τ and α as well as the curve $\alpha(\tau)$ (figs. 3.11 and 3.12) illustrate the numerical results reported in Tabs. A.13 and A.14. Due to the particular distribution of τ, the correction factor for the virial mass μ has a median value close to one and so the evolutionary-corrected mass distribution $\mathcal{N}_e$ is not significantly different from the observed distribution $\mathcal{N}_{obs}$ (see fig. 3.13). This holds for both $GH83$ and $GH83(D \leq 20\ Mpc)$. Moreover no significant change in $\mathcal{N}_e(\mathcal{M})$ is due to the choice of the value for $\Omega = 0.2$ or 1. Although this is not true in particular for the distributions of τ, α and μ in the whole $GH83$, the general conclusions about the unevolved dynamical state of groups are not dependent on Ω.

3.2.4 A procedure to recover distant faint groups

The number fraction of groups with mass not exceeding a given value $\mathcal{M}$ is defined as the mass distribution of a given catalogue $\mathcal{N}_{obs}(\mathcal{M})$:

$$\mathcal{N}_{obs}(\mathcal{M}) = \begin{cases} 0 & \text{if } \mathcal{M} \leq min(\mathcal{M}_j) = \mathcal{M}_1 \\ j/N_{obs} & \text{if } \mathcal{M} \in [\mathcal{M}_j, \mathcal{M}_{j+1}) \\ 1 & \text{if } \mathcal{M} \geq max(\mathcal{M}_j) = \mathcal{M}_{N_{obs}} \end{cases} \tag{3.10}$$

with: $\mathcal{M}_j \leq \mathcal{M}_{j+1}$, for $j = 1, \ldots, N_{obs}$.

This expression holds on the assumption that there is no relation between the group mass and its position within $\mathcal{V}$. This is an assumption to be tested.

Up to now what we have is only the observed distribution. In fact we do not (unfortunately) have the opportunity to observe all the groups that are present within $D_\star$ because there may be many groups too far away and too faint to be detected. In fact, recalling the discussion about GIA in chapter 1, a bound system of galaxies is defined to be a group if the number n_g of its member galaxies is equal to or greater than 3. Suppose that a given group has $n_g \geq 3$ members with luminosities L_i and $L_i \geq L_{i+1}$, with $i = 1, \ldots, n_g$. If this group is obtained running a GIA on a magnitude complete galaxy sample with limit at m_c, then there exists an upper limit $D_g^{(v)}$ to the distance within which the group is visible and beyond which it disappears since its third brightest member has luminosity L_3 smaller than the completeness value at that distance $L_c^{(v)} = L(m_c, D_g^{(v)})$. If we want to study the groups of galaxies within a certain distance ($D_\star$) from the earth, the ideal condition would be realised in the case that for all the observed groups the relation $D_g^{(v)} \geq D_\star$ holds. In that case we could be quite confident that the catalogued groups are all the groups present within $D_\star$

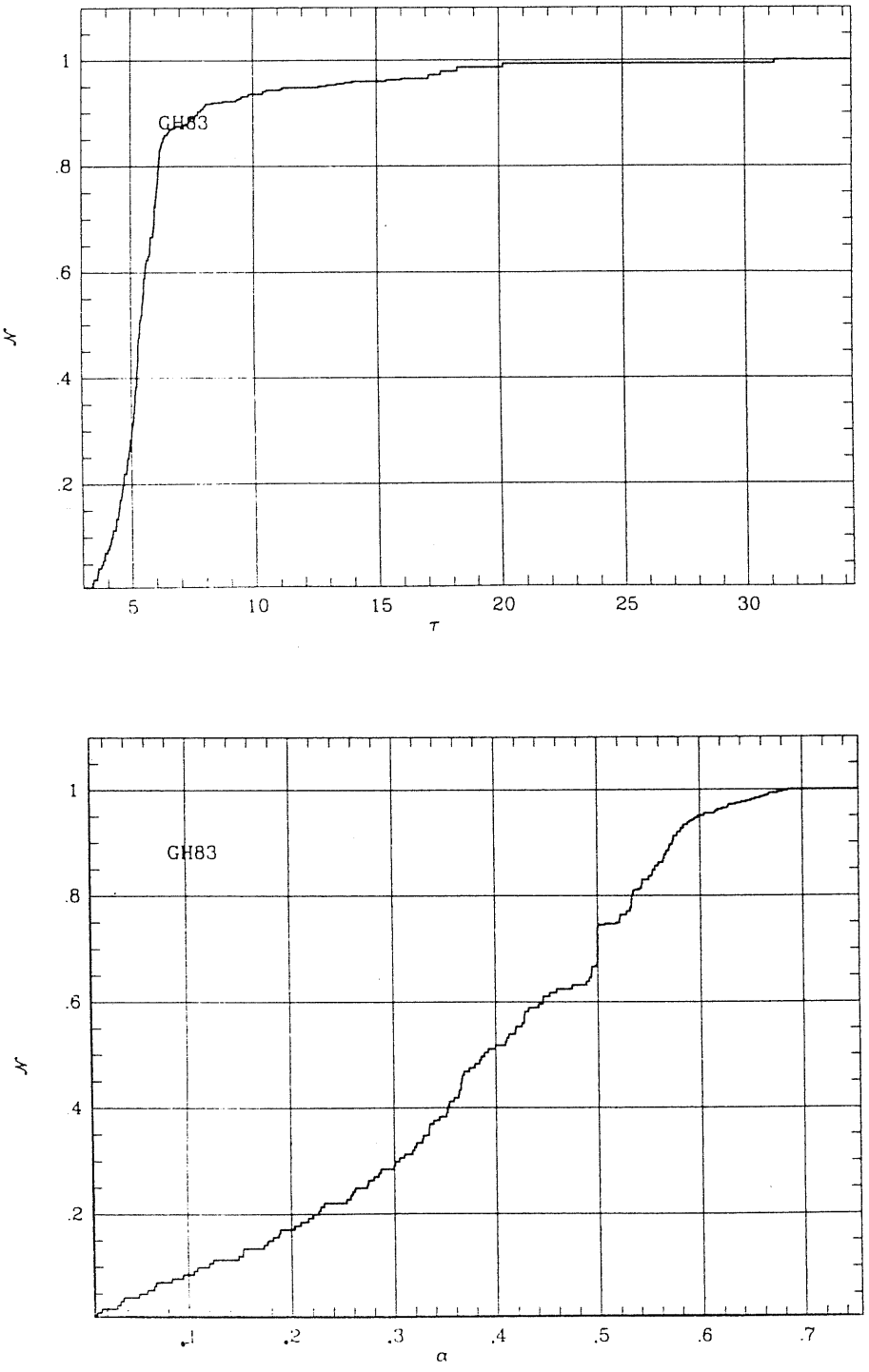

Figure 3.11: The distributions of the dynamical state τ (upper) and the virial α (lower) for the $GH83$ groups in the case $\Omega = 0.2$.

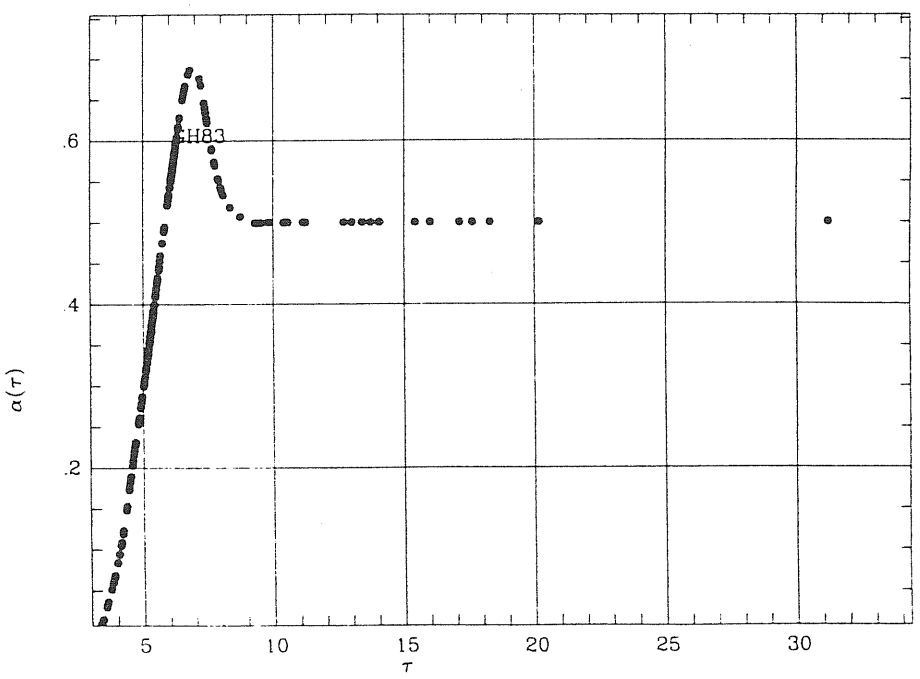

Figure 3.12: The curve $\alpha(\tau)$ for the $GH83$ groups in the case $\Omega = 0.2$.

and none (or nearly none) is missed by the galaxy survey or by the G.I.A. Unfortunately, this is not the case and some of the $GH83(D \leq 20Mpc)$ have $D_g^{(v)} < D_\star = 20Mpc$. This means that it is possible that an unknown amount of groups like these is present between $D_g^{(v)}$ and $D_\star$ but we do not observe them. In this case it is necessary to account for these *lost* groups. In order to estimate the number of unseen groups associated with a given value of $D_g^{(v)}$, it is necessary to assume a model for the number density of groups within $D_\star$. Let us suppose that the number density distribution $\rho_n(\vec{r})$ of groups within a spherical volume $\mathcal{V}(D_\star)$ with radius $D_\star$ and centre on the earth is known, and $\vec{r}$ indicates the position of groups within the volume $\mathcal{V}(D_\star)$. In this case it is possible to compute the fraction of groups within a distance D from us as:

$$n(D) = n_0 \int_{\mathcal{V}(D)} \rho_n(\vec{r}) d\vec{r} \tag{3.11}$$

so that $n(0) = 0$ and $n(D_\star) = 1$. If a group, say the j^{th} group in the catalogue, is observed at a distance D_j from us, but would disappear at $D_j^{(v)} < D_\star$, then there is a fraction of the whole volume $\mathcal{V}(D_\star)$ that could contain more groups similar to the j^{th}. If we call $N_{est}(j)$ the total number

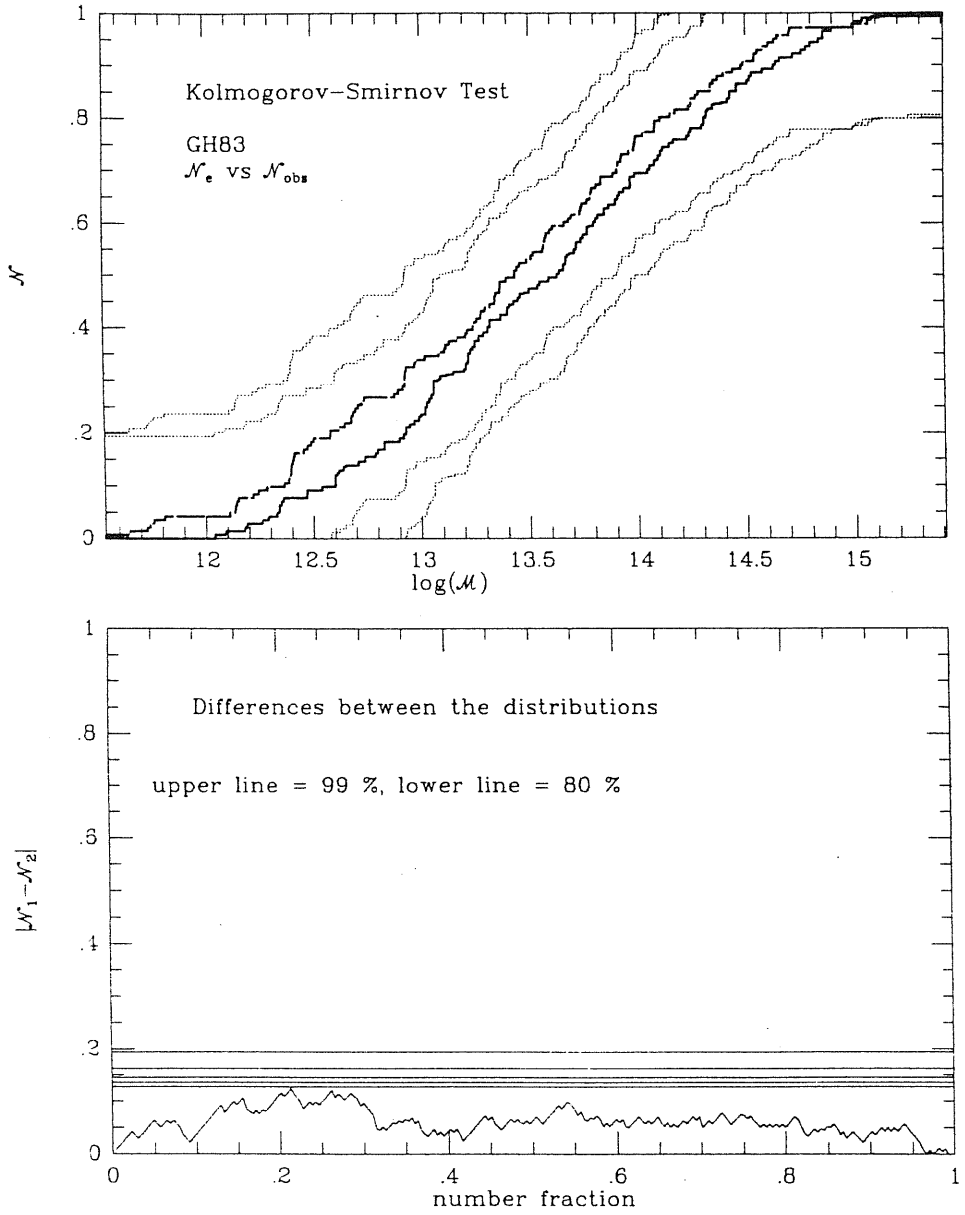

Figure 3.13: The Kolmogorov-Smirnov comparison between the observed and evolutionary corrected mass ($\mathcal{M}_{Vu}$) distributions of the GH83 groups in the case of $\Omega = 0.2$. The observed distribution is indicated by the long dashed step function, while the corrected distribution is indicated by the solid step function.

of groups similar to the j^{th} which are present within $\mathcal{V}(D_\star)$, then:

$$N_{est}(j) = \frac{n(D_\star)}{n(D_j^{(v)})}, \tag{3.12}$$

on the assumption that the spatial distribution is independent of the brightness of groups. Now $n(D)$ depends on the geometry of the mass distribution within $\mathcal{V}(D_\star)$. For a given $\rho_n(\vec{r})$, $N_{est}(j)$ is determined only by the value of $D_j^{(v)}$ that depends on the third brightest galaxy of the groups ($L_3(j)$) and on the completeness limit m_c. Groups with small L_3 have a small $D^{(v)}$ and hence a large N_{est}. Only the absolute values of the various $N_{est}(j)$ depend on the geometry (i.e., ρ_n), while the property of a given group to have the largest $N_{est}(j)$ depends only on $D_j^{(v)}$ and is independent of $\rho_n(\vec{r})$, due to the non decreasing dependence of $n(D)$ for growing D for every $\rho_n(\vec{r})$.

Once the value of $N_{est}(j)$ is known, an assumption is required about the mass of the lost $N_{est}(j) - 1$ groups. It is unreasonable that all should have the same $\mathcal{M}(j)$ mass as the observed groups. A more acceptable estimation of their mass can be obtained by spreading the $N_{est} - 1$ values of the mass in an interval of amplitude $\delta\mathcal{M}(j)$ around $\mathcal{M}(j)$, where $\delta\mathcal{M}(j)$ is the uncertainty in the mass value estimated by numerical simulations and accounting for the projection and incompleteness effects. Following the results of Giuricin et al. (1984), the spreading law can be obtained assuming that the measurements of $log(\mathcal{M})$ are distributed with a Gaussian law around the true values with a standard deviation given by $\varepsilon(n_g, N_g)$ (see page 39). After the spreading is applied the mass distribution accounting for the contribution of distant faint groups is available: $\mathcal{N}_c(\mathcal{M})$. The properties of $\mathcal{N}_c(\mathcal{M})$ depend essentially on the distribution of $N_{est}(j)$ and on the masses $\mathcal{M}(j)$ of those groups having the highest N_{est}. If the distribution of $N_{est}(j)$ is strongly peaked on one or few values of j, then it is likely that $\mathcal{N}_c(\mathcal{M})$ is significantly different from the observed distribution $\mathcal{N}_{obs}(\mathcal{M})$, unless the highest $N_{est}(j)$ occur for groups with a mass close to the median value of the observed distribution. In this case the observed distribution is reinforced and the confidence bands around it shrink, thus increasing the resolution of KS statistics.

It is not advisable to apply the faint distant groups correction to more than one mass estimator. In fact, it is possible that the peaks of the distribution of $N_{est}(j)$ occur for groups having different values of mass depending on the estimator. If the difference among masses is large, then the independence of $\mathcal{N}_{obs}(\mathcal{M})$ on the mass estimator is not transferred to $\mathcal{N}_c(\mathcal{M})$. For large enough values of $max_j\{N_{est}(j)/\sum_k N_{est}(k)\}$, the spreading is unable to remove the dependence of the corrected distribution on the estimator, although it can reduce it.

In the particular case of $GH83(D \leq 20\ Mpc)$ it is possible to ap-

ply the method described to recover faint distant groups since there are a certain number of groups for which $D^{(v)} < D_\star = 20\ Mpc$. As a model for the local spatial distribution of groups within 20 Mpc, the same empirical law discussed for $T87(D \leq 20\ Mpc)$ is assumed (eq. 3.18). That expression for $n(D)$ holds also if applied to $T87$ groups occupying the same volume of $GH83(D \leq 20\ Mpc)$ and the parameters D_0 and ν keep the same value as for the whole $T87(D \leq 20\ mpc)$. The corrected mass distribution is then obtained from the distribution $\mathcal{N}_e(\mathcal{M})$ by accounting for the dynamical state of the groups. The result is that the total number of groups including faint and bright objects is $\sum_j N_{est}(j) = 53$ and $max_j\{N_{est}(j)/\sum_k N_{est}(k)\} = 0.11$, which occurs for group number 22. The peak is not too high, in fact the significance of the KS comparison between $\mathcal{N}_c(\mathcal{M})$ and $\mathcal{N}_e(\mathcal{M})$ is $S = 0.999$ (see fig. 3.14), which indicates no difference. The quite high value of the ratio:

$$\frac{N_{obs}}{\sum_j N_{est}(j)} = 0.72 \tag{3.13}$$

is probably due to the high value of the completeness limit $m_c = 14.5$ of the catalogue, meaning that only few groups ($\sim 30\%$) are lacking because of their distance and low brightness. This result seems to indicate that the mass distribution of the $GH83(D \leq 20\ Mpc)$ groups is quite well representative of the groups' true mass distribution.

As a concluding remark I can say that, although I actually used the expression in eq. 3.18, other kinds of $n(D)$ have been tried. In particular power laws: $\rho_n(D_{Virgo}) \propto D_{Virgo}^{-2}$ where D_{Virgo} is the distance of groups from the centre of the Virgo cluster. This expression with $\nu = 2$ is suggested (Tully 1982; Yahil, Sandage and Tamman 1980) to describe the spatial distribution of galaxies around the Virgo cluster, but only within 10 Mpc from its centre. Other expressions for $\rho_n(\vec{r})$ were power laws with steeper and shallower values of ν, or depressed at high distances by an exponential cutoff. However all these sorts of law suffer from the unjustified assumption of spherical symmetry and continuity. It is shown, on the contrary, (Tully 1982) that the matter distribution around the Local Supercluster is clumped in clouds and flattened about a plane. Simple power laws are too poor an approximation to the observed distribution that can hardly be modelled in a satisfactory way by simple analytical expressions. It seems to me that a good solution to this problem is to adopt the empirical distribution of a quite rich catalogue in the examined region, namely the Tully catalogue. The procedure to recover lost groups was tested in the case of $T87(D \leq 20\ Mpc)$ assuming two possible values of the completeness limit m_c. The result was that for a deep enough value of m_c the procedure could give quite reliable results. Since the value of m_c is higher by two magnitudes (neglecting the correction for

absorption) than the value of the $T87$ sample it is likely that $\mathcal{N}_c(\mathcal{M})$ estimated for $GH83(D \leq 20\ Mpc)$ is actually a fair representation of the real mass distribution. In any case it does not differ from the observed distribution. The distribution of group mass corrected for the evolutionary effect and accounting for faint distant groups has the following statistical features: $min\{\mathcal{M}\} = 11.64$, $max\{\mathcal{M}\} = 14.63$, $mean\{\mathcal{M}\} = 13.11$, $st.dev.\{\mathcal{M}\} = 0.61$, $median\{\mathcal{M}\} = 13.15^{13.29}_{12.95}$, $Q_1 = 12.63$, $Q_3 = 13.63$.

3.2.5 Summary

Let me single out the main results of the above analysis:

- a non-negligible selection bias affects the catalogue and can be reduced below significant values by limiting the analysis out to 20 Mpc from us; the mass distribution of the main estimators shows a marginal stability relative to this cutoff; in any case the whole-catalogue distribution of masses is dominated by the distant fraction of $GH83$ groups for all estimators;

- the statistical analysis of groups in the nearby fraction and in the whole catalogue as well, seems to indicate that no significant difference exists between the mass distribution obtained using different estimators, i.e., all the considered estimators are homogeneous and show nearly the same statistical behaviour;

- the dynamical state of these groups is generally far from relaxation, in fact nearly 90% of the groups have not yet reached the virial equilibrium regime; however the correction accounting for unrelaxation does not alter the mass distribution;

- a tentative correction is introduced in order to recover the groups that are missed by the catalogue because of their great distance or low luminosity. The result indicates that nearly 70% of the whole number of groups present within 20 Mpc are observed, but this percentage depends on the assumed model for the spatial distribution of groups;

- the mass distribution seems to show good stability relative to the correction for lost groups, which means that it is likely to be a fair representation of the real mass distribution. This result holds independently of the model for the spatial distribution of groups.

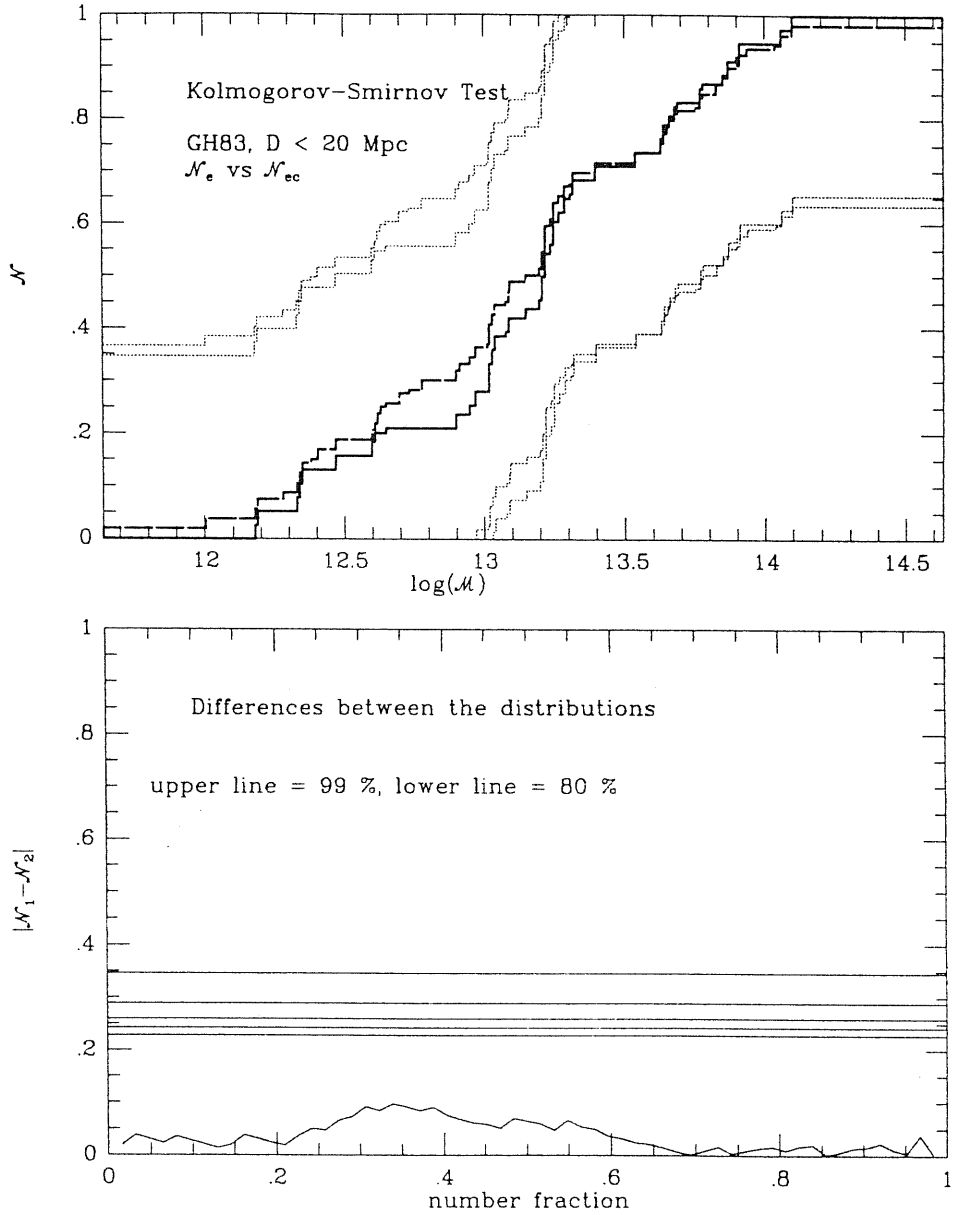

Figure 3.14: The KS test comparing the observed $\mathcal{N}_e(\mathcal{M})$ (solid) and corrected $\mathcal{N}_{ec}(\mathcal{M})$ (long-dashed) distributions

3.3 Analysis of T87 groups

3.3.1 Generalities

As reported in the previous chapter, T87 counts $N = 157$ groups distributed over all the unobscured sky and reaching a maximum distance of $D_{max} = 29 Mpc$. Since Tully (1987b) does not give the exact limits of the coordinate range covered by his catalogue, the solid angle $\mathcal{A}_{T87}$ and hence the volume $\mathcal{V}_{T87}$ are estimated quite roughly. We have that $\mathcal{A}_{T87} = 8.72\ sterad$, corresponding to $\sim 70\%$ of the whole sky. The volume spanned is then:

$$\mathcal{V}_{T87} = 7.1 \cdot 10^4\ Mpc^3 \tag{3.14}$$

and the average number density of observed groups is:

$$\bar{\rho}_n^{(obs)}(T87) = 2.2 \cdot 10^{-3}\ Mpc^{-3}. \tag{3.15}$$

The characteristic values of the available physical parameters for the $T87$ groups are listed in Tab. A.17, while the maps of groups' positions are shown in fig.s 3.15 and 3.16. In many cases some or all group members have unknown magnitude. In these cases the total observed luminosity L_{sg} accounts only for the members with known B_T^0, while it is zero if B_T^0 is missing for all members. The quoted values of L_{sg}, L_{min} and L_{max} refer only to the subset of groups having at least one member with known magnitude and hence $L_{max} > 0$. This subset counts $N_{obs}(L_{max} > 0) = 151$ groups[5]. Only six groups are completely lacking in B_T^0. On the other hand, if I consider only the subset containing groups with $L_{min} > 0$, so that all members have known values of B_T^0, I get $N_{obs}(L_{min} > 0) = 52$ -one third of the whole catalogue. No significant difference is found on comparing the mass distributions of all estimators in $T87(L_{min} > 0)$ and $T87$. In fact, the KS test for every mass estimator gives $S > 0.50$. The same result is obtained by comparing $T87(L_{min} > 0)$ and $T87(L_{max} = 0)$. It is then possible to deduce that faint members do not alter significantly the mass distributions of the $T87$ groups. This is due to the similarity of the mass distributions of groups containing only members with known magnitudes and the groups that also contain galaxies of unknown magnitude.

Because of the lack of magnitudes it is not possible to consider the luminosity-weighted parameters for the whole $T87$. In the case of $T87(L_{min} > 0)$ the whole set of weighted parameters is available. For this subset of bright groups the KS comparison between weighted and unweighted parameters indicates no significant dependence of the distribution on the adopted

[5]The parameters marked by a $\star$ in tabs. A.17, A.19, A.24, A.20 and A.22 refer to these groups.

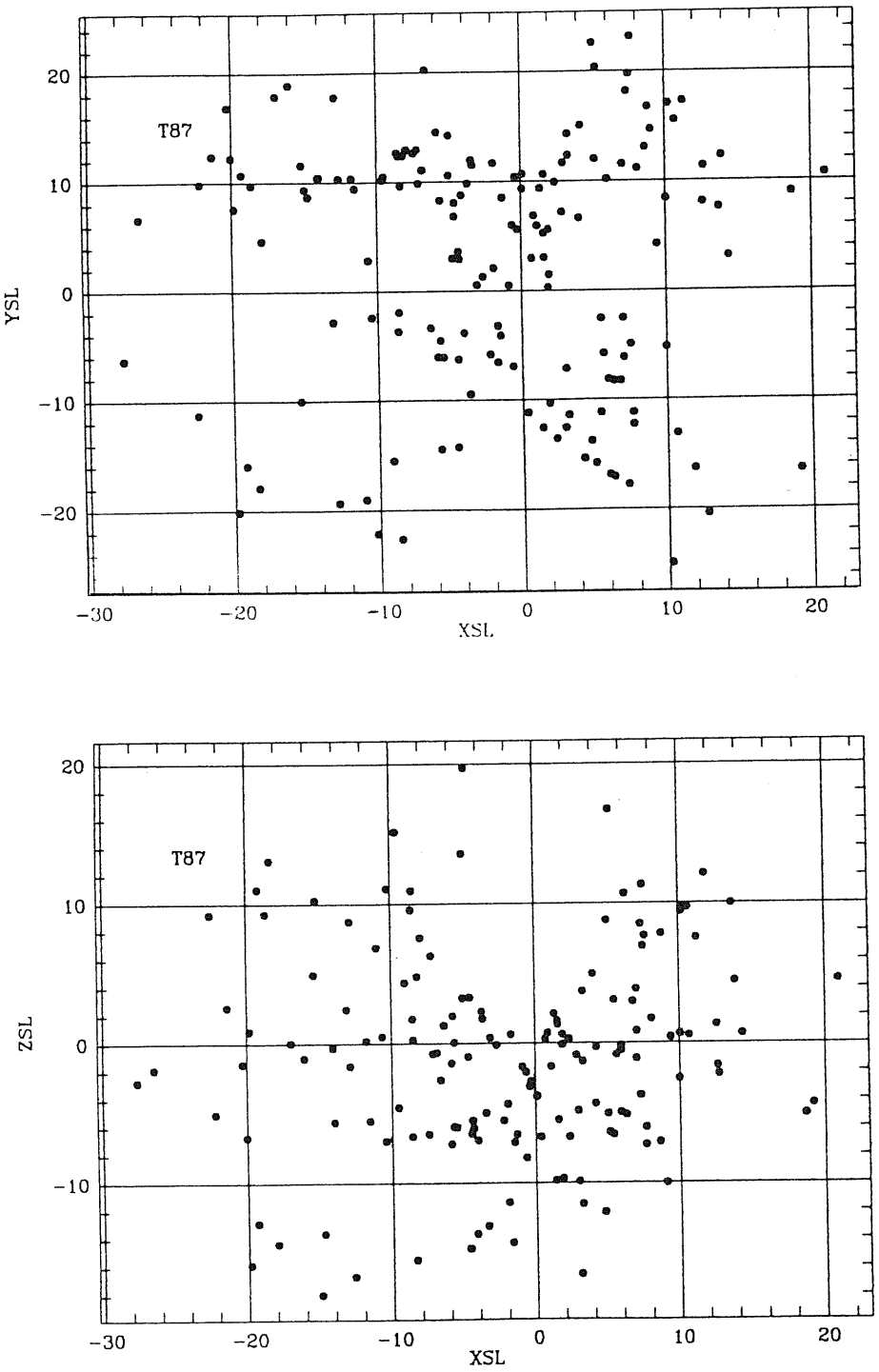

Figure 3.15: The T87 map in the supergalactic coordinate frame (part 1), the values of the coordinates are given in Mpc.

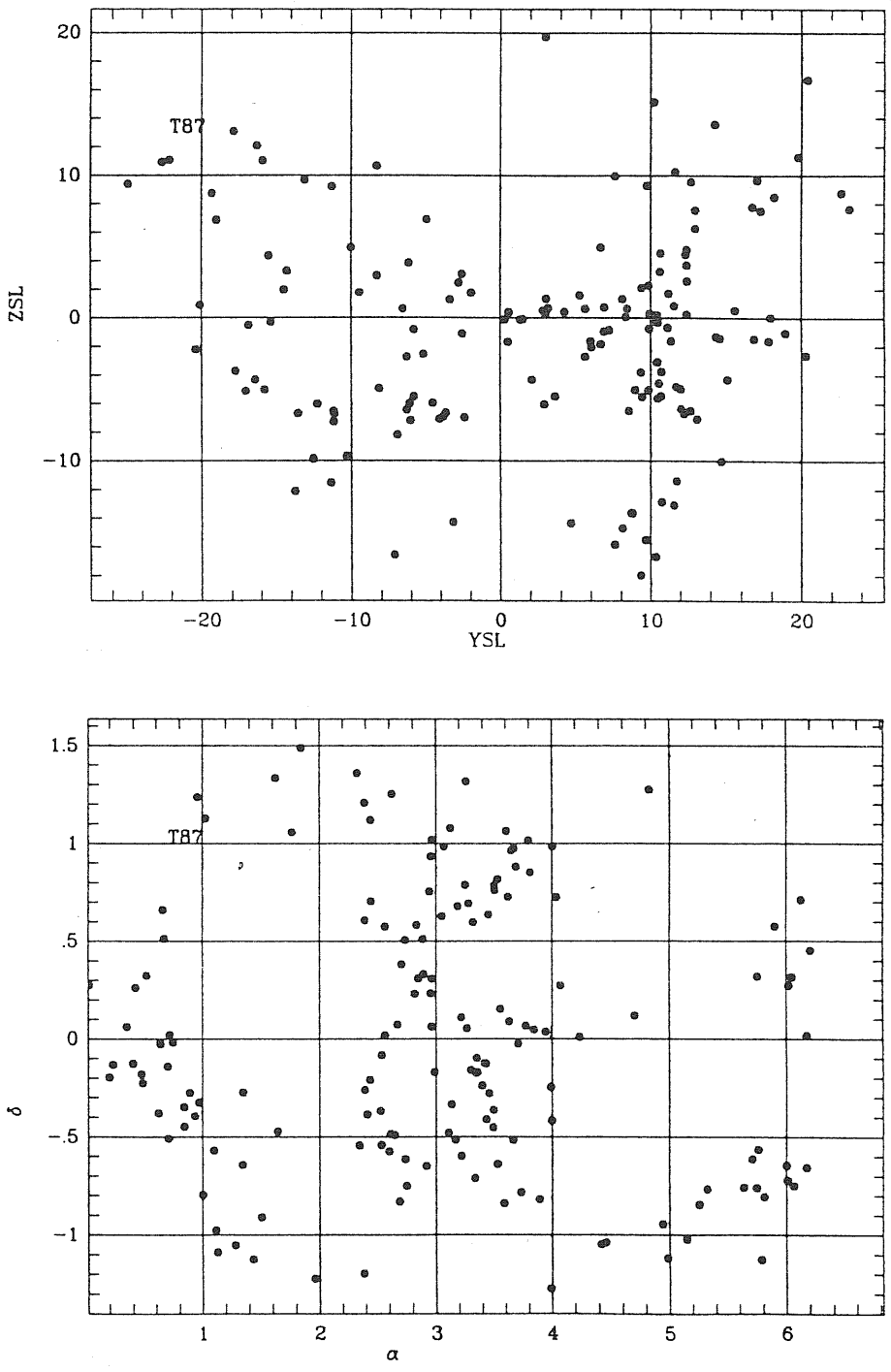

Figure 3.16: The T87 group coordinate maps (part 2). Upper graph: positions in the supergalactic coordinate frame (in units of Mpc. Lower graph: the (α, δ) map in units of rad.

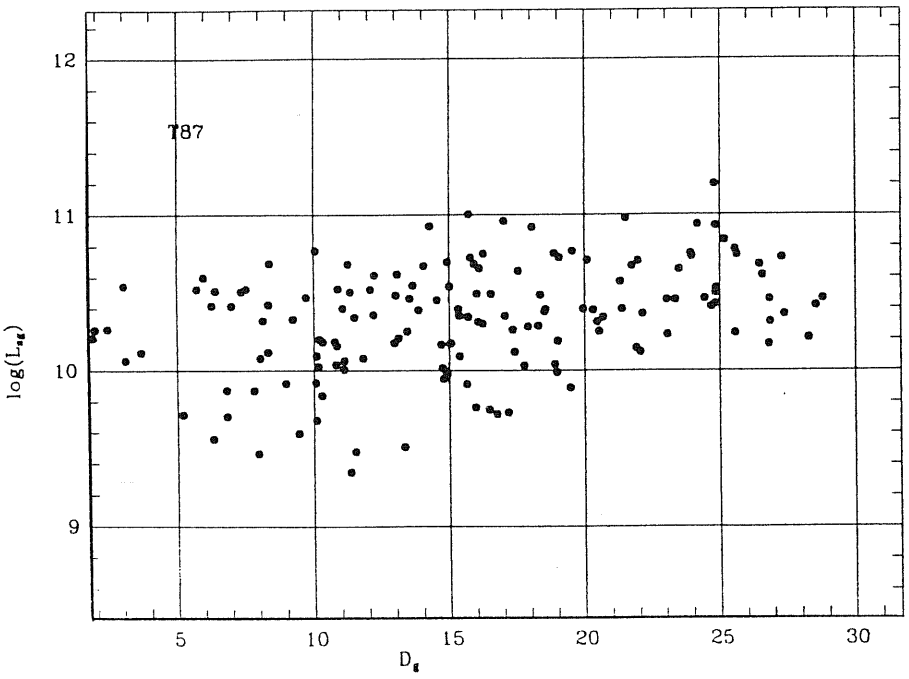

Figure 3.17: The group luminosity versus distance for the $T87$ groups.

weighting procedure, in agreement with the result I obtained for catalogues complete in magnitude (namely $GH83$ and $RGH89$). The stability of parameters against the weights w of luminosities can be due to the lack of morphological segregation in the $T87(L_{min} > 0)$ groups, or, more probably, to the particular population of these groups. In fact the median value of the spiral fraction is $n(S) = 0.61^{0.67}_{0.50}$, and $n(I.\&P.) = 0.00^{0.20}_{0.00}$, while $n(S0) = 0.18^{0.25}_{0.00}$ and $n(E) = 0.00^{0.00}_{0.00}$. These values indicate that the median fraction of galaxies with $T \leq -1$ having $w \geq 1$ is much smaller than later type galaxies having $w = 1$. For this reason I decided to benefit from the richness of the whole $T87$ catalogue and to avoid luminosity-weighted parameters.

It is worth noting that the KS comparison between $\log(\sigma_v)$ and $\log(V_n)$ is very high ($S = 1.00$) and so the correction for observational errors on the velocities is small.

From Tab. A.19 it seems that a strong observational bias is present as is indicated by the high value of the correlation coefficient $r[\log(L_{sg}), D_g] = 0.35$ with $S = 8.3 \cdot 10^{-6}$ (see also fig. 3.17. A non-negligible correlation with distance is also shown by the virial mass, the velocity dispersion and the virial radius. The author of the catalogue (Tully 1987b) pointed out that one of the two contributions to the galaxy sample is complete in B^0_T

within 3000 Km/s and the other is complete for galaxies of Sc type or later within 1500 Km/s and the incompleteness becomes significant above 2000 Km/s. I considered $T87(D \leq 20\ Mpc)$, the subcatalogue of groups within 20 Mpc, and found that $r[\log(L_{sg}), D_g] = 0.18$ with $S = 0.054$ and $N_{obs}(D \leq 20\ Mpc, L_{max} > 0) = 110$, while for $T87(D \leq 19\ Mpc)$: $r[\log(L_{sg}), D_g] = 0.16$ with $S = 0.096$ and $N_{obs}(D \leq 19\ Mpc, L_{max} > 0) = 106$ without significant differences in the other properties of the two subcatalogues. It seems that limiting the catalogue out to 20 Mpc reduces to a satisfactory amount the observational bias of L_{sg} with distance (see Tab. A.22). Unfortunately the correlation with distance shown by $\mathcal{M}_{Vu}$, σ_v and R_{Vu} is still significant although reduced. In order to obtain a negligible correlation for these parameters, the limit in distance must be lowered to 13 Mpc. In this case only 56 groups form the nearby fraction of the catalogue. Moreover, no significant difference is found between the mass distribution of groups within 20 Mpc and 13 Mpc. So the limit in distance does not alter significantly the mass distribution of the nearby fraction of the catalogue. It is also worth noting also that no significant difference is found between the mass distribution of groups in $T87(D \leq 13\ Mpc)$ and the whole catalogue. This is in agreement with the similar conclusion about the stability of the mass distribution with respect to the limit in distance. It seems better to accept the presence of a bias in the mass and to have the same distance limit for all the catalogues instead of reducing this limit and so losing statistical resolution and the opportunity to compare the nearby fractions of different catalogues.

3.3.2 Analysis of groups physical parameters

Considering only groups within 20 Mpc, it is possible to reduce below the 95% significance level the observational bias and still have a large fraction of the whole catalogue, namely $N_{obs}(D \leq 20\ Mpc) = 113$ with $N_{obs}(D \leq 20\ Mpc, L_{max} > 0) = 110$ and $N_{obs}(D \leq 20\ Mpc, L_{min} > 0) = 35$. The volume occupied by $T87(D \leq 20\ Mpc)$ is

$$\mathcal{V}_{T87(D \leq 20\,Mpc)} = 2.3 \cdot 10^4\ Mpc^3 \tag{3.16}$$

and the average number density of observed groups is:

$$\bar{\rho}_n^{(obs)}[T87(D \leq 20\ Mpc)] = 5.0 \cdot 10^{-3}\ Mpc^{-3}. \tag{3.17}$$

In Tab. A.20 the main statistical values of $T87(D \leq 20\ Mpc)$ are listed, while Tab. A.24 indicates the stability of group parameter distributions between $T87$ and the nearby fraction. From the values of S it is possible to deduce that the observational bias, although non-negligible, does not affect

significantly the statistical properties of the $T87$ groups. For this reason the results of the analysis in the case of the whole $T87$ will also be reported.

In Tab. A.23 the results of the pairwise KS comparison between different mass estimator distributions are reported. No significant difference is indicated, except for the case of the average mass $\mathcal{M}_{Av}$ that shows a significantly different behaviour, but is of little relevance as already explained (see page 42). The group mass distribution has the same statistical properties independent of which estimator is used, in agreement with the results obtained in the other catalogues. This conclusion also holds for the whole $T87$. The comparison between the virial mass $\mathcal{M}_{Vu}$ and the projected mass $\mathcal{M}_P$[6] distributions is shown in fig. 3.18. Applying the KW test to the distributions of all mass estimators I obtained for $T87(D \leq 20\ Mpc)$ a significance $S = 0.08$, while excluding the average mass the significance is $S = 0.68$. In the case of $T87$ I have $S = 0.008$ for all five mass estimators, while $S = 0.57$ if the average mass is excluded. This confirms the results obtained using the KS pairwise comparison and indicates that, except for the average mass, the set of mass estimators has the same underlying distribution. A second relevant test concerns the evolutionary state of groups. By use of the method described in §1.4.7 and assuming $\Omega = 0.2$, I checked the hypothesis of virialization of the $T87$ groups. The results indicate that a large fraction of groups are undergoing dynamical evolution. In fact $\sim 80\%$ of the $T87(D \leq 20\ Mpc)$ groups have $\tau \leq 3 \cdot \pi = 9.42$ and hence are falling in the unrelaxed region of the $\alpha(\tau)$ curve. As a consequence of this fact the distribution of mass corrected for dynamical evolution $\mathcal{N}_e(\mathcal{M})$ is significantly different from the observed distribution $\mathcal{N}_{obs}(\mathcal{M})$ (see fig. 3.19). This is due to the distribution of α, in fact the median value is $0.31^{0.34}_{0.27}$, correspondingly the median of the correction factor μ for the mass is $1.60^{1.83}_{1.46}$.

It is interesting to note also that the first and third quartiles of the correction factor are respectively 1.23 and 2.33. This means that 75% of the $T87$ groups have their mass increased by a factor ≥ 1.23. Then it is clear that the effect of the correction is not negligible. The same conclusion is reached for $T87(D \leq 20\ Mpc)$: the mass corrected for the non-virialization effect is significantly larger than the observed value computed on the assumption that groups are virialized. The main statistical values of the distribution of the corrected mass, α, τ and μ are listed in Tabs. A.25 and A.26 and illustrated in figs. 3.20 and 3.21. A different situation is produced by assuming $\Omega = 1$. In this case we again have that a large fraction of groups is in the pre-virialization phase, but μ is smaller than that obtained in the $\Omega = 0.2$ case. In fact, comparing the observed and

[6]Tully (1987b) advises to use $f_P = 20/\pi$ instead of $32/\pi$ (see eq. 1.137) in the expression of the projected mass estimator. However He also point out that the virial and projected mass estimators show differences quite small relative to their uncertainties. Hence I preferred to use the same expression for the projected mass estimators for all catalogues.

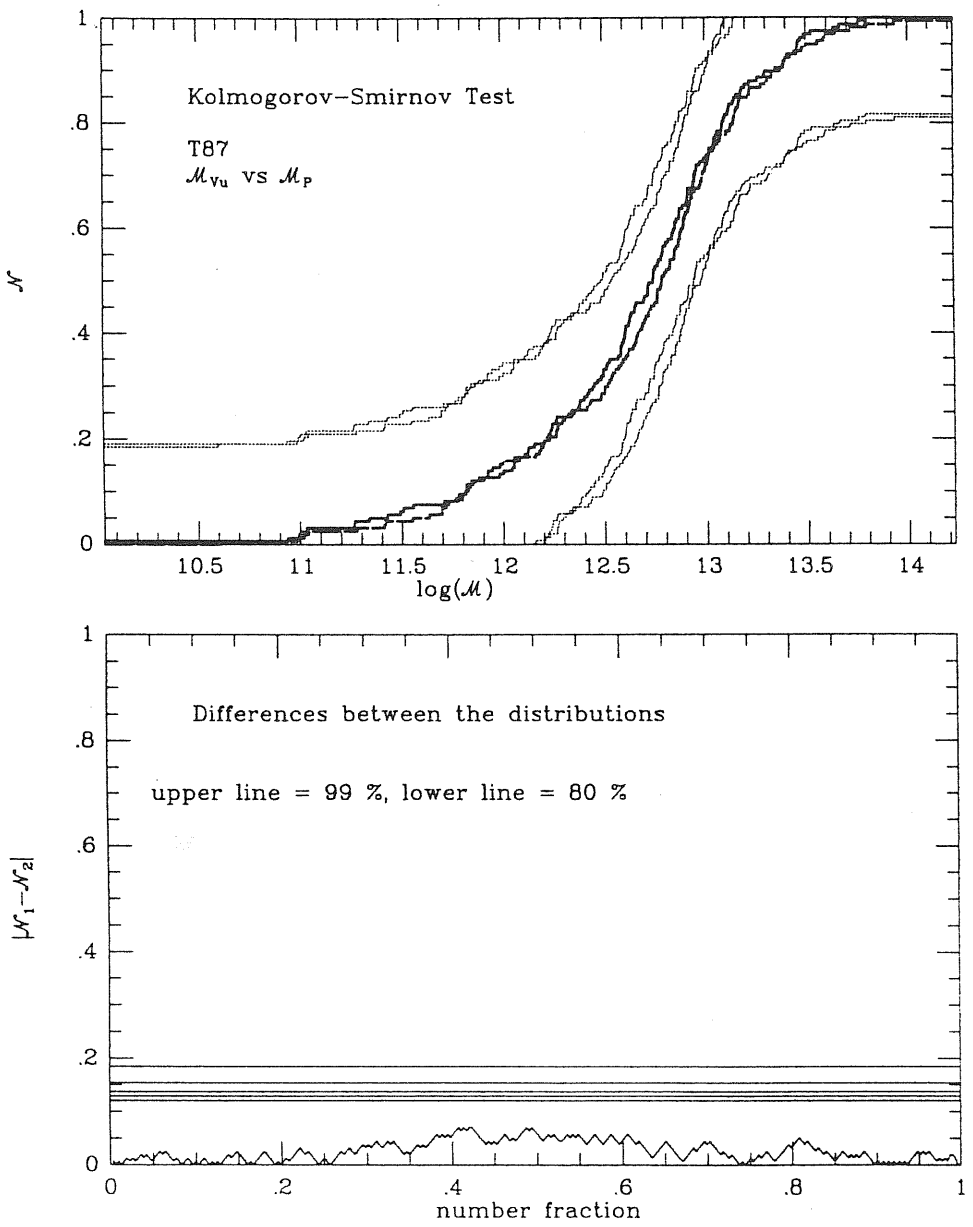

Figure 3.18: The KS comparison between the virial mass $\mathcal{M}_{Vu}$ (solid line) and the projected mass $\mathcal{M}_P$ (long-dashed line) distributions for the $T87$ groups.

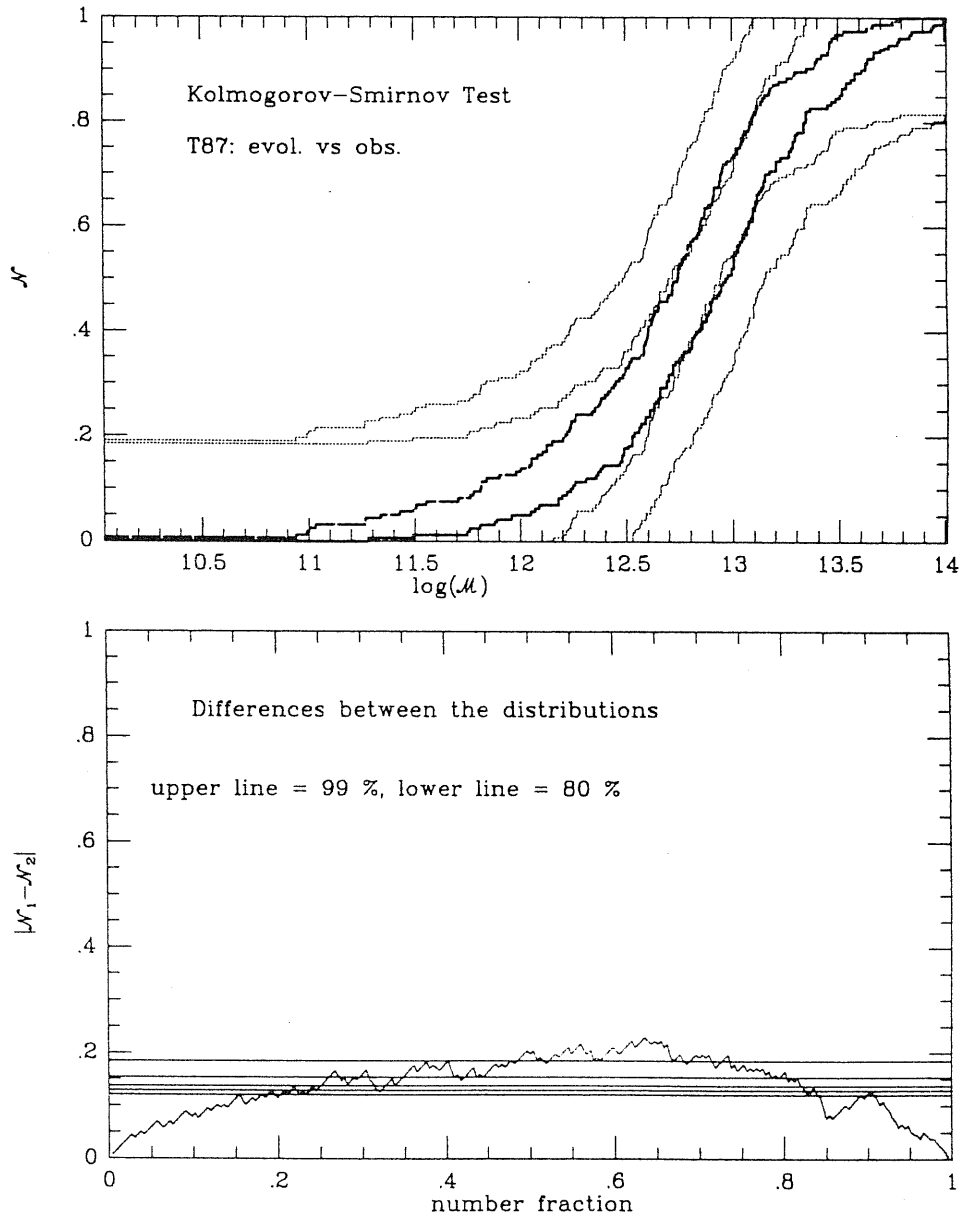

Figure 3.19: The KS comparison between the observed (long-dashed line) and evolutionary corrected (solid line) mass distributions of the $T87$ groups for $\Omega = 0.2$.

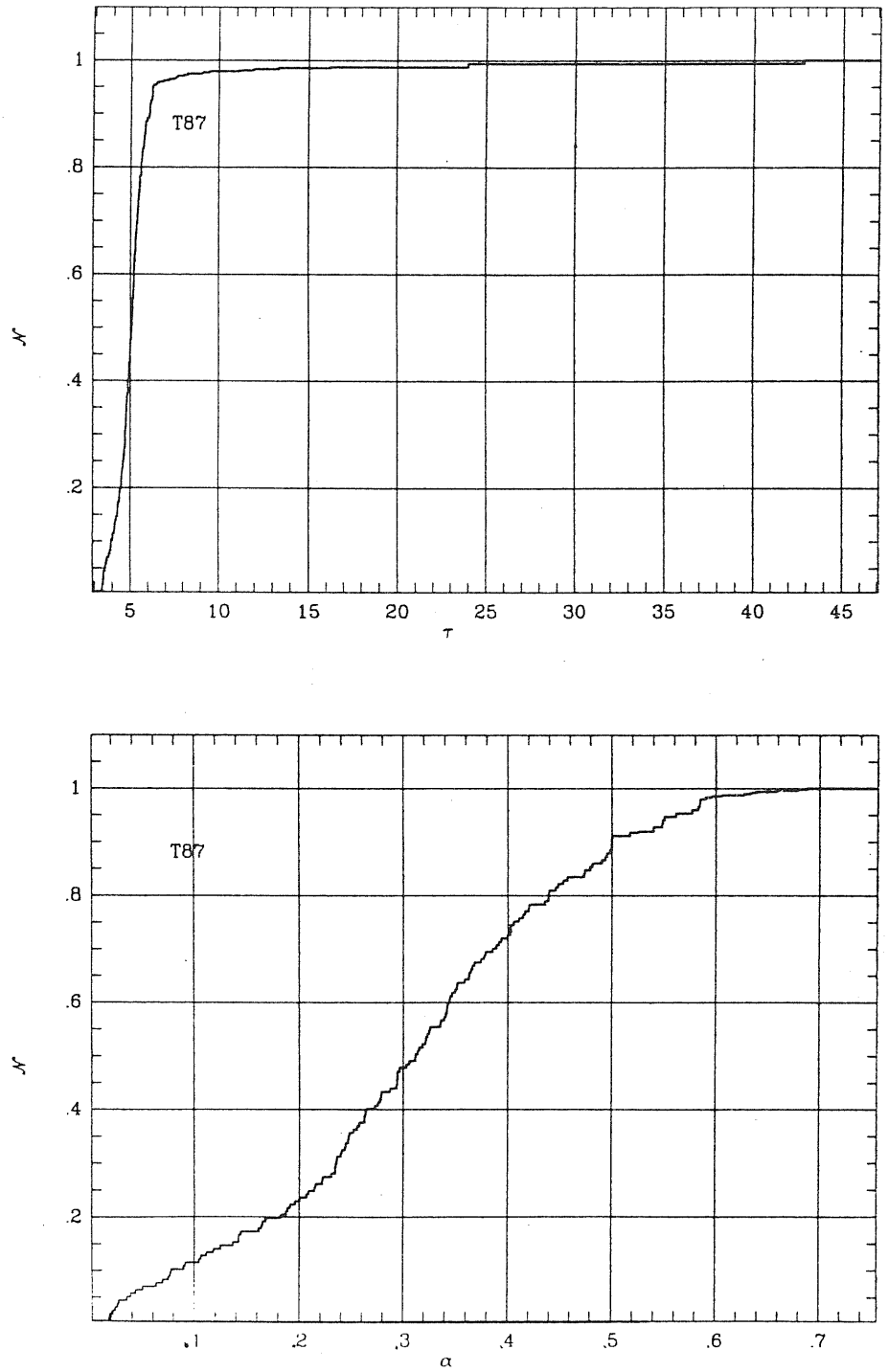

Figure 3.20: The distributions of the dynamical state τ (upper) and of the virial α (lower) for the $T87$ groups in the case $\Omega = 0.2$.

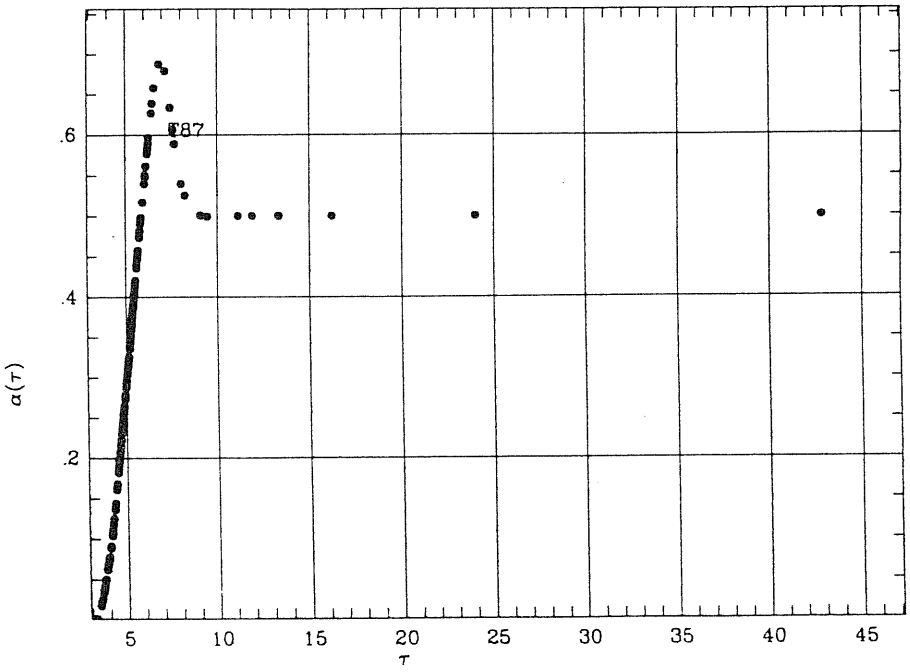

Figure 3.21: The curve $\alpha(\tau)$ for the $T87$ groups for $\Omega = 0.2$.

corrected mass distributions assuming $\Omega = 1$ for the $T87$ groups, the KS test gives a significance value $S < 10^{-3}$. Running the same test for the $T87(D \leq 20\ Mpc)$ groups, I obtained $S < 10^{-3}$ in agreement with the result for $\Omega = 0.2$. In any case if we compare the corrected mass distributions obtained for $T87$ using 0.2 and 1 for Ω we obtain $S = 0.39$. The same comparison for $T87(D \leq 20\ Mpc)$ gives $S = 0.44$, indicating in both cases no significant difference. On the other hand, for τ, α and μ the difference is significant for both $T87$ and its nearby fraction. These results are reported in Tab. A.28. It seems that the extent of the evolutionary correction relative to the observed mass distribution is dependent on the value assumed for Ω, but the corrected distribution is insensitive to the value of Ω. For this reason I consider only $\mathcal{N}_c(\mathcal{M})$ for $\Omega = 0.2$ as for the other catalogues.

3.3.3 A test of the procedure to recover faint distant groups

I considered the following test in order to determine the reliability of the procedure to recover low luminosity groups that might be missed by the observations in a magnitude complete galaxy sample. Let us take $T87(D \leq 20\ Mpc)$ and the claimed completeness of the galaxy sample with the limit

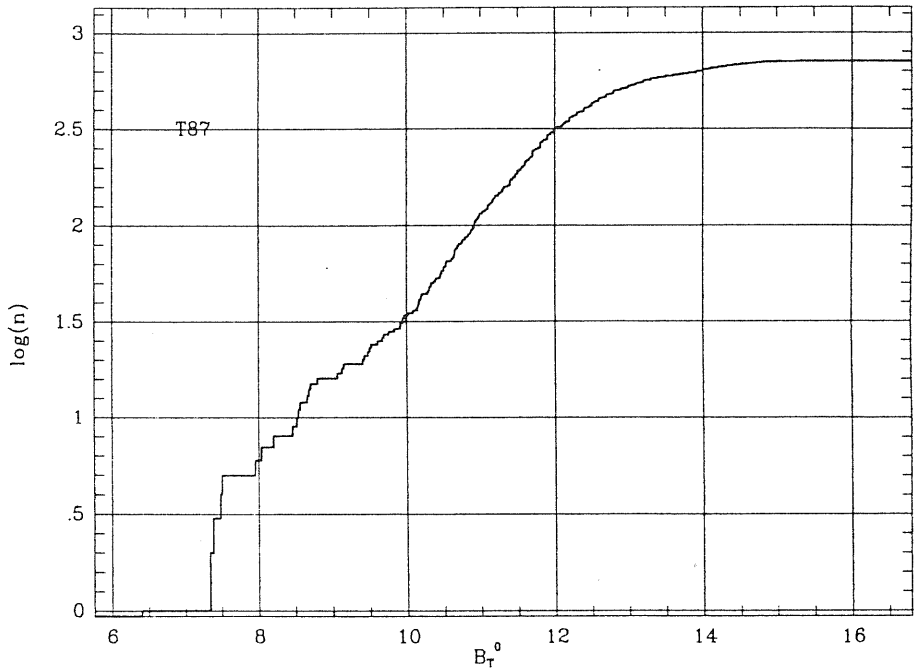

Figure 3.22: The B_T^0 magnitude distribution for the $T87$ galaxies.

$B_T^0 \leq m_c = 12$. This value is poorly determined as appears from fig. 3.22, and in fact the author himself suggested a value of $m_c = 12.5$ in a paper published in 1988 (Tully 1988) about the luminosity function of the NGB catalogue. Both values of m_c are considered here.

Now it is reasonable to ask what mass distribution $\mathcal{N}_{obs}^{(m_c)}(\mathcal{M})$ we would observe in the case that only the galaxies brighter than m_c were present in the groups or, in other words, what we would have as the mass distribution if only the complete fraction of the galaxy sample were considered. Using the KS test we can compare $\mathcal{N}_{obs}^{(m_c)}(\mathcal{M})$ with $\mathcal{N}_{obs}(\mathcal{M})$ for each mass estimator. The results are reported in Tab. A.29 and shown in fig. 3.23 for the virial mass $\mathcal{M}_{Vu}$. Note that the number of groups surviving the $m_c = 12$ cutoff is $N_{obs}^{(12)} = 40$, and $N_{obs}^{(12.5)} = 54$. From the results of Tab. A.29 it is possible to see that only $\mathcal{M}_{Vu}$ and $\mathcal{M}_{Av}$ are stable against the exclusion of faint galaxies. The other estimators show quite a strong sensitivity to the value of m_c([7]) and hence to the presence of faint galaxies. It is now possible to apply the procedure to recover lost groups to $\mathcal{N}_{obs}^{(m_c)}(\mathcal{M})$ in order to test the effect of the correction relative to the observed distribution $\mathcal{N}_{obs}(\mathcal{M})$. To this aim we need a model for the spatial distribution of groups within

[7] Nearly the same conclusion holds if the whole $T87$ is considered.

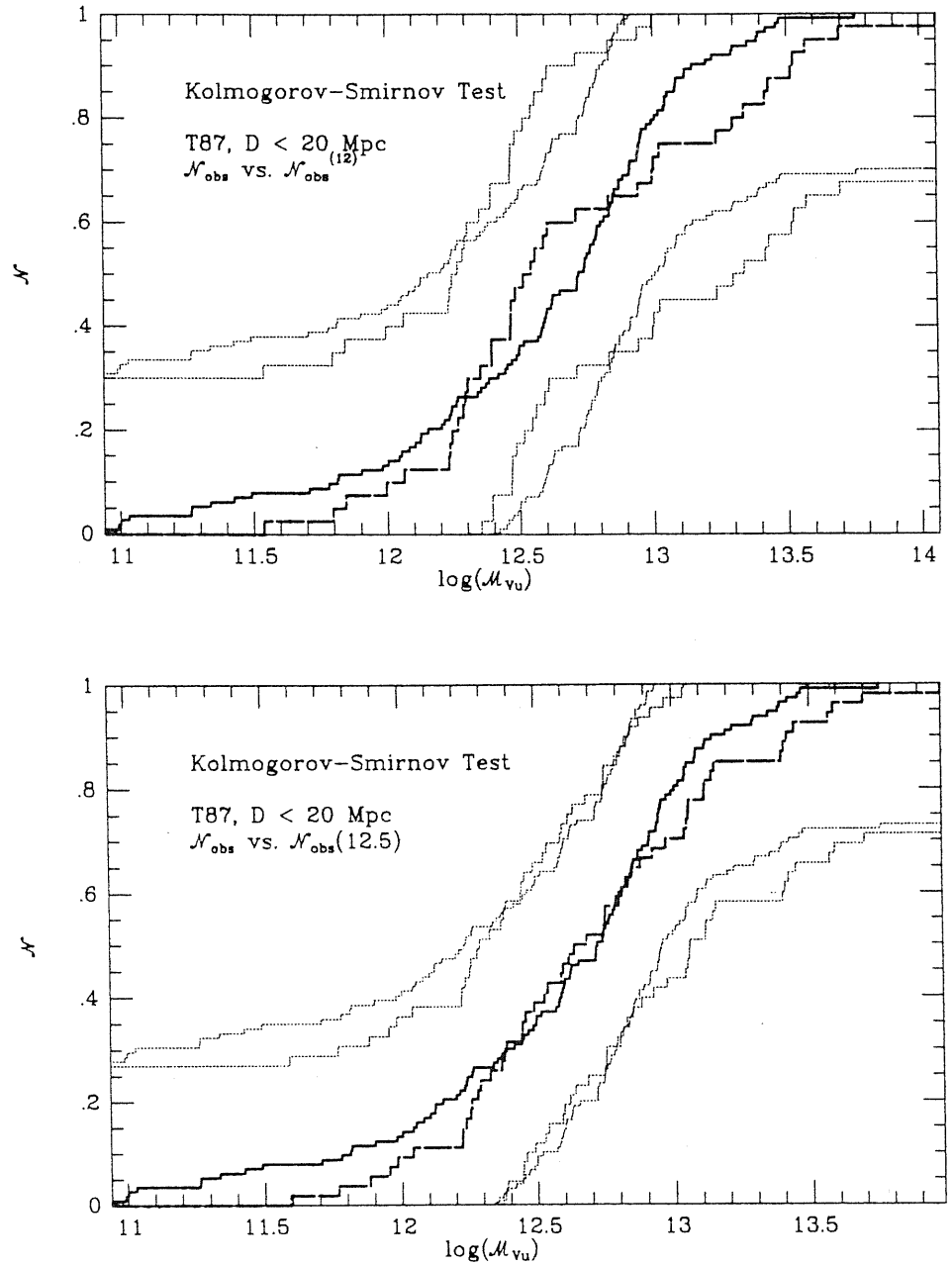

Figure 3.23: The KS comparison between the observed mass distribution $\mathcal{N}_{obs}(\mathcal{M}$ (solid line) and the distribution $\mathcal{N}_{obs}^{(m_c)}(\mathcal{M})$ (long-dashed line) obtained excluding faint members of $T87$ groups for $\mathcal{M}_{Vu}$ and $m_c = 12$ (upper) and $m_c = 12.5$ (lower).

the considered volume ($D \leq 20\ Mpc$). This information comes from the distribution of $T87(D \leq 20\ Mpc)$ groups that can be described by the empirical law:

$$n(D) = n_0 \cdot \arctan\left[\left(\frac{D}{D_0}\right)^{\nu}\right], \tag{3.18}$$

where $n(D)$ is the fraction of groups lying within a distance D from us, $D_0 = 20\ Mpc$ and $\nu = 2$ are parameters obtained from fitting the observed distribution and shown in fig. 3.24. Using this relation we can estimate the number of groups that should be present within $D_\star = 20\ Mpc$ but that are missed because of the limit in magnitude at m_c. For the j^{th} group with visibility distance $D_g^{(v)}(j) \leq D_\star$ the total estimated number of such groups is:

$$N_{est}(j) = \frac{\rho_n(D_\star)}{\rho_n[D_g^{(v)}(j)]} \geq 1. \tag{3.19}$$

Therefore we can estimate the corrected mass distribution $\mathcal{N}_c^{(m_c)}(\mathcal{M})$ by spreading the $N_{est}(j)$ values of the group mass around the value of the mass observed for the j^{th} group following the same procedure described in §3.2.4. Let us first compare $\mathcal{N}_c^{(m_c)}(\mathcal{M})$ with $\mathcal{N}_{obs}^{(m_c)}(\mathcal{M})$ in order to see the effect of the correction relative to the complete-sample distribution. The values of the significance of the KS test for various mass estimators are reported in Tab. A.30. It is possible to say that the recovery procedure is quite effective in estimating the total number of groups for both values of m_c, in fact $\sum_j N_{est}(j, m_c = 12) = 119$ and $\sum_j N_{est}(j, m_c = 12.5) = 110$. When comparing the real observed mass distribution $\mathcal{N}_{obs}(\mathcal{M})$ with the estimated distribution $\mathcal{N}_c^{(m_c)}(\mathcal{M})$ corrected for faint distant groups, a good agreement is found for $\mathcal{M}_{Vu}$ and $\mathcal{M}_P$, while a marginal agreement is shown by $\mathcal{M}_{Me}$ and $\mathcal{M}_{Av}$ on the assumption that $m_c = 12.5$. On the other hand, if $m_c = 12$, only $\mathcal{M}_{Vu}$ shows a marginal agreement, while for all other estimators the agreement is not good. In other words, the real distribution $\mathcal{N}_{obs}(\mathcal{M})$ is fairly estimated only for the most stable mass estimator in particular $\mathcal{M}_{Vu}$, and only in the case of $m_c = 12.5$ (see Tab. A.31 and fig. 3.25). The procedure gives a reliable estimate of the real distribution only in the case that the magnitude limit is deep enough so that the fraction of members that are lost is not so high as to significantly alter the distribution of the most sensitive mass estimators such as $\mathcal{M}_P$. This can also be explained by noting that a low value of the completeness limit leads to a distribution in $N_{est}(j)$ that is strongly peaked around the value of the group having the smallest $D_g^{(v)}$. In the case that the value of the mass of the group with a high value of $N_{est}(j)$ is far enough from the median of the sample mass, the corrected distribution will be significantly altered by this high value of the weight N_{est} relative to the observed distribution. If, on the the other hand, the value of m_c is deep enough, then the highest value of $N_{est}(j)$ is not so

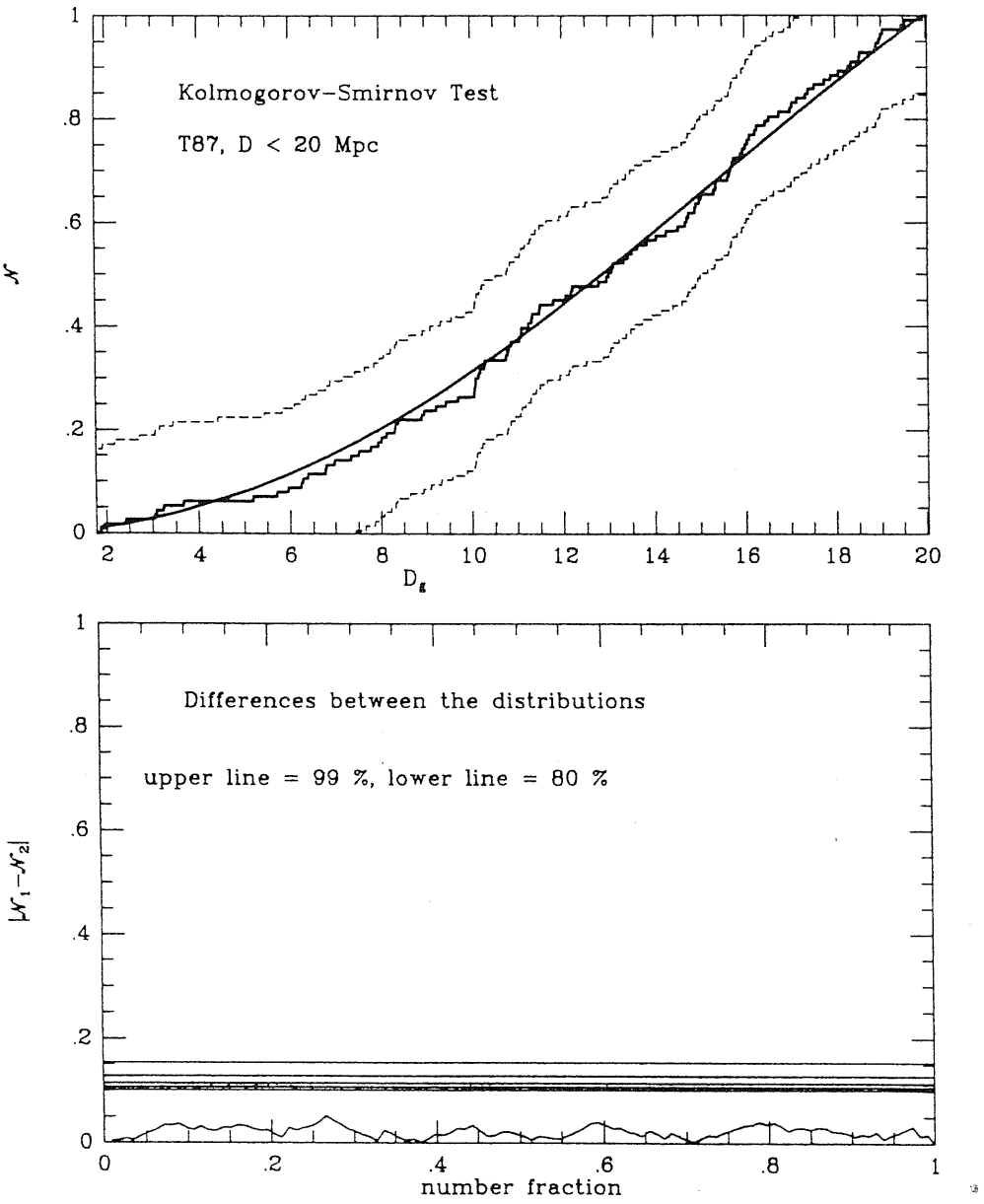

Figure 3.24: The spatial distribution of the $T87(D \leq 20\ Mpc)$ groups.

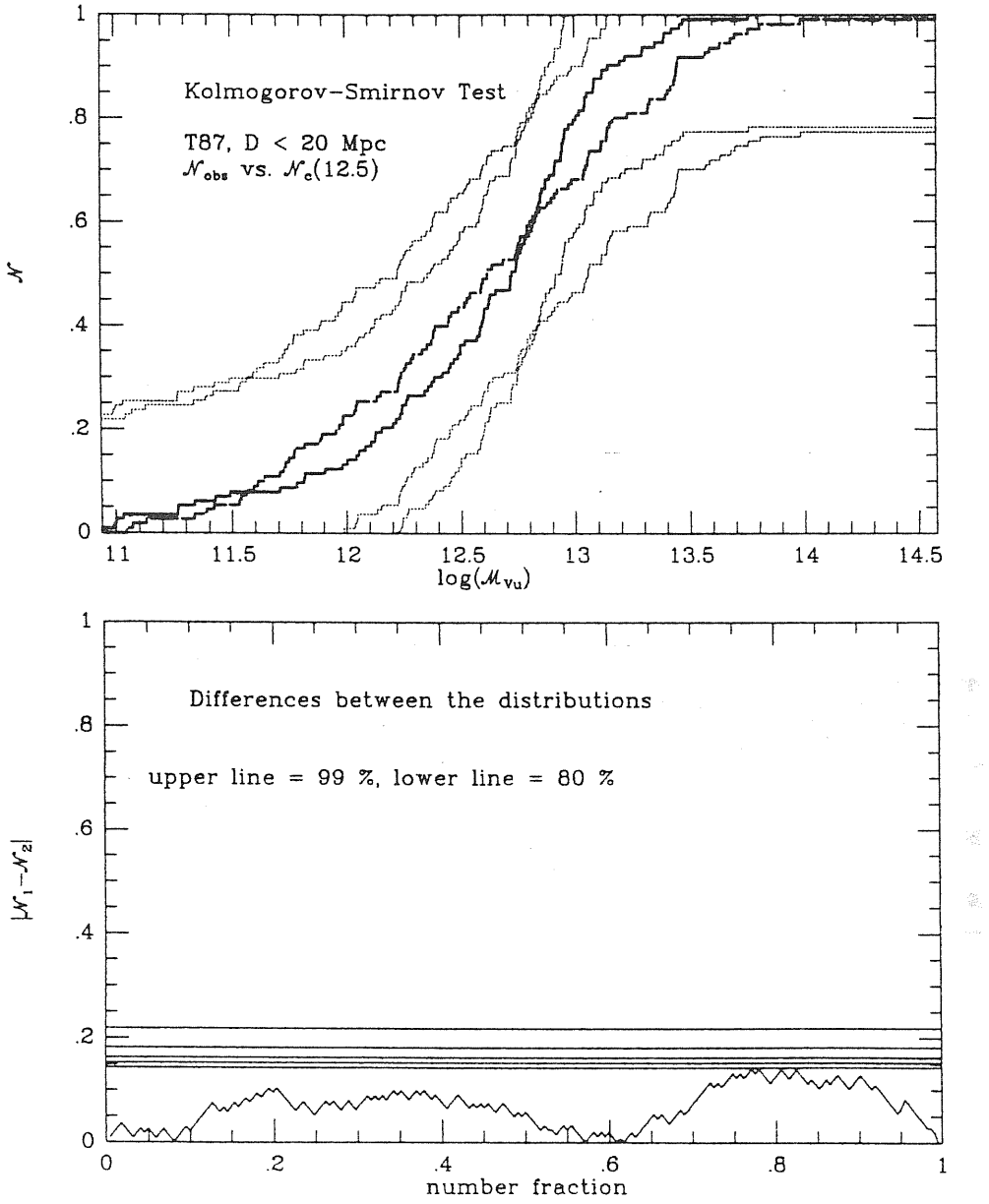

Figure 3.25: The KS comparison between the observed mass distribution $\mathcal{N}_{obs}(\mathcal{M})$ (solid line) and the distribution obtained from the faint distant groups recovery procedure $\mathcal{N}_c^{(m_c)}(\mathcal{M})$ for $\mathcal{M}_{Vu}$ and the $T87(D \leq 20\ Mpc)$ groups.

large and the correction to the magnitude-complete observed distribution of group mass is not significantly altered. In general, the value of N_{est} depends more strongly on the visibility distance $D_g^{(v)}$ rather than on the law assumed for $\rho_n(D)$ or $n(D)$. It might also be argued that a high value of N_{est} for a group having a mass smaller than the sample median may recover the low-mass tail of the real distribution, but the rather weak though significant correlation between the mass and total luminosity does not support this point of view.

In conclusion it is possible to say that the method discussed here is likely to work reliably as long as the magnitude limit is deep enough. If the completeness limit m_c is unknown, a good indication of the reliability of the corrected distribution may be obtained by analysing the stability of mass distributions relative to the inclusion or exclusion of galaxies fainter than m_c. On the other hand, the good stability shown by $\mathcal{M}_{Vu}$ offers a good way out of the problem, avoiding assumptions about m_c and $n(D)$.

3.3.4 Summary

The main results obtained for the $T87$ groups are:

- a significant bias is present in the observed properties of groups and can be reduced (to an acceptable level) by considering only groups within 20 Mpc. However the effect of the bias is very weak because of the fact that the mass distribution of groups results quite stable with respect to the limit in distance for various values of this limit;

- the observed mass distribution is independent of the estimator used, in agreement with the results of other catalogues, so that all the considered mass estimators give homogeneous mass distributions;

- nearly 90% of groups do not satisfy the virialization condition but are in a regime of strong dynamical evolution preceding virial equilibrium; the correction accounting for the unrelaxed dynamical state of groups significantly alters the mass distribution independent of the value assumed for Ω;

- a test of the procedure to recover groups missed by observations because of their low luminosity seems to indicate that, assuming $m_c = 12.5$ as the completeness limit for the galaxy sample, the procedure works quite well.

3.4 Analysis of V84 groups

3.4.1 Generalities

This is a quite rich catalogue and the characteristics of the galaxy sample from which it is obtained are described in §2.6. The supergalactic coordinate map is shown in figs. 3.26 and 3.27. The solid angle covered by V84 amounts to $\mathcal{A}_{V84} = 4.51$ *sterad* roughly estimated by the (α, δ) map (fig. 3.27) and corresponding to $\sim 36\%$ of the whole sky. The depth of V84 is similar to T87: $D_g \leq 32\ Mpc$,

The volume spanned is then:

$$\mathcal{V}_{V84} = 4.9 \cdot 10^4\ Mpc^3 \tag{3.20}$$

and the average number density of observed groups is:

$$\bar{\rho}_n^{(obs)}(V84) = 2.2 \cdot 10^{-3}\ Mpc^{-3}. \tag{3.21}$$

The main parameters of groups and their statistically relevant values are listed in Tabs. A.32 and A.33.

Here the luminosity-weighted quantities are missing since the value of the magnitude is not available for each group member[8]. Moreover, the galaxy sample is not complete. From fig. 3.28 it is possible to notice that the logarithm of the counts deviates from a straight line (corresponding to a complete sample) near $B_T \sim 12$, but this value is not very well determined. For this reason the corrections applied in the case of GH83 are not possible for V84. An idea of the observational bias is obtained by considering the correlation of the main parameters and the distance. The Spearman correlation coefficients r and their significance S are reported in Tab. A.34. It is important to notice the value of r for the pair $(\log(L_s), D_g)$: $r = 0.43$ and its significance $S = 2.1 \cdot 10^{-6}$ that indicates a strong bias with distance (see fig. 3.29). In agreement with the procedure adopted in the previous analysis, if I consider only groups within 20 Mpc from us the former values of r and S are reduced to: $r = 0.21$ and $S = .055$ which are within an acceptable range, although the correlation is still marginally significant. The stability of the mass estimators and of other physical parameters relative to the distance limit is rather strong as is indicated by the results in Tab. A.39. The correlation of the mass $\mathcal{M}_{Vu}$ with distance is reduced by the limit in distance, but is still significant. The same holds for the virial radius, while for the velocity dispersion the correlation is weakly significant in the nearby fraction of the catalogue. On the other hand, if I consider a smaller volume

[8]Recall that in V84 galactic magnitudes are in the B_T system and without correction for absorbtion, so that the suitable conversion factors are to be used in order to compare the quoted luminosities with other catalogues.

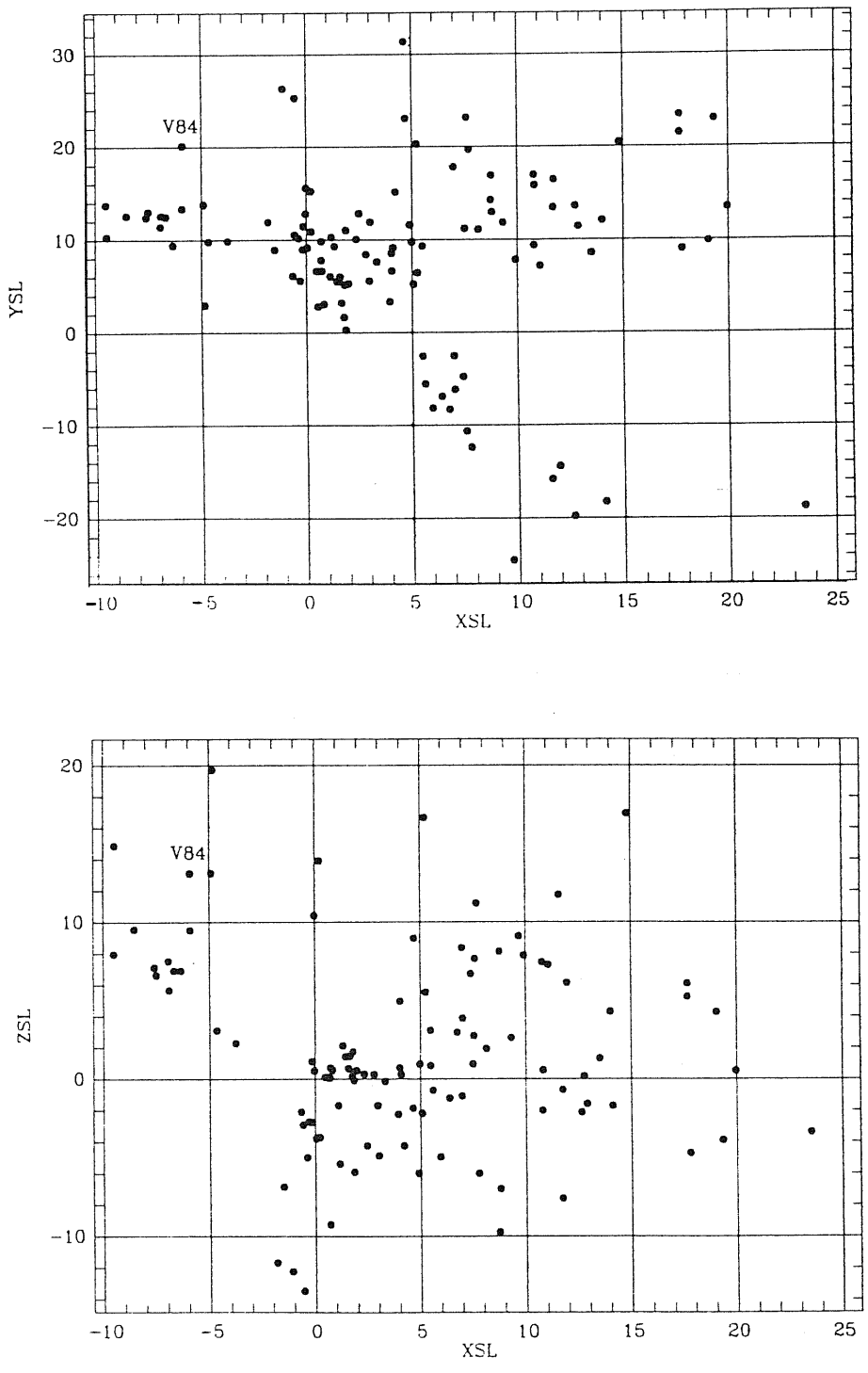

Figure 3.26: The V84 map in the supergalactic coordinate frame (part 1); the values of the coordinates are given in *Mpc*.

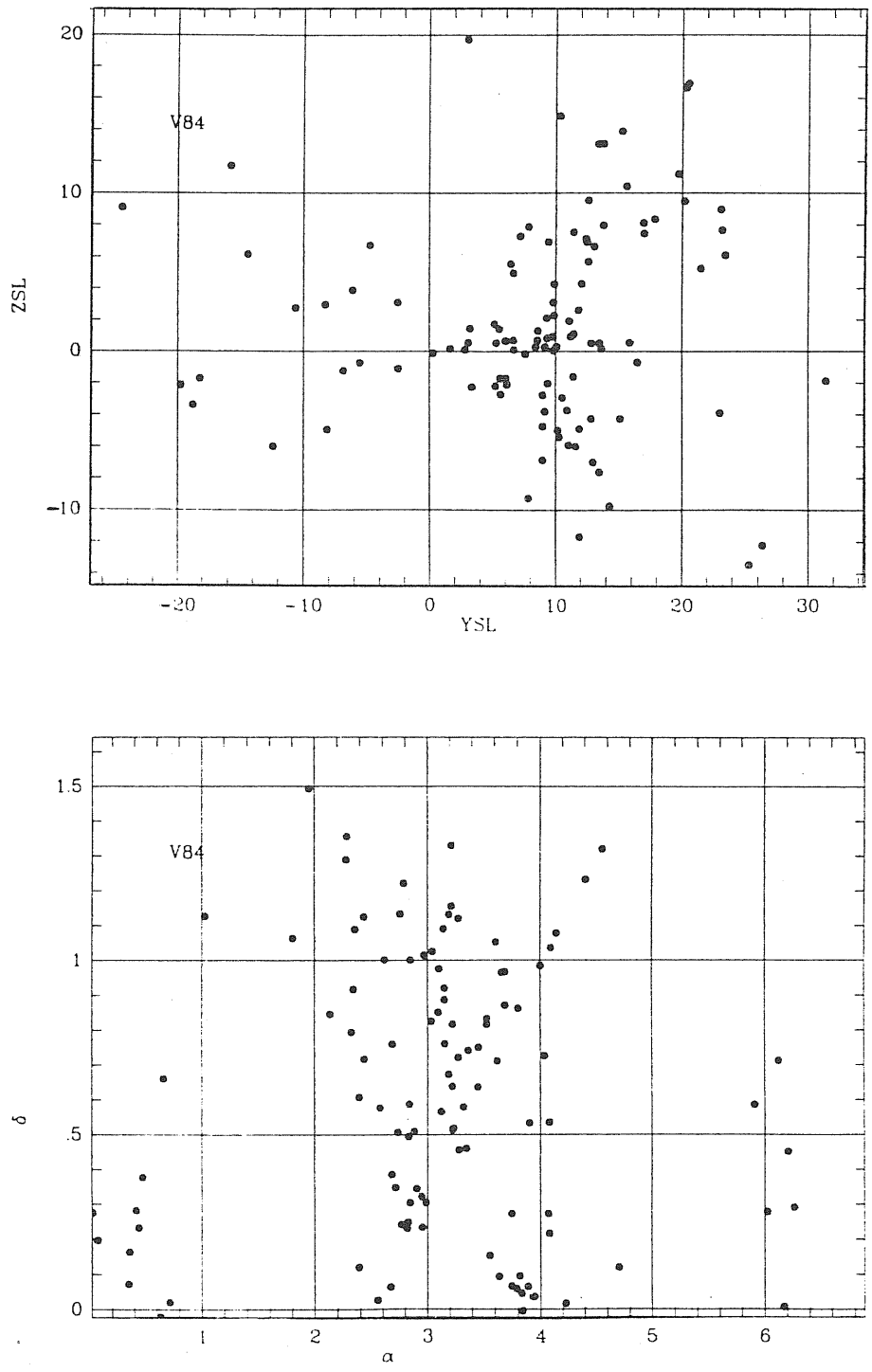

Figure 3.27: The V84 group coordinate maps (part 2). Upper graph: positions in the supergalactic coordinate frame in units of Mpc. Lower graph: the (α, δ) map in units of rad.

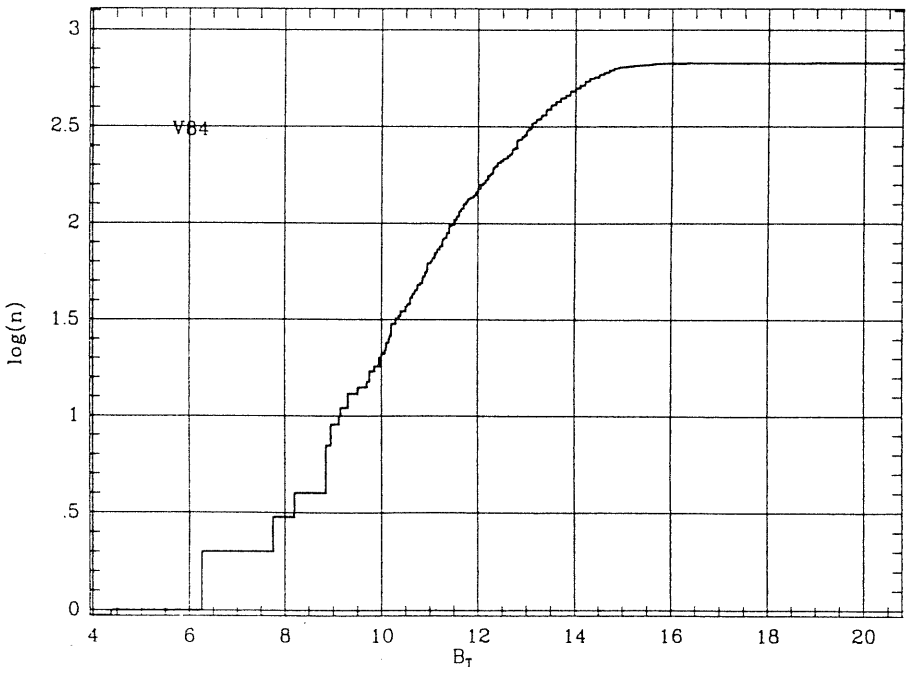

Figure 3.28: The B_T magnitude distribution for the $V84$ galaxies.

as for example $D \leq 15\ Mpc$ the available number of groups decreases to 58, the bias is more effectively reduced but I would lose nearly one half of V84 and no significant difference occurs between the parameter distributions of groups within 20 Mpc and 15 Mpc. No significant difference is found between the distributions of main parameters comparing the whole $V84$ and $V84(D \leq 15\ Mpc)$, hence the stability of the parameters relative to the limit in distance is rather strong and the effect of the observational bias can be considered weak to a good level of significance. As is concluded in the analysis of the $T87$ groups, the limit at 20 Mpc is a good compromise among the necessity to reduce the bias, to have a rich nearby fraction of the catalogue and the opportunity to compare the nearby fractions of different catalogues.

3.4.2 Analysis of groups physical parameters

The values of group parameters and correlations for the nearby fraction of V84 (hereafter $V84(D \leq 20\ Mpc)$) are listed in Tabs. A.36, A.37 and A.35. The volume spanned is then:

$$\mathcal{V}_{V84(D\leq 20\ Mpc)} = 1.2 \cdot 10^4\ Mpc^3 \tag{3.22}$$

and the average number density of observed groups is:

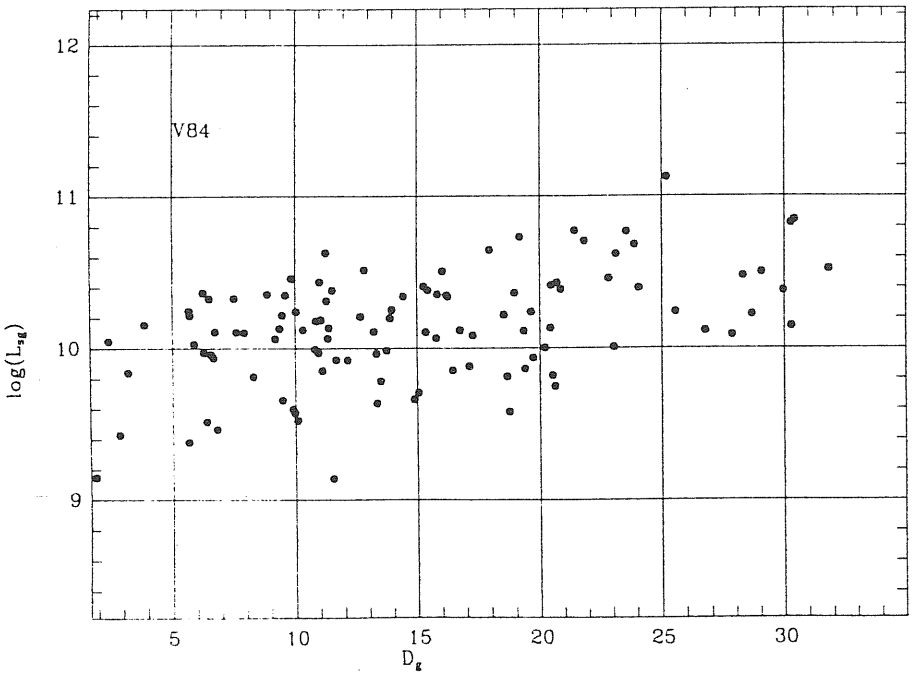

Figure 3.29: The group luminosity versus distance for the $V84$ groups.

$$\bar{\rho}_n^{(obs)}[V84(D \leq 20\ Mpc)] = 6.8 \cdot 10^{-3}\ Mpc^{-3}. \tag{3.23}$$

The number of groups in $V84(D \leq 20\ Mpc)$ is, in fact, 82: a large fraction of the whole catalogue. For this reason it is unlikely that the distributions of the parameters of groups in V84 and $V84(D \leq 20\ Mpc)$ are very different. In fact this is confirmed by a KS analysis (see Tab. A.39).

A first crucial point is the dependence of the observed distribution on the particular mass estimator. Again the KS analysis confirms with good statistical significance the irrelevance of the choice of the estimator. The result of this test on both V84 and $V84(D \leq 20\ Mpc)$ is reported in Tab. A.38. It appears clearly that in every case S is larger than any critical level (i.e., 0.01, 0.05, 0.10), leading to the conclusion that no evidence of variation exists between each pair of distributions. The KS comparison between the virial mass $\mathcal{M}_{Vu}$ and the projected mass $\mathcal{M}_P$ is shown in fig. 3.30. It is worth noting that the smallest values of S are obtained when one of the members of the pair is $\mathcal{M}_{Av}$ indicating that this is probably less reliable than other estimators. The same conclusion is reached on applying the KW test. In fact, for the whole $V84$ the KW significance is $S = 0.49$ and for $V84(D \leq 20\ Mpc)$ $S = 0.58$. These values indicate that the hypothesis that all mass estimators have the same underlying distribution is true.

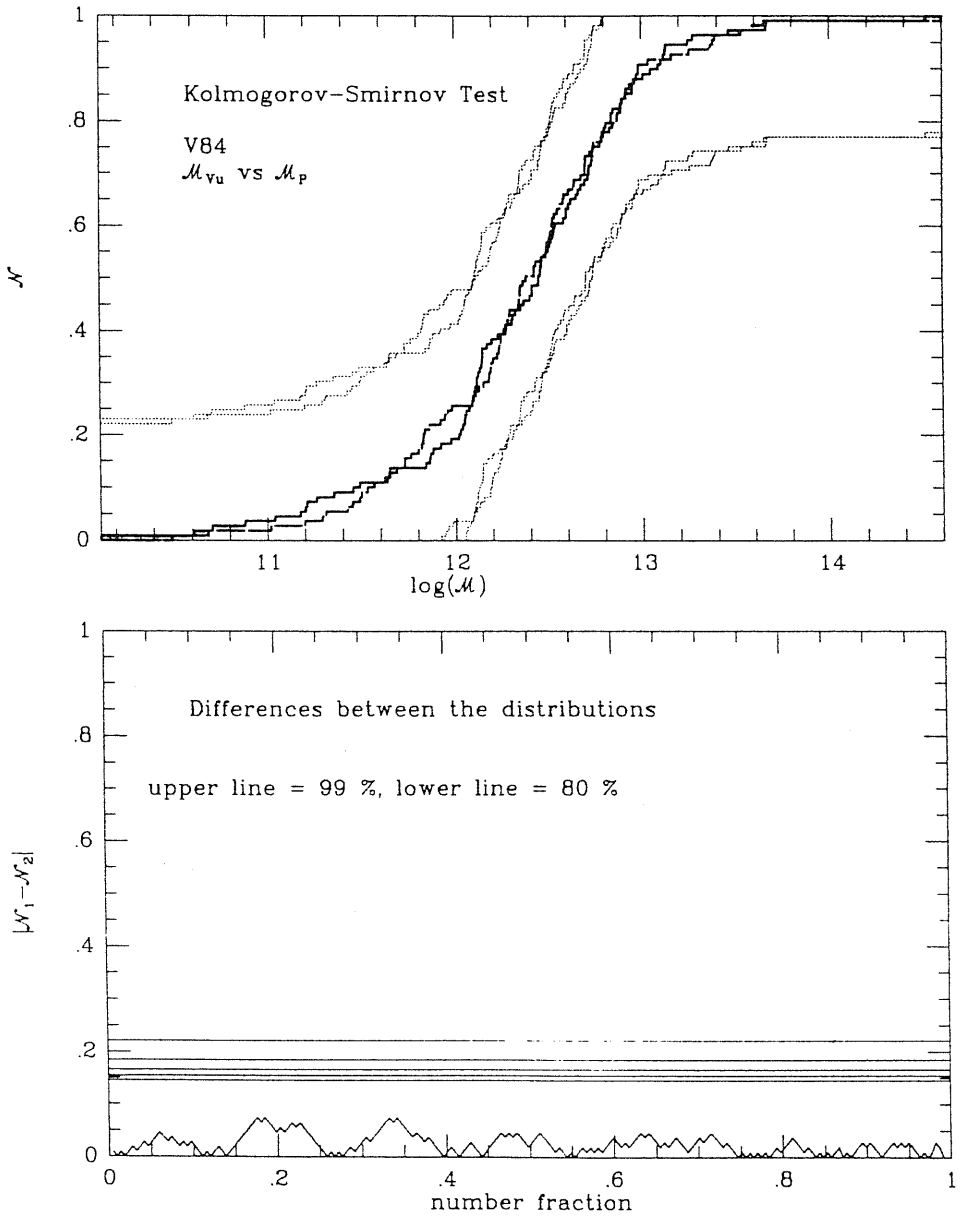

Figure 3.30: The KS comparison between the virial mass $\mathcal{M}_{Vu}$ (solid line) and the projected mass $\mathcal{M}_P$ (long-dashed line) distributions of $V84$ groups.

The unweighted virial mass $\mathcal{M}_{Vu}$ is taken as representative, and this is the particular mass estimator I refer to when considering the mass of groups in general.

For the sake of completeness I applied the same test to the fully corrected velocity dispersion σ_v and the observed velocity dispersion V_n. The conclusion is again that no significant difference exists between these estimators either in the $V84$ or in the $V84(D \leq 20\ Mpc)$ groups. The significance of the KS test is $S = 1.00$ for both V84 and $V84(D \leq 20\ Mpc)$.

I applied to $V84(D \leq\ Mpc)$ the test concerning the correction to the virial mass due to the non-stationary dynamical state of groups. Comparing in the usual way the observed and evolutionary-corrected mass distributions it results that there exists a non-negligible difference between the two distributions as is shown in fig 3.31. The significance of the difference is $S = 0.04$ for $V84(D \leq 20\ Mpc)$ and $S = 0.04$ for the whole of $V84$ (see Tabs. A.42). The median value with 99% confidence limits of $\log(\mathcal{M}_{Vu})$ is $12.50^{12.68}_{12.37}$ for $V84(D \leq 20\ Mpc)$ and $12.59^{12.75}_{12.43}$ for $V84$. The statistical features of other parameter distributions are reported in Tabs. A.40 and A.41. From the positions occupied by groups on the $\alpha(\tau)$ curve and the distribution of τ (see figs. 3.32 and 3.33) it appears that only a few of them are in the virialized regime, while approximately 95% of the groups (considering the whole catalogue) are undergoing dynamical evolution and have $\tau \leq 3\pi$.

These results are obtained with $\Omega = 0.2$, but comparing to what is found for $\Omega = 1$ I obtained no relevant change in the results for the mass distribution (see Tab. A.43). It is then more correct to refer to the evolutionary-corrected mass distribution since it seems that the hypothesis of stationary state is not satisfied, at least for these groups.

In the case of V84 the lack of completeness in magnitude does not allow us to perform the correction for lost groups as was done for GH83. In effect I tried to obtain a fictitious sample complete in magnitude by excluding from V84 all the galaxies with unknown or too weak magnitude, taking a limit from visual inspection of fig. 3.28 at $m_c = 12$ or 12.5. Then I applied the correction in the way described for GH83, but the results showed that the distribution estimated by this correction is close to the initial one and that it is close to the original uncleaned catalogue distribution as long as the clearing procedure does not alter significantly the distribution of the mass. In conclusion, it is more correct to consider the original uncleaned catalogue instead of introducing other assumptions which are not tested and which do not appreciably improve the resulting information.

3.4.3 Summary

About V84 groups it is possible to say:

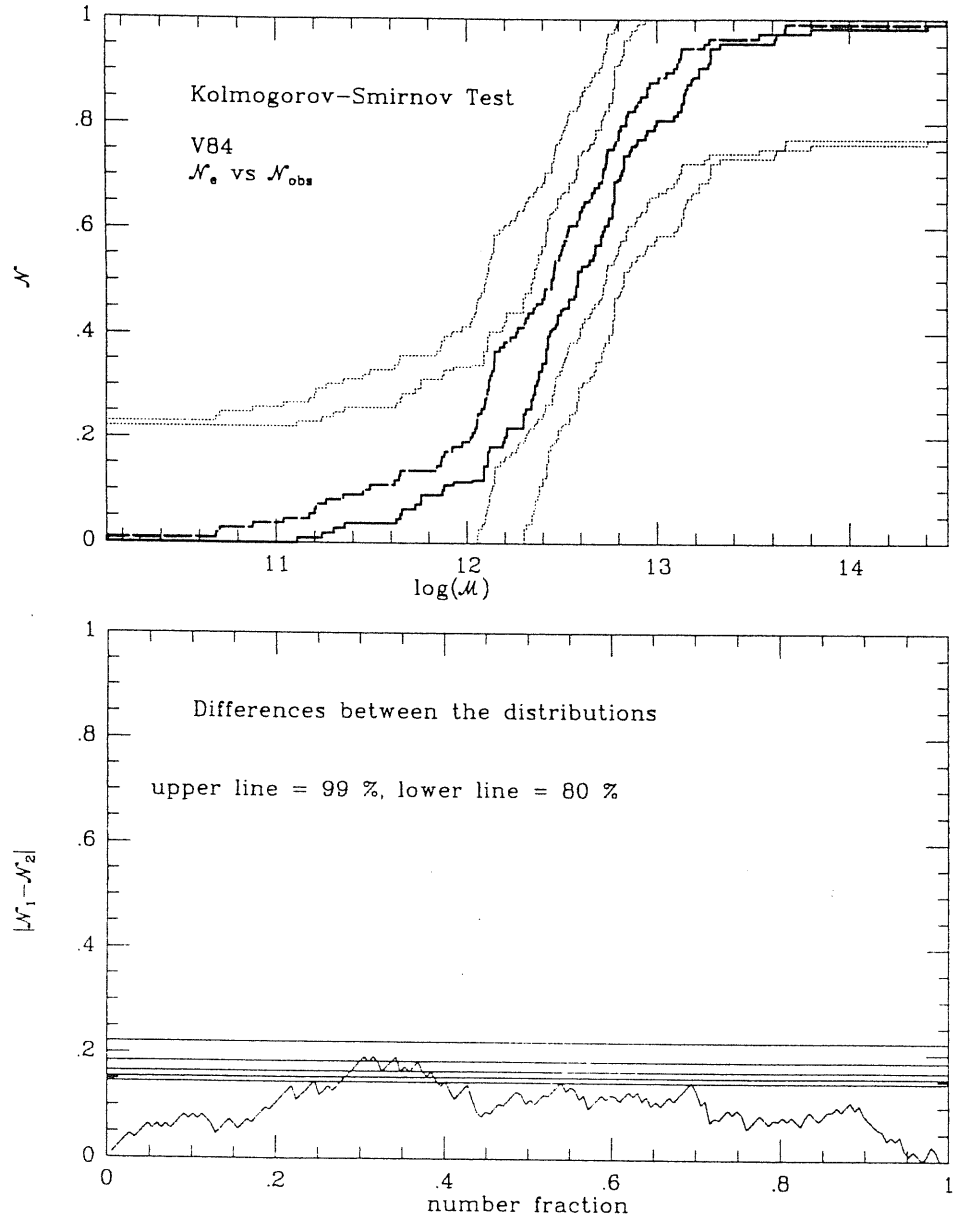

Figure 3.31: The KS comparison between the observed (long-dashed) and evolutionary corrected (solid) mass distribution of the $V84$ groups ($\Omega = 0.2$).

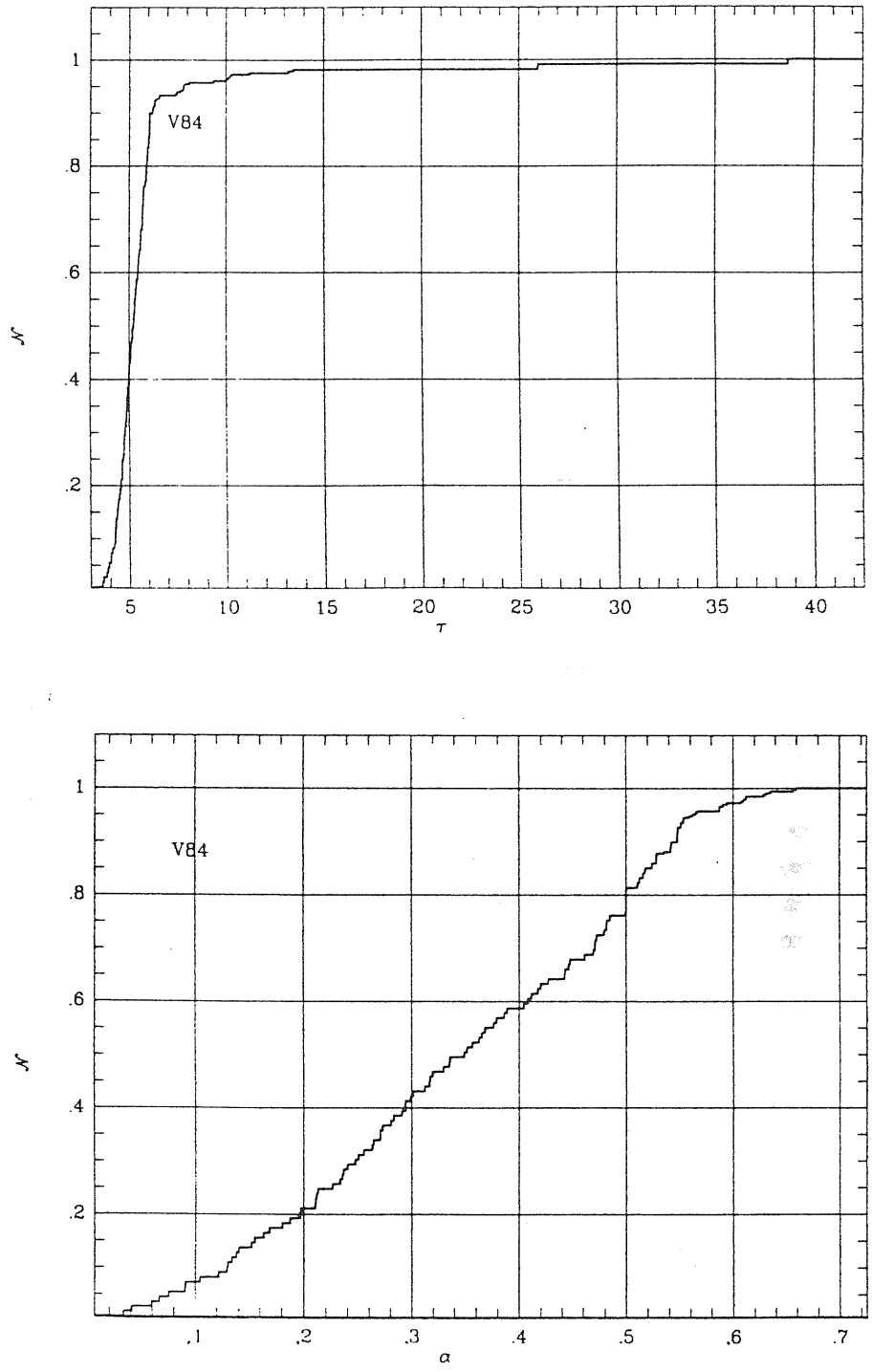

Figure 3.32: The distribution of the dynamical state τ (upper) and the virial α (middle) for the $V84$ groups for $\Omega = 0.2$.

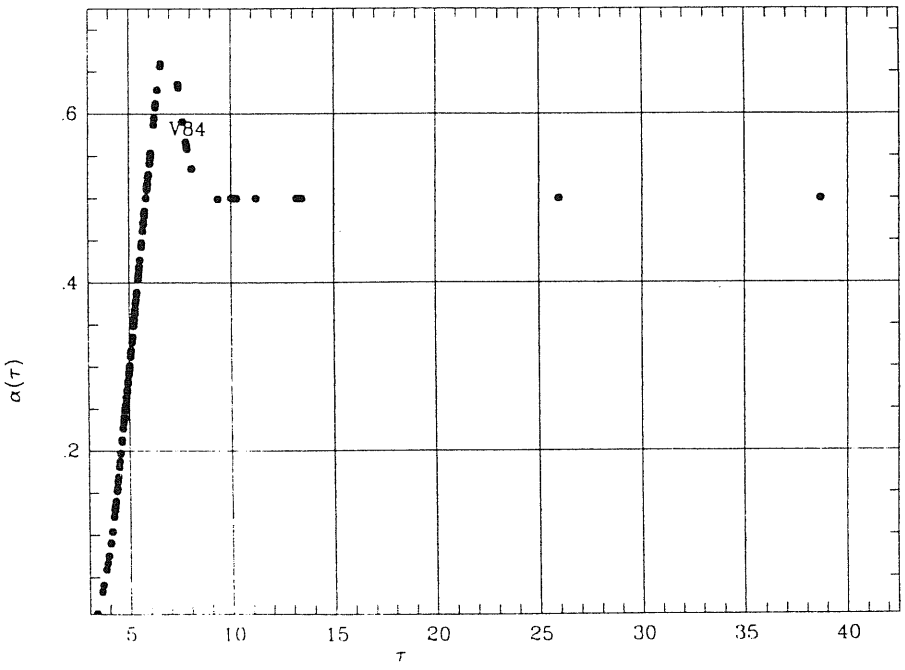

Figure 3.33: The curve $\alpha(\tau)$ for the $V84$ groups for $\Omega = 0.2$.

- the catalogue is affected by observational bias, but limiting the analysis out to 20 Mpc from us reduces this bias to an acceptable level; in any case for all parameter distributions no difference is found between the nearby fraction and the whole catalogue;
- the observed mass distribution seems to show no sensitivity to the particular estimator used, so it is possible to say that all mass estimators are homogeneous;
- the assumption of stationariness in the dynamics of groups seems not to be verified by approximately 95% of the examined groups, in fact the dynamical state of these groups lies in a range characterized by strong evolution, consequently the mass distribution corrected in order to account for non-virialization significantly differs from the observed one; this result holds for two different values of Ω.

3.5 Analysis of $RGH89$ groups

I report here the results obtained from the analysis of RGH89 groups. This catalogue comprises $N_{obs} = 49$ groups of the first slice of the whole

Ramella et al. (1989) catalogue. They are distributed out to quite a large distance ($D_{max} = 113\ Mpc$). The supergalactic coordinate map and the (α, δ) map are shown in figs. 3.34 and 3.35, covering a solid angle $\mathcal{A}_{RGH89} = 0.16\ sterad$ corresponding to 1% of the whole sky. The volume spanned is then:

$$\mathcal{V}_{RGH89} = 7.5 \cdot 10^4\ Mpc^3 \tag{3.24}$$

and the average number density of observed groups is:

$$\bar{\rho}_n^{(obs)}(RGH89) = 6.5 \cdot 10^{-4}\ Mpc^{-3}. \tag{3.25}$$

The original slice contained 72 groups, but some of these were quite close to the border of the surveyed area and so, in order to avoid groups with real members beyond the slice limits, I removed them from the catalogue. In any case the results discussed here do not change significantly if the whole set, including border-line groups, is considered.

From Tab. A.46 it seems that a strong observational bias affects this catalogue: some of the main group parameters such as $\mathcal{M}$, L_{sg} etc. are correlated with distance from us (see fig. 3.36). Because of the high value of the minimum distance $D_{min} = 32\ Mpc$ and the small value of N_{obs}, it is useless to consider a distance cut $D_\star$ in order to reduce this bias, so the whole catalogue is considered with this warning in mind. The main statistical values of group parameters are listed in Tabs. A.44 and A.45. The most relevant correlations between these parameters are reported in Tab. A.46.

Since the morphological types T of the member galaxies are not available, I can consider only the case $w = 1$ in the luminosity-weighted parameters. For this reason no morphological segregation can be tested.

The main result of the analysis is the stability of the mass distribution for different choices of the estimator to a high level of significance. This result is obtained by comparing pairwise the mass distributions of different estimators. The significance of the KS test statistics is listed in Tab. A.47 for all pairs and in fig. 3.40 for a particular pair. The conclusion of the KS pairwise test is confirmed by the result of the Kruskal-Wallis (KW) test $S_{KW} = 0.90$ which indicates that all the mass estimators are drawn from the same parent distribution.

It was argued by Ramella et al. (1989) that nearly 30% of groups having 3 or 4 members are probably an accidental superposition of galaxies due to the geometry of the large scale structure. It is possible to account for this information by using a bootstrap technique to resample the observed groups and rejecting 30% of the groups which have less than 5 members. We can obtain this resampling if groups with more than 4 members are labelled with a weight $w_b = 1$, and the remaining groups have $w_b = 2/3$. For each

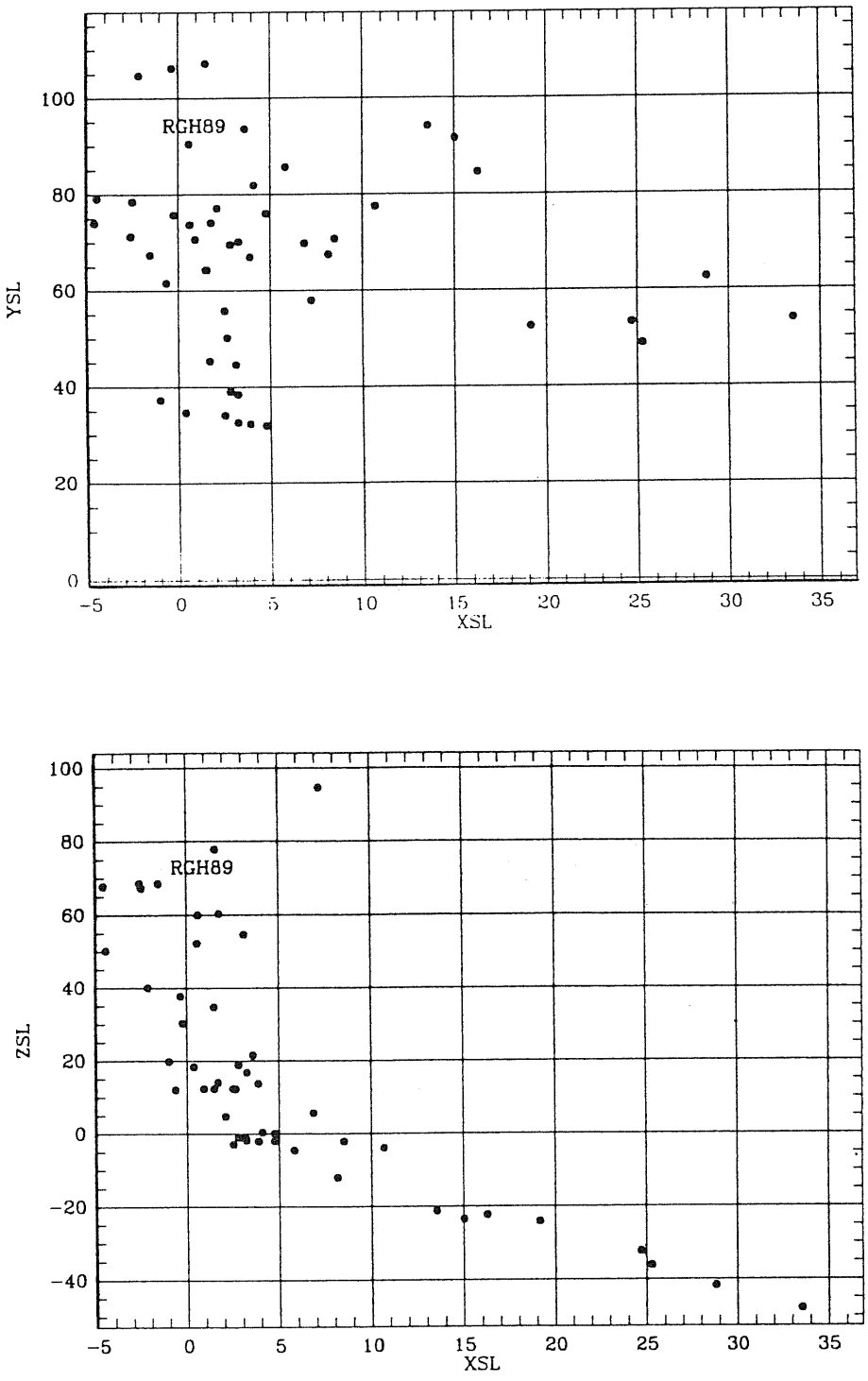

Figure 3.34: The RGH89 map in the supergalactic coordinate frame (part 1); the values of the coordinates are given in *Mpc*.

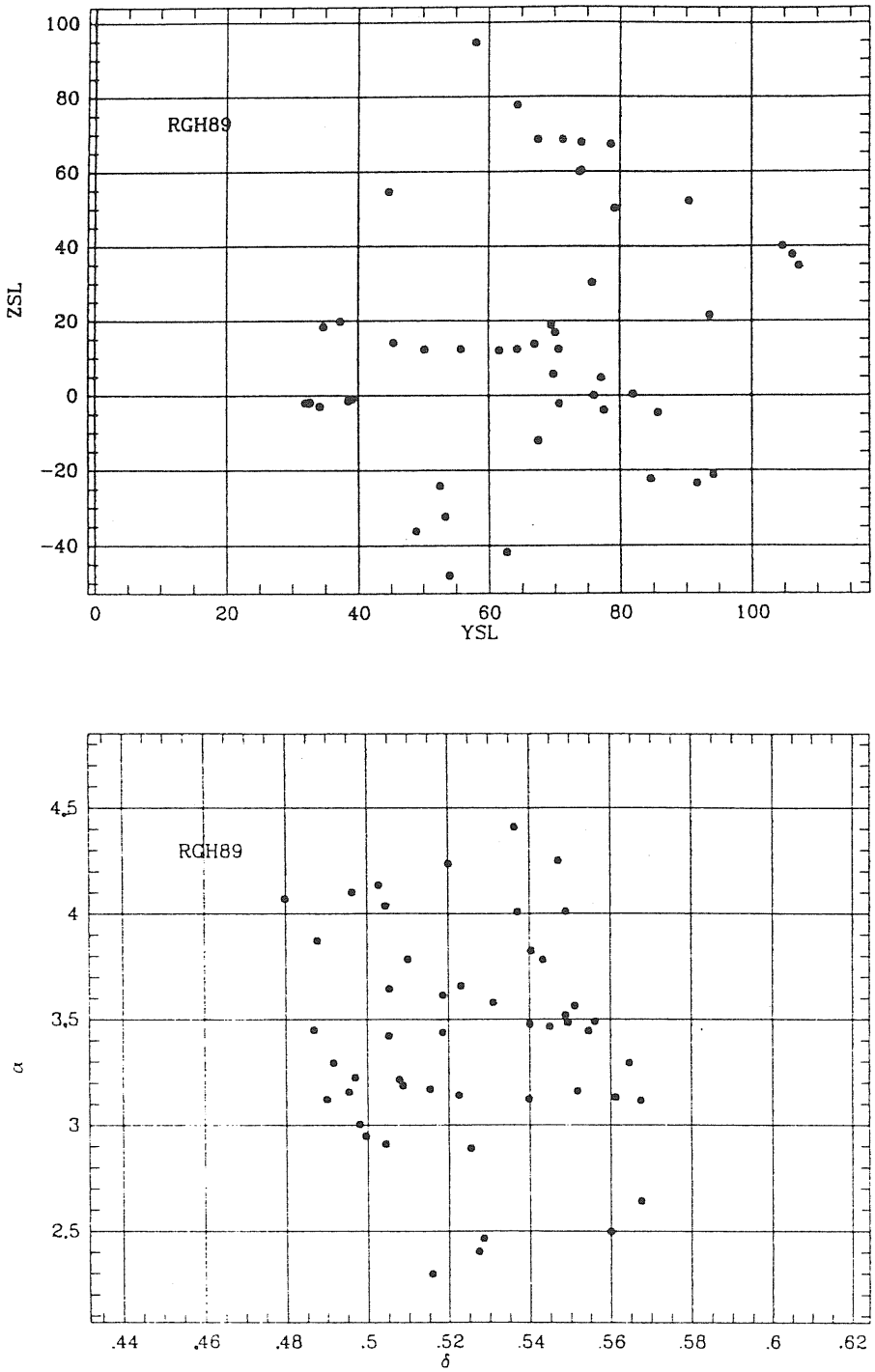

Figure 3.35: The RGH89 group coordinate maps (part 2). Upper graph: positions in the supergalactic coordinate frame in units of *Mpc*. Lower graph: the (α, δ) map in units of *rad*.

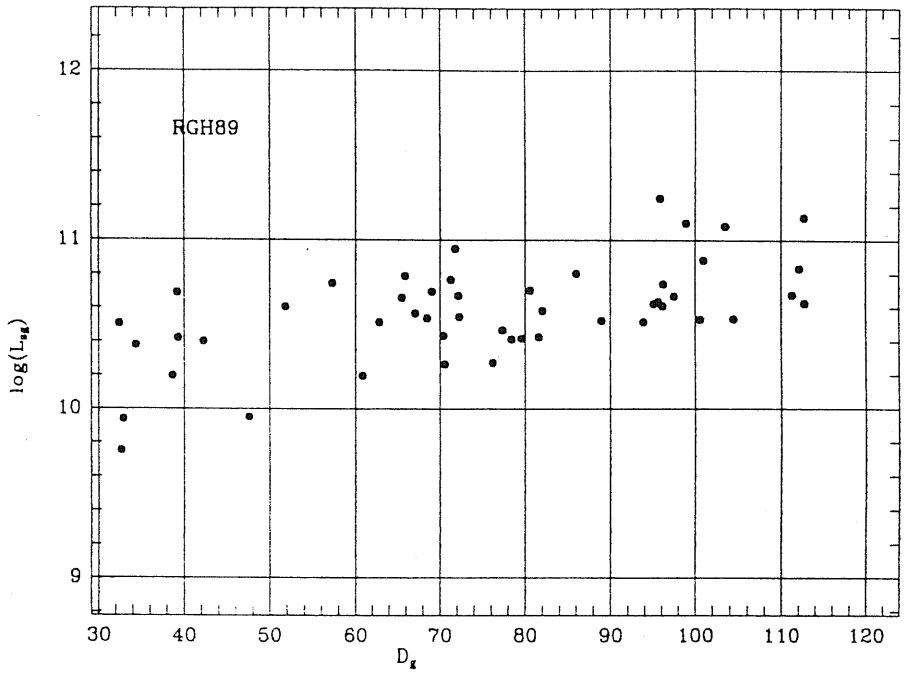

Figure 3.36: The group luminosity versus distance for the *RGH*89 catalogue.

resampled set of groups the KS test can show how much the resampled mass distribution $\mathcal{N}_b(\mathcal{M})$ differs from the original one $\mathcal{N}_{obs}(\mathcal{M})$. Performing this procedure a sufficient number of times to reach stable conclusions, say 10^3 or 10^4 times, it is possible to have an idea of the relevance of accidental superpositions on the mass distribution, on the assumption that the initial hypothesis is correct. Applying this procedure the following results are obtained: for every mass estimator the KS test gives a significant ($S \leq 0.05$) difference with a frequency $f_{0.05} \leq 0.1\%$. This result is confirmed by several runs of the procedure and for several recipes for the resampling weights w_b. It seems that, if this procedure is correct, then the presence of unphysical groups due to accidental superpositions has a negligible effect on the observed mass distribution for every mass estimator.

The RGH89 groups seem to show a distribution of $\mathcal{M}_{Vu}$ which is insensitive to the correction of the mass accounting for the possible unrelaxed dynamical state of groups. This is due to the particular distribution of α and τ (see figs. 3.37 and 3.38). Only a small fraction of groups is in the virialized regime, as is indicated by the median value of $\tau = 5.73$ which is smaller than the lower limit $3 \cdot \pi$ of the virialized dynamical regime. The median value of α is 0.47 and so the median correction factor for the virial mass is close to 1 (see Tab. A.49). It is then reasonable that the observed and corrected distributions of $\mathcal{M}_{Vu}$ do not differ significantly, in fact the KS comparison between these distributions gives $S = 0.96$ for $\Omega = 0.2$ so that the difference is not significant. The same test between the observed mass distribution and that obtained when correcting for evolutionary effects assuming $\Omega = 1$ gives $S = 0.86$. In fact the distributions of the corrected virial mass, the dynamical state τ, the virial α and the correction factor μ are not sensitive to the adopted value of Ω, as is shown by the high significance of KS statistics obtained on comparing the distributions of these parameters for the two values of Ω (see Tab. A.50).

Concluding this section I stress that:

- RGH89 groups are affected by a strong observational bias which is very difficult to remove or reduce;
- no significant difference seems to exist between the mass distributions obtained using different estimators, i.e., all mass estimators are homogeneous;
- approximately 90% of these groups are undergoing dynamical evolution and have not yet reached virial equilibrium. Nevertheless, the particular distribution of the correction factor accounting for non-virialization does not significantly alter the mass distribution of groups.

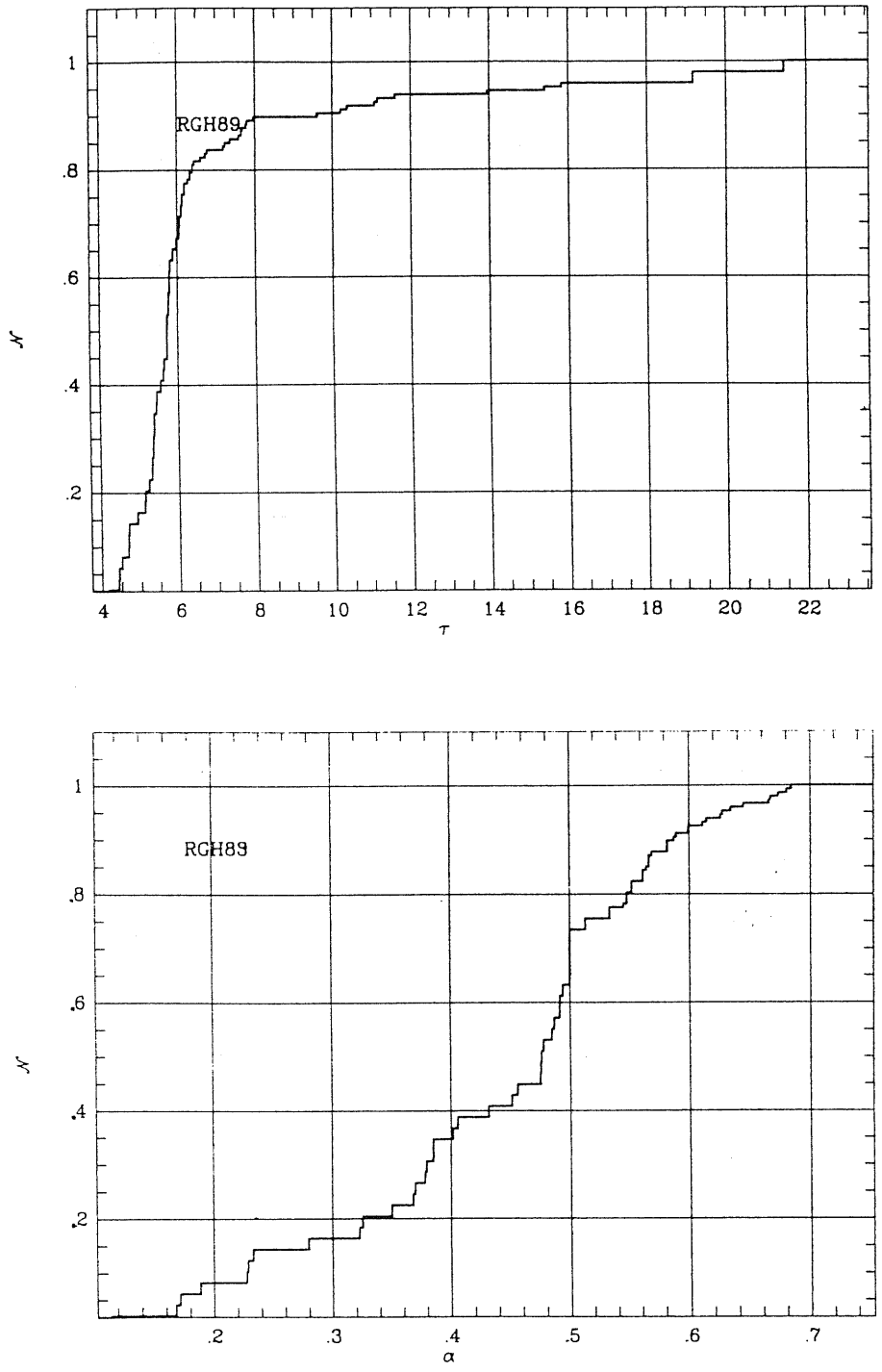

Figure 3.37: The distributions of the dynamical state τ (upper) and of the virial α (lower) for the $RGH89$ groups in the case $\Omega = 0.2$.

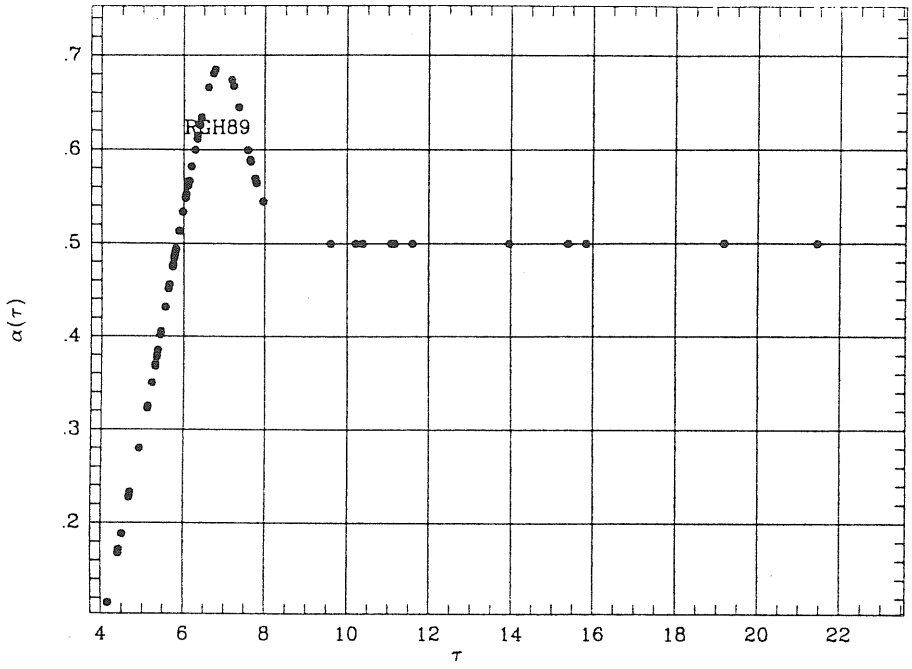

Figure 3.38: The curve $\alpha(\tau)$ for the $RGH89$ groups in the case $\Omega = 0.2$.

3.6 Analysis of S89 groups

This catalogue originally contained 87 groups. Since the observational error of the red-shift for member galaxies is not available, an indicative value of $\Delta V = 25\ Km/s$ is assumed for all members. This corresponds to the median value of the red-shift uncertainty for $GH83$. As a consequence of $\Delta V > 0$ some of the $S89$ groups have $\sigma_v^2 < 0$ and are then excluded from the analysis. The number of such groups is quite small, only 3, and so the properties of groups are not affected by this assumption, and a non-zero value for ΔV does seem reasonable.

The $S89$ groups cover a solid angle $\mathcal{A}_{S89} = 1.74\ sterad$ corresponding to 14% of the whole sky. The volume spanned is then:

$$\mathcal{V}_{S89} = 3.0 \cdot 10^5\ Mpc^3 \tag{3.26}$$

and the average number density of observed groups is:

$$\bar{\rho}_n^{(obs)}(S89) = 2.8 \cdot 10^{-4}\ Mpc^{-3}. \tag{3.27}$$

The positions of these groups in supergalactic and (α, δ) coordinate frames are shown in figs. 3.41 and 3.42.

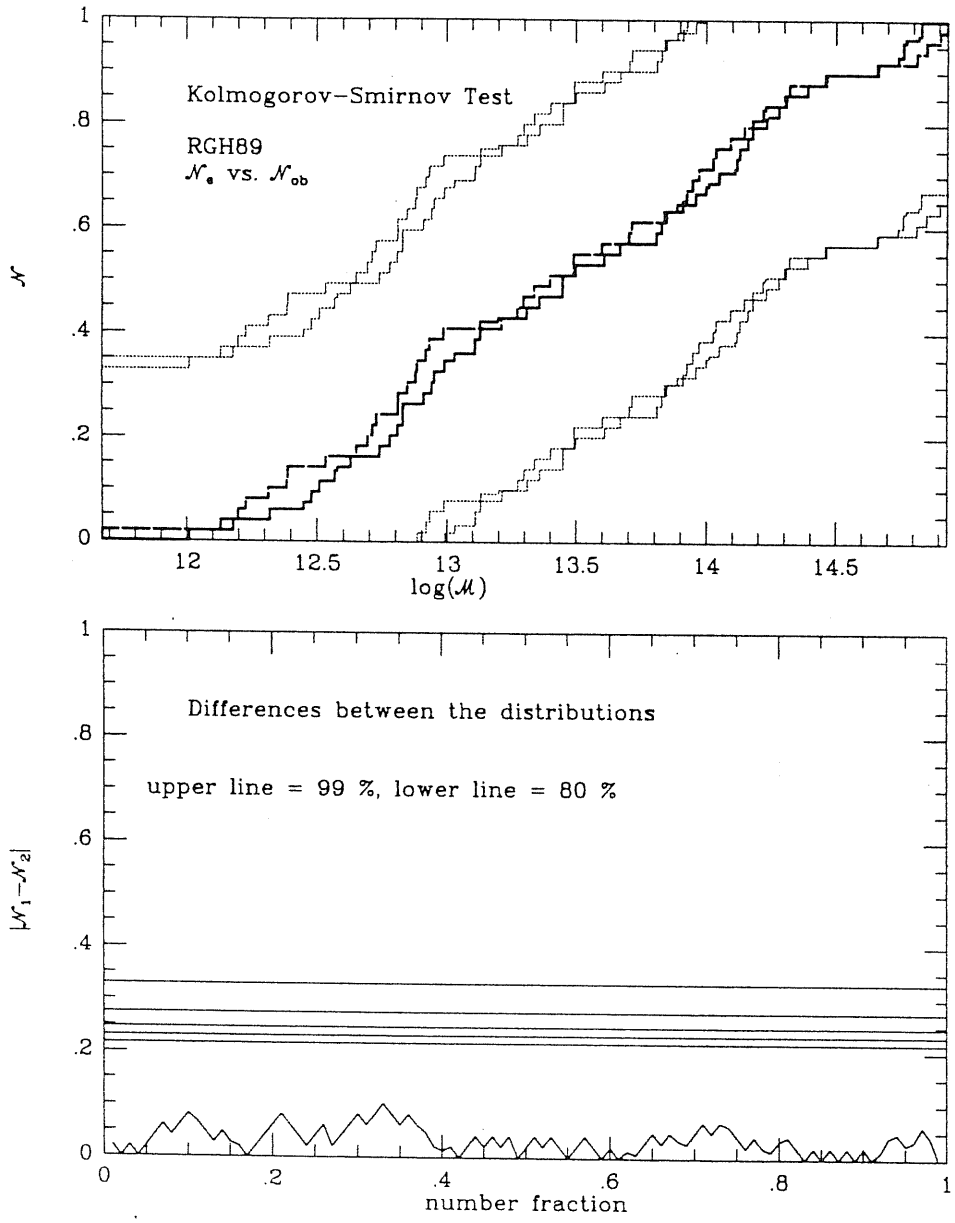

Figure 3.39: The KS comparison between the observed (long-dashed) and evolutionary corrected (solid) mass distribution of the $RGH89$ groups ($\Omega = 0.2$).

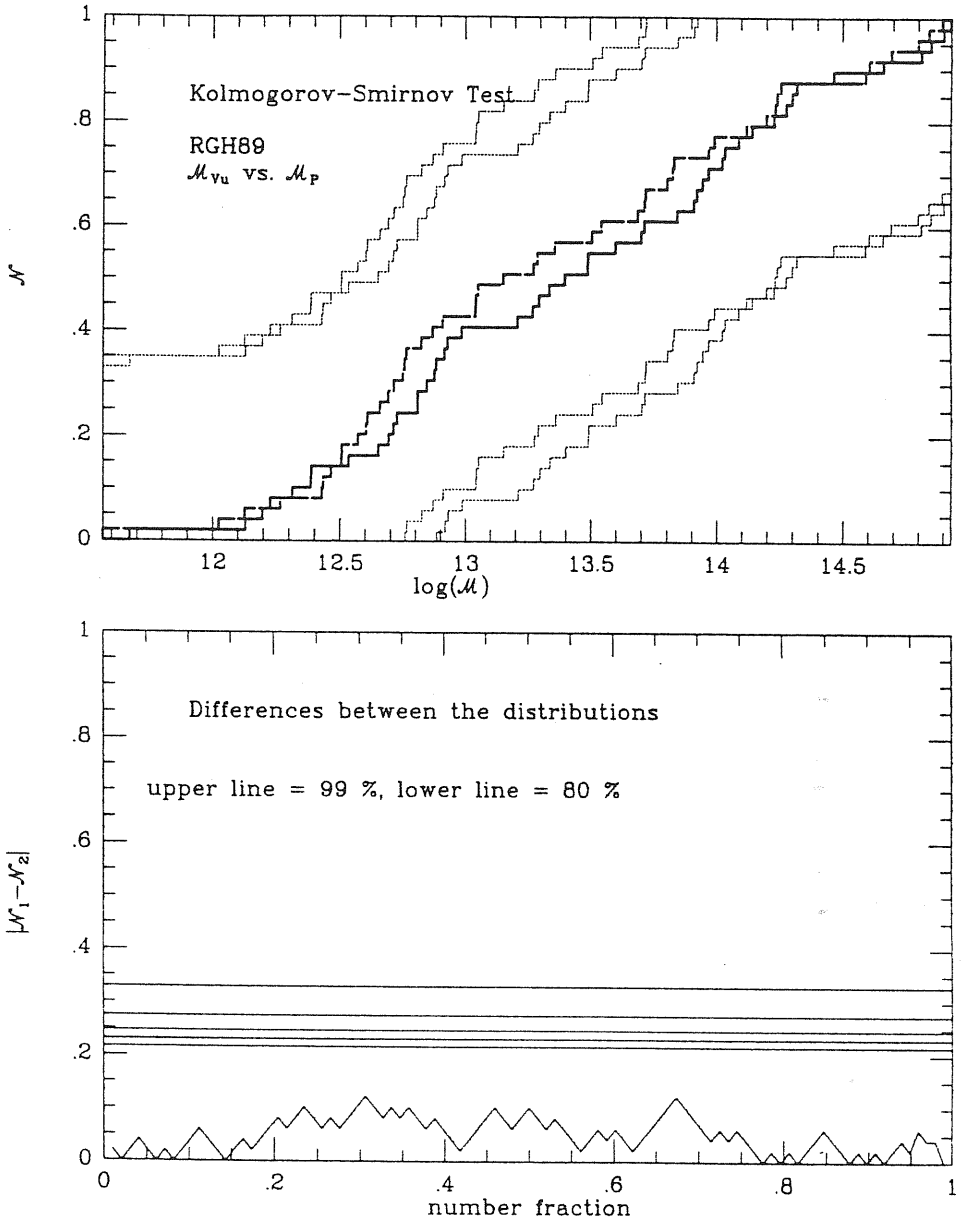

Figure 3.40: The KS-test comparison between $\mathcal{N}_{obs}(\mathcal{M}_{Vu})$ (solid line) and $\mathcal{N}_{obs}(\mathcal{M}_P)$ (long-dashed line).

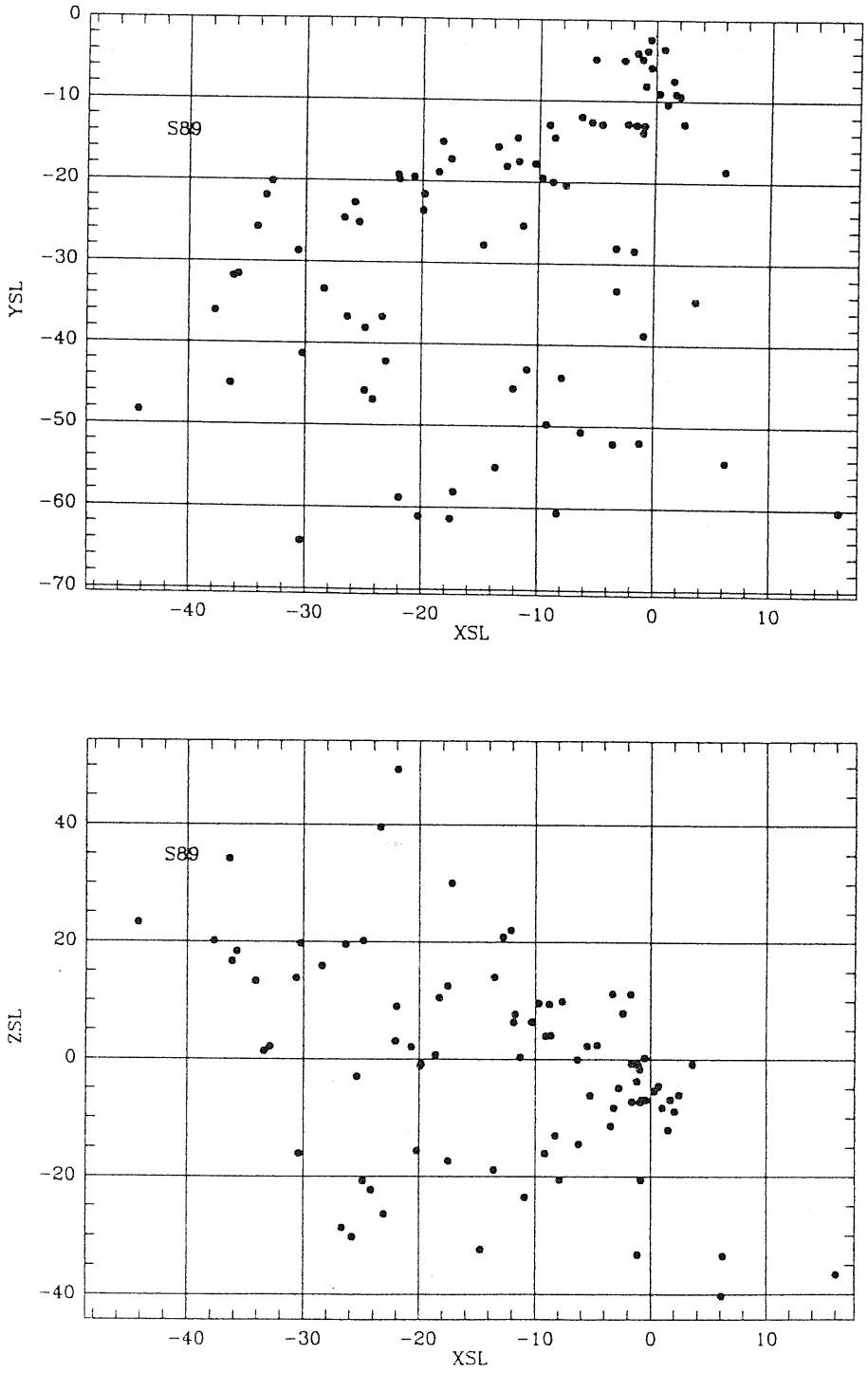

Figure 3.41: The S89 map in the supergalactic coordinate frame (part 1);, the values of the coordinates are given in Mpc.

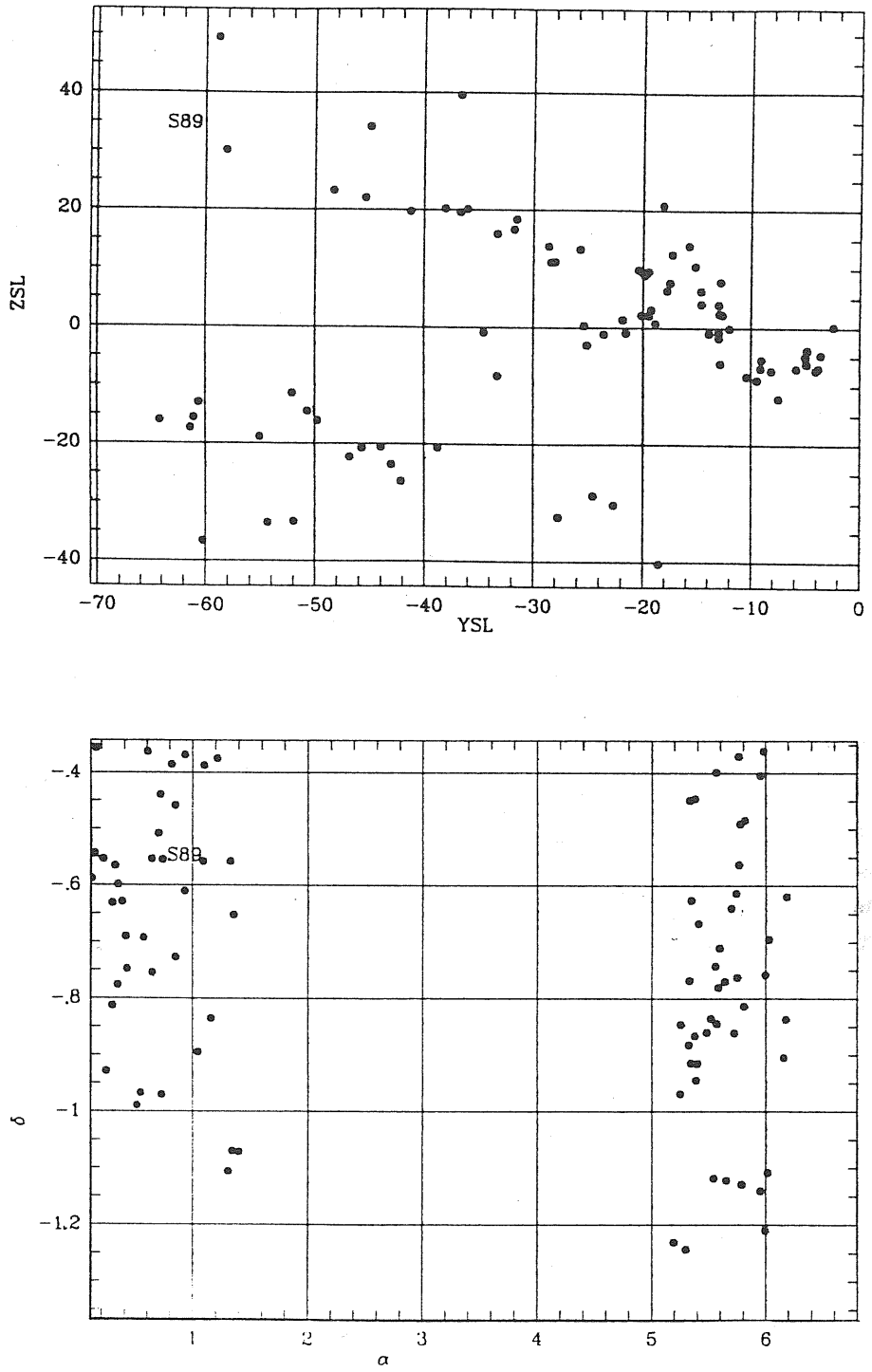

Figure 3.42: The S89 group coordinate maps (part 2). Upper graph: positions in the supergalactic coordinate frame in units of Mpc. Lower graph: the (α, δ) map in units of rad.

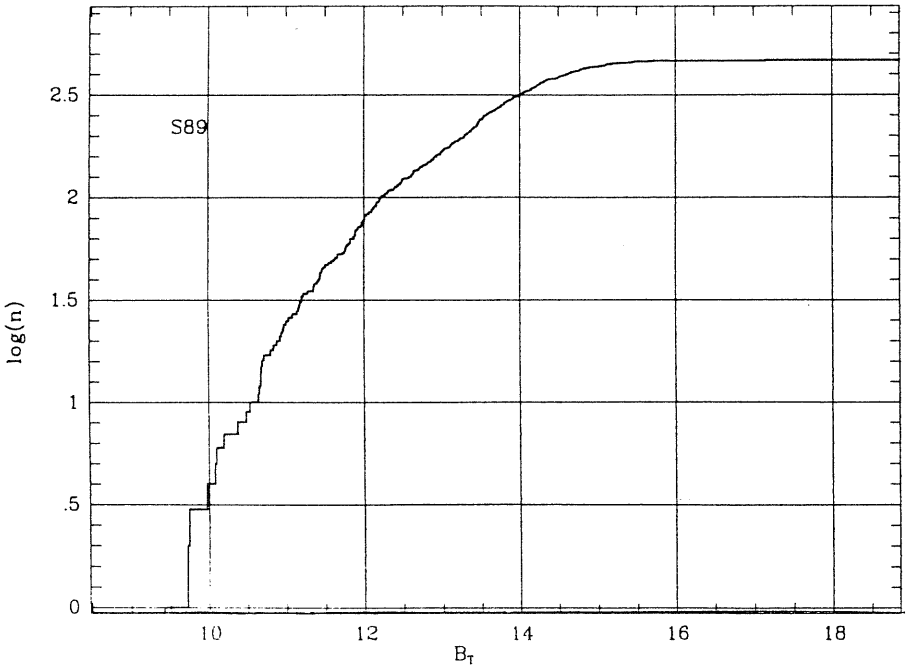

Figure 3.43: The B_T magnitude distribution of the $S89$ galaxies.

Since for some of the member galaxies the magnitude is not available, the quoted values of L_{sg}, L_{min}, L_{max} and $\mathcal{M}_{Vu}/L_{sg}$ refer only to groups having at least one member with known luminosity, namely to $N_{obs}(L_{max} > 0) = 83$ groups. These quantities are marked by $(\star)$ in all the tables of results.

The original galaxy sample of the $S89$ catalogue is complete in diameter, and only about 10% of the sample galaxies were lacking radial velocity measurements (Maia et al. 1989). This completeness is not easily translated into magnitude.

From fig. 3.43 it seems that a possible value for the completeness limit m_c is 12 or 12.5. If we take $m_c = 12.5$ and exclude all the fainter galaxies in the $S89$ groups, only nine groups survive and two of them lie beyond 20 Mpc from us. So the magnitude complete sample is too poor for a statistical analysis. All luminosity-weighted parameters are then ignored and no recovering of faint distant groups is possible. On the other hand $S89$ is quite a rich catalogue and can give us information about the mass distribution of southern groups which can be compared with the $GH83$ and $RGH89$ groups obtained with the same GIA, but with different search parameters in the case of $RGH89$. Maia et al. (1989) stressed that although the galaxy sample of S89 is different from GH83, the resulting group properties are

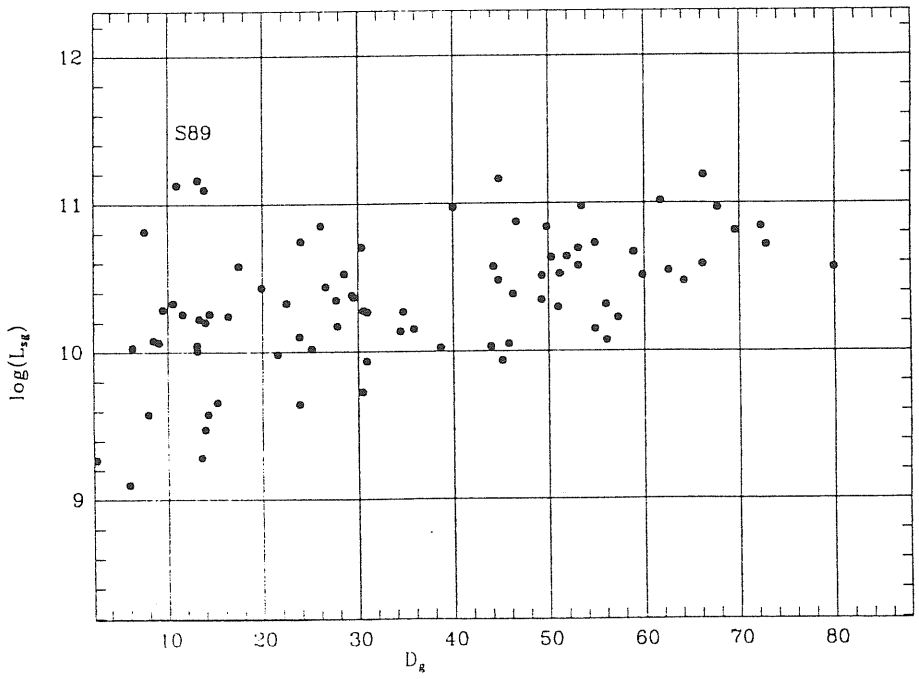

Figure 3.44: The group luminosity versus distance for the $S89$ catalogue.

similar and can be compared.

The general features of the $S89$ groups are indicated in Tabs. A.51 and A.52, while Tab. A.53 reports the correlations between the main parameters. It is possible to notice that the high value of $r[\log(L_{sg}), D_g] = 0.47$ with $S = 1.5 \cdot 10^{-5}$ suggests the presence of a non-negligible observational bias (see fig. 3.44).

If we consider the subcatalogue of groups within 20 Mpc from us, $S89(D \leq 20\ Mpc)$, the correlation is significantly reduced: $r[\log(L_{sg}), D_g] = 0.25$ with $S = 0.23$, but only 25 groups satisfy the constraint on the distance. A strong reduction is also shown by the correlation between the mass and the distance. The 20 Mpc limit effectively reduces the observational biases for the main parameters below the significant values. The parameters of $S89(D \leq 20\ Mpc)$ are described in Tabs. A.55 and A.56, and the correlations in Tab. A.57. The effect of the observational bias on the mass distribution is not significant indeed the KS comparison of the distribution of each mass estimator among $S89(D \leq 20\ Mpc)$, $S89$ and $S89(D > 20\ Mpc)$ gives no evidence for significant differences (see Tab. A.54 and fig. 3.45). In other words, the mass distribution shows good stability relative to the observational bias. For this reason the results of the analysis are reported for both $S89$ and the nearby subcatalogue. The

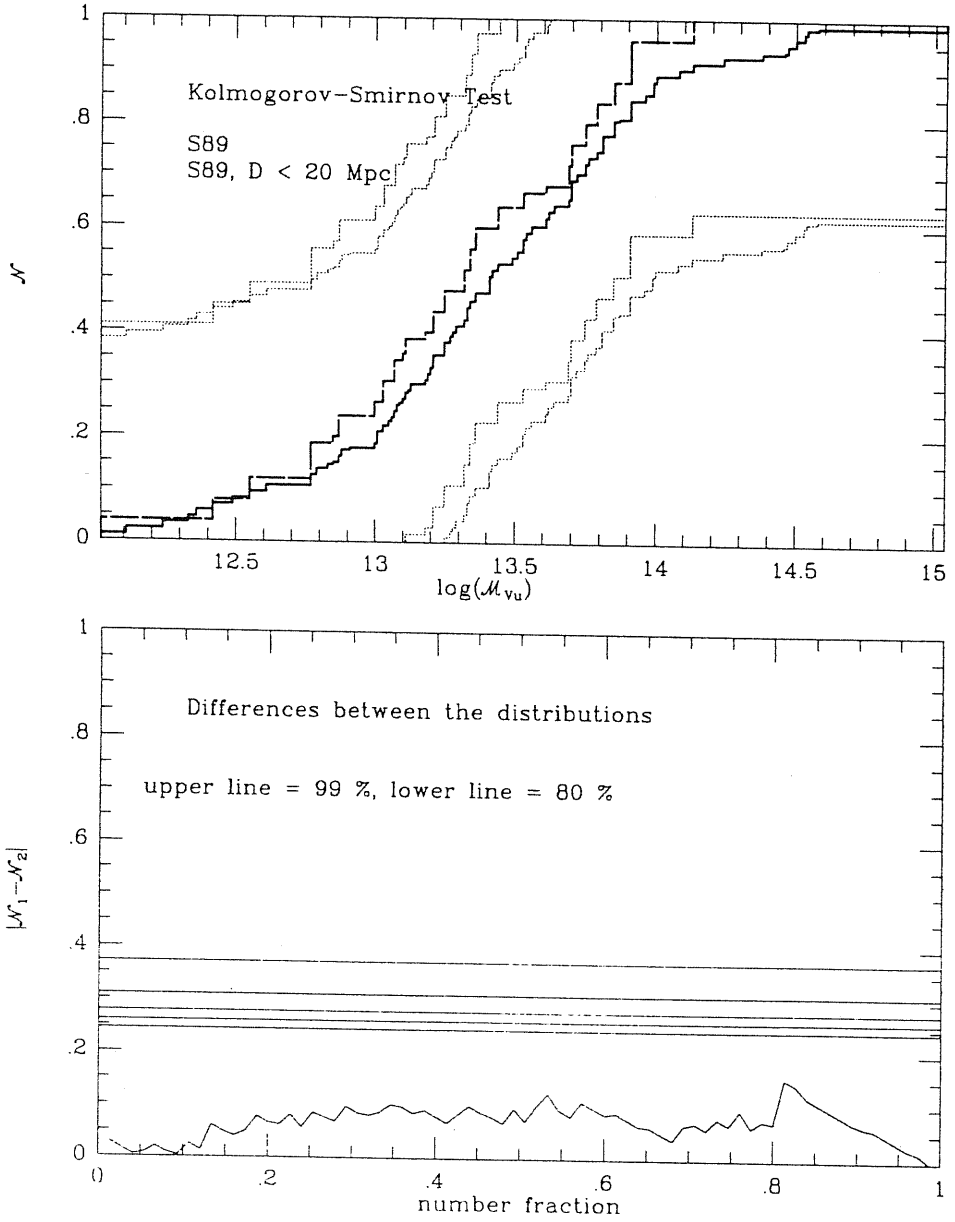

Figure 3.45: The KS comparison between the mass distribution of the groups of the whole *S*89 (solid line) and its nearby fraction (long-dashed line) for $\mathcal{M}_{Vu}$.

volume spanned by the nearby portion of $S89$ is then:

$$\mathcal{V}_{S89(D\leq 20\ Mpc)} = 4.6 \cdot 10^3\ Mpc^3 \tag{3.28}$$

and the average number density of observed groups is:

$$\bar{\rho}_n^{(obs)}[S89(D \leq 20\ Mpc)] = 5.4 \cdot 10^{-4}\ Mpc^{-3}. \tag{3.29}$$

A first result concerns the comparison among various mass estimators. As is reported in Tab. A.58, in no case does the KS test give evidence of significant differences between different estimators. The only significant ($S = 0.04$) difference is found between $\mathcal{M}_P$ and $\mathcal{M}_{Av}$, but the value of S is quite close to the critical value and the average mass estimator deserves little attention since, as already discussed, it has no physical grounds, but is defined as an extension of the expression giving $\mathcal{M}_P$ (see page 42). This holds for both $S89$ and its nearby fraction. The graph shown in fig. 3.46 gives a visual idea of the numerical results of Tab. A.58. The hypothesis that all mass estimators share the same underlying distribution can be tested by the KW test. The resulting significance is $S = 0.11$ for $S89$ and $S = 0.78$ for $S89(D \leq 20\ Mpc)$. This means that the hypothesis is true in both cases. A second test concerns the dynamical state of the groups. Using the method described in §1.4.7, I obtained the results shown in Tabs. A.59 and A.60. The curve $\alpha(\tau)$ and the distribution of τ and α are shown in figs. 3.47 and 3.48. These indicate that a large fraction ($\sim 90\%$) of groups fall in the region $\tau \leq 3 \cdot \pi$ and so are still undergoing dynamical evolution. In any case the value of the mass correction factor μ is distributed in such a way that the mass is not significantly altered by this correction (see fig. 3.49), except for the case $\Omega = 1.0$ (see Tab. A.61). However, the corrected mass distribution $\mathcal{N}_e(\mathcal{M})$ does not depend on Ω. This result holds for both $S89$ and $S89(D \leq 20\ Mpc)$ (see Tab. A.62). The lack of dependence on Ω is shared by α, τ and μ. Due to the stability of $\mathcal{N}_e(\mathcal{M})$, the value of $\Omega = 0.2$ is retained as reference value, for consistency with the analysis of other catalogues.

Summarizing the results about $S89$ groups, it is possible to say that:

- a non-negligible bias affects the catalogue, but can be reduced to a negligible level by limiting the analysis to groups within 20 Mpc from us; in any case it seems that the mass distribution is not strongly affected by the bias;
- no significant dependence is found for the mass distribution on the estimator used: all mass estimators are homogeneous;
- approximately 90% of the groups are undergoing dynamical evolution and hence do not satisfy the virialization condition. However,

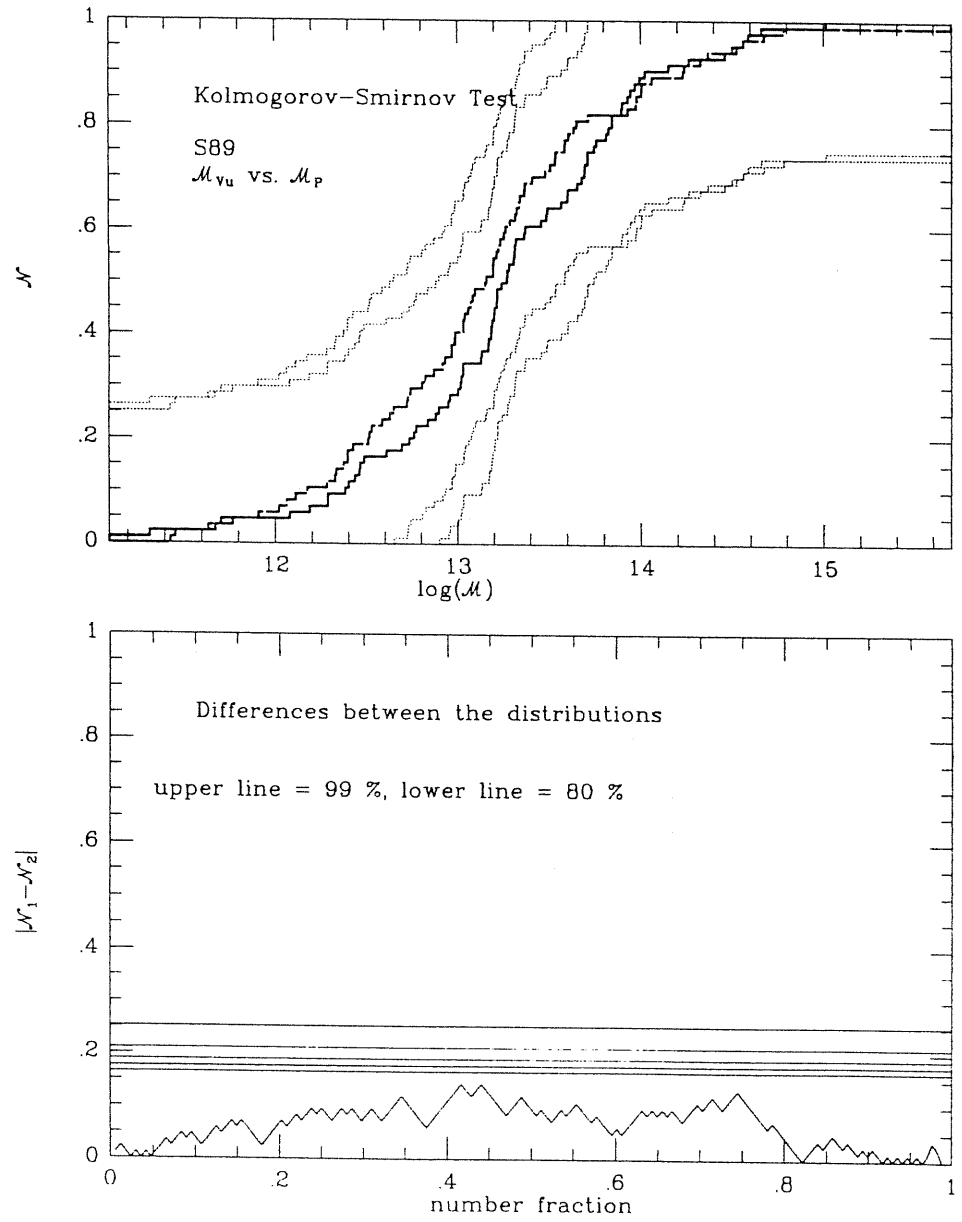

Figure 3.46: The KS comparison between the distributions of $\mathcal{M}_{Vu}$ (solid) and $\mathcal{M}_P$ (long-dashed) for the $S89$ groups.

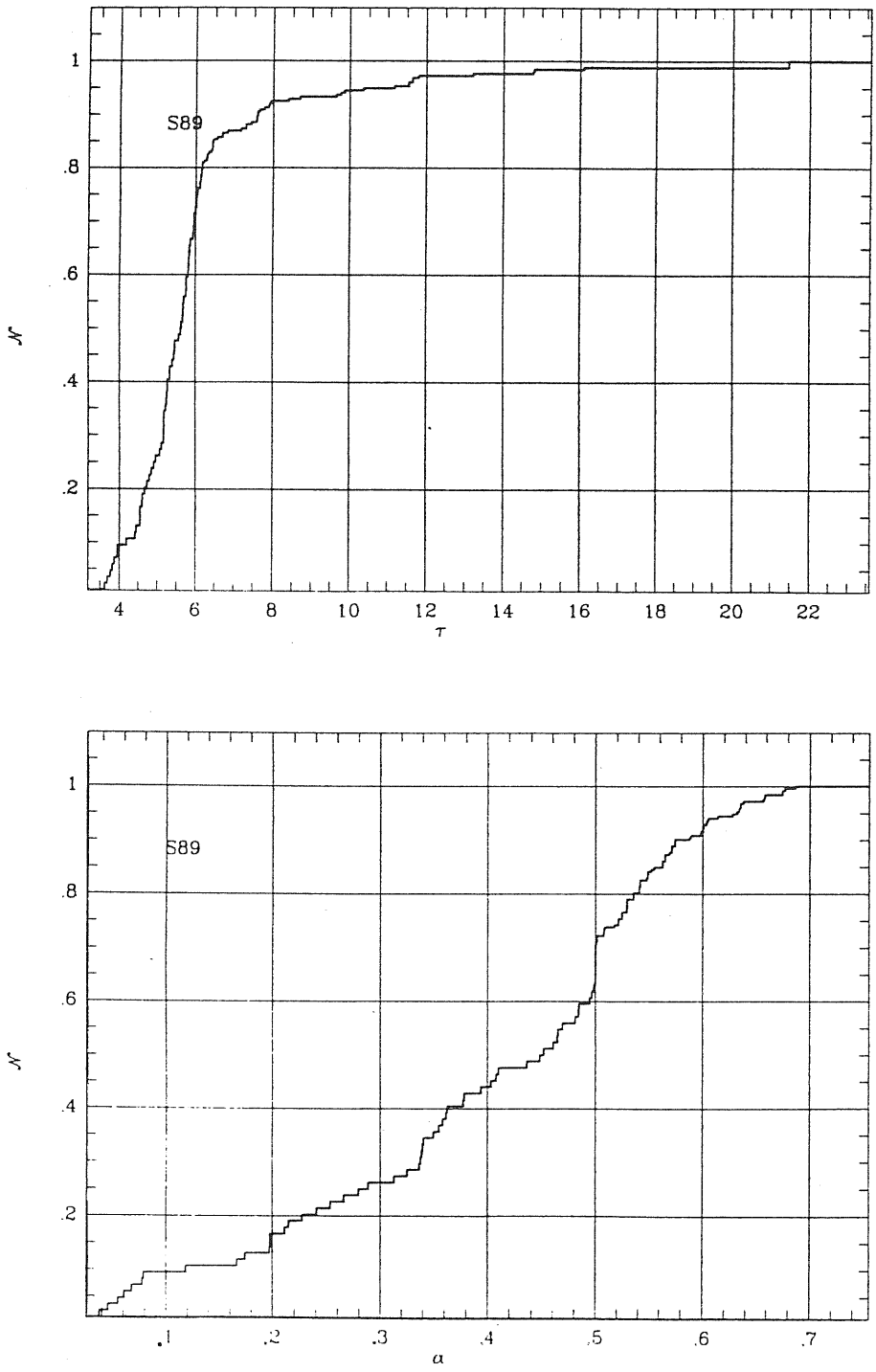

Figure 3.47: The distributions of the dynamical state τ (upper) and of the virial α (lower) for the $S89$ groups in the case $\Omega = 0.2$.

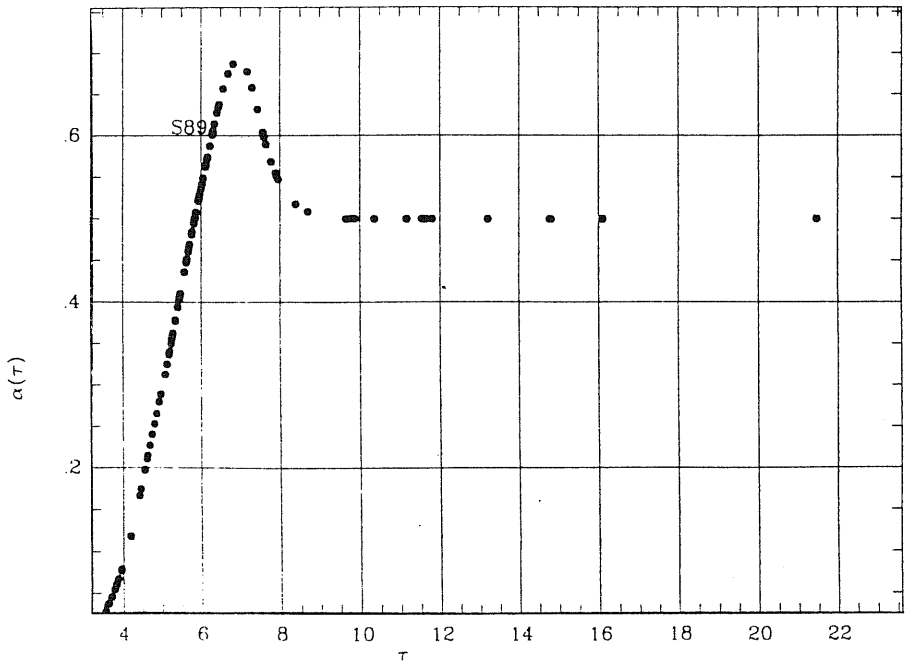

Figure 3.48: The curve $\alpha(\tau)$ for the $S89$ groups in the case $\Omega = 0.2$.

the mass distribution is not significantly altered by the correction accounting for the non-virialization, which is due to the particular distribution of the correction factor.

3.7 Comparison among catalogues

In this section I want to compare the distributions of the main physical parameters of groups observed in different catalogues, and to analyse the features they share and those that distinguish them. The analysis is carried out considering both the whole catalogues and their nearby portions. This is because of the presence of non-negligible biases which in some cases are significantly reduced if only groups within 20 Mpc from us are considered. The largest unbiased portion of each catalogue is also considered. This is defined by the subcatalogues of groups within the largest limiting distance from us which show no significant correlation of the main physical parameters (such as the mass, velocity dispersion and virial radius) with distance. Fortunately, as will be seen from the results, the presence of this bias does not alter the main conclusions.

On the basis of the information available from the observations, the

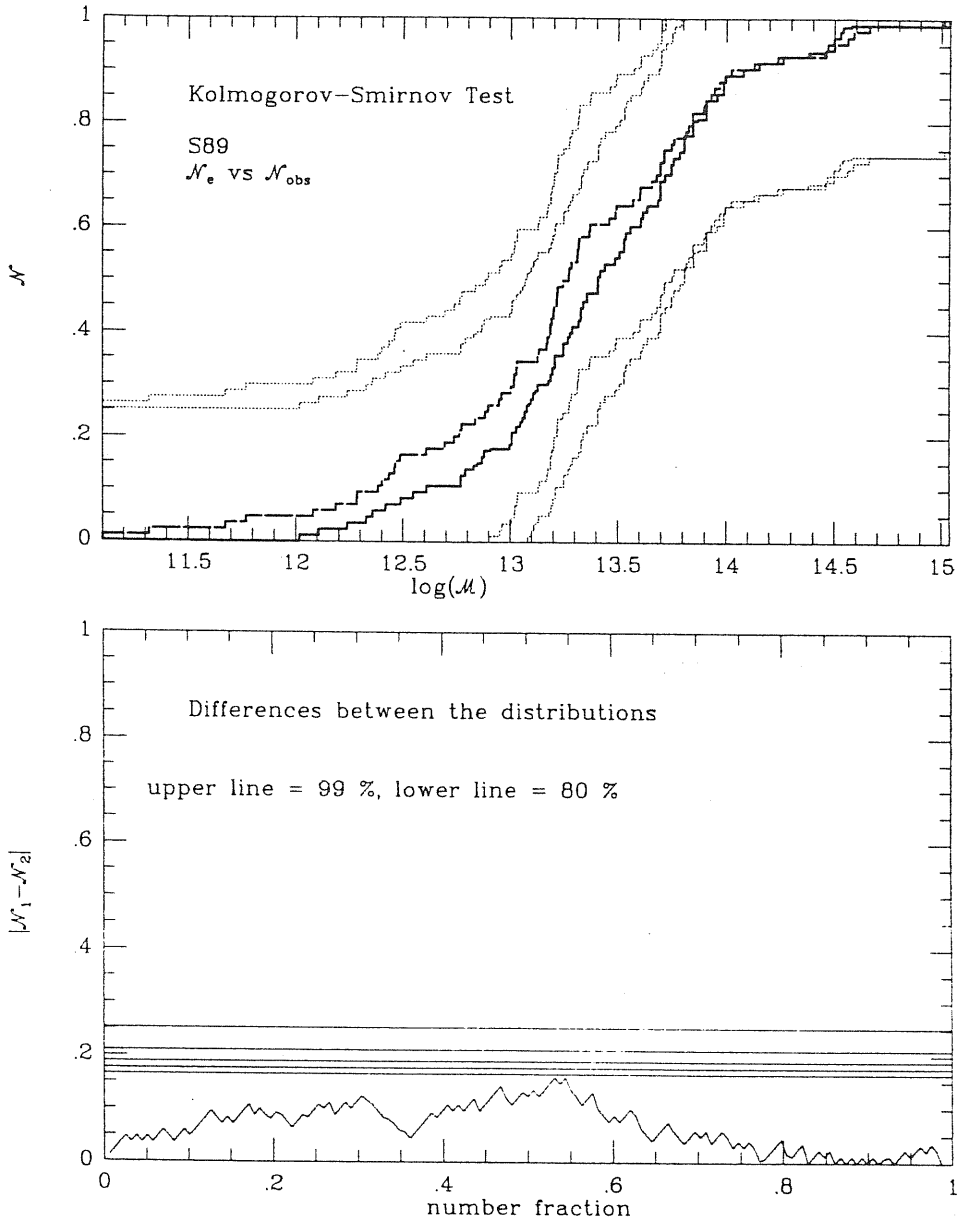

Figure 3.49: The Kolmogorov-Smirnov comparison between the observed (long-dashed) and evolutionary corrected (solid) mass distribution of the $S89$ groups for $\Omega = 0.2$.

estimation of physical parameters of groups of galaxies is described. In particular the hypotheses underlying the derivation of the mass estimators are stressed. One of these hypotheses concerns the dynamical state of groups. It is generally assumed in the literature that these galaxy systems have reached a steady state called virial equilibrium. It is here verified, by adopting a method described by Giuricin et al. (1988), that nearly all the groups in all catalogues are in a phase characterized by strong dynamical evolution. They do not satisfy one of the basic assumptions of the virial theorem, in that they are rather dynamically young galaxy systems. Due to this result, a suitable correction for the mass of groups is introduced to account for the non-virialized dynamical state. Only three of the considered catalogues show a mass distribution not significantly altered by this correction: $GH83$, $S89$ and $RGH89$, while both $T87$ and $V84$ do show a significant effect of the correction on the mass distribution.

For one of the catalogues ($GH83$) within 20 Mpc from us, it is possible to recover the contribution to the mass distribution due to faint and distant groups missed by the observations. Adopting a reasonable model for the space distribution of groups, the observed mass distribution of groups turns out to be well representative of the *total* mass distribution of groups accounting also for faint distant objects. The same stability is found for different models of the local spatial distribution of groups.

Let me consider first the mass distributions $\mathcal{N}_e(\mathcal{M})$ corrected for non-virialization for all the five catalogues. The main statistical quantities relative to these distributions are summarized in Tab A.63 ([9]). Applying the Kruskal-Wallis test to the set $\mathcal{C} = \{GH83,\ T87,\ RGH89,\ S89,\ V84\}$ I obtain a significance $S = 4 \cdot 10^{-34}$([10]). This value indicates that the masses of groups in these catalogues do not share the same underlying (or parent) distribution. In other words the set $\mathcal{C}$ is not homogeneous with respect to the mass distribution. The same conclusion holds if I consider the observed mass distribution, i.e., not corrected for the non-virialized dynamical state. In this case the KW test gives $S = 2 \cdot 10^{-30}$, suggesting that the correction for non-virialization does not alter the inhomogeneity of catalogues. In fig. 3.50 the mass distribution for all the catalogues is shown: the difference among them is quite clear. If I exclude from $\mathcal{C}$ the $V84$ groups, the KW test gives $S = 3.2 \cdot 10^{-17}$ and the set is still significantly inhomogeneous. If I exclude the groups of $T87$ and retain those of $V84$, I have $S = 6 \cdot 10^{-31}$ and again the set is inhomogeneous. Homogeneity is obtained by excluding

[9]In this table the last two columns list the values of the first Q_1 and third Q_3 quartiles of the distributions, defined respectively by: $\mathcal{N}(Q_1) = 0.25$ and $\mathcal{N}(Q_3) = 0.75$.

[10]Usually, the hypothesis tested is rejected as false in the case that the significance S is smaller than a critical value, otherwise the hypothesis is considered true. The most commonly used critical value for tests of this kind is $S_c = 0.05$ corresponding to a level of statistical confidence of 95%, other critical values are 0.01 and 0.10.

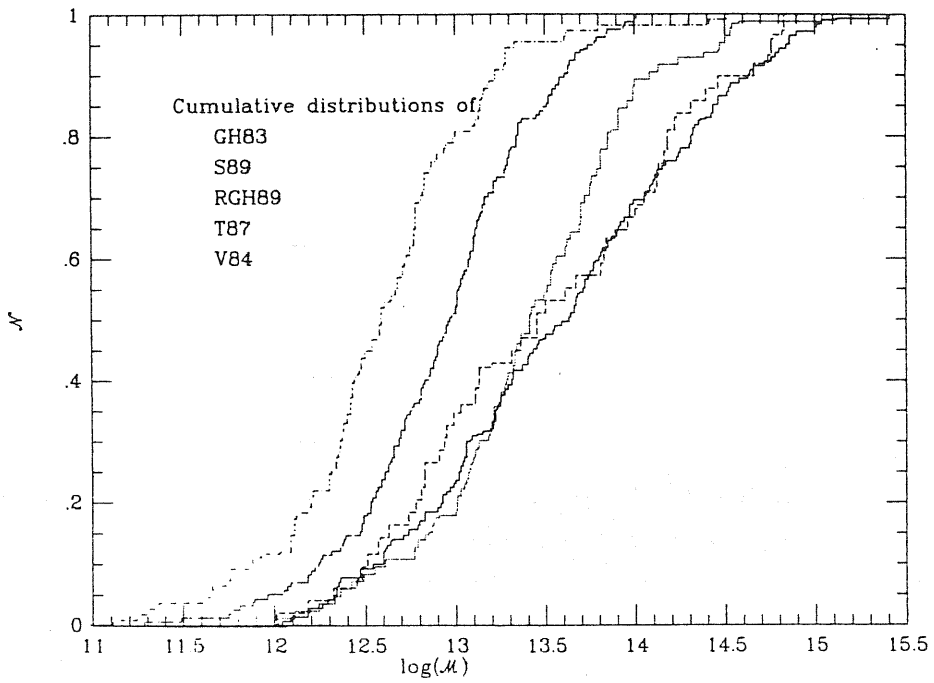

Figure 3.50: The mass distribution function of all catalogues: $GH83$ (solid), $S89$ (dashed), $RGH89$ (short-dashed), $T87$ (long-dashed) and $V84$ (dot-dashed).

both the $T87$ and $V84$ groups from the set $\mathcal{C}$. In fact in this case the KW test gives $S = 0.20$, which is well above all critical values. This means that groups in the catalogues of the set $\mathcal{C}_{f.o.f.} = \{GH83,\ S89,\ RGH89\}$ have masses with the same underlying distribution, or, in other words, $\mathcal{C}_{f.o.f.}$ forms a homogeneous set of catalogues (based on the friends-of-friends identification algorithm) relative to the mass distribution of groups of galaxies. The striking fact is that the catalogues of this set share little or no volume of space, have been obtained from different galaxy samples. Their common property is the group identification algorithm (GIA) although in the case of $RGH89$ the search parameters are different from both $GH83$ and $S89$. On the other hand, $GH83$ and $S89$ are obtained from rather different galaxy samples (Maia et al. 1989). In fact this might explain the significant difference found by the KS-test pairwise comparison, but, in any case, the difference between $GH83$ and $S89$ is not strong enough to compromise the homogeneity of $\mathcal{C}_{f.o.f.}$. Moreover comparing $\mathcal{N}_e(\mathcal{M})$ between the $T87$ and $V84$ groups by the KS test one obtains a significant difference ($S < 10^{-3}$). This can be interpreted by observing that, although a hierarchical clustering procedure is adopted to obtain both catalogues, the criterion to identify groups in the two catalogues are different. In the case of $T87$ the groups are systems of galaxies with luminosity density exceeding a critical value, while in $V84$ the number density is used instead of luminosity density. However, it is not possible to exclude the possibility that other properties of these catalogues contribute significantly to cause the difference between the group parameters of $T87$ and $V84$. Moreover the KS comparison between these two catalogues cannot be confirmed by the KW test since only two catalogues which are not in the $\mathcal{C}_{f.o.f.}$ are available[11]. This conclusion, reached using the KW test, is confirmed by the pairwise comparison using the KS test (see Tab. A.64). The relevance of the observational bias relative to the inhomogeneity of the catalogues is likely to be negligible-indeed the results do not change significantly if only the region of space within 20 Mpc from us is considered (see also fig. 3.51). On the other hand it is possible to note that the limit at 20 Mpc effectively reduces the bias of the mass, velocity dispersion and virial radius only for $GH83$ and $S89$, while a residual and non-negligible correlation of these parameters with distance is also present in the nearby fraction of the $T87$ and $V84$ catalogues. In order to test the role of the bias for the inhomogeneity of catalogues, I allow the distance limit to change for different catalogues. I considered the value of the distance limit $D_\star$ which defines the richest nearby fraction of each catalogue free of correlation between the mass and the distance from us. I obtained,

[11]The Kruskal-Wallis (KW) test is a proper tool in the case of three or more distributions. If only two distributions are available, the KS test is more appropriate (Ledermann, 1982).

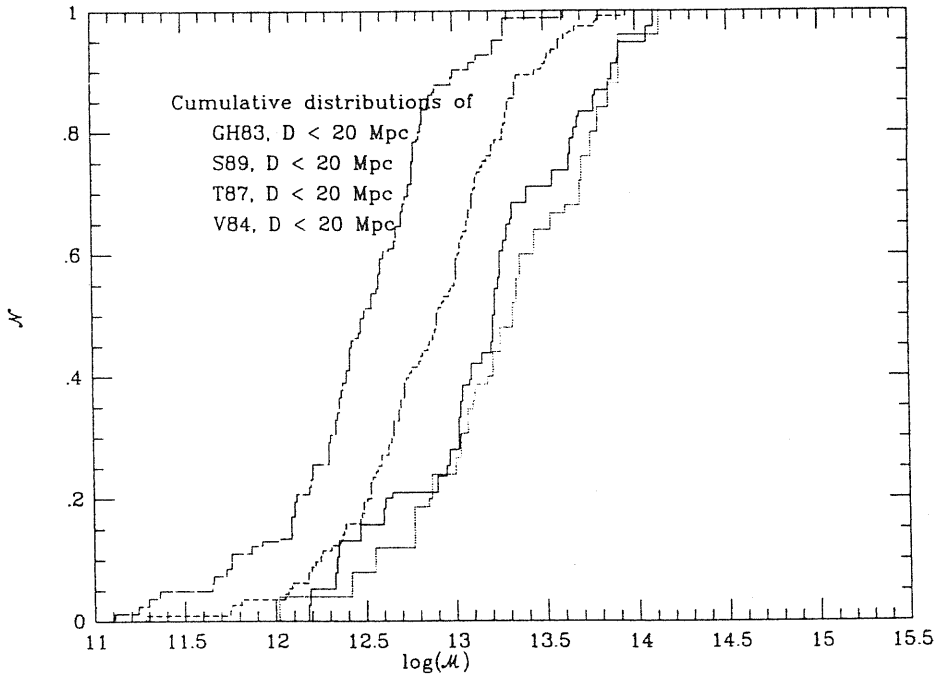

Figure 3.51: The mass distribution for groups within 20 Mpc. The various catalogues by: $GH83$ (solid), $S89$ (short-dashed), $T87$ (dashed) and $V84$ (long-dashed).

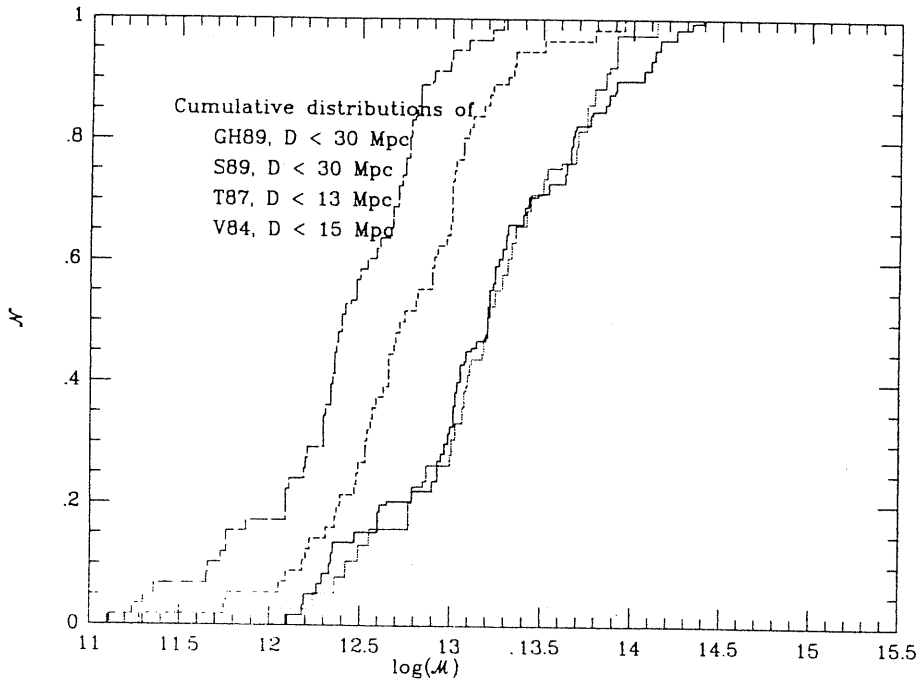

Figure 3.52: The mass distribution for the bias-free subcatalogues. The various catalogues are indicated in the same way as in fig. 3.51.

in this way, a subset of bias-free fraction of catalogues: $C_{bf} = \{GH83(D \leq 30\ Mpc),\ T87(D \leq 13\ Mpc),\ S89(D \leq 30\ Mpc),\ V84(D \leq 15\ Mpc)$. The mass distributions for these subcatalogues are shown in fig. 3.52. The KW test applied to this set gives $S = 9 \cdot 10^{-20}$ and so the inhomogeneity is still present. Using the KS test it is possible to compare the mass distributions of groups in the bias-free fractions of $GH83$ and $S89$, and in fact no significant difference is found, in agreement with the result obtained from the KW test. A further test is performed between the groups of $GH83$ and $T87$ considering only the volume within 20 Mpc from us and the solid angle shared by both catalogues. This allows me to compare the properties of the two catalogues in the same region of physical space. The result I obtained is a significant difference between the two mass distributions. This probably means that the two catalogues sample that region of space in rather different ways. It is possible to conclude that the observational bias has very little or no relevance for the detected inhomogeneity of the set of catalogues (at least for the mass distribution). Moreover for every catalogue the mass distributions of groups within 20 Mpc and in the richest bias-free fraction of the catalogue are not significantly different. These results seem to indicate that the inhomogeneity is stronger than the observational bias.

The homogeneity property of different catalogues relative to the mass distribution is a consequence of the relation of this distribution to the distributions of other, more basic, parameters. It is worth analysing the homogeneity of the catalogues relative to the distributions of the velocity dispersion σ_v, the virial radius R_{Vu}, the crossing time $\mathcal{T}_V$, the dynamical state τ, the virial α and, for the sake of completeness, of the mean pairwise separation R_p. It is interesting to note that the complete set $\mathcal{C}$ is not homogeneous for any parameter considered (see Tab. A.64), and this result also holds if only the region within 20 Mpc from us is considered (see Tab. A.65). Homogeneity is obtained for all parameters, except R_p, by the set $\mathcal{C}_{f.o.f.}$. Moreover, if we consider only groups within 20 Mpc, only two catalogues are available $GH83$ and $S89$ which have similar distributions for all parameters including R_p. These results are confirmed by the pairwise comparison using the KS test: $\mathcal{C}_{f.o.f.}$ is a homogeneous set of catalogues, while $T87$ and $V84$ show parameters distributed in (two) different ways. In fact no parameters show distributions which are similar in $V84$ and $T87$, except a marginal similarity ($S = 0.096$) obtained for the crossing time (see Tab. A.66).

Because of the strong dependence of the mass on the velocity dispersion, the distributions of σ_v for all catalogues are shown in fig. 3.53. The similarity of the behaviour of $\mathcal{M}$ and σ_v is clear.

The conclusion that can be drawn from this analysis is that, although other factors possibly related to the underlying galaxy samples may play a non-negligible role, the main property that makes the set of all the studied catalogues not homogeneous is the GIA adopted to produce the catalogue. This holds not only when the mass distribution is concerned, but for all the physical parameters of groups of galaxies. In this sense the results obtained here are stronger than the results obtained by Nolthenius and White (1987). They considered a set of group catalogues obtained using one GIA, namely the friends-of-friends algorithm, but with different search parameters. Their results gave inhomogeneous mass distributions. Probably the fact that in this work no significant difference is detected between group catalogues obtained with the friends-of-friends algorithm but with different search parameters, namely $GH83$ and $S89$ versus $RGH89$, is due to the low number of groups in each catalogue. The relevance of the search parameter is probably a higher order effect relative to the difference in GIA. This conclusion suggests that a new more reliable definition for groups of galaxies, and hence a new GIA, is necessary in order to overcome the inhomogeneity of catalogues.

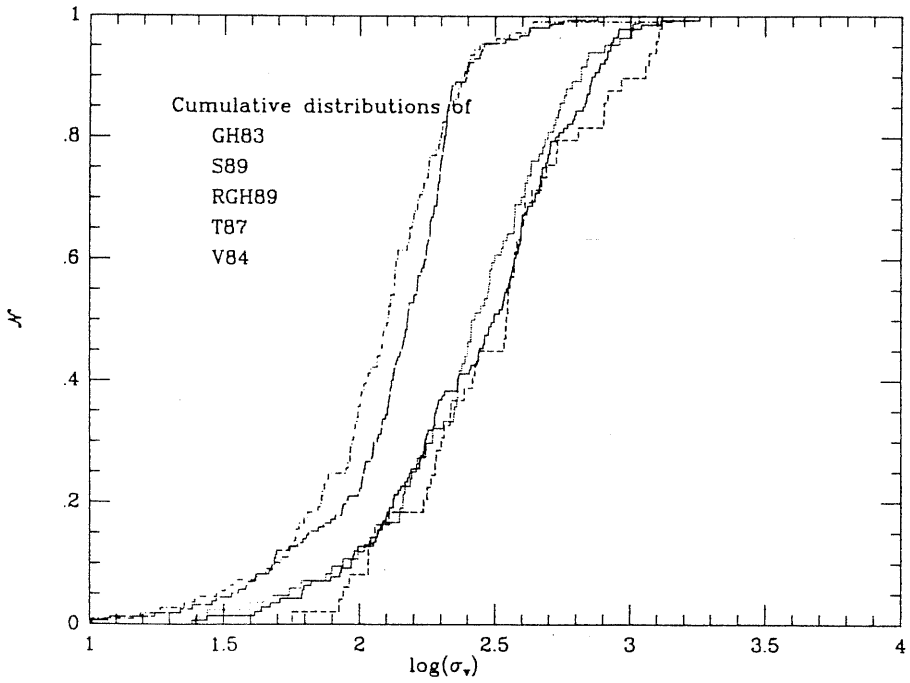

Figure 3.53: The velocity dispersion σ_v distribution for all catalogues. The various catalogues are indicated as in the previous fig. 3.50.

Summary and Conclusion

The problem of the estimation of the mass distribution of galaxy groups has been considered. The data base for the analysis of this problem is obtained from five different catalogues of groups. The main features of the examined catalogues are considered to be: a) the depth, completeness, coordinate range and possibly the correction for absorption and systemic motions of the galaxy sample; b) the procedure adopted in order to identify groups of galaxies and the values of the parameters used to run this procedure.

The catalogues considered in the present work are different for nearly all of the main features quoted above.

The main physical parameters of groups are estimated for each catalogue. The quantities characterising the statistical properties of these parameters are reported. Particular attention is paid to the dynamical state of these galaxy systems since it is strictly related to the mass estimate. Using a general method described by Giuricin et al. (1988), it is found that for all catalogues a large fraction ($\sim 90\%$) of groups is dynamically young and has not yet reached the virial equilibrium phase. The fact that the steady dynamical state required by the hypotheses of the virial theorem is largely unsatisfied by groups has significant consequences only for the mass distribution of groups in two catalogues: $T87$ and $V84$. In fact, it is possible to correct the mass by accounting for non-virialization effect. The observed and evolutionary-corrected mass distributions differ significantly for the groups of $T87$ and $V84$, while they are quite similar for groups in $RGH89$, $S89$ and $GH83$. It is worth noting that these three catalogues share the same GIA.

Due to its completeness property, it was possible to apply to the nearby portion $GH83(D \leq 20\ Mpc)$ a procedure to recover the mass of faint distant groups. On the basis of a reasonable model for the spatial distribution of groups within the examined volume, a good agreement is found between the shape of the mass distributions of observed groups and the distribution

accounting for observed as well as faint distant groups. The stability of the shape of the mass distribution against various models for the spatial distribution of groups is not shared by the estimated total number and total mass of groups within the examined volume.

Once the corrected mass distributions are obtained for each catalogue, they can be compared with the use of suitable statistical tools. It results that the set of five different catalogues considered is significantly inhomogeneous relative not only to the mass but also to all the main physical parameters of groups. In other words, different catalogues contain groups with significantly different physical properties. A subset of catalogues that is homogeneous is formed by $S89$, $RGH89$ and $GH83$. These three catalogues share no region of physical space, come from different underlying galaxy samples, but are produced from the same identification algorithm (although in the case of $RGH89$ the search parameters are different from those used in $GH83$ and $S89$). On the other hand, the remaining catalogues $T87$ and $V84$ are obtained from identification algorithms which differ from those of all other catalogues. More over, their underlying galaxy samples are different. As a consequence the masses of their member groups are different, and show no similarity with any of the other catalogues considered. These results seem to suggest that the property of the catalogues which is mainly responsible for the inhomogeneity of the groups' physical parameters is the identification algorithm used to produce the group catalogues, even though other features of the catalogue may also play a non-negligible role. Probably a good way to test this point could be to use numerical simulations of galaxy clustering on sufficiently large scales and to compare the performance of different group identification algorithms. It would be interesting to see if the inhomogeneity described in this work persists in the same sense in numerical simulations.

The effect of the observational bias on the quoted results is also tested. In particular the analysis is performed on a nearby fraction of each catalogue obtained by considering only groups within 20 Mpc from us. The choice of this value is the best compromise between the requirement of a large enough number of groups and the need to reduce the observational bias below significant values. A value of the distance limit common to all catalogues seems to allow a more meaningful comparison among their nearby fractions. No change in the main conclusions reported above is observed if only the nearby fractions of the catalogues are considered. The distance limit reduces the bias to negligible values for some of the catalogues. If the limit is allowed to change from one catalogue to another, it is possible to define for each catalogue the richest bias-free (nearby) fraction of that catalogue. Also in the case of the set formed by the bias-free fractions of the catalogues, no change is observed in the main results. It is then possible to conclude that the inhomogeneity of the catalogues is not

significantly affected by the observational bias.

A much greater amount of observations is now available relative to the initial work of Gott and Turner (1977), but a new analysis of the concept of group is necessary. The presence of the inhomogeneity among different catalogues suggests the need for the introduction of a (new) definition for groups of galaxies and hence a (new) group identification algorithm that allows us to overcome the inhomogeneity of different catalogues. Also for this problem numerical simulations will probably be of great help.

As far as present day catalogues are concerned, it is possible to ask a) if, although inhomogeneous, the mass distribution of groups in each catalogue is in agreement with the Press and Schechter theory; b) what are the Press and Schechter function parameters $\mathcal{M}_\star$ and n for each catalogue; and finally c) what are the variation of these parameters among different catalogues, i.e., what is the effect of the inhomogeneity on the values of the fitted parameters. It is in fact possible that the shapes of the mass distributions of groups in different catalogues are similar, yielding similar values of n, while the largest variations affect only $\mathcal{M}_\star$.

All these problems will hopefully be analysed in the near future. Moreover, this analysis will include another class of galaxy systems, compact groups. The comparison of open and compact group properties could give interesting information. The accomplishment of this project would hopefully provide observational constraints for both cosmological and astrophysical theories.

Appendix A

Tables of results

This appendix contains the tables which are referred to in chapter 3. They list the results of the analysis of various group catalogues I have considered.

A.1 The GH83 Groups

Table A.1: List of GH83 parameters.

par.	min.	max.	mean	st. dev.	median
D_g	2.46	77.68	37.39	20.06	$34.87^{42.37}_{29.11}$
$D_g^{(v)}$	7.11	87.89	50.19	19.41	$50.69^{56.81}_{45.34}$
n_g	3	23	5.57	3.57	4^{5}_{4}
N_g	4.	80.	20.54	13.88	$17.^{18.}_{15.}$
λ_g	0.13	1.00	0.57	0.26	$0.58^{0.67}_{0.46}$
ν_g	0.17	1.00	0.32	0.18	$0.25^{0.28}_{0.21}$
$\log(R_{Vu})$	-0.45	0.93	0.16	0.32	$0.15^{0.25}_{0.02}$
$\log(R_V)$	-0.45	1.26	0.22	0.35	$0.21^{0.33}_{0.09}$
$\log(R_V(w=3))$	-0.52	1.21	0.23	0.36	$0.27^{0.34}_{0.08}$
$\log(R_V(w=5))$	-0.55	1.16	0.26	0.37	$0.26^{0.39}_{0.12}$
$\log(R_V(w=10))$	-0.51	1.21	0.32	0.40	$0.32^{0.47}_{0.21}$
$\log(R_p)$	-0.96	0.72	-0.11	0.30	$-0.13^{-0.05}_{-0.20}$
$\log(\mathcal{T}_V)$	-1.57	0.74	-0.61	0.44	$-0.62^{-0.55}_{-0.73}$
$\log(\sigma_v)$	1.38	3.26	2.43	0.36	$2.50^{2.57}_{2.36}$
$\log(V_n)$	1.33	3.25	2.40	0.36	$2.47^{2.55}_{2.32}$
$\log(V_g(w=1))$	1.46	3.24	2.35	0.37	$2.40^{2.51}_{2.26}$
$\log(V_g(w=3))$	1.38	3.27	2.32	0.38	$2.37^{2.46}_{2.24}$
$\log(V_g(w=5))(\star)$	1.28	3.27	2.31	0.39	$2.35^{2.46}_{2.24}$
$\log(V_g(w=10))(\star)$	1.13	3.28	2.27	0.40	$2.34^{2.41}_{2.18}$
$\log(L_{min})$	7.77	10.23	9.48	0.53	$9.62^{9.73}_{9.46}$
$\log(L_{max})$	8.99	10.78	10.08	0.29	$10.11^{10.20}_{10.05}$
$\log(L_{sg})$	9.40	11.24	10.52	0.35	$10.52^{10.66}_{10.45}$
$\log(L_{Tg})$	9.47	11.81	10.82	0.54	$10.85^{10.98}_{10.64}$
$\log(\mathcal{M}_{vir}/L_{Tg})$	0.74	4.06	2.47	0.72	$2.50^{2.66}_{2.31}$

Table A.2: List of GH83 mass estimators-statistical parameters.

par.	min.	max.	mean	st. dev.	median
$\log(\mathcal{M}_{vir})$	11.55	15.23	13.29	0.85	$13.31^{13.52}_{13.00}$
$\log(\mathcal{M}_{vir}(w=3))$	11.30	15.24	13.24	0.88	$13.28^{13.53}_{12.95}$
$\log(\mathcal{M}_{vir}(w=5))$	11.15	15.24	13.24	0.83	$13.26^{13.52}_{12.95}$
$\log(\mathcal{M}_{vir}(w=10))$	10.98	15.25	13.24	0.89	$13.24^{13.52}_{12.99}$
$\log(\mathcal{M}_{Vu})$	11.54	15.25	13.39	0.83	$13.43^{13.66}_{13.21}$
$\log(\mathcal{M}_{VT})$	11.76	15.23	13.36	0.78	$13.36^{13.58}_{13.18}$
$\log(\mathcal{M}_{P})$	11.33	15.38	13.34	0.87	$13.41^{13.56}_{13.10}$
$\log(\mathcal{M}_{Me})$	11.59	15.33	13.38	0.80	$13.41^{13.66}_{13.26}$
$\log(\mathcal{M}_{Av})$	11.74	15.41	13.51	0.81	$13.53^{13.73}_{13.26}$

Table A.3: Spearman correlation coefficient r and its significance S for GH83.

pair	$\mid r \mid$	S	$\mid r \mid = 0$?
(n_g, D_g)	0.36	< 0.001	NO
(N_g, D_g)	0.55	< 0.001	NO
$(\log(L_{sg}), D_g)$	0.63	< 0.001	NO
$(\log(L_{Tg}), D_g)$	0.86	< 0.001	NO
$(\log(L_{min}), D_g)$	0.98	< 0.001	NO
$(\log(L_{max}), D_g)$	0.56	< 0.001	NO
$(\log(\mathcal{M}_{vir}), D_g)$	0.44	< 0.001	NO
$(\log(\mathcal{M}_{Vu}), D_g)$	0.43	< 0.001	NO
$(\log(\mathcal{M}_{VT}), D_g)$	0.41	< 0.001	NO
$(\log(\mathcal{M}_{P}), D_g)$	0.37	< 0.001	NO
$(\log(\sigma_v), D_g)$	0.27	0.001	NO
$(\log(R_{Vu}), D_g)$	0.25	< 0.001	NO
$(\log(L_{sg}), n_g)$	0.31	< 0.001	NO
$(\log(L_{Tg}), N_g)$	0.77	< 0.001	NO

Table A.4: Spearman correlation coefficient r and its significance S for $GH83(D \leq 20Mpc)$.

pair	$\mid r \mid$	S	$\mid r \mid = 0$?
(n_g, D_g)	0.08	0.63	YES
(N_g, D_g)	0.59	< 0.001	NO
$(\log(L_{sg}), D_g)$	0.05	0.77	YES
$(\log(L_{Tg}), D_g)$	0.13	0.42	YES
$(\log(L_{min}), D_g)$	0.81	< 0.001	NO
$(\log(L_{max}), D_g)$	0.28	0.09	YES
$(\log(\mathcal{M}_{vir}), D_g)$	0.19	0.25	YES
$(\log(\mathcal{M}_{Vu}), D_g)$	0.15	0.35	YES
$(\log(\mathcal{M}_{VT}), D_g)$	0.15	0.35	YES
$(\log(\mathcal{M}_P), D_g)$	0.23	0.16	YES
$(\log(\sigma_v), D_g)$	0.16	0.33	YES
$(\log(R_{Vu}), D_g)$	0.24	0.14	YES
$(\log(\mathcal{M}_{Vu}), \log(\sigma_v))$	0.95	< 0.001	NO
$(\log(\mathcal{M}_{Vu}), \log(R_{Vu}))$	0.17	0.31	YES
$(\log(L_{sg}), n_g)$	0.75	< 0.001	NO
$(\log(L_{Tg}), N_g)$	0.66	< 0.001	NO

Table A.5: Spearman correlation coefficient r and its significance S for $GH83(D \leq 30Mpc)$. The number of groups in this subcatalogue is 59.

pair	$\mid r \mid$	S	$\mid r \mid = 0$?
(n_g, D_g)	0.06	0.64	YES
(N_g, D_g)	0.54	< 0.001	NO
$(\log(L_{sg}), D_g)$	0.19	0.14	YES
$(\log(L_{Tg}), D_g)$	0.33	0.009	NO
$(\log(L_{min}), D_g)$	0.89	< 0.001	NO
$(\log(L_{max}), D_g)$	0.04	0.76	YES
$(\log(\mathcal{M}_V), D_g)$	0.07	0.58	YES
$(\log(\mathcal{M}_{Vu}), D_g)$	0.006	0.97	YES
$(\log(\mathcal{M}_{VT}), D_g)$	0.006	0.96	YES
$(\log(\mathcal{M}_P), D_g)$	0.04	0.77	YES
$(\log(L_{sg}), n_g)$	0.70	< 0.001	NO
$(\log(L_{Tg}), N_g)$	0.74	< 0.001	NO

Table A.6: Spearman correlation coefficient r and its significance S for $GH83(D \leq 25Mpc)$. The number of groups in this subcatalogue is 48.

pair	$\mid r \mid$	S	$\mid r \mid = 0$?
(n_g, D_g)	0.07	0.63	NO
(N_g, D_g)	0.58	< 0.001	NO
$(\log(L_{sg}), D_g)$	0.18	0.22	YES
$(\log(L_{Tg}), D_g)$	0.28	0.046	NO
$(\log(L_{min}), D_g)$	0.86	< 0.001	NO
$(\log(L_{max}), D_g)$	0.09	0.54	YES
$(\log(\mathcal{M}_V), D_g)$	0.02	0.87	YES
$(\log(\mathcal{M}_{Vu}), D_g)$	0.11	0.46	YES
$(\log(\mathcal{M}_{VT}), D_g)$	0.10	0.48	YES
$(\log(\mathcal{M}_P), D_g)$	0.13	0.38	YES
$(\log(L_{sg}), n_g)$	0.71	< 0.001	NO
$(\log(L_{Tg}), N_g)$	0.70	< 0.001	NO

Table A.7: The KS test significances S of differences revealed by the comparison of mass and other main parameter distributions. ($GH83(D \leq 20\ Mpc)$ versus $GH83$ in column A and versus $GH(D > 20\ Mpc)$ in column B, while in column C: $GH83$ versus $GH83(D > 20\ Mpc)$.

estimator	col. A	col. B	col C.
$\mathcal{M}_{Vu}$	0.07	0.009	0.80
$\mathcal{M}_{vir}$	0.08	0.007	0.79
$\mathcal{M}_{vir}(w=3)$	0.18	0.03	0.90
$\mathcal{M}_{vir}(w=5)$	0.18	0.03	0.90
$\mathcal{M}_{vir}(w=10)$	0.15	0.02	0.88
$\mathcal{M}_{VT}$	0.04	0.03	0.79
$\mathcal{M}_{P}$	0.09	0.01	0.86
$\mathcal{M}_{Me}$	0.04	0.002	0.68
$\mathcal{M}_{Av}$	0.03	0.001	0.62
n_g	0.61	0.26	0.99
N_g	< 0.001	< 0.001	0.12
$\log(\sigma_v)$	0.43	0.16	0.99
$\log(T_V)$	0.26	0.06	0.94
$\log(R_p)$	< 0.001	< 0.001	0.22
$\log(R_{Vu})$	0.01	< 0.001	0.48
$\log(\mathcal{M}_{vir}/L_{Tg})$	0.62	0.28	0.99

Table A.8: List of $GH83(D \leq 20Mpc)$ parameters.

par.	min.	max.	mean	st. dev.	median
D_g	2.46	19.66	13.88	4.60	$14.64^{17.18}_{11.87}$
$D_g^{(v)}$	7.11	75.37	30.09	15.73	$29.13^{37.10}_{17.48}$
n_g	3	23	6.26	4.08	5^{7}_{4}
N_g	4.00	39.00	12.24	8.82	$9.00^{14.00}_{6.00}$
λ_g	0.82	1.00	0.90	0.06	$0.89^{0.93}_{0.85}$
ν_g	0.39	1.00	0.56	0.18	$0.50^{0.59}_{0.44}$
$\log(R_V)$	-0.44	1.26	0.11	0.38	$0.4^{0.21}_{-0.14}$
$\log(R_V(w=3))$	-0.52	1.21	0.13	0.38	$0.045^{0.28}_{-0.14}$
$\log(R_V(w=5))$	-0.55	1.16	0.16	0.39	$0.069^{0.39}_{-0.11}$
$\log(R_V(w=10))$	-0.51	1.07	0.21	0.41	$0.11^{0.50}_{-0.04}$
$\log(R_{Vu})$	-0.44	0.40	-0.02	0.23	$-0.03^{0.13}_{-0.17}$
$\log(R_p)$	-0.83	0.08	-0.30	0.20	$-0.25^{-0.20}_{-0.40}$
$\log(T_V)$	-1.32	0.69	-0.70	0.47	$-0.79^{-0.58}_{-1.04}$
$\log(\sigma_v)$	1.38	2.84	2.35	0.35	$2.45^{2.60}_{2.14}$
$\log(V_n)$	1.33	2.82	2.33	0.35	$2.41^{2.58}_{2.13}$
$\log(V_g(w=1))$	1.48	2.79	2.19	0.35	$2.23^{2.39}_{2.07}$
$\log(V_g(w=3))$	1.48	2.83	2.17	0.36	$2.22^{2.39}_{1.99}$
$\log(V_g(w=5))$	1.48	2.84	2.15	0.37	$2.24^{2.39}_{1.95}$
$\log(V_g(w=10))$	1.37	2.82	2.12	0.39	$2.23^{2.37}_{1.91}$
$\log(L_{min})$	7.77	9.39	8.77	0.34	$8.81^{8.97}_{8.70}$
$\log(L_{max})$	8.99	10.39	9.87	0.33	$9.88^{10.02}_{9.76}$
$\log(L_{sg})$	9.40	10.95	10.21	0.37	$10.28^{10.40}_{10.06}$
$\log(L_{Tg})$	9.47	10.98	10.26	0.38	$10.34^{10.44}_{10.07}$
$\log(\mathcal{M}_{vir}/L_{Tg})$	1.07	4.00	2.61	0.69	$2.51^{2.94}_{2.27}$

Table A.9: List of $GH83(D \leq 20Mpc)$ groups mass estimators-statistical parameters.

par.	min.	max.	mean	st. dev.	median
$\log(\mathcal{M}_{vir})$	11.67	14.93	13.18	0.74	$13.28^{13.51}_{12.63}$
$\log(\mathcal{M}_{vir}(w=3))$	11.67	14.87	13.19	0.74	$13.28^{13.52}_{12.64}$
$\log(\mathcal{M}_{vir}(w=5))$	11.67	14.83	13.22	0.73	$13.30^{13.52}_{12.62}$
$\log(\mathcal{M}_{vir}(w=10))$	11.67	14.73	13.28	0.74	$13.32^{13.59}_{12.62}$
$\log(\mathcal{M}_{Vu})$	11.54	14.03	13.04	0.68	$13.19^{13.43}_{12.62}$
$\log(\mathcal{M}_{VT})$	11.76	13.97	13.04	0.63	$13.19^{13.42}_{12.59}$
$\log(\mathcal{M}_{P})$	11.58	14.23	13.03	0.68	$13.10^{13.47}_{12.62}$
$\log(\mathcal{M}_{Me})$	11.59	14.09	13.06	0.68	$13.18^{13.49}_{12.73}$
$\log(\mathcal{M}_{Av})$	12.11	14.17	13.14	0.62	$13.19^{13.47}_{12.77}$

Table A.10: Pairwise KS test of different velocity dispersion estimator distributions observed in $GH83(D \leq 20Mpc)$ (upper half) and in $GH83$ (lower half).

♣	σ_v	V_n	$V_g(1)$	$V_{g(3)}$	$V_g(5)$	$V_g(10)$
σ_v	♣	0.90	0.14	0.14	0.08	0.04
V_n	0.78	♣	0.24	0.14	0.14	0.08
$V_g(1)$	0.15	0.59	♣	0.99	0.98	0.54
$V_g(3)$	0.06	0.20	0.98	♣	0.99	0.90
$V_g(5)$	0.05	0.20	0.87	0.99	♣	0.98
$V_g(10)$	0.03	0.02	0.26	0.69	0.94	♣

Table A.11: Pairwise KS test of different mass estimator distributions observed in $GH83(D \leq 20Mpc)$ (upper half) and in $GH83$ (lower half).

♣	$\mathcal{M}_{Vu}$	$\mathcal{M}_{VT}$	$\mathcal{M}_{P}$	$\mathcal{M}_{Me}$	$\mathcal{M}_{Av}$	$\mathcal{M}_{V}^{(1)}$	$\mathcal{M}_{V}^{(3)}$	$\mathcal{M}_{V}^{(5)}$	$\mathcal{M}_{V}^{(10)}$
$\mathcal{M}_{Vu}$	♣	0.99	0.90	0.98	0.98	0.98	0.90	0.90	0.54
$\mathcal{M}_{VT}$	0.98	♣	0.90	0.98	0.98	0.90	0.90	0.73	0.37
$\mathcal{M}_{P}$	0.78	0.78	♣	0.98	0.90	0.90	0.73	0.54	0.54
$\mathcal{M}_{Me}$	0.99	0.94	0.94	♣	0.98	0.90	0.73	0.73	0.54
$\mathcal{M}_{Av}$	0.78	0.59	0.40	0.59	♣	0.98	0.90	0.90	0.90
$\mathcal{M}_{V}^{(1)}$	0.98	0.78	0.59	0.87	0.94	♣	0.99	0.99	0.90
$\mathcal{M}_{V}^{(3)}$	0.87	0.59	0.40	0.87	0.98	0.95	♣	1.00	0.98
$\mathcal{M}_{V}^{(5)}$	0.78	0.59	0.40	0.78	0.99	0.98	0.99	♣	0.99
$\mathcal{M}_{V}^{(10)}$	0.59	0.40	0.26	0.49	0.98	0.87	0.94	0.99	♣

Table A.12: Pairwise KS test of different virial radius estimator distributions observed in $GH83(D \leq 20Mpc)$ (upper half) and in $GH83$ (lower half).

♣	R_{Vu}	$R_V(1)$	$R_V(3)$	$R_V(5)$	$R_V(10)$
R_{Vu}	♣	0.54	0.14	0.04	0.01
$R_V(1)$	0.40	♣	0.98	0.54	0.37
$R_V(3)$	0.12	0.87	♣	0.98	0.37
$R_V(5)$	0.02	0.49	0.98	♣	0.54
$R_V(10)$	< 0.001	0.24	0.15	0.69	♣

Table A.13: List of $GH83$ mass corrected for the evolutionary effect and related parameters.

par.	min.	max.	mean	st. dev.	median
		$\Omega = 0.2$			
$\log(\mathcal{M}_{Vu})$	12.04	15.41	13.58	0.77	$13.63^{13.80}_{13.31}$
τ	3.34	31.21	6.16	3.41	$5.38^{5.61}_{5.24}$
α	0.008	0.69	0.38	0.17	$0.39^{0.45}_{0.36}$
μ	0.73	61.31	2.98	7.25	$1.29^{1.42}_{1.12}$
		$\Omega = 1$			
$\log(\mathcal{M}_{Vu})$	12.13	15.51	13.66	0.77	$13.72^{13.87}_{13.42}$
τ	3.29	24.17	5.46	2.13	$5.15^{5.38}_{5.00}$
α	0.005	0.68	0.34	0.17	$0.33^{0.39}_{0.30}$
μ	0.73	98.63	4.15	11.65	$1.51^{1.68}_{1.28}$

Table A.14: List of $GH83(D \leq 20\ Mpc)$ mass corrected for the evolutionary effect and related parameters.

par.	min.	max.	mean	st. dev.	median
		$\Omega = 0.2$			
$\log(\mathcal{M}_{Vu})$	12.18	14.10	13.18	0.52	$13.21^{13.40}_{13.02}$
τ	3.36	17.62	6.43	2.79	$5.66^{6.20}_{5.29}$
α	0.01	0.69	0.42	0.17	$0.45^{0.53}_{0.37}$
μ	0.73	48.60	3.08	8.01	$1.09^{1.36}_{0.94}$
		$\Omega = 1$			
$\log(\mathcal{M}_{Vu})$	12.24	14.16	13.25	0.51	$13.30^{13.48}_{13.09}$
τ	3.31	13.64	5.64	1.57	$5.43^{5.98}_{5.06}$
α	0.006	0.66	0.39	0.18	$0.40^{0.50}_{0.31}$
μ	0.75	77.74	4.35	12.85	$1.24^{1.61}_{0.99}$

Table A.15: Effect of the evolutionary correction: significance S of KS test comparison between the observed and corrected distributions.

Ω	$GH83$	$GH83(D \leq 20\ Mpc)$
0.2	0.24	0.37
1.0	0.09	0.24

Table A.16: Effect of Ω on the evolutionary correction: significance S of KS test comparison between the corrected distributions obtained for two values of Ω for $GH83$.

par.	$GH83$	$GH83(D \leq 20\ Mpc)$
$\mathcal{M}_{V_u}$	0.81	0.54
τ	0.03	0.17
α	0.02	0.42
μ	0.02	0.54

A.2 The T87 groups

Table A.17: List of T87 parameters.

par.	min.	max.	mean	st. dev.	median
D_g	1.88	28.78	15.77	6.70	$15.67^{17.05}_{13.64}$
n_g	3	22	5.69	3.68	4^{5}_{4}
$\log(R_{Vu})$	-0.63	0.54	0.02	0.24	$0.04^{0.07}_{-0.05}$
$\log(R_p)$	-1.20	0.09	-0.30	0.22	$-0.27^{-0.23}_{-0.33}$
$\log(\mathcal{T}_V)$	-1.70	1.11	-0.43	0.41	$-0.46^{-0.39}_{-0.53}$
$\log(\sigma_v)$	0.93	2.88	2.12	0.30	$2.18^{2.24}_{2.12}$
$\log(L_{min})(\star)$	7.08	10.70	9.56	0.69	$9.79^{9.89}_{9.57}$
$\log(L_{max})(\star)$	7.74	10.64	9.71	0.62	$9.89^{10.01}_{9.70}$
$\log(L_{sg})(\star)$	9.35	11.20	10.33	0.35	$10.36^{10.45}_{10.28}$
$\log(\mathcal{M}_{Vu}/L_{sg})(\star)$	-1.47	3.55	2.25	0.65	$2.33^{2.42}_{2.20}$

Table A.18: List of T87 mass estimators-statistical parameters.

$\log(\mathcal{M}_{Vu})$	10.04	13.79	12.62	0.62	$12.74^{12.84}_{12.60}$
$\log(\mathcal{M}_{VT})$	11.28	13.82	12.74	0.52	$12.80^{12.89}_{12.68}$
$\log(\mathcal{M}_P)$	10.60	14.22	12.68	0.61	$12.79^{12.88}_{12.67}$
$\log(\mathcal{M}_{Me})$	11.01	13.86	12.69	0.53	$12.79^{12.87}_{12.65}$
$\log(\mathcal{M}_{Av})$	11.42	13.94	12.87	0.50	$12.92^{13.04}_{12.77}$

Table A.19: Spearman correlation coefficient r and its significance S for $T87$.

pair	$\mid r \mid$	S	$\mid r \mid = 0$?
$(\log(L_{sg}), D_g)(\star)$	0.35	$< 10^{-3}$	NO
$(\log(L_{min}), D_g)(\star)$	0.51	$< 10^{-3}$	NO
$(\log(L_{max}), D_g)(\star)$	0.27	$< 10^{-3}$	NO
$(\log(\mathcal{M}_{Vu}), D_g)$	0.20	$8 \cdot 10^{-3}$	NO
$(\log(\sigma_v), D_g)$	0.18	0.02	NO
$(\log(R_{Vu}), D_g)$	0.16	0.04	NO
$(\log(L_{sg}/\mathcal{M}_{Vu}), D_g)(\star)$	0.01	0.87	YES
$(\log(L_{sg}), \log(\sigma_v))(\star)$	0.36	$< 10^{-3}$	NO
$(\log(L_{sg}), \log(R_{Vu}))(\star)$	0.07	0.41	YES
$(\log(\sigma_v), \log(R_{Vu}))$	0.06	0.44	YES
$(\log(\mathcal{M}_{Vu}), \log(L_{sg}))(\star)$	0.36	$< 10^{-3}$	NO
$(\log(\mathcal{M}_{Vu}), \log(\sigma_v))$	0.88	0.00	NO
$(\log(\mathcal{M}_{Vu}), \log(R_{Vu}))$	0.35	$< 10^{-3}$	NO
$(\log(L_{sg}/\mathcal{M}_{Vu}), \log(R_{Vu}))(\star)$	0.25	0.002	NO

Table A.20: List of $T87(D \leq 20\ Mpc)$ parameters.

par.	min.	max.	mean	st. dev.	median
D_g	1.88	19.93	12.45	4.55	$13.01^{14.76}_{11.05}$
n_g	3	22	6.21	3.97	5^{6}_{4}
$\log(R_{Vu})$	-0.49	0.52	0.005	0.21	$-0.004^{0.06}_{-0.06}$
$\log(R_p)$	-1.04	0.09	-0.31	0.21	$-0.28^{-0.23}_{-0.36}$
$\log(\mathcal{T}_V)$	-1.28	1.11	-0.43	0.36	$-0.48^{-0.39}_{-0.55}$
$\log(\sigma_v)$	1.07	2.75	2.10	0.28	$2.17^{2.23}_{2.11}$
$\log(L_{min})(\star)$	7.08	10.43	9.40	0.73	$9.56^{9.80}_{9.34}$
$\log(L_{max})(\star)$	7.74	10.63	9.64	0.64	$9.85^{9.99}_{9.65}$
$\log(L_{sg})(\star)$	9.35	11.00	10.26	0.35	$10.31^{10.39}_{10.18}$
$\log(\mathcal{M}_{Vu}/L_{sg})(\star)$	-1.47	3.55	2.27	0.66	$2.33^{2.48}_{2.16}$

Table A.21: List of $T87(D \leq 20\ Mpc)$ mass estimators-statistical parameters.

$\log(\mathcal{M}_{Vu})$	10.94	13.76	12.58	0.58	$12.72^{12.84}_{12.57}$
$\log(\mathcal{M}_{VT})$	11.28	13.77	12.67	0.51	$12.77^{12.87}_{12.63}$
$\log(\mathcal{M}_P)$	10.60	14.23	12.64	0.61	$12.77^{12.89}_{12.62}$
$\log(\mathcal{M}_{Me})$	11.01	13.78	12.63	0.53	$12.74^{12.84}_{12.57}$
$\log(\mathcal{M}_{Av})$	11.41	13.74	12.79	0.50	$12.86^{13.00}_{12.66}$

Table A.22: Spearman correlation coefficient r and its significance S for $T87(D \leq 20\ Mpc)$.

pair	$\mid r \mid$	S	$\mid r \mid = 0$?
$(\log(L_{sg}), D_g)(\star)$	0.18	0.054	YES
$(\log(L_{min}), D_g)(\star)$	0.57	$< 10^{-3}$	NO
$(\log(L_{max}), D_g)(\star)$	0.25	0.008	NO
$(\log(\mathcal{M}_{Vu}), D_g)$	0.22	0.02	NO
$(\log(\sigma_v), D_g)$	0.20	0.04	NO
$(\log(R_{Vu}), D_g)$	0.24	0.01	NO
$(\log(L_{sg}/\mathcal{M}_{Vu}), D_g)(\star)$	0.12	0.21	YES
$(\log(L_{sg}), \log(\sigma_v))(\star)$	0.35	$< 10^{-3}$	NO
$(\log(L_{sg}), \log(R_{Vu}))(\star)$	0.11	0.23	YES
$(\log(\sigma_v), \log(R_{Vu}))$	0.02	0.70	YES
$(\log(\mathcal{M}_{Vu}), \log(L_{sg}))(\star)$	0.35	$< 10^{-3}$	NO
$(\log(\mathcal{M}_{Vu}), \log(\sigma_v))$	0.89	0.00	NO
$(\log(\mathcal{M}_{Vu}), \log(R_{Vu}))$	0.39	$< 10^{-3}$	NO
$(\log(L_{sg}/\mathcal{M}_{Vu}), \log(R_{Vu}))(\star)$	0.18	0.053	YES

Table A.23: Pairwise KS test of different mass estimator distributions observed in $T87$ and $T87(D \leq 20\ Mpc)$.

pair	$S(T87)$	$S[T87(D \leq 20\ Mpc)]$
$(\mathcal{M}_{Vu}, \mathcal{M}_{VT})$	0.47	0.77
$(\mathcal{M}_{Vu}, \mathcal{M}_{P})$	0.83	0.77
$(\mathcal{M}_{Vu}, \mathcal{M}_{Me})$	0.56	0.55
$(\mathcal{M}_{Vu}, \mathcal{M}_{Av})$	0.006	0.02
$(\mathcal{M}_{VT}, \mathcal{M}_{P})$	0.75	0.98
$(\mathcal{M}_{VT}, \mathcal{M}_{Me})$	0.96	0.98
$(\mathcal{M}_{VT}, \mathcal{M}_{Av})$	0.051	0.08
$(\mathcal{M}_{P}, \mathcal{M}_{Me})$	0.75	0.94
$(\mathcal{M}_{P}, \mathcal{M}_{Av})$	0.03	0.21
$(\mathcal{M}_{Me}, \mathcal{M}_{Av})$	0.03	0.11

Table A.24: KS test significances S of differences revealed by the comparison of mass and other parameters distributions. ($T87(D \leq 20\ Mpc)$ versus $T87$ in column A and versus $T87(D > 20\ Mpc)$ in column B, while in column C: $T87$ versus $T87(D > 20\ Mpc)$.

estimator	col. A	col. B	col C.
$\mathcal{M}_{Vu}$	0.87	0.02	0.17
$\mathcal{M}_{VT}$	0.93	0.055	0.26
$\mathcal{M}_{P}$	0.99	0.38	0.74
$\mathcal{M}_{med}$	0.99	0.17	0.49
$\mathcal{M}_{Av}$	0.86	0.02	0.16
n_g	0.97	0.099	0.37
$\log(\sigma_v)$	0.97	0.16	0.38
$\log(T_V)$	0.99	0.39	0.75
$\log(R_p)$	0.94	0.06	0.28
$\log(R_{Vu})$	0.79	0.01	0.11
$\log(\mathcal{M}_{Vu}/L_{Tg})(\star)$	0.99	0.81	0.95

Table A.25: List of $T87$ mass corrected for the evolutionary effect and related parameters.

par.	min.	max.	mean	st. dev.	median
		$\Omega = 0.2$			
$\log(\mathcal{M}_{Vu})$	11.28	14.01	12.93	0.52	$12.97^{13.07}_{12.85}$
τ	3.23	47.75	5.44	3.53	$5.06^{5.19}_{4.88}$
α	$1.6 \cdot 10^{-3}$	0.69	0.31	0.15	$0.31^{0.34}_{0.27}$
μ	0.73	304.40	4.96	24.48	$1.60^{1.83}_{1.46}$
		$\Omega = 1$			
$\log(\mathcal{M}_{Vu})$	11.37	14.14	13.02	0.52	$13.07^{13.15}_{12.92}$
τ	3.21	33.15	5.09	2.65	$4.81^{4.95}_{4.65}$
α	$1.0 \cdot 10^{-3}$	0.65	0.26	0.14	$0.26^{0.29}_{0.22}$
μ	0.77	500.07	7.33	40.27	$1.93^{2.25}_{1.74}$

Table A.26: List of $T87(D < 20\ Mpc)$ mass corrected for the evolutionary effect and related parameters.

par.	min.	max.	mean	st. dev.	median
		$\Omega = 0.2$			
$\log(\mathcal{M}_{Vu})$	11.28	13.95	12.87	0.47	$12.90^{13.03}_{12.72}$
τ	3.23	16.20	5.09	1.04	$5.08^{5.22}_{4.88}$
α	$1.6 \cdot 10^{-3}$	0.69	0.31	0.14	$0.31^{0.35}_{0.27}$
μ	0.73	304.40	5.27	28.64	$1.59^{1.83}_{1.43}$
		$\Omega = 1$			
$\log(\mathcal{M}_{Vu})$	11.37	14.08	12.96	0.47	$12.99^{13.13}_{12.86}$
τ	3.21	12.54	4.84	0.82	$4.83^{4.98}_{4.65}$
α	$1.0 \cdot 10^{-3}$	0.65	0.26	0.13	$0.26^{0.29}_{0.22}$
μ	0.77	500.70	7.89	47.14	$1.91^{2.25}_{1.70}$

Table A.27: Effect of the evolutionary correction: significance S of KS test comparison between the observed and corrected distributions.

Ω	$T87$	$T87(D \leq 20\ Mpc)$
0.2	< 0.001	0.002
1.0	$< 10^{-3}$	< 0.001

Table A.28: Effect of Ω on the evolutionary correction: significance S of KS test comparison between the corrected distributions obtained for two values of Ω for $T87$.

par.	$T87$	$T87(D \leq 20\ Mpc)$
$\mathcal{M}_{Vu}$	0.39	0.44
τ	0.005	0.01
α	0.006	0.02
μ	0.02	0.01

Table A.29: The effect of the magnitude limit m_c on the observed mass distributions for $T87(D \leq 20\ Mpc)$.

par.	$S(m_c = 12)$	$S(m_c = 12.5)$
$\log(\mathcal{M}_{Vu})$	0.30	0.68
$\log(\mathcal{M}_{VT})$	0.06	0.78
$\log(\mathcal{M}_{P})$	$8.2 \cdot 10^{-3}$	0.82
$\log(\mathcal{M}_{Me})$	0.02	0.67
$\log(\mathcal{M}_{Av})$	0.48	0.71

Table A.30: The effect of the correction on the m_c-complete mass distributions on $T87(D \leq 20\ Mpc)$: KS significance of $\mathcal{N}_c^{(m_c)}(\mathcal{M})$ vs. $\mathcal{N}_{obs}^{(m_c)}(\mathcal{M})$.

par.	$S(m_c = 12)$	$S(m_c = 12.5)$
$\log(\mathcal{M}_{Vu})$	0.11	0.30
$\log(\mathcal{M}_P)$	0.25	0.36
$\log(\mathcal{M}_{Me})$	0.17	0.24
$\log(\mathcal{M}_{Av})$	0.36	0.53

Table A.31: The efficiency of faint distant groups recovery for $T87(D \leq 20\ Mpc)$: KS significance of $\mathcal{N}_c^{(m_c)}(\mathcal{M})$ vs. $\mathcal{N}_{obs}(\mathcal{M})$.

par.	$S(m_c = 12)$	$S(m_c = 12.5)$
$\log(\mathcal{M}_{Vu})$	0.053	0.22
$\log(\mathcal{M}_P)$	$< 10^{-3}$	0.11
$\log(\mathcal{M}_{Me})$	$< 10^{-3}$	0.06
$\log(\mathcal{M}_{Av})$	0.008	0.06

A.3 The V84 groups

Table A.32: List of V84 parameters.

par.	min.	max.	mean	st. dev.	median
D_g	1.87	31.79	15.00	7.24	$13.87^{16.25}_{11.32}$
n_g	3	19	5.91	2.78	5^{6}_{4}
$\log(R_{Vu})$	-0.65	0.71	-0.13	0.23	$-0.13^{-0.07}_{-0.20}$
$\log(R_p)$	-1.15	0.54	-0.44	0.28	$-0.42^{-0.36}_{-0.51}$
$\log(\bar{T}_V)$	-1.66	0.77	-0.53	0.40	$-0.54^{-0.42}_{-0.67}$
$\log(\sigma_v)$	1.01	3.16	2.06	0.31	$2.10^{2.14}_{2.01}$
$\log(\bar{L}_{min})$	6.79	9.73	8.60	0.55	$8.70^{8.84}_{8.50}$
$\log(\bar{L}_{max})$	8.75	10.51	9.82	0.33	$9.86^{9.92}_{9.74}$
$\log(\bar{L}_{sg})$	9.14	11.12	10.14	0.36	$10.13^{10.24}_{10.08}$
$\log(\mathcal{M}_{Vu}/\bar{L}_{sg})$	-2.28	3.90	2.12	0.75	$2.16^{2.28}_{2.04}$

Table A.33: List of V84 mass estimators-statistical parameters.

$\log(\mathcal{M}_{Vu})$	10.12	14.51	12.36	0.66	$12.45^{12.58}_{12.19}$
$\log(\mathcal{M}_{VT})$	11.16	14.52	12.46	0.55	$12.49^{12.62}_{12.29}$
$\log(\mathcal{M}_P)$	10.50	14.60	12.37	0.63	$12.38^{12.52}_{12.24}$
$\log(\mathcal{M}_{Me})$	11.01	14.45	12.42	0.58	$12.45^{12.62}_{12.26}$
$\log(\mathcal{M}_{Av})$	11.19	13.69	12.49	0.54	$12.50^{12.66}_{12.42}$

Table A.34: Spearman correlation coefficient r and its significance S for V84.

pair	$\mid r \mid$	S	$\mid r \mid = 0$?
$(\log(L_{sg}), D_g)$	0.43	< 0.001	NO
$(\log(L_{min}), D_g)$	0.77	< 0.001	NO
$(\log(L_{max}), D_g)$	0.32	< 0.001	NO
$(\log(\mathcal{M}_{Vu}), D_g)$	0.36	< 0.001	NO
$(\log(\sigma_v), D_g)$	0.29	0.002	NO
$(\log(R_{Vu}), D_g)$	0.31	0.001	NO
$(\log(\mathcal{M}_{Vu}), \log(L_{sg}))$	0.41	< 0.001	NO
$(\log(\mathcal{M}_{Vu}), \log(\sigma g))$	0.90	< 0.001	NO
$(\log(\mathcal{M}_{Vu}), \log(R_{Vu}))$	0.30	0.002	NO
$(\log(L_{sg}), \log(\sigma_g))$	0.39	< 0.001	NO
$(\log(L_{sg}), \log(R_{Vu}))$	0.14	0.15	YES
$(\log(\sigma_v), \log(R_{Vu}))$	0.09	0.37	YES

Table A.35: Spearman correlation coefficient r and its significance S for $V84(D \leq 20\ Mpc)$.

pair	$\mid r \mid$	S	$\mid r \mid = 0$?
$(\log(L_{sg}), D_g)$	0.21	0.055	YES
$(\log(L_{min}), D_g)$	0.75	< 0.001	NO
$(\log(L_{max}), D_g)$	0.15	0.18	YES
$(\log(\mathcal{M}_{Vu}), D_g)$	0.23	0.034	NO
$(\log(\sigma_v), D_g)$	0.21	0.056	YES
$(\log(R_{Vu}), D_g)$	0.25	0.023	NO
$(\log(\mathcal{M}_{Vu}), \log(L_{sg}))$	0.30	0.006	NO
$(\log(\mathcal{M}_{Vu}), \log(\sigma_v))$	0.90	< 0.001	NO
$(\log(\mathcal{M}_{Vu}), \log(R_{Vu}))$	0.18	0.10	YES
$(\log(L_{sg}), \log(\sigma_v))$	0.27	0.01	NO
$(\log(L_{sg}), \log(R_{Vu}))$	0.11	0.30	YES
$(\log(\sigma_v), \log(R_{Vu}))$	0.20	0.09	YES

Table A.36: List of $V84(D \leq 20\ Mpc)$ parameters.

par.	min.	max.	mean	st. dev.	median
D_g	1.87	19.71	11.73	4.67	$11.29^{13.32}_{10.03}$
n_g	3	13	5.82	2.55	5^{6}_{4}
$\log(R_{Vu})$	-0.65	0.40	-0.17	0.22	$-0.16^{-0.09}_{-0.25}$
$\log(R_p)$	-1.15	0.15	-0.49	0.26	$-0.47^{-0.40}_{-0.57}$
$\log(T_V)$	-1.49	0.77	-0.52	0.39	$-0.54^{-0.42}_{-0.65}$
$\log(\sigma_v)$	1.01	2.62	2.02	0.29	$2.09^{2.13}_{1.99}$
$\log(L_{min})$	6.79	9.29	8.46	0.53	$8.57^{8.70}_{8.35}$
$\log(L_{max})$	8.75	10.49	9.76	0.33	$9.75^{9.88}_{9.70}$
$\log(L_{sg})$	9.14	10.73	10.05	0.33	$10.11^{10.20}_{9.98}$
$\log(\mathcal{M}_{Vu}/L_{sg})$	-2.28	3.25	2.05	0.78	$2.10^{2.26}_{1.98}$

Table A.37: List of $V84(D \leq 20\ Mpc)$ mass estimators-statistical parameters.

$\log(\mathcal{M}_{Vu})$	10.12	13.13	12.24	0.59	$12.32^{12.51}_{12.13}$
$\log(\mathcal{M}_{VT})$	11.16	13.17	12.35	0.48	$12.37^{12.56}_{12.21}$
$\log(\mathcal{M}_P)$	10.50	13.25	12.23	0.55	$12.29^{12.46}_{12.19}$
$\log(\mathcal{M}_{Me})$	11.01	13.15	12.30	0.51	$12.34^{12.51}_{12.17}$
$\log(\mathcal{M}_{Av})$	11.19	13.29	12.37	0.49	$12.46^{12.58}_{12.23}$

Table A.38: Pairwise KS test of different mass estimator distributions observed in V84 and $V84(D \leq 20Mpc)$.

pair	$S(V84)$	$S[V84(D \leq 20\ Mpc)]$
$(\mathcal{M}_{Vu}, \mathcal{M}_{VT})$	0.52	0.55
$(\mathcal{M}_{Vu}, \mathcal{M}_{P})$	0.93	0.83
$(\mathcal{M}_{Vu}, \mathcal{M}_{Med})$	0.98	0.98
$(\mathcal{M}_{Vu}, \mathcal{M}_{Av})$	0.52	0.58
$(\mathcal{M}_{VT}, \mathcal{M}_{P})$	0.52	0.45
$(\mathcal{M}_{VT}, \mathcal{M}_{Med})$	0.75	0.83
$(\mathcal{M}_{VT}, \mathcal{M}_{Av})$	0.85	0.83
$(\mathcal{M}_{P}, \mathcal{M}_{Med})$	0.75	0.71
$(\mathcal{M}_{P}, \mathcal{M}_{Av})$	0.19	0.18
$(\mathcal{M}_{Med}, \mathcal{M}_{Av})$	0.52	0.58

Table A.39: KS test significances S of differences revealed by the comparison of mass estimator distributions. $(V84(D \leq 20\ Mpc)$ versus $V84$ in column A and versus $V84(D > 20\ Mpc)$ in column B, while in column C: $V84$ versus $V84(D > 20\ Mpc)$.

estimator	col. A	col. B	col C.
$\mathcal{M}_{Vu}$	0.90	0.02	0.13
$\mathcal{M}_{VT}$	0.88	0.01	0.10
$\mathcal{M}_{P}$	0.62	$< 10^{-3}$	0.01
$\mathcal{M}_{med}$	0.72	0.002	0.03
$\mathcal{M}_{Av}$	0.65	$< 10^{-3}$	0.02
n_g	1.00	0.99	0.99
$\log(\sigma_v)$	0.96	0.052	0.22
$\log(T_V)$	0.99	0.73	0.94
$\log(R_p)$	0.78	0.004	0.051
$\log(R_{Vu})$	0.94	0.04	0.19
$\log(\mathcal{M}_{Vu}/L_{Tg})(\star)$	0.99	0.12	0.36

Table A.40: List of $V84$ mass corrected for the evolutionary effect and related parameters.

par.	min.	max.	mean	st. dev.	median
		$\Omega = 0.2$			
$\log(\mathcal{M}_{Vu})$	11.11	14.51	12.59	0.57	$12.59^{12.75}_{12.43}$
τ	3.33	36.66	5.81	3.93	$5.22^{5.47}_{4.97}$
α	0.007	0.66	0.34	0.16	$0.35^{0.41}_{0.29}$
μ	0.76	68.31	2.72	6.68	$1.43^{1.72}_{1.22}$
		$\Omega = 1$			
$\log(\mathcal{M}_{Vu})$	11.19	14.54	12.67	0.56	$12.66^{12.82}_{12.52}$
τ	3.29	30.52	5.38	2.97	$5.00^{5.26}_{4.74}$
α	0.005	0.62	0.30	0.16	$0.30^{0.36}_{0.24}$
μ	0.81	106.20	3.63	10.38	$1.68^{2.06}_{1.39}$

Table A.41: List of $V84(D \leq 20\ Mpc)$ mass corrected for the evolutionary effect and related parameters.

par.	min.	max.	mean	st. dev.	median
		$\Omega = 0.2$			
$\log(\mathcal{M}_{Vu})$	11.11	13.61	12.47	0.48	$12.50^{12.68}_{12.37}$
τ	3.33	25.96	5.58	2.60	$5.22^{5.45}_{4.97}$
α	0.007	0.66	0.34	0.16	$0.35^{0.41}_{0.29}$
μ	0.76	68.31	2.90	7.62	$1.43^{1.72}_{1.23}$
		$\Omega = 1$			
$\log(\mathcal{M}_{Vu})$	11.19	13.73	12.55	0.48	$12.56^{12.75}_{12.47}$
τ	3.29	20.49	5.21	1.92	$5.00^{5.24}_{4.74}$
α	0.005	0.62	0.30	0.15	$0.30^{0.35}_{0.24}$
μ	0.81	106.20	3.91	11.87	$1.68^{2.06}_{1.41}$

Table A.42: Effect of evolutionary correction: significance S of KS test comparison between the observed and corrected distributions.

Ω	$V84$	$V84(D \leq 20\ Mpc)$
0.2	0.04	0.04
1.0	0.006	0.005

Table A.43: Effect of Ω on the evolutionary correction: significance S of KS test comparison between the corrected distributions obtained for two values of Ω for $V84$.

par.	$V84$	$V84(D \leq 20\ Mpc)$
$\mathcal{M}_{Vu}$	0.49	0.53
τ	0.04	0.18
α	0.08	0.18
μ	0.14	0.14

A.4 The RGH89 groups

Table A.44: List of RGH89 parameters.

par.	min.	max.	mean	st. dev.	median
D_g	32.36	112.68	75.37	23.68	$76.17^{88.94}_{67.04}$
$D_g^{(v)}$	37.45	135.44	86.94	22.58	$88.94^{95.28}_{78.35}$
n_g	3	13	4.7	2.28	4^{5}_{3}
N_g	10	156	42.6	27.5	38^{41}_{31}
λ_g	0.13	0.81	0.40	0.21	$0.36^{0.43}_{0.23}$
ν_g	0.07	0.31	0.13	0.07	$0.11^{0.12}_{0.08}$
$\log(R_{Vu})$	-0.51	0.51	0.07	0.26	$0.08^{0.22}_{-0.06}$
$\log(R_V)$	-1.03	0.06	-0.25	0.24	$-0.17^{-0.13}_{-0.27}$
$\log(R_p)$	-0.46	0.51	0.09	0.26	$0.09^{0.24}_{-0.06}$
$\log(\mathcal{T}_V)$	-1.40	$-4 \cdot 10^{-4}$	-0.76	0.33	$-0.79^{-0.61}_{-0.94}$
$\log(\sigma_v)$	1.75	3.12	2.50	0.34	$2.54^{2.60}_{2.31}$
$\log(V_g(1))$	1.74	3.13	2.44	0.35	$2.47^{2.56}_{2.26}$
$\log(V_n)$	1.68	3.10	2.45	0.35	$2.48^{2.56}_{2.26}$
$\log(L_{min})$	9.01	10.13	9.73	0.29	$9.78^{9.90}_{9.70}$
$\log(L_{max})$	9.42	10.58	10.13	0.25	$10.17^{10.25}_{10.04}$
$\log(L_{sg})$	9.75	11.25	10.57	0.29	$10.58^{10.67}_{10.50}$
$\log(L_{Tg})$	9.85	12.02	11.03	0.47	$11.06^{11.25}_{10.87}$
$\log(\mathcal{M}_V/L_{Tg})$	0.33	3.87	2.30	0.80	$2.48^{2.69}_{1.83}$

Table A.45: List of RGH89 mass estimators-statistical parameters.

par.	min.	max.	mean	st. dev.	median
$\log(\mathcal{M}_V)$	11.65	14.92	13.45	0.83	$13.35^{13.93}_{12.93}$
$\log(\mathcal{M}_{Vu})$	11.67	14.93	13.43	0.84	$13.40^{13.93}_{12.88}$
$\log(\mathcal{M}_{VT})$	11.81	14.89	13.38	0.80	$13.29^{13.82}_{12.82}$
$\log(\mathcal{M}_P)$	11.57	14.90	13.31	0.84	$13.16^{13.72}_{12.76}$
$\log(\mathcal{M}_{Me})$	12.02	14.85	13.38	0.80	$13.40^{13.69}_{12.80}$
$\log(\mathcal{M}_{Av})$	11.71	14.91	13.46	0.83	$13.39^{13.82}_{12.92}$

Table A.46: Spearman correlation coefficient r and its significance S for RGH89.

pair	$\mid r \mid$	S	$\mid r \mid = 0$?
$(\log(L_{sg}), D_g)$	0.55	$< 10^{-3}$	NO
$(\log(L_{Tg}), D_g)$	0.88	$< 10^{-3}$	NO
$(\log(L_{min}), D_g)$	0.97	$< 10^{-3}$	NO
$(\log(L_{max}), D_g)$	0.46	$< 10^{-3}$	NO
$(\log(\mathcal{M}_{Vu}), D_g)$	0.30	0.035	NO
$(\log(\sigma_v), D_g)$	0.21	0.15	YES
$(\log(R_{Vu}), D_g)$	0.38	0.008	NO
$(\log(L_{Tg}/\mathcal{M}_{Vu}), D_g)$	0.22	0.12	YES
$(\log(L_{Tg}), \log(\sigma_v))$	0.34	0.015	NO
$(\log(L_{Tg}), \log(R_{Vu}))$	0.34	0.016	NO
$(\log(\sigma_v), \log(R_{Vu}))$	0.46	10^{-3}	NO
$(\log(\mathcal{M}_{Vu}), \log(L_{sg}))$	0.38	0.006	NO
$(\log(\mathcal{M}_{Vu}), \log(L_{Tg}))$	0.41	0.003	NO
$(\log(L_{Tg}/\mathcal{M}_{Vu}), \log(R_p))$	0.36	0.01	NO
$(\log(L_{Tg}/\mathcal{M}_{Vu}), \log(R_{Vu}))$	0.48	$< 10^{-3}$	NO

Table A.47: Pairwise KS test of different mass estimator distributions observed in *RGH*89.

pair	S	pair	S
$(\mathcal{M}_{Vu}, \mathcal{M}_V)$	0.99	$(\mathcal{M}_{Vu}, \mathcal{M}_{VT})$	0.85
$(\mathcal{M}_{Vu}, \mathcal{M}_P)$	0.86	$(\mathcal{M}_{Vu}, \mathcal{M}_{Me})$	0.86
$(\mathcal{M}_{Vu}, \mathcal{M}_{Av})$	0.99	$(\mathcal{M}_V, \mathcal{M}_{VT})$	0.70
$(\mathcal{M}_V, \mathcal{M}_P)$	0.53	$(\mathcal{M}_V, \mathcal{M}_{Me})$	0.70
$(\mathcal{M}_V, \mathcal{M}_{Av})$	0.96	$(\mathcal{M}_{VT}, \mathcal{M}_P)$	0.96
$(\mathcal{M}_{VT}, \mathcal{M}_{Me})$	0.96	$(\mathcal{M}_{VT}, \mathcal{M}_{Av})$	0.96
$(\mathcal{M}_P, \mathcal{M}_{Me})$	0.96	$(\mathcal{M}_P, \mathcal{M}_{Av})$	0.70
$(\mathcal{M}_{Me}, \mathcal{M}_{Av})$	0.70	-	-

Table A.48: Pairwise KS test of different velocity dispersion and virial radius estimator distributions observed in $RGH89$.

pair	S
(σ_v, V_n)	0.70
(σ_v, V_g)	0.38
(V_n, V_g)	0.96
(R_{Vu}, R_V)	0.96

Table A.49: List of $RGH89$ mass corrected for the evolutionary effect and related parameters.

par.	min.	max.	mean	st. dev.	median
		$\Omega = 0.2$			
$\log(\mathcal{M}_{Vu})$	12.01	14.83	13.49	0.77	$13.45^{14.00}_{12.99}$
τ	4.17	21.44	6.63	3.39	$5.73^{5.98}_{5.37}$
α	0.11	0.68	0.44	0.13	$0.48^{0.50}_{0.38}$
μ	0.73	4.36	1.33	0.69	$1.05^{1.30}_{1.00}$
		$\Omega = 1$			
$\log(\mathcal{M}_{Vu})$	12.11	14.88	13.55	0.76	$13.55^{14.04}_{13.05}$
τ	3.99	16.92	5.90	2.16	$5.12^{5.76}_{5.15}$
α	0.008	0.68	0.40	0.14	$0.42^{0.48}_{0.33}$
μ	0.74	5.83	1.54	0.97	$1.18^{1.50}_{1.03}$

Table A.50: Effect of Ω on the evolutionary correction: significance S of KS test comparison between the corrected distributions obtained for two values of Ω for $RGH89$.

par.	S
$\mathcal{M}_{Vu}$	0.99
τ	0.19
α	0.12
μ	0.22

A.5 The S89 groups

Table A.51: List of $S89$ parameters.

par.	min.	max.	mean	st. dev.	median
D_g	2.47	79.94	35.60	20.34	$30.95^{45.12}_{26.01}$
n_g	3	61	6.32	10.02	3^{4}_{3}
$\log(R_{Vu})$	-0.45	0.61	0.09	0.23	$0.12^{0.19}_{0.08}$
$\log(R_p)$	-0.97	1.49	-0.28	0.32	$-0.27^{-0.22}_{-0.38}$
$\log(\mathcal{T}_V)$	-1.40	0.44	-0.64	0.42	$-0.74^{-0.56}_{-0.83}$
$\log(\sigma_v)$	1.40	3.03	2.40	0.35	$2.42^{2.53}_{2.36}$
$\log(V_n)$	1.40	3.04	2.41	0.35	$2.43^{2.54}_{2.37}$
$\log(L_{min})(\star)$	7.59	10.35	9.35	0.66	$9.54^{9.72}_{9.27}$
$\log(L_{max})(\star)$	8.85	10.94	10.07	0.39	$10.11^{10.21}_{10.01}$
$\log(L_{sg})(\star)$	9.10	11.19	10.36	0.45	$10.35^{10.52}_{10.25}$
$\log(\mathcal{M}_{Vu}/L_{sg})(\star)$	-1.33	4.37	2.84	0.83	$2.92^{3.06}_{2.66}$

Table A.52: List of $S89$ mass estimators-statistical parameters.

par.	min.	max.	mean	st. dev.	median
$\log(\mathcal{M}_{Vu})$	11.10	15.01	13.26	0.73	$13.26^{13.49}_{13.17}$
$\log(\mathcal{M}_{VT})$	11.58	15.03	13.30	0.68	$13.27^{13.51}_{13.18}$
$\log(\mathcal{M}_P)$	11.46	15.70	13.15	0.78	$13.15^{13.32}_{12.97}$
$\log(\mathcal{M}_{Me})$	11.36	15.50	13.24	0.75	$13.22^{13.42}_{13.02}$
$\log(\mathcal{M}_{Av})$	11.24	15.08	13.41	0.72	$13.40^{13.67}_{13.25}$

Table A.53: Spearman correlation coefficient r and its significance S for $S89$.

pair	$\mid r \mid$	S	$\mid r \mid = 0$?
$(\log(L_{sg}), D_g)(\star)$	0.47	< 0.001	NO
$(\log(L_{min}), D_g)(\star)$	0.82	< 0.001	NO
$(\log(L_{max}), D_g)(\star)$	0.55	< 0.001	NO
$(\log(\mathcal{M}_{Vu}), D_g)$	0.25	0.02	NO
$(\log(\sigma_v), D_g)$	0.16	0.14	YES
$(\log(R_{Vu}), D_g)$	0.34	0.001	NO
$(\log(\mathcal{M}_{Vu}/L_{sg}), D_g)(\star)$	0.06	0.53	YES
$(\log(\mathcal{M}_{Vu}), \log(L_{sg}))(\star)$	0.41	< 0.001	NO
$(\log(\mathcal{M}_{Vu}), \log(\sigma_v))$	0.93	< 0.001	NO
$(\log(\mathcal{M}_{Vu}), \log(R_{Vu}))$	0.29	0.001	NO
$(\log(L_{sg}), \log(\sigma_v))(\star)$	0.39	< 0.001	NO
$(\log(L_{sg}), \log(R_{Vu}))(\star)$	0.15	0.16	YES
$(\log(\sigma_v), \log(R_{Vu}))$	0.02	0.88	YES
$(\log(\mathcal{M}_{Vu}/L_{sg}), \log(R_{Vu}))(\star)$	0.18	0.095	YES

Table A.54: The KS test significances S of differences revealed by the comparison between some group parameter distributions of $S89$ versus $S89(D \leq 20\ Mpc)$ (in col. A), of $S89(D \leq 20\ Mpc)$ versus $S89(D > 20\ Mpc)$ (in col. B) and $S89(D > 20\ Mpc)$ versus $S89$ (in col. C).

par.	A	B	C
$\log(\mathcal{M}_{Vu})$	0.74	0.46	0.99
$\log(\mathcal{M}_{VT})$	0.74	0.46	0.99
$\log(\mathcal{M}_P)$	0.95	0.81	0.99
$\log(\mathcal{M}_{med})$	0.82	0.57	0.99
$\log(\mathcal{M}_{Av})$	0.57	0.28	0.99
n_g	0.36	0.08	0.94
$\log(\sigma_v)$	0.98	0.90	0.99
$\log(R_{Vu})$	0.22	0.053	0.92
$\log(R_p)$	0.31	0.06	0.92
$\log(T_V)$	0.67	0.29	0.99
$\log(\mathcal{M}_{Vu}/L_{sg})(\star)$	0.39	0.10	0.96

Table A.55: List of $S89(D \leq 20\ Mpc)$ parameters.

par.	min.	max.	mean	st. dev.	median
D_g	2.47	19.89	11.83	3.98	$13.13^{13.98}_{9.06}$
n_g	3	61	11.68	17.16	5^{6}_{3}
$\log(R_{Vu})$	-0.43	0.27	0.01	0.19	$0.08^{0.18}_{-0.11}$
$\log(R_p)$	-0.75	1.18	-0.35	0.23	$-0.40^{-0.22}_{-0.48}$
$\log(\mathcal{T}_V)$	-1.40	0.22	-0.71	0.40	$-0.80^{-0.59}_{-0.93}$
$\log(\sigma_v)$	1.39	2.82	2.39	0.34	$2.41^{2.62}_{2.31}$
$\log(V_n)$	1.40	2.82	2.39	0.34	$2.42^{2.62}_{2.31}$
$\log(L_{min})(\star)$	7.59	9.92	8.63	0.61	$8.56^{8.98}_{8.19}$
$\log(L_{max})(\star)$	8.85	10.37	9.81	0.43	$9.90^{10.10}_{9.50}$
$\log(L_{sg})(\star)$	9.10	11.16	10.13	0.57	$10.20^{10.33}_{9.66}$
$\log(\mathcal{M}_{Vu}/L_{sg})(\star)$	-1.33	4.12	2.92	1.07	$3.06^{3.39}_{2.77}$

Table A.56: List of $S89(D \leq 20\ Mpc)$ mass estimators-statistical parameters.

par.	min.	max.	mean	st. dev.	median
$\log(\mathcal{M}_{Vu})$	11.10	14.15	13.16	0.71	$13.22^{13.71}_{12.95}$
$\log(\mathcal{M}_{VT})$	11.58	14.16	13.20	0.63	$13.23^{13.72}_{12.96}$
$\log(\mathcal{M}_P)$	11.46	14.33	13.04	0.68	$13.09^{13.37}_{12.63}$
$\log(\mathcal{M}_{Me})$	11.36	14.26	13.12	0.68	$13.13^{13.70}_{12.77}$
$\log(\mathcal{M}_{Av})$	11.72	14.20	13.23	0.64	$13.27^{13.73}_{13.00}$

Table A.57: Spearman correlation coefficient r and its significance S for $S89(D \leq 20\ Mpc)$.

pair	$\mid r \mid$	S	$\mid r \mid = 0$?
$(\log(L_{sg}), D_g)(\star)$	0.25	0.23	YES
$(\log(L_{min}), D_g)(\star)$	0.60	< 0.001	NO
$(\log(L_{max}), D_g)(\star)$	0.32	0.12	YES
$(\log(\mathcal{M}_{Vu}), D_g)$	0.08	0.70	YES
$(\log(\sigma_v), D_g)$	0.17	0.41	YES
$(\log(R_{Vu}), D_g)$	0.12	0.55	YES
$(\log(\mathcal{M}_{Vu}/L_{sg}), D_g)(\star)$	0.01	0.95	YES
$(\log(\mathcal{M}_{Vu}), \log(L_{sg}))(\star)$	0.56	< 0.003	NO
$(\log(\mathcal{M}_{Vu}), \log(\sigma_v))$	0.92	< 0.001	NO
$(\log(\mathcal{M}_{Vu}), \log(R_{Vu}))$	0.27	0.19	YES
$(\log(L_{sg}), \log(\sigma_v))(\star)$	0.52	< 0.01	NO
$(\log(L_{sg}), \log(R_{Vu}))(\star)$	0.29	0.16	YES
$(\log(\sigma_v), \log(R_{Vu}))$	0.05	0.82	YES
$(\log(\mathcal{M}_{Vu}/L_{sg}), \log(R_{Vu}))(\star)$	0.18	0.39	YES

Table A.58: Pairwise KS test of different mass estimator distributions observed in $S89$ and $S89(D \leq 20Mpc)$.

pair	$S(S89)$	$S[S89(D \leq 20\ Mpc)]$
$(\mathcal{M}_{Vu}, \mathcal{M}_{VT})$	0.99	0.99
$(\mathcal{M}_{Vu}, \mathcal{M}_{P})$	0.36	0.91
$(\mathcal{M}_{Vu}, \mathcal{M}_{Med})$	0.59	0.91
$(\mathcal{M}_{Vu}, \mathcal{M}_{Av})$	0.47	0.99
$(\mathcal{M}_{VT}, \mathcal{M}_{P})$	0.19	0.70
$(\mathcal{M}_{VT}, \mathcal{M}_{Med})$	0.36	0.91
$(\mathcal{M}_{VT}, \mathcal{M}_{Av})$	0.59	0.99
$(\mathcal{M}_{P}, \mathcal{M}_{Med})$	0.72	0.91
$(\mathcal{M}_{P}, \mathcal{M}_{Av})$	0.04	0.47
$(\mathcal{M}_{Med}, \mathcal{M}_{Av})$	0.14	0.70

Table A.59: List of $S89$ mass corrected for the evolutionary effect and related parameters.

par.	min.	max.	mean	st. dev.	median
$\Omega = 0.2$					
$\log(\mathcal{M}_{Vu})$	12.02	15.04	13.42	0.59	$13.41^{13.63}_{13.25}$
τ	3.54	21.44	6.01	2.50	$5.61^{5.82}_{5.26}$
α	0.03	0.69	0.40	0.17	$0.45^{0.50}_{0.36}$
μ	0.73	17.76	2.15	2.85	$1.12^{1.39}_{1.00}$
$\Omega = 1$					
$\log(\mathcal{M}_{Vu})$	12.17	15.09	13.49	0.58	$13.50^{13.71}_{13.35}$
τ	3.45	16.93	5.56	1.82	$5.40^{5.61}_{5.04}$
α	0.02	0.65	0.36	0.17	$0.39^{0.45}_{0.30}$
μ	0.77	26.37	2.76	4.23	$1.26^{1.63}_{1.11}$

Table A.60: List of $S89(D \leq 20\ Mpc)$ mass corrected for the evolutionary effect and related parameters.

par.	min.	max.	mean	st. dev.	median
$\Omega = 0.2$					
$\log(\mathcal{M}_{Vu})$	12.02	14.13	13.28	0.52	$13.32^{13.70}_{13.03}$
τ	3.81	21.44	6.51	3.54	$5.75^{6.02}_{5.33}$
α	0.06	0.66	0.42	0.16	$0.48^{0.50}_{0.38}$
μ	0.76	8.26	1.76	1.90	$1.04^{1.32}_{1.00}$
$\Omega = 1$					
$\log(\mathcal{M}_{Vu})$	12.17	14.17	13.34	0.50	$13.38^{13.75}_{13.08}$
τ	3.67	16.93	6.05	2.62	$5.54^{5.80}_{5.12}$
α	0.04	0.61	0.38	0.15	$0.43^{0.49}_{0.32}$
μ	0.81	11.61	2.18	2.74	$1.16^{1.54}_{1.01}$

Table A.61: Effect of the evolutionary correction: significance S of KS test comparison between the observed and corrected distributions.

Ω	$S89$	$S89(D \leq 20\ Mpc)$
0.2	0.24	0.91
1.0	0.04	0.70

Table A.62: Effect of Ω on the evolutionary correction: significance S of KS test comparison between the corrected distributions obtained for two values of Ω for $S89$.

par.	$S89$	$S89(D \leq 20\ Mpc)$
$\mathcal{M}_{Vu}$	0.87	0.99
τ	0.27	0.78
α	0.09	0.27
μ	0.17	0.25

A.6 Comparison among catalogues

Table A.63: Summary of statistical features of the mass distributions of groups in different catalogues. The reported numbers indicate the decimal logarithms of the masses in solar units.

cat.	min.	max	mean	st.dev.	median	Q_1	Q_3
$GH83$	12.04	15.41	13.58	0.77	$13.63^{13.80}_{13.31}$	13.02	14.15
$RGH89$	12.01	14.83	13.49	0.77	$13.45^{14.00}_{12.99}$	12.83	14.13
$S89$	12.02	15.04	13.42	0.58	$13.41^{13.62}_{13.25}$	13.08	13.81
$T87$	11.28	14.01	12.93	0.52	$12.97^{13.07}_{12.85}$	12.61	13.28
$V84$	11.11	14.51	12.59	0.57	$12.59^{12.75}_{12.43}$	12.31	12.87

Table A.64: The Kruskal-Wallis test significance S for the set C of whole catalogues (line A) and within 20 Mpc from us (line B).

par.	$\mathcal{M}$	τ	α	$\mathcal{T}_V$	σ_v	R_{Vu}	R_p
A	$< 10^{-3}$	$< 10^{-3}$	$< 10^{-3}$	$< 10^{-3}$	$< 10^{-3}$	$< 10^{-3}$	$< 10^{-3}$
B	$< 10^{-3}$	$< 10^{-3}$	$< 10^{-3}$	$< 10^{-3}$	$< 10^{-3}$	$< 10^{-3}$	$< 10^{-3}$

Table A.65: The significance S of the Kruskal-Wallis test for the set $C_{f.o.f.}$ of whole catalogues (line A) and of the KS pairwise test significance for $GH83$ and $S89$ within 20 Mpc from us (line B).

par.	$\mathcal{M}$	τ	α	$\mathcal{T}_V$	σ_v	R_{Vu}	R_p
A	0.20	0.13	0.13	0.13	0.49	0.20	$< 10^{-3}$
B	0.73	0.69	0.94	0.79	0.71	0.47	0.17

Table A.66: The KS test for pairwise comparison between catalogues (here R89 stands for RGH89).

pair	$\mathcal{M}$	τ	α	$\mathcal{T}_V$	R_{Vu}	σ_v	R_p
GH83,T87	$< 10^{-3}$	$< 10^{-3}$	$< 10^{-3}$	$< 10^{-3}$	$< 10^{-3}$	$< 10^{-3}$	$< 10^{-3}$
GH83,S89	0.03	0.84	0.39	0.41	0.04	0.59	$< 10^{-3}$
GH83,V84	$< 10^{-3}$	0.02	0.04	0.13	$< 10^{-3}$	$< 10^{-3}$	$< 10^{-3}$
GH83,R89	0.72	0.08	0.08	0.03	0.17	0.79	0.001
T87,S89	$< 10^{-3}$	$< 10^{-3}$	$< 10^{-3}$	$< 10^{-3}$	0.002	$< 10^{-3}$	0.52
T87,V84	$< 10^{-3}$	0.04	0.04	0.06	$< 10^{-3}$	0.03	$< 10^{-3}$
T87,R89	$< 10^{-3}$	$< 10^{-3}$	$< 10^{-3}$	$< 10^{-3}$	0.32	$< 10^{-3}$	0.03
S89,V84	$< 10^{-3}$	0.03	0.005	0.03	$< 10^{-3}$	$< 10^{-3}$	0.002
S89,R89	0.12	0.17	0.75	0.27	0.38	0.26	0.04
V84,R89	$< 10^{-3}$	0.001	0.001	0.002	$< 10^{-3}$	$< 10^{-3}$	$< 10^{-3}$

Table A.67: The KS test for pairwise comparison between catalogues within 20 Mpc from us.

pair	$\mathcal{M}$	τ	α	$\mathcal{T}_V$	R_{Vu}	σ_v	R_p
GH83,T87	0.005	$< 10^{-3}$	$< 10^{-3}$	$< 10^{-3}$	0.49	$< 10^{-3}$	0.88
GH83,S89	0.73	0.69	0.94	0.79	0.47	0.71	0.17
GH83,V84	$< 10^{-3}$	0.002	0.003	0.02	0.02	$< 10^{-3}$	$< 10^{-3}$
T87,S89	0.006	$< 10^{-3}$	$< 10^{-3}$	$< 10^{-3}$	0.30	$< 10^{-3}$	0.15
T87,V84	$< 10^{-3}$	0.03	0.01	0.096	$< 10^{-3}$	0.02	$< 10^{-3}$
S89,V84	$< 10^{-3}$	0.049	0.03	0.03	10^{-3}	$< 10^{-3}$	0.15

Bibliography

[1] Aarseth S.J. and Saslaw W.C., 1972: *Ap. J.*, **172**, 17.

[2] Arp H., 1970: *Nature*, **225**, 1033.

[3] Arp H. and Sulentic J.W., 1985: *Ap. J.*, **244**, 805.

[4] Bahcall J.N. and Tremaine S., 1981 (BT): *Ap. J.*, **244**, 805.

[5] Barnes J., 1984: *Mon. Not. R. Astr. Soc.*, **208**, 873.

[6] Binggeli B., Sandage A. and Tamman G.A., 1985: *Astron. J.*, **90**, 1681.

[7] Binggeli B., Sandage A. and Tamman G.A., 1988: *Ann. Rev. Astr. & Astrophys.*, **26**, 509.

[8] Byrd G.G. and Valtonen M.J., 1985: *Ap. J.*, **289**, 535.

[9] Cavaliere A, Danese G. and De Zotti G.F., 1977: *Ap. J.*, **217**, 6.

[10] Cavaliere A., Santangelo P., Tarquini G. and Vittorio N., 1986: *Ap. J.*, **305**, 651.

[11] Chamaraux P., van Woerden H., Goss W.M., Mebold U. and Tully R.B., 1989: in preparation.

[12] Colafrancesco S., Lucchin S. and Matarrese S, 1989: *Ap. J.*, **345**, 3.

[13] da Costa L.N., Pellegrini P.S., Sargent W.L., Torny J., Davis M., Mekisin A., Latham D.W., Menzies J.W. and Coulson I.A., 1988: *Ap. J.*, **327**, 544.

[14] Danese L., De Zotti G. and di Tullio G., 1979: *Astron. & Astrophys.*, **82**, 322.

[15] Davis M., Efstathiou G., Frenk C.S. and White S.D.M., 1985: *Ap. J*, **292**, 371.

[16] de Lapparent V., Geller M.J. and Huchra J.P., 1989: preprint.

[17] de Vaucouleurs G., 1975: in *Galaxies and the Universe*, eds.: A. Sandage and J. Kristien, Chicago: University of Chicago Press, pag. 557.

[18] de Vaucouleurs G., de Vaucouleurs A. and Corwin H, 1976: *Second Reference Catalogue of Bright Galaxies*, Austin: Univerity of Texas Press.

[19] Efstathiou G., Frenk C. S. and White S.D.M., 1988: *Mon. Not. R. Astr. Soc.*, **235**, 715.

[20] Evrard A.E., 1987: *Ap. J.*, **316**, 36.

[21] Faber S.M. and Gallagher J.S., 1979: *Ann. Rev. Astron. & Astrophys.*, **17**, 135.

[22] Felten J.E., 1985: *Comments on Astrophys.*, **11**, 53.

[23] Fisher J.R. and Tully R.B., 1981: *Ap. J. Suppl. S.*, **47**, 139.

[24] Geller M.J. and Huchra J.P., 1983 (GH83): *Ap. J. Suppl. S.*, **52**, 61.

[25] Geller M.J., 1988: in *Large Scale Structure of the Universe*, SAAS-FEE lectures.

[26] Girardi M, Biviano A., Giuricin G., Mardirossian F. and Mezzetti M, 1990: *Ap. J.*, in press.

[27] Giuricin G., Mardirossian M. and Mezzetti M., 1982: *Ap. J.*, **255**, 361.

[28] Giuricin G., Mardirossian F., Mezzetti M. and Santangelo P., 1984: *Ap. J.*, **277**, 38.

[29] Giuricin G., Mardirossian F. and, Mezzetti M., 1985: *Astron. & Astrophys. Suppl. S.*, **62**, 157.

[30] Giuricin G., Mezzetti M., Ramella M. and Mardirossian F., 1986: *Astron. & Astrophys.*, **157**, 129.

[31] Giuricin G., Gondolo. P., Mardirossian F., Mezzetti M., Ramella M., 1988: *Astron. & Astrophys.*, **199**, 85.

[32] Giuricin G., Mardirossian F., Mezzetti M. and Pisani A., 1989: *Ap. J.*, **345**, 101.

[33] Gott J.R.III and Rees M.J., 1975: *Astron. & Astrophys.*, **45**, 365.

[34] Gott J.R. and Turner E.L., 1977 (GT77): *Ap. J.*, **213**, 309.

[35] Gunn J.E. and Gott J.R., 1972: *Ap. J.*, **176**, 1.

[36] Heisler J., Tremaine S. and Bahcall J.N., 1985: *Ap. J.*, **298**, 8.

[37] Huchra J.P., 1976: *Astron. J.*, **81**, 952.

[38] Huchra J.P. and Geller M.J., 1982 (HG82): *Ap. J.*, **257**, 423.

[39] Huchra J.P., Geller M.J., de Lapparent V. and Corwin H., 1988: in preparation.

[40] Huchra J.P., Davis M., Latham D. and Torny J., 1983: *Ap. J. Suppl. S.*, **52**, 89.

[41] Jaakola T., 1971: *Nature*, **234**, 534.

[42] Jackson J.C., 1975: *Mon. Not. R. Astr. Soc.*, **173**, 41p.

[43] Kendall M. and Stuart A., 1977: *The Advanced Theory of Statistics*, London, C. Griffin.

[44] Lauberts A., 1982: *The ESO-Uppsala Survey of the ESO(B) Atlas*, ESO, Munich.

[45] Lauberts A. and Valentijn E.A., 1989: *The Surface Photometry Catalogue of the ESO-Uppsala Galaxies*, ESO.

[46] Ledermann W., 1982: *Handbook of Applicable Mathematics*, John Wiley & Sons, vol.VI.

[47] Limber D.N., 1959: *Ap. J.*, **130**, 414.

[48] Lucchin F., 1990a: preprint.

[49] Lucchin F., 1990b: *Introduzione alla Cosmologia*, Zanichelli, Bologna.

[50] Lynden-Bell D., 1967: *Mon. Not. R. Astr. Soc.*, **136**, 101.

[51] Lynden-Bell D., Faber S.M., Burstein D., Davies R.L., Dressler A., Terlevich R.J. and Wegner G., 1988: *Ap. J.*, **326**, 19.

[52] Maia M.A.G., da Costa L.N. and Latham D.W., 1989: *Ap. J. Suppl. S.*, **69**, 809.

[53] Materne J., 1978: *Astron. & Astrophys.*, **63**, 401.

[54] Materne J., 1979: *Astron. & Astrophys.*, **74**, 235.

[55] Merritt D., 1983: *Ap. J.*, **264**, 24.

[56] Mezzetti M, Pisani A., Giuricin G. and Mardirossian F., 1985: *Astron. & Astrophys.*, **143**, 188.

[57] Mezzetti M., Girardi M., Giuricin G. and Mardirosian F., 1988: in preparation.

[58] Nilson P., 1973: *Uppsala General Catalog of Galaxies*, Uppsala Obs. Annals V, vol. 1.

[59] Nolthenius R. and White S.D.M., 1987: *Mon. Not. R. Astr. Soc.*, **235**, 505.

[60] Peacock J.A., 1990: *Contribution Paper to the* 10^{th} *Moriond Astrophysical Meeting*, Les Arcs, preprint.

[61] Peebles P.J.E., 1970: *Astron. J.*, **75**, 13.

[62] Perea J., del Olmo A. and Moles M., 1990: *Ap. J.*, in press.

[63] Press W.H. and Schechter P, 1974: *Ap. J.*, **187**, 425.

[64] Ramella M., Geller M.J. and Huchra J.P., 1989 (RGH89): *Ap. J.*, .

[65] Reif K., Mebold U., Goss M., van Woerden H. and Siegman B., 1982: *Astron. & Astrophys. Suppl. S.*, **50**, 451.

[66] Rood H.J. and Dickel J., 1978: *Ap. J.*, **224**, 724.

[67] Rood H.J., 1980: *A Catalog of Galaxy Red-Shifts.*

[68] Rubin V.C., Ford W.K., Thonnard N. and Burstein D., 1982: *Ap. J.*, **261**, 439.

[69] Schechter P., 1976: *Ap. J.*, **203**, 297.

[70] Sandage A., 1975: *Ap. J.*, **202**, 563.

[71] Sandage A., 1978: *Astron. J.*, **83**, 904.

[72] Sandage A. and Tamman G., 1975: *Ap. J.*, **196**, 313.

[73] Sandage A. and Tamman G., 1981: *Revised Shapley-Ames Catalog of Bright Galaxies*, Canergie Institution, Washington DC.

[74] Sargent W.L.W. and Turner E.L., 1977: *Ap. J. Lett.*, **212**, L3.

[75] Saslaw W.C., 1985: *Gravitational Physics of Stellar and Galactic Systems*, Cambridge University Press.

[76] Shapley H. and Ames A., 1932: *Harvard Ann.*, vol. **88**, No. 2.

[77] Shu F.H., 1978: *Ap. J.*, **225**, 83.

[78] Smith H. Jr., 1977: *Astron. & Astrophys.*, **61**, 305.

[79] Smith H.Jr., 1982: *Ap. J.*, **259**, 423.

[80] Smith H.Jr., 1984: *Ap. J.*, **285**, 16.

[81] Stauffer D., 1985: *Introduction to Percolation Theory*, Taylor & Francis, London and Philadelphia.

[82] van Morrsel G.A., 1982: *Ph. D. Thesis*, University of Groningen, Netherlands.

[83] Vennik J. and Kaasik A., 1982: *Astrofizika*, **18**, 523.

[84] Vennik J. and Kaasik A., 1984: in preparation.

[85] Vennik J., 1984 (V84): *Tartu Astrophys. Obs.*, No. **73**, 3.

[86] Vennik J., 1986: *Astron. Nach.*, **307**, 157.

[87] Tully R.B., 1980: *Ap. J.*, **237**, 390.

[88] Tully R.B., 1982: *Ap. J.*, **257**, 389.

[89] Tully R.B., 1987a: *Nearby Galaxy Catalog*, Cambridbe University Press.

[90] Tully R.B., 1987b (T87): *Ap. J.*, **321**, 280.

[91] Tully R.B. and Fisher J.R., 1987: *Nearby Galaxies Atlas*, Cambridge University Press, Cambribge.

[92] Tully R.B., 1988: *Astron. J.*, **96**, 73.

[93] Turner E.L. and Gott J.R., 1976: *Ap. J.*, **209**, 6.

[94] White S.D.M., Huchra J.P., Latham D. and Davies M., 1983: *Mon. Not. R. Astr. Soc.*, **203**, 701.

[95] Yahil A., 1977: *Ap. J.*, **217**, 27.

[96] Yahil A., Sandage A. and Tamman G.A., 1980: *Ap. J.*, **242**, 448.

[97] Zwicky F., 1933: *Helv. Phys. Acta*, **6**, 10.